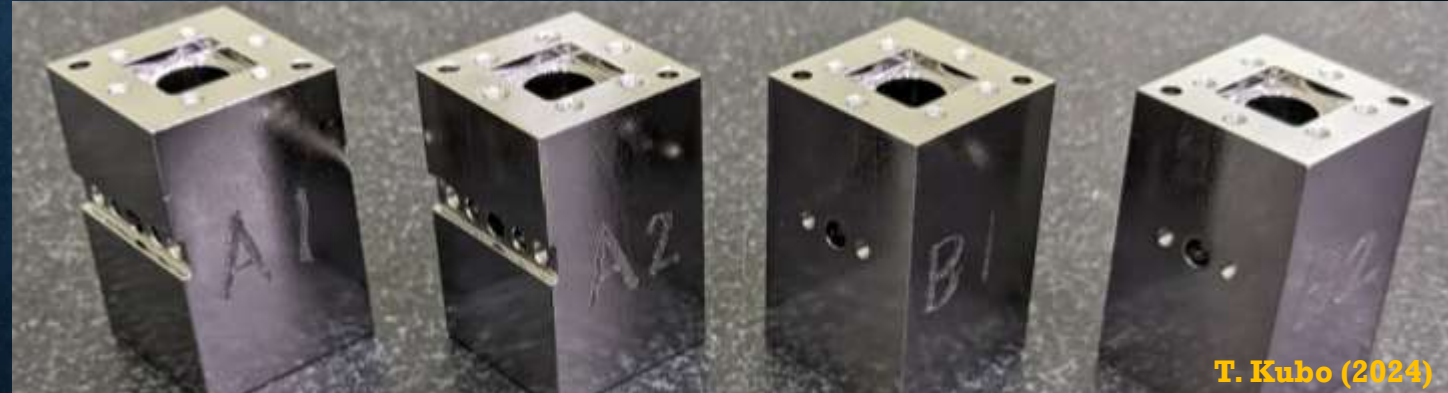
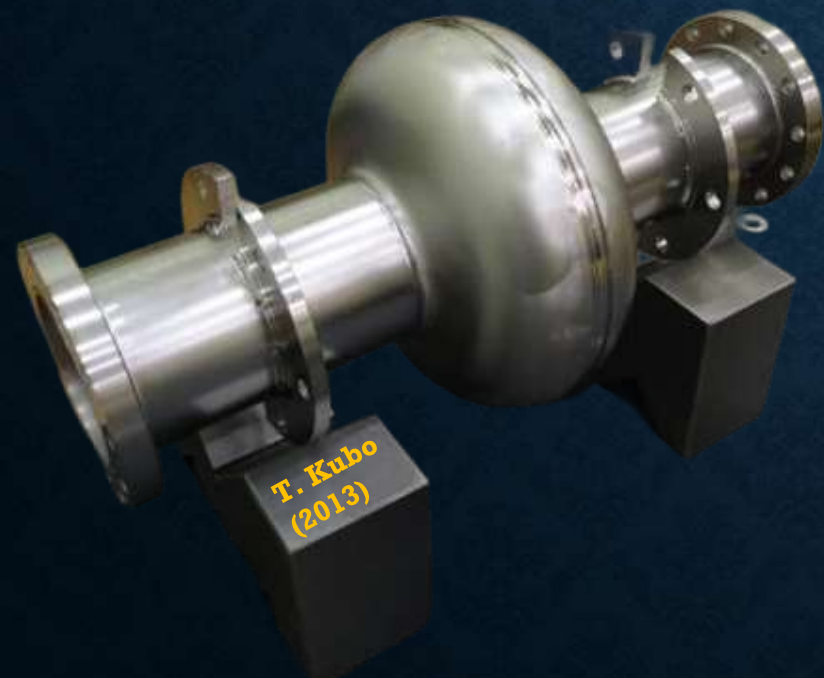


HIGH ENERGY ACCELERATOR SCIENCE SEMINAR, OCT. 29, 2025

SUPERCONDUCTING RESONANT CAVITIES

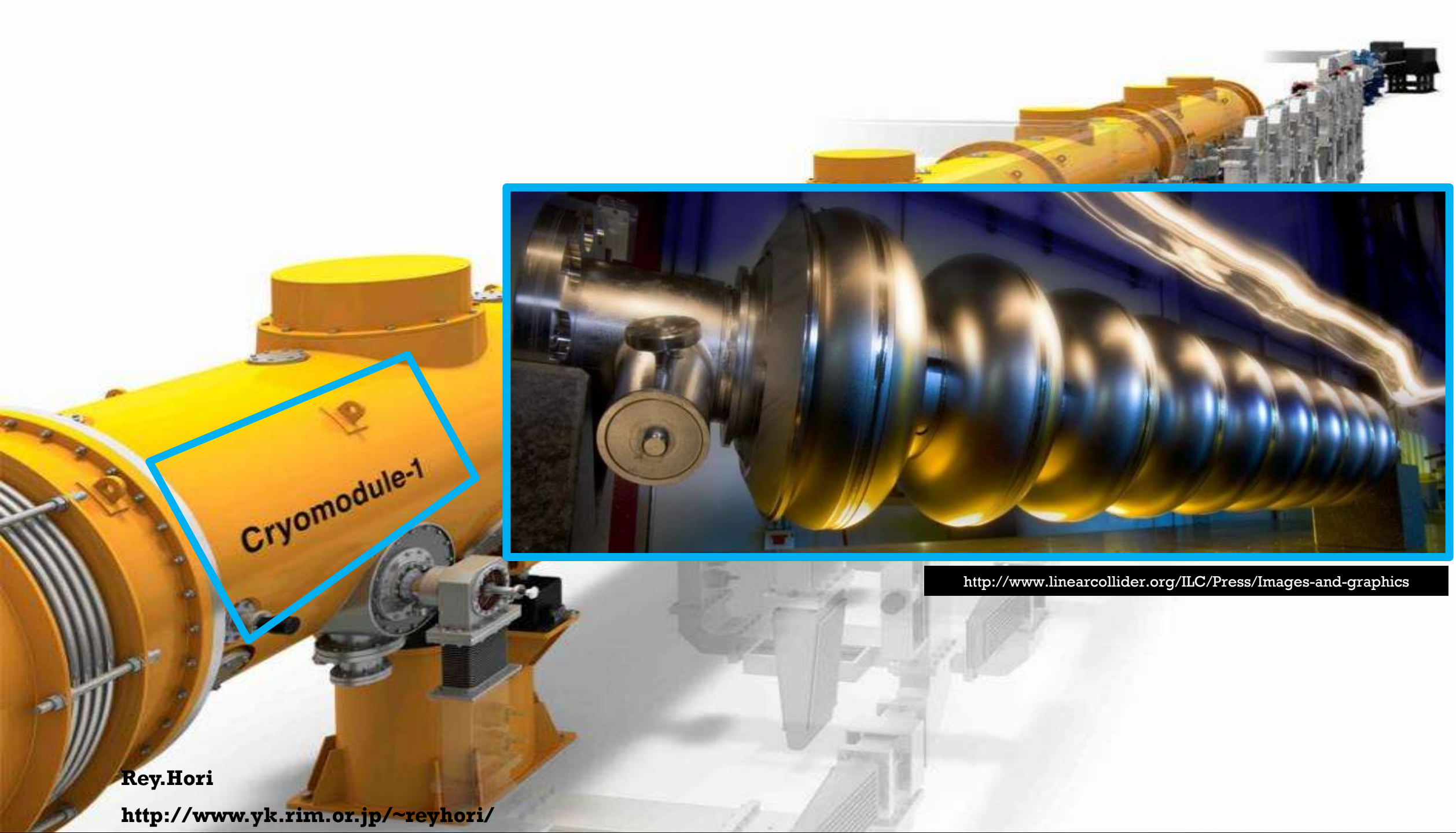
Takayuki KUBO
KEK iCASA





Rey.Hori

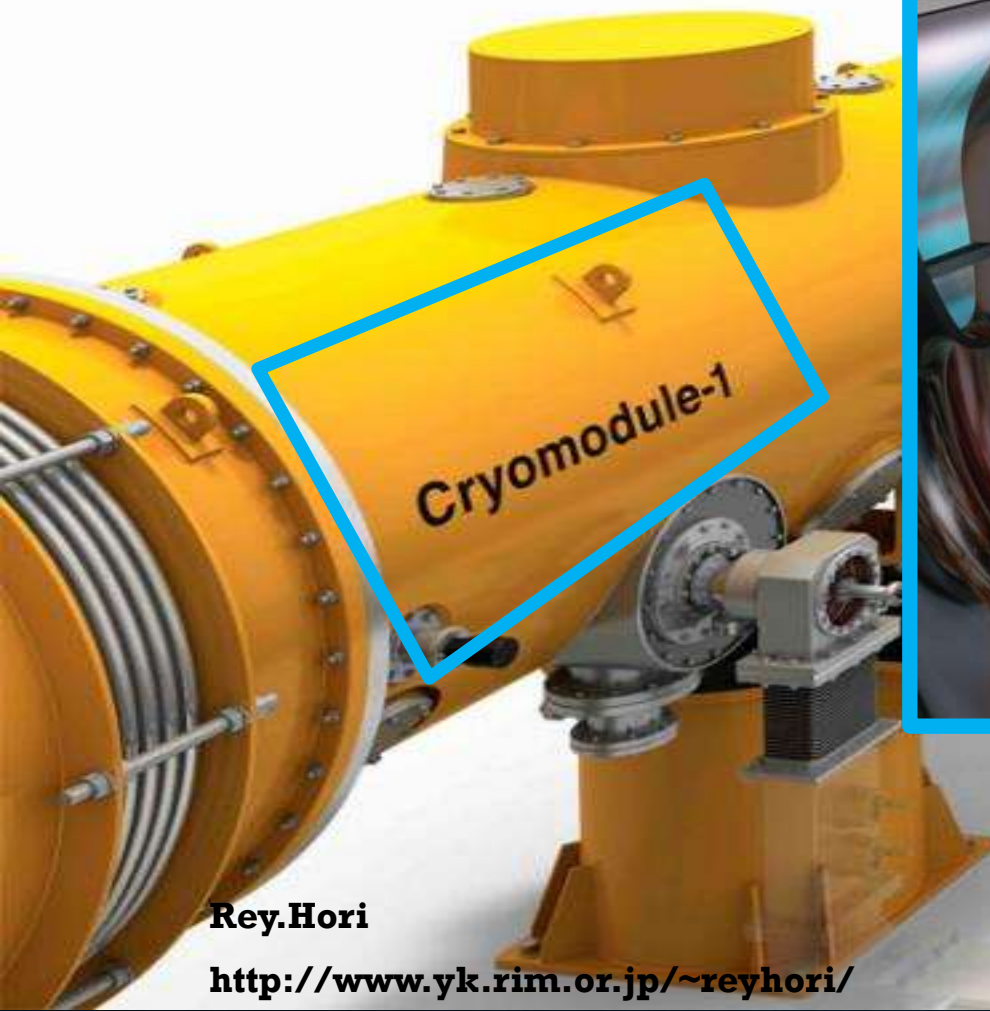
<http://www.yk.rim.or.jp/~reyhori/>



<http://www.linearcollider.org/ILC/Press/Images-and-graphics>

Rey.Hori

<http://www.yk.rim.or.jp/~reyhori/>

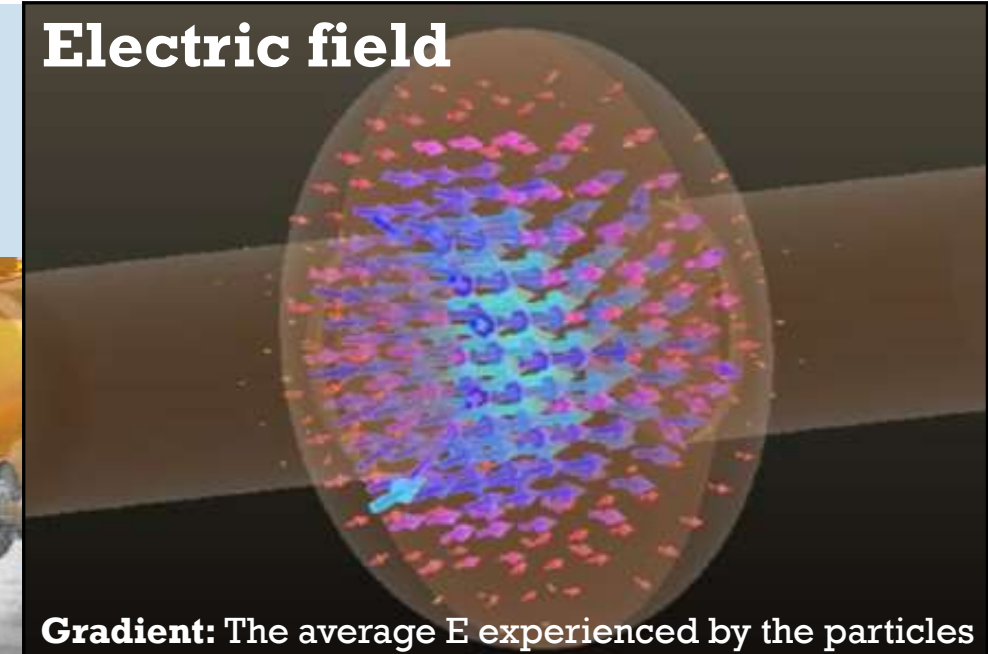
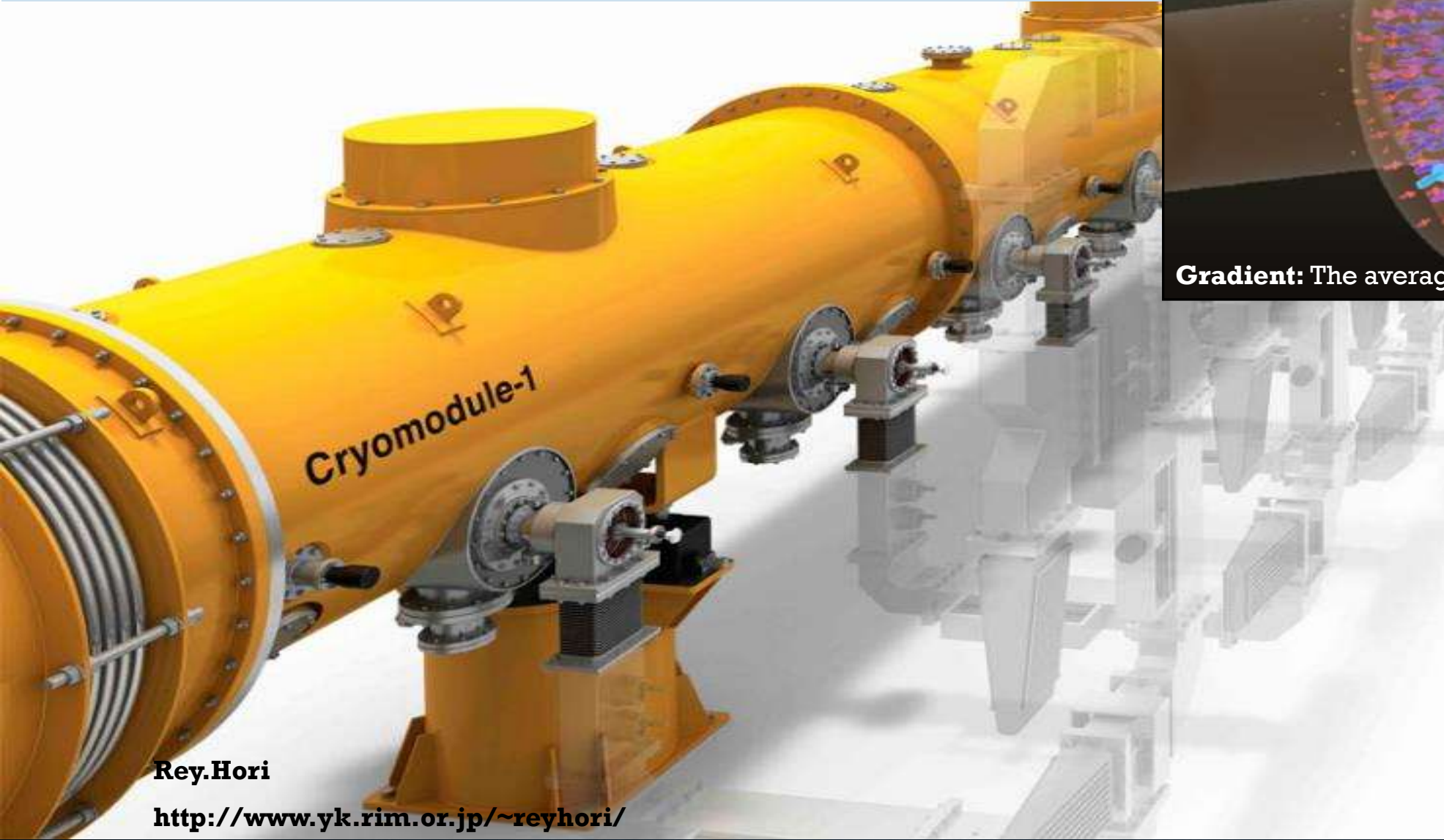


<http://www.linearcollider.org/ILC/Press/Images-and-graphics>

Rey.Hori

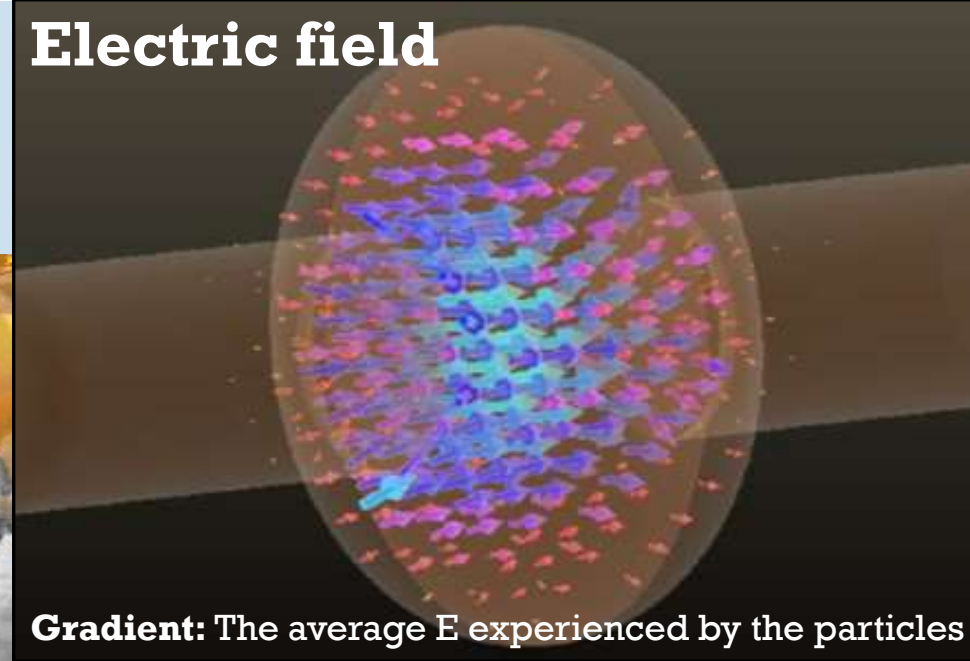
<http://www.yk.rim.or.jp/~reyhori/>

Key Performance Metrics (1): Gradient E_{acc} (microwave amplitude)



Gradient: The average E experienced by the particles

Key Performance Metrics (1): Gradient E_{acc} (microwave amplitude)



Gradient: The average E experienced by the particles

Key Performance Metrics (2): Quality factor Q_0 (photon lifetime)



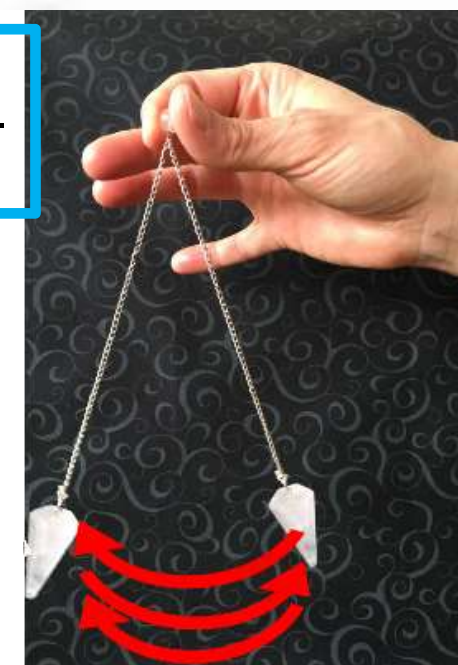
Rey.Hori

<http://www.yk.rim.or.jp/~reyhori/>

$$Q_0 = \frac{\omega U}{P} \sim \frac{U}{P_1}$$

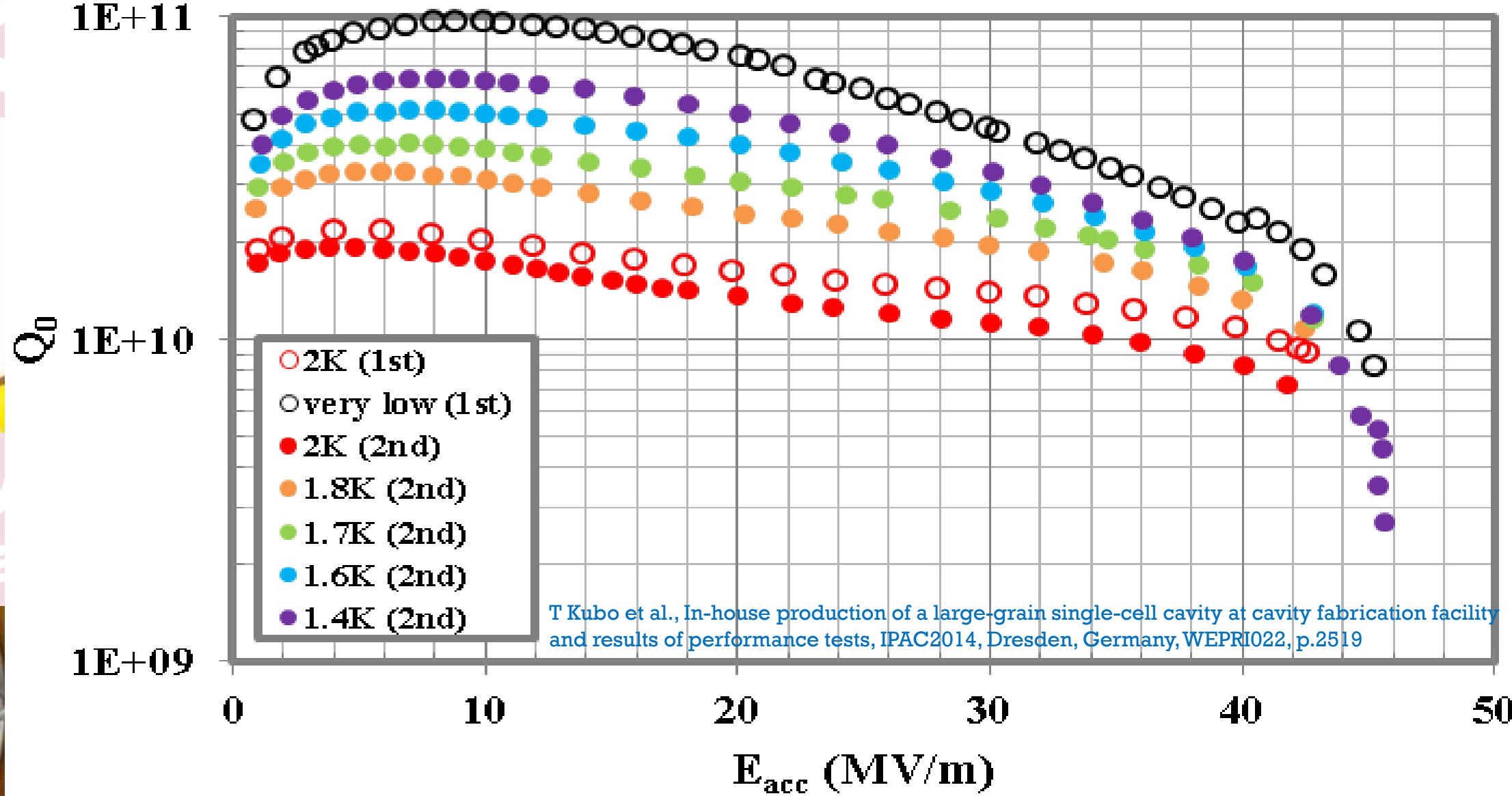
P_1 : dissipation per
RF cycle

Q_0 : how many cycles it
takes for the stored
energy to completely
dissipate

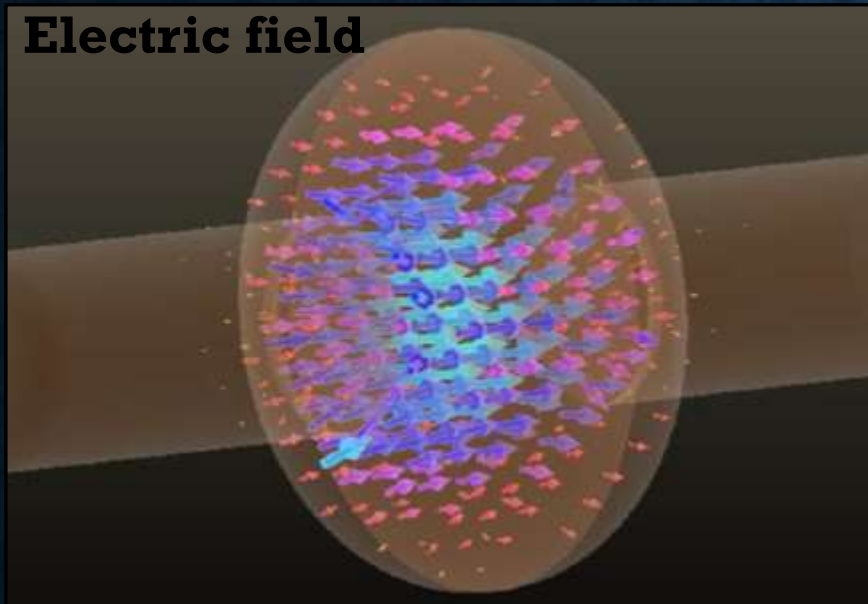


Key Performance Metrics (1)

Electric field

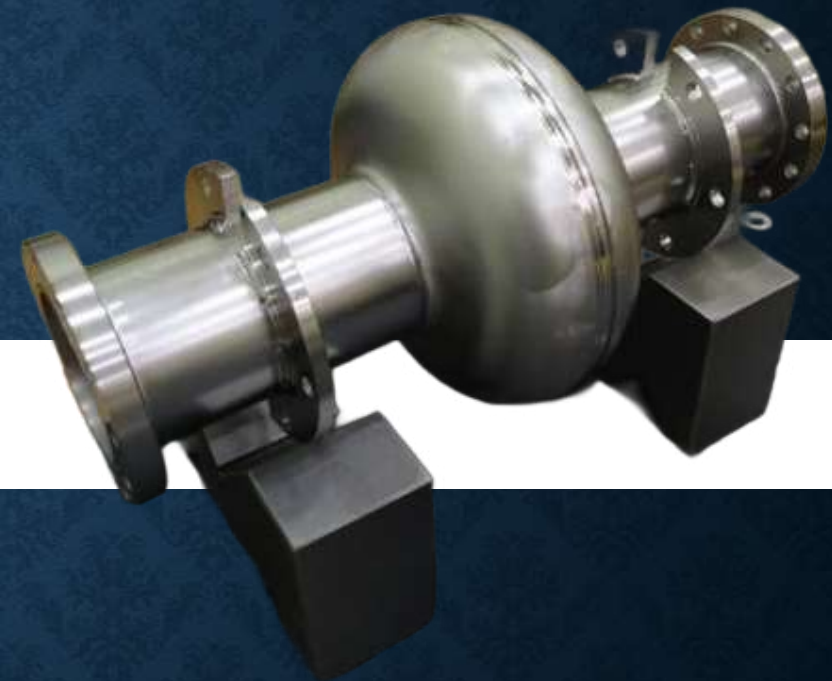
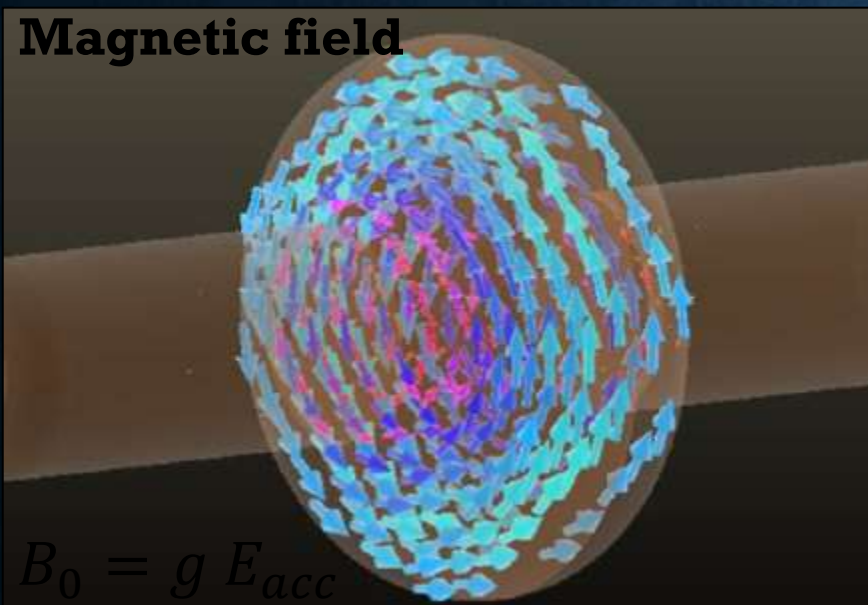


Electric field

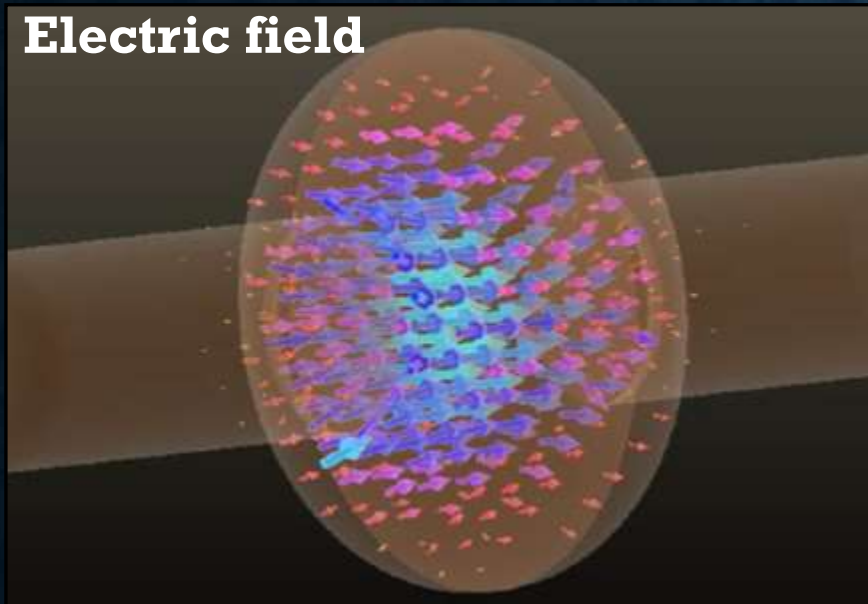


What Limits the Gradient?

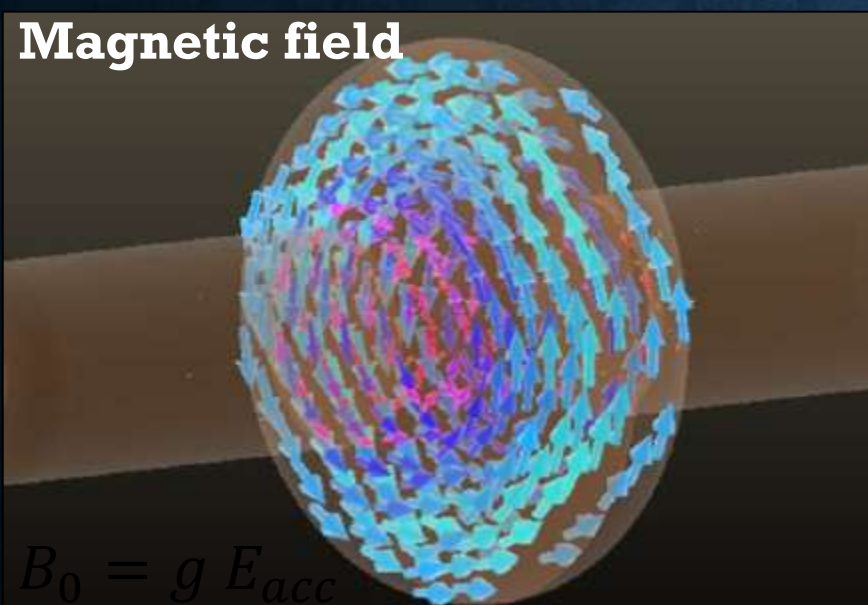
Magnetic field



Electric field



Magnetic field



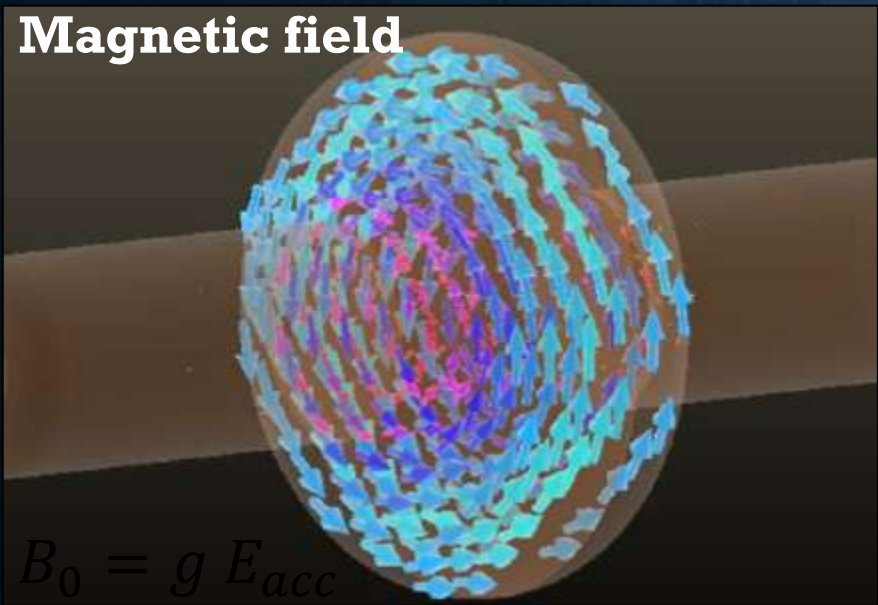
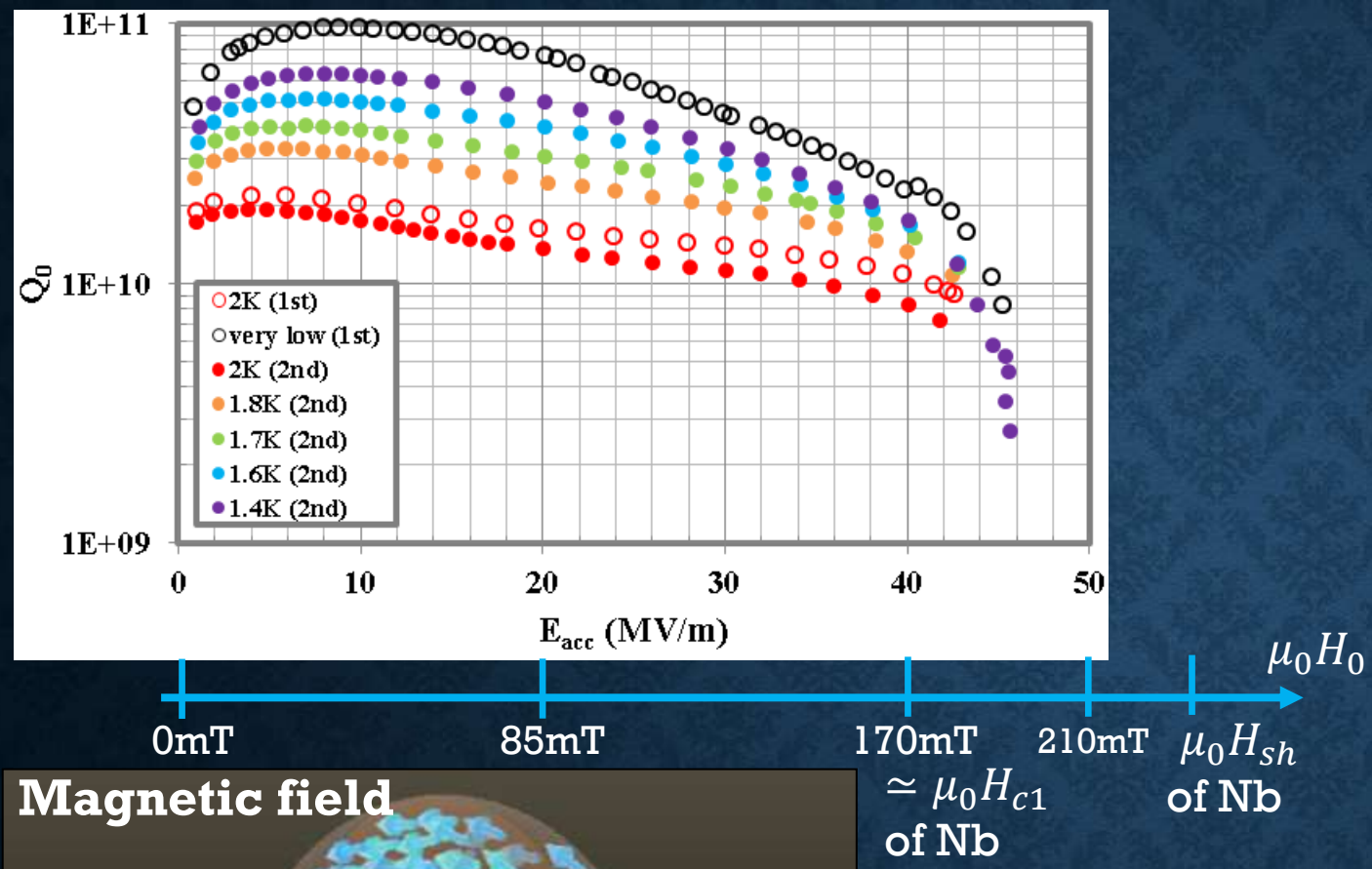
$$B_0 = g E_{acc}$$

Relation between the gradient (E_{acc}) and the surface RF magnetic field (B_0)

The accelerating field E_{acc} is proportional to the amplitude B_0 of the microwave magnetic field on the inner surface (bottom figure), that is,

$$B_0 = g E_{acc}$$

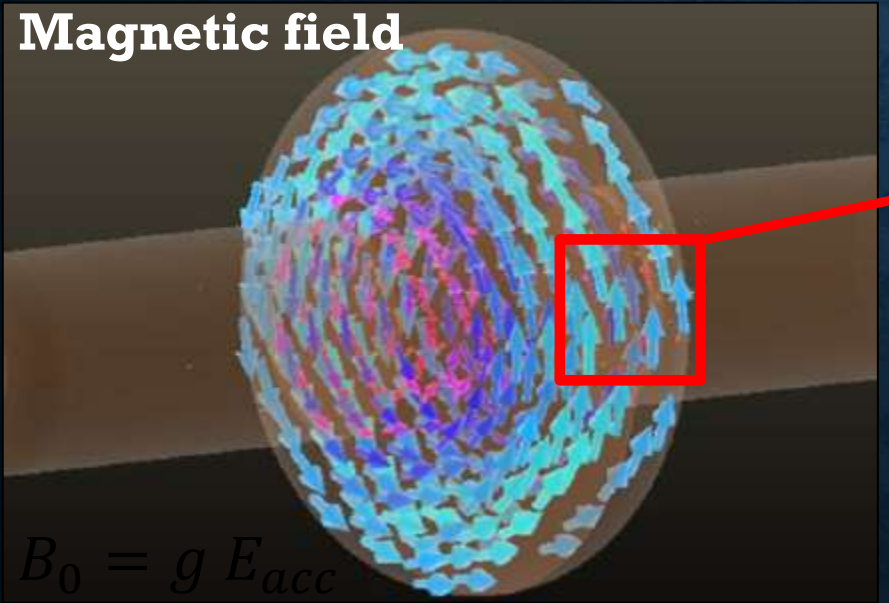
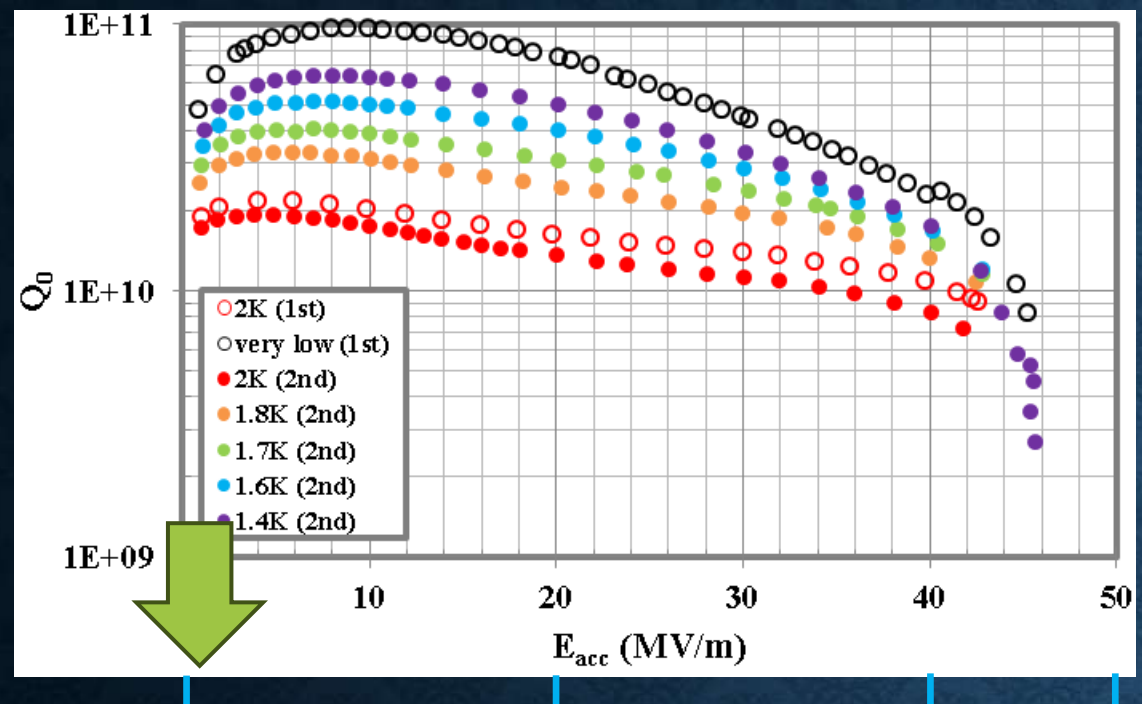
Here, g is a geometry-dependent constant determined by the cavity design [e.g., $g = 4.26 \text{ mT/(MV/m)}$ for the TESLA shape].



$\mu_0 H_0$

0mT 85mT 170mT 210mT $\mu_0 H_{sh}$
 $\simeq \mu_0 H_{c1}$
of Nb

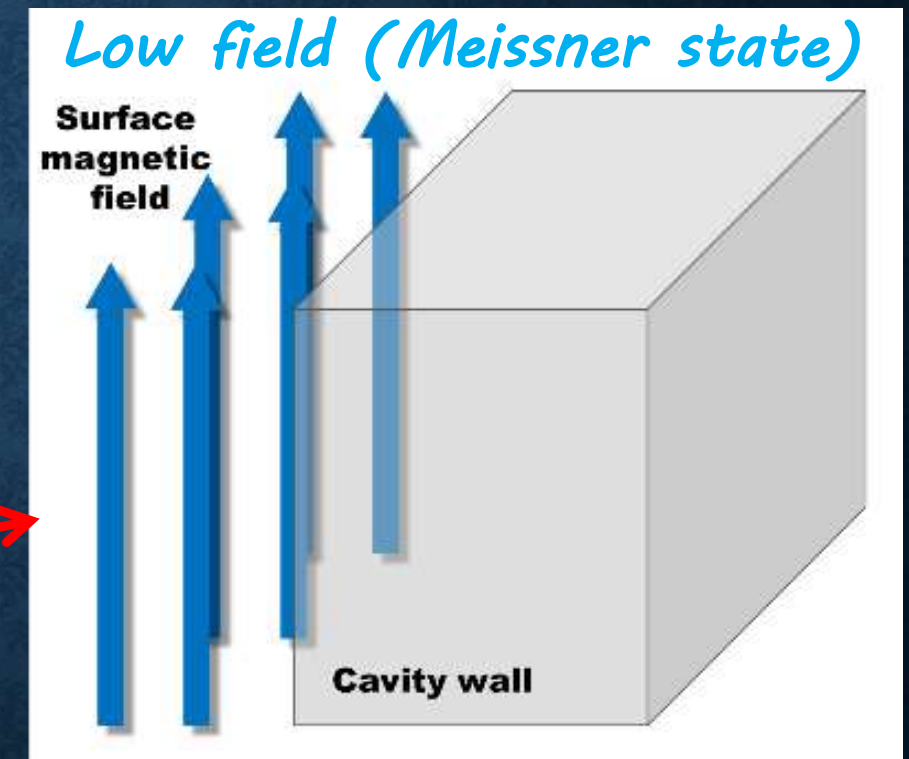
$$B_0 = g E_{acc}$$

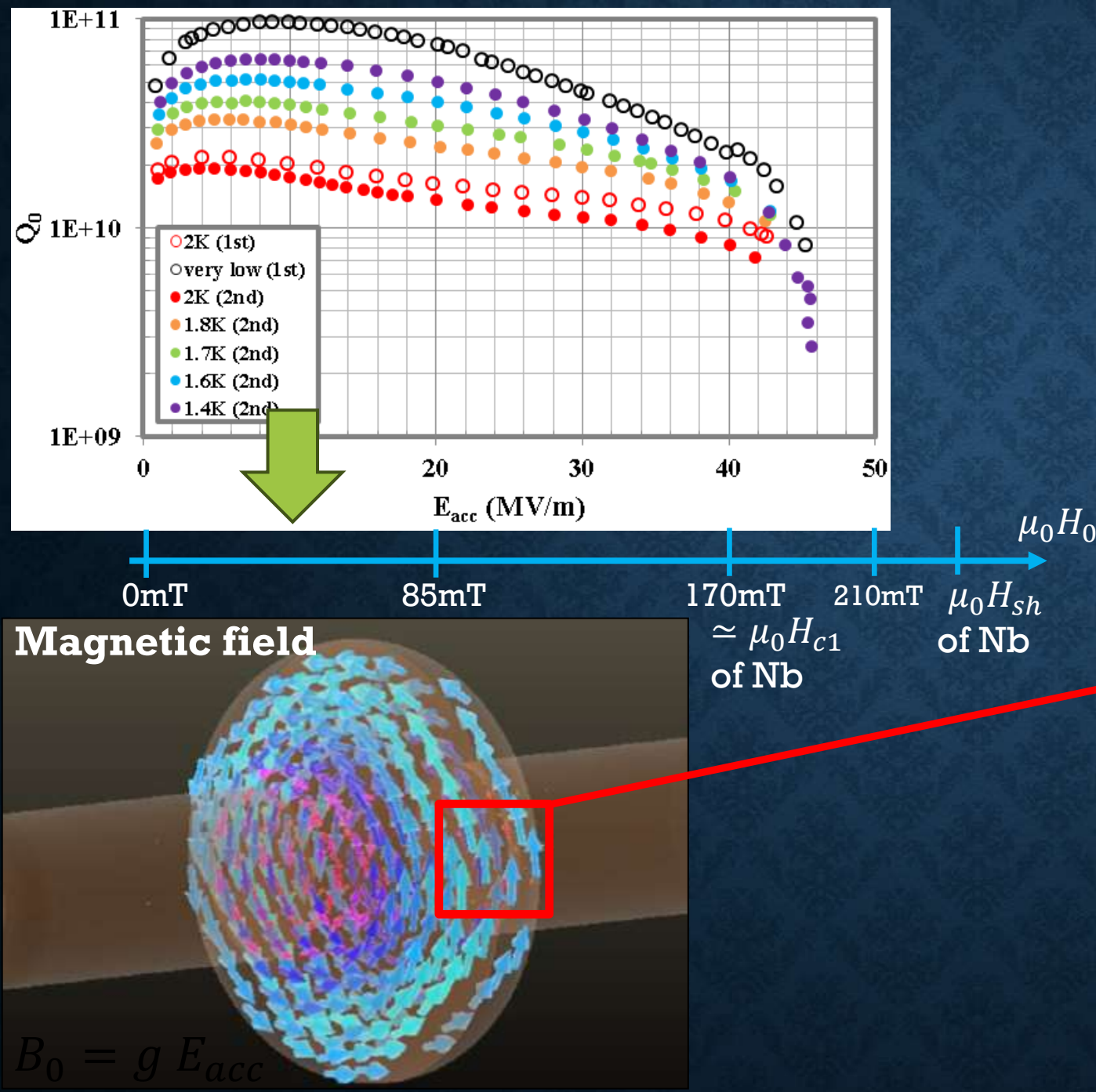


$$B_0 = g E_{acc}$$

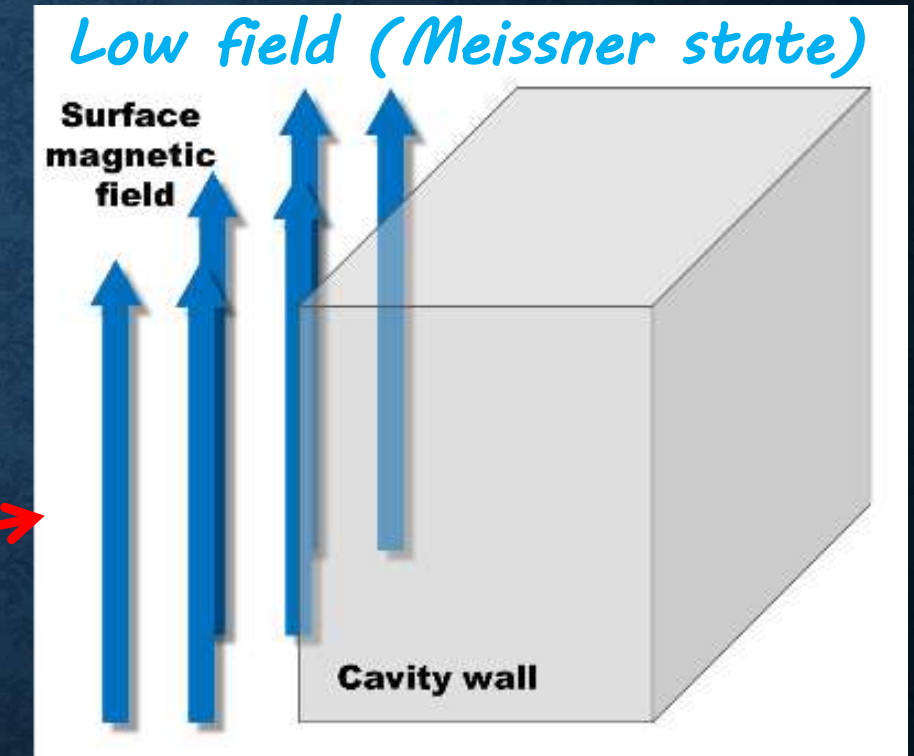
0mT 85mT 170mT 210mT $\mu_0 H_0$
 $\simeq \mu_0 H_{c1}$ of Nb

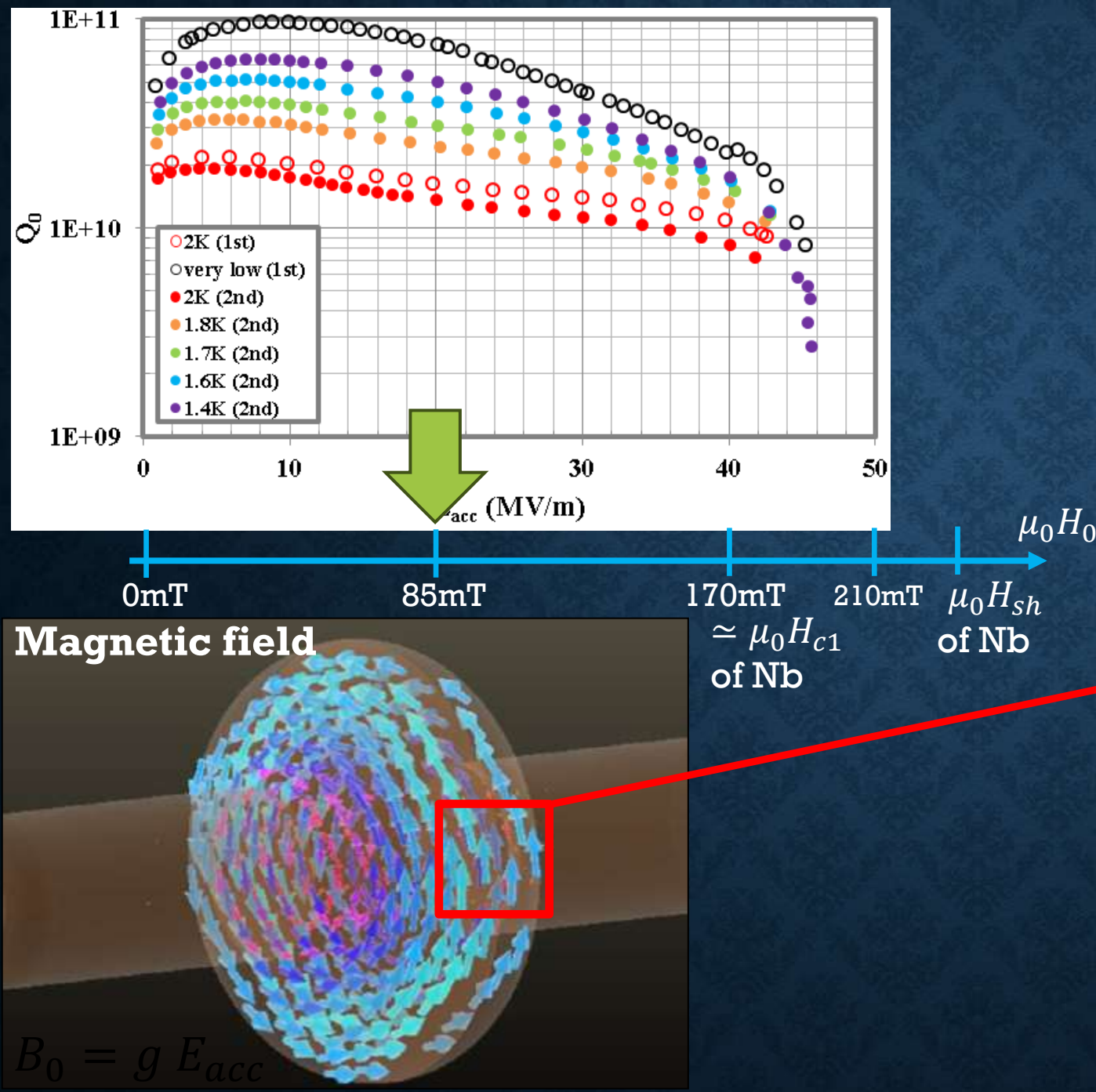
(□_□_□) good



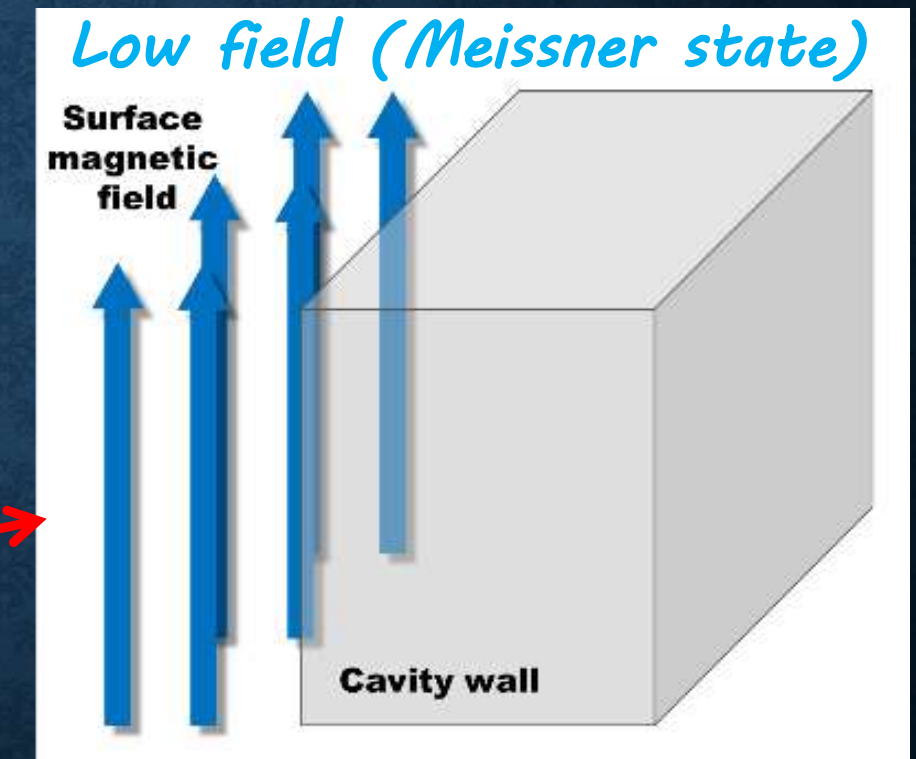


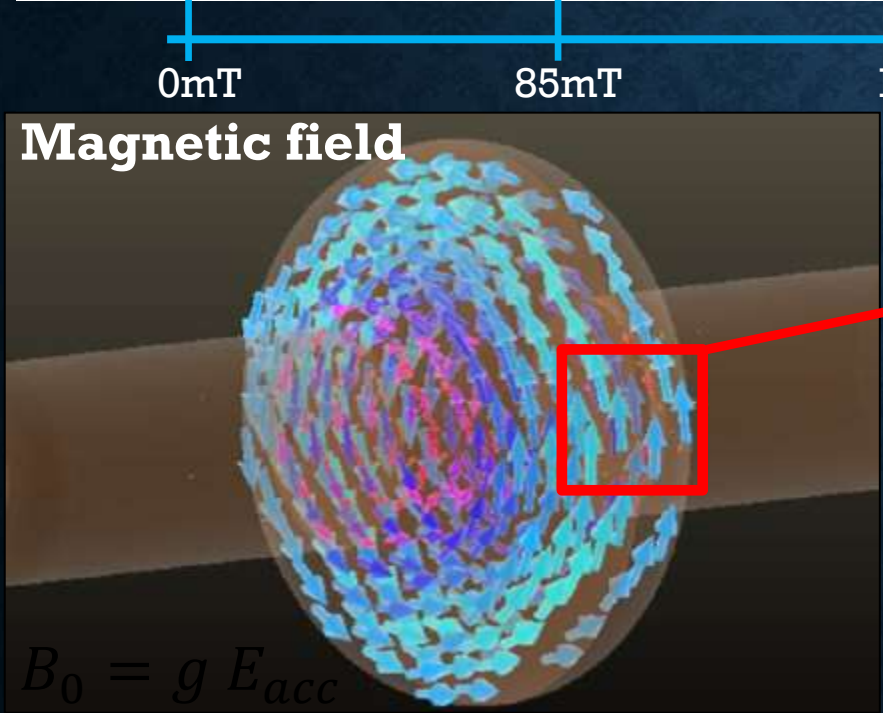
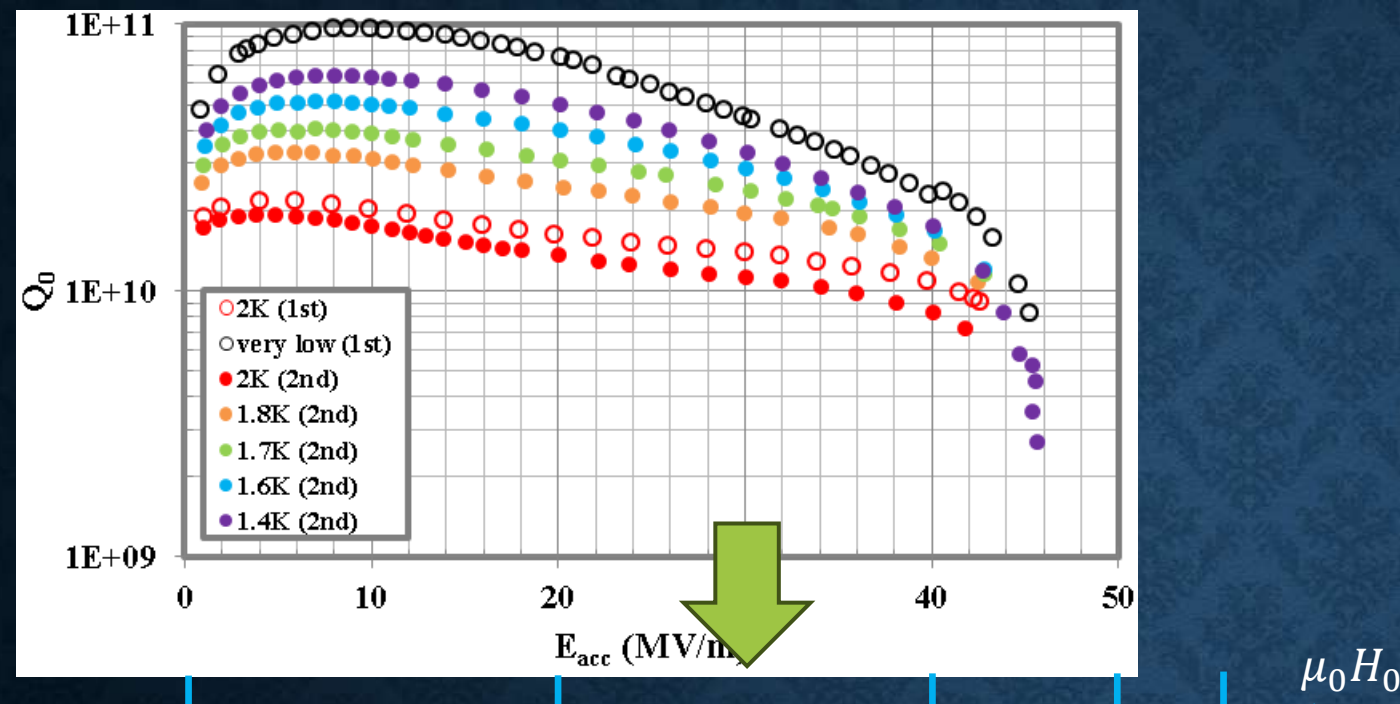
($\square - \square$) good





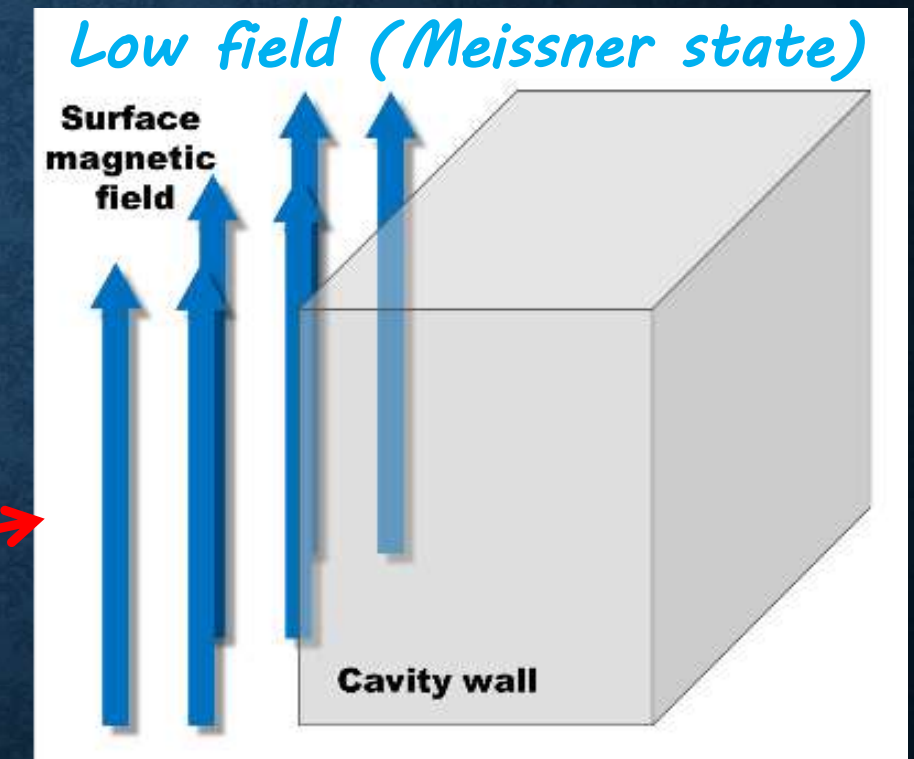
(□_□_□) good

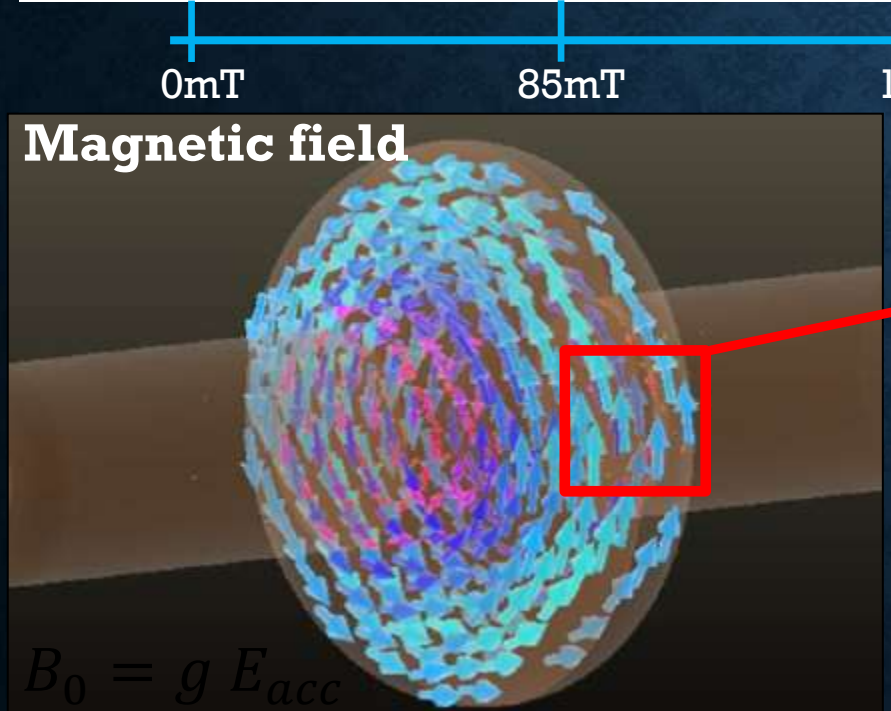
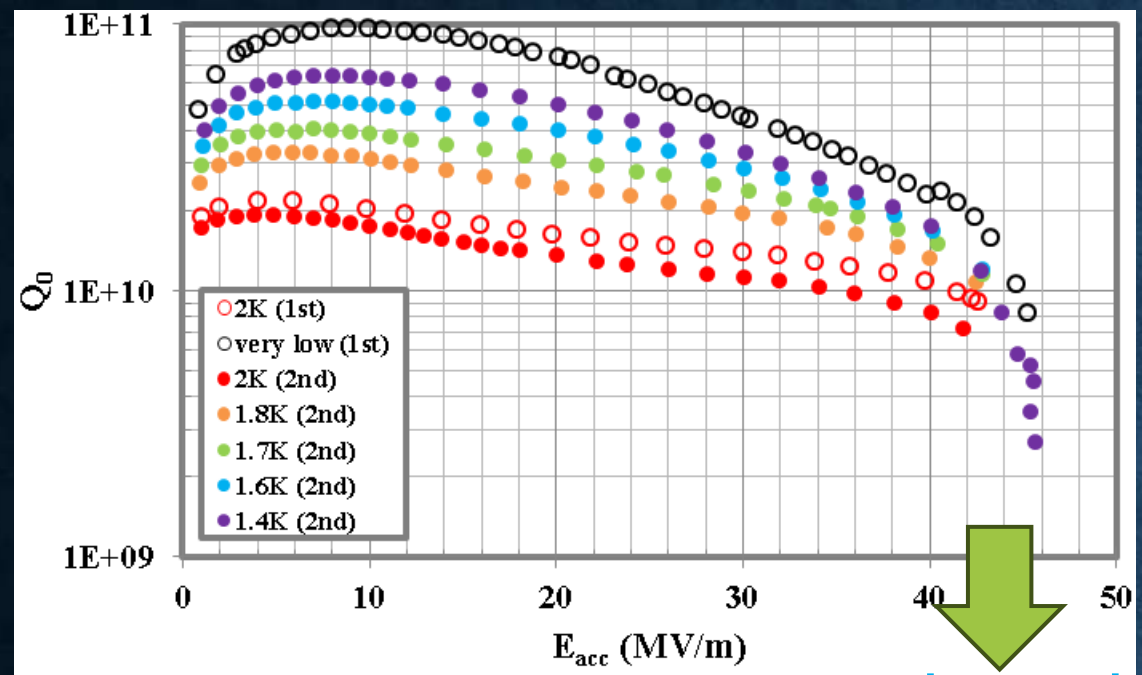




0mT 85mT $170mT \simeq \mu_0 H_{c1}$ of Nb $210mT \mu_0 H_{sh}$ of Nb

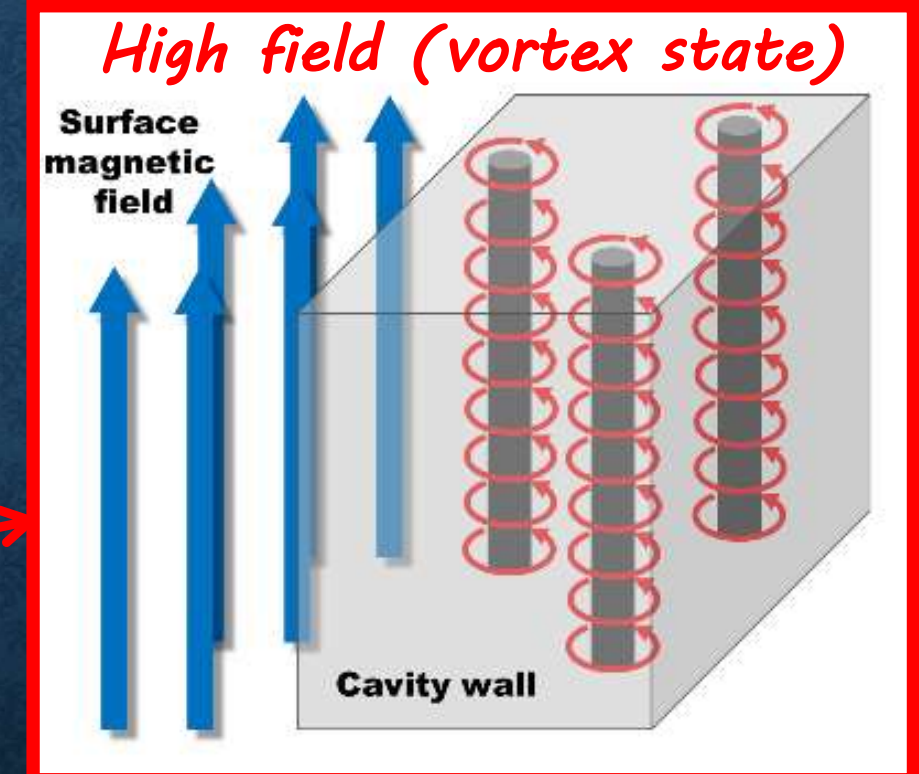
($\square - \square$) good

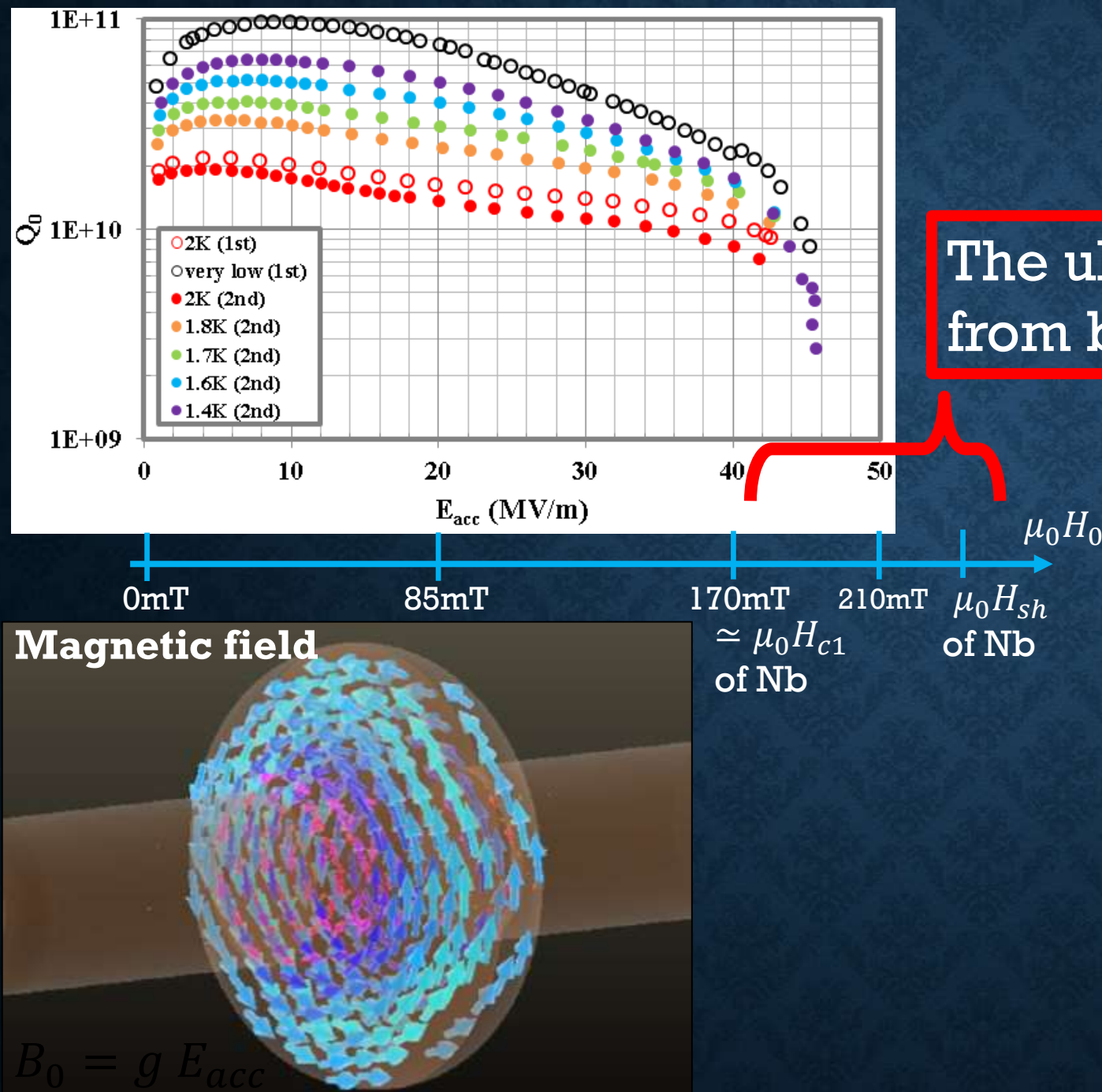




0mT 85mT $170\text{mT} \simeq \mu_0 H_{c1}$ of Nb $210\text{mT} \mu_0 H_{sh}$ of Nb

＼(^o^)／ オワタ



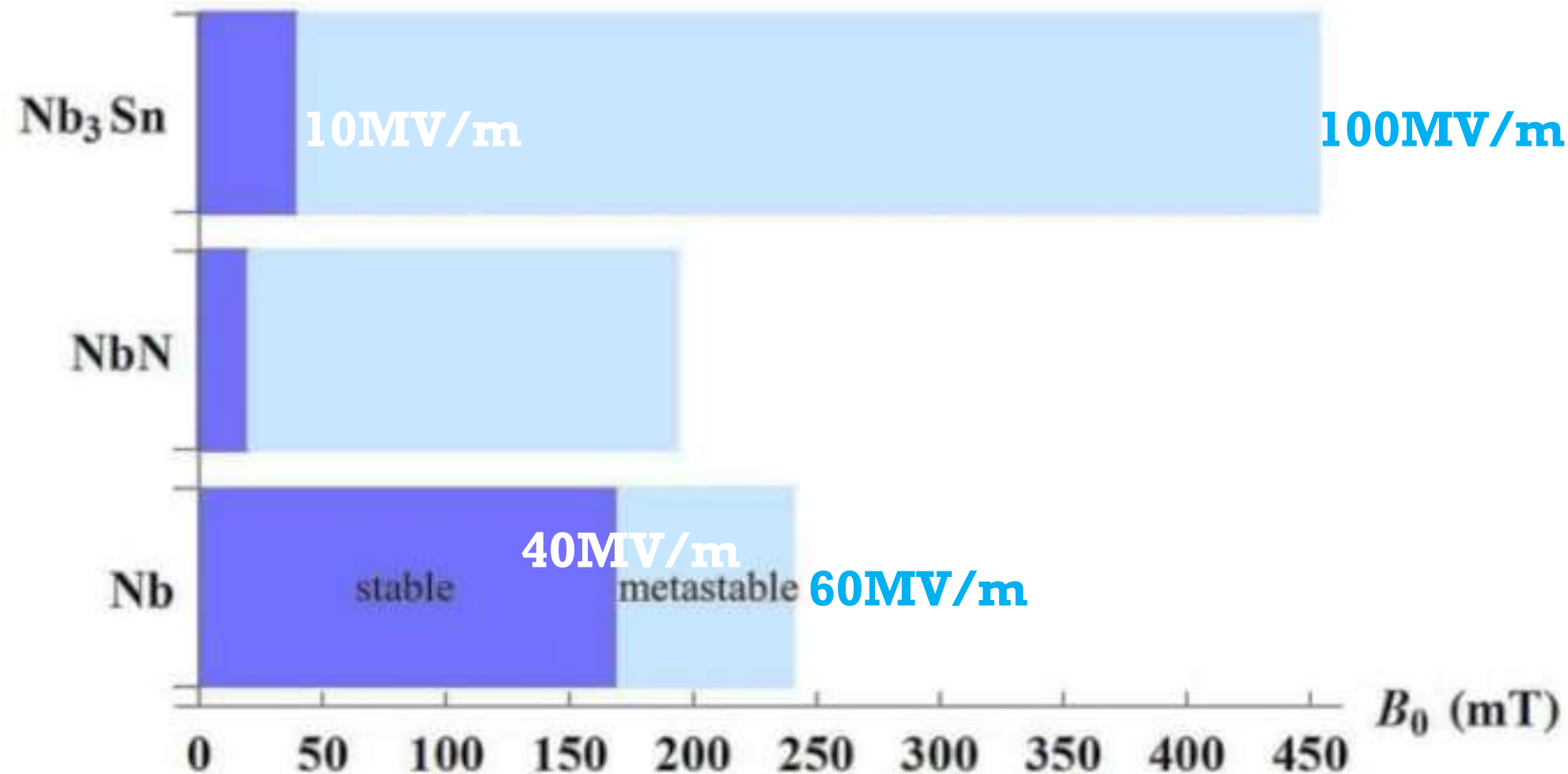


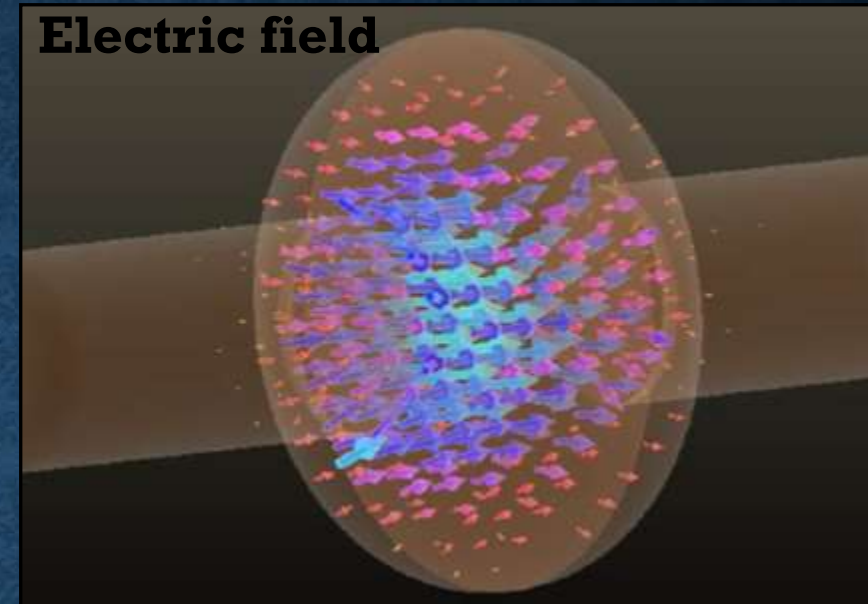
The ultimate limit of cavities made from bulk material is considered as

$$B_{c1} \leq B_0^{max} < B_{sh}$$

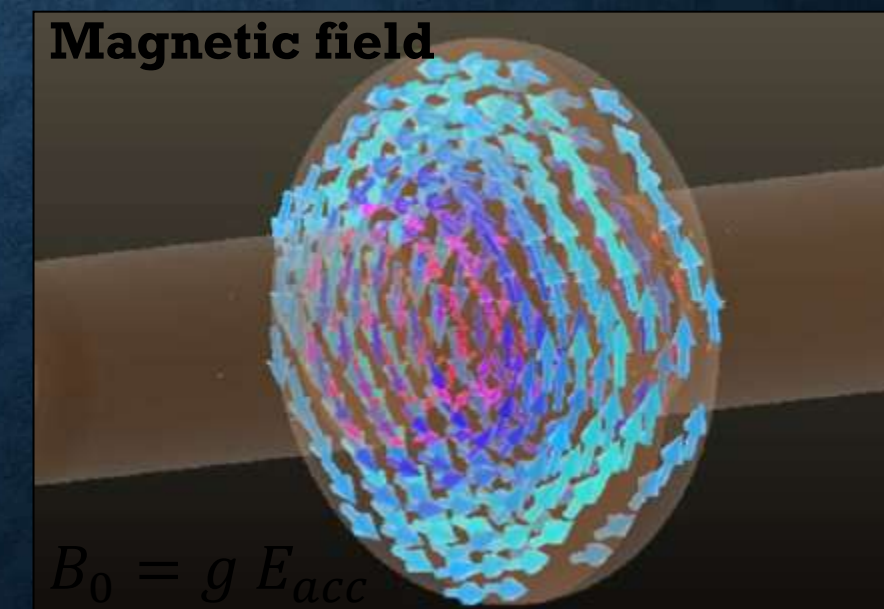
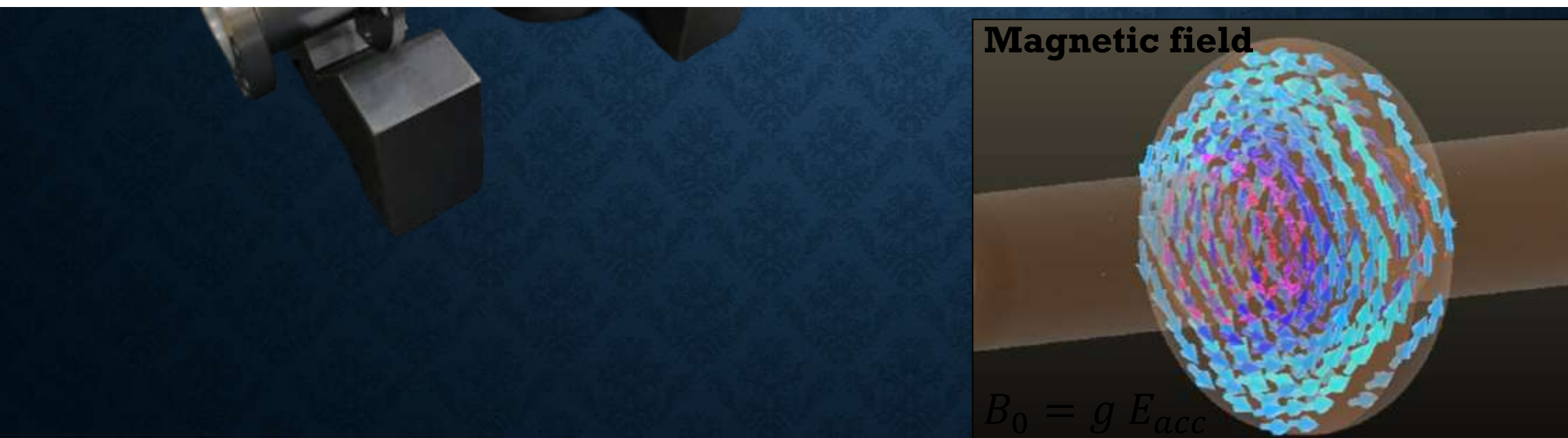
B_{c1} : the lower critical field, above which the Meissner state becomes energetically unfavorable.

B_{sh} : the superheating field, which represents the stability limit of the Meissner state.



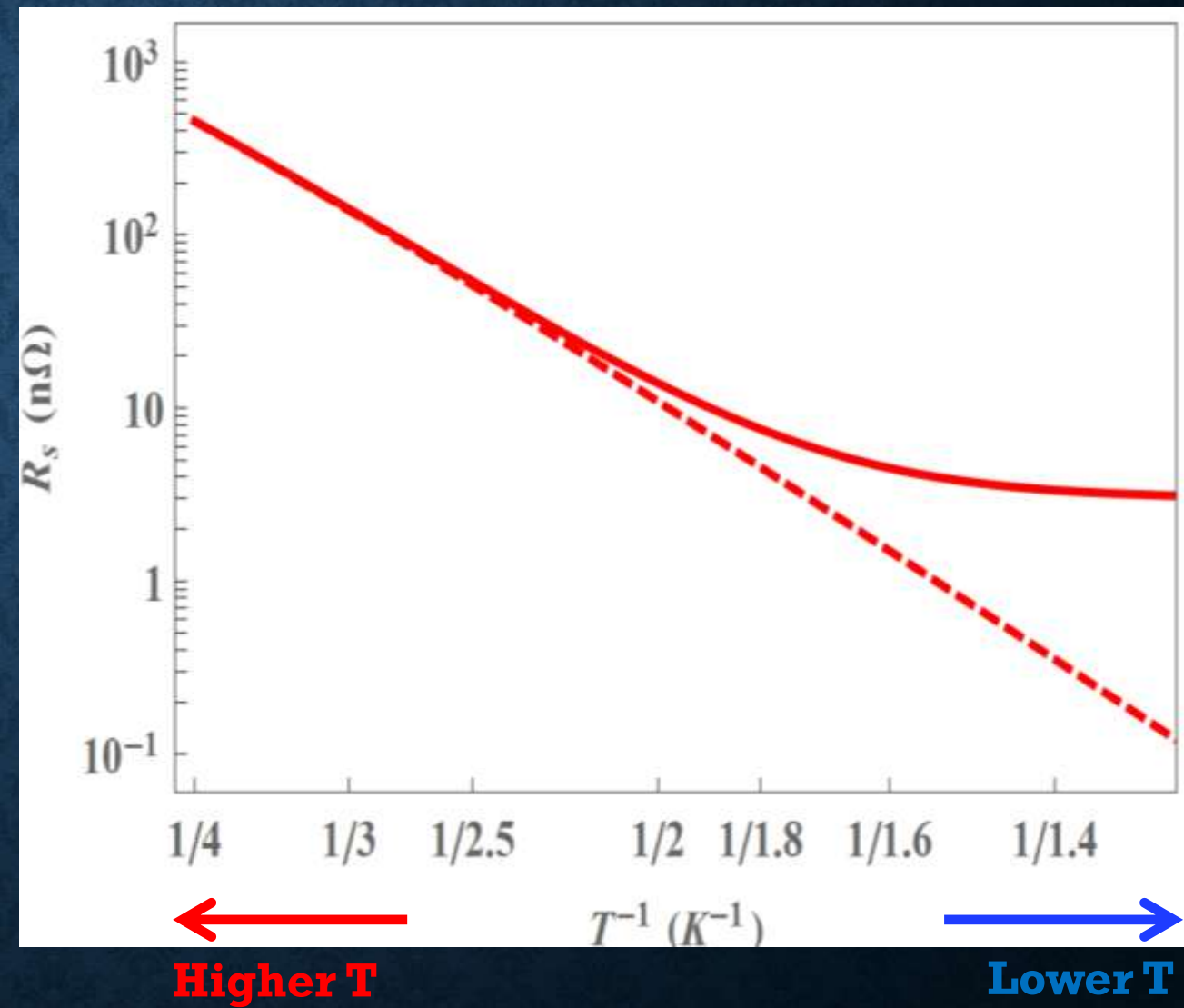
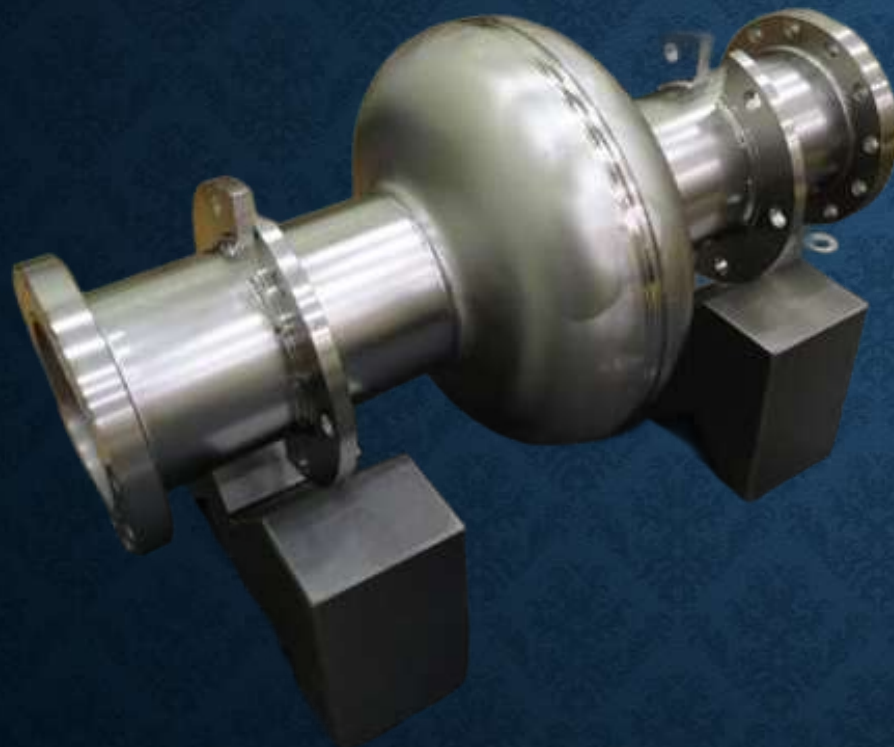


What Limits the Quality Factor?

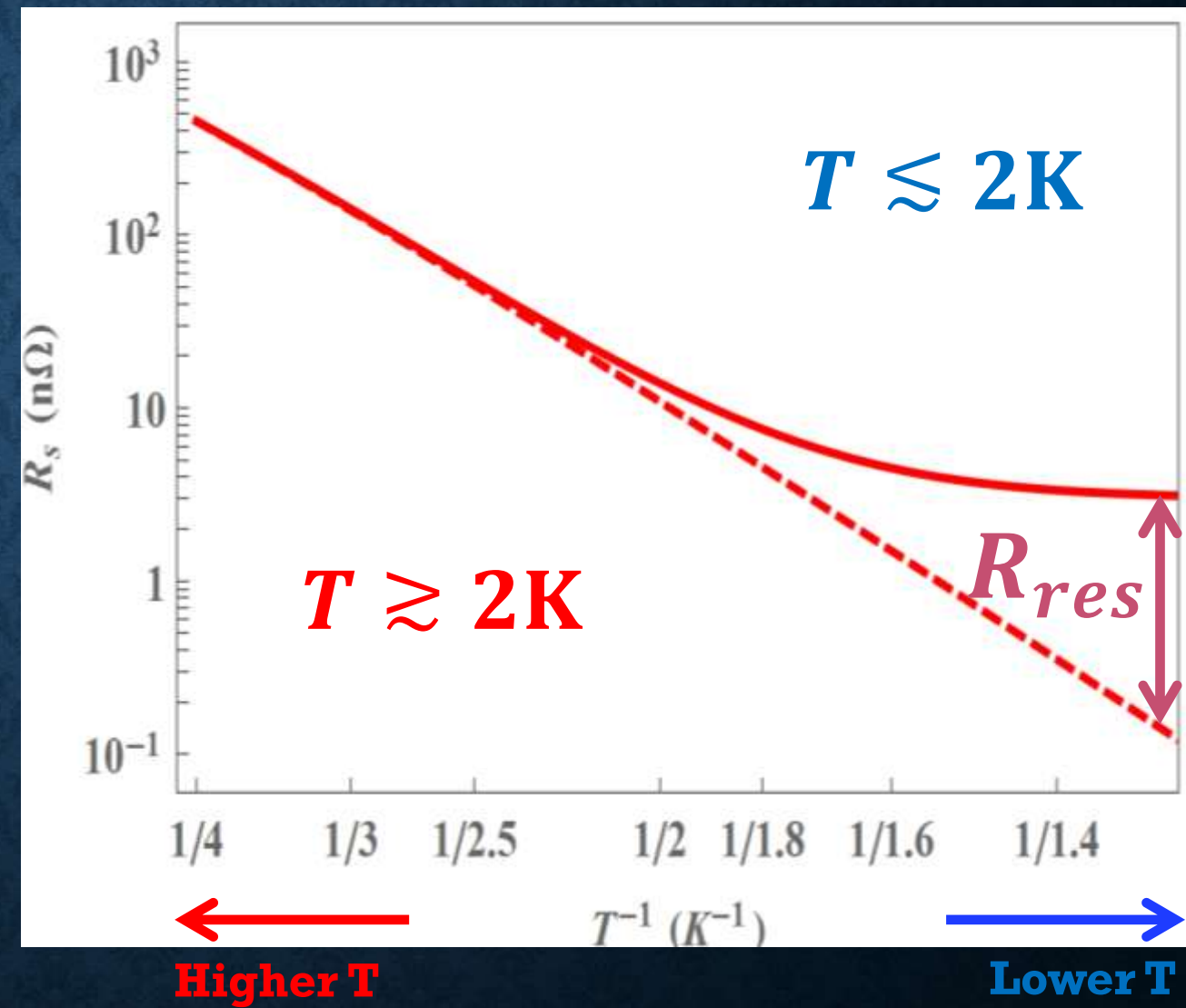
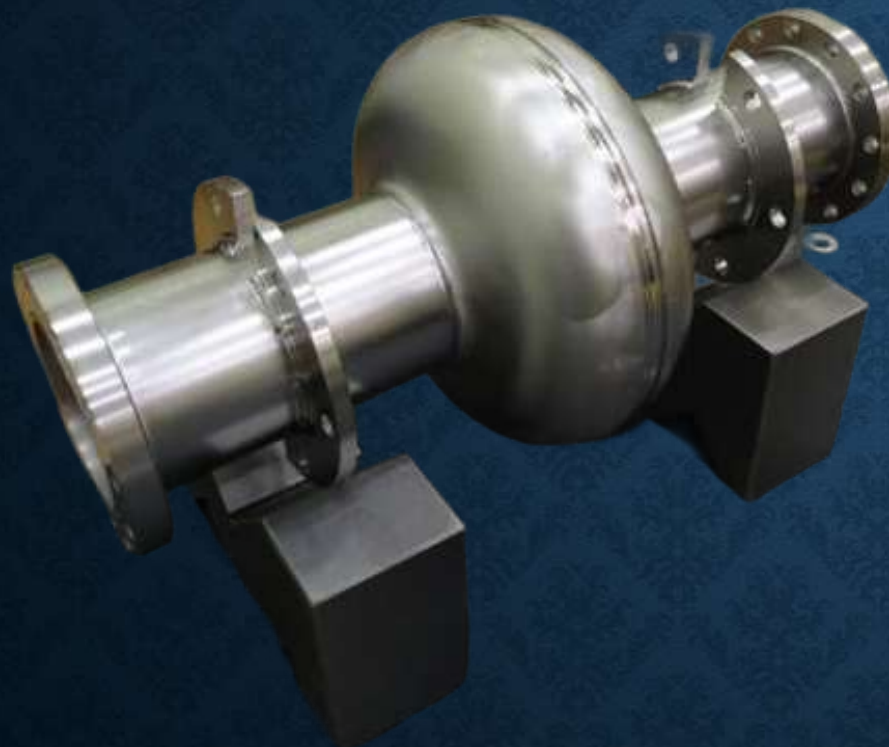


$$B_0 = g E_{acc}$$

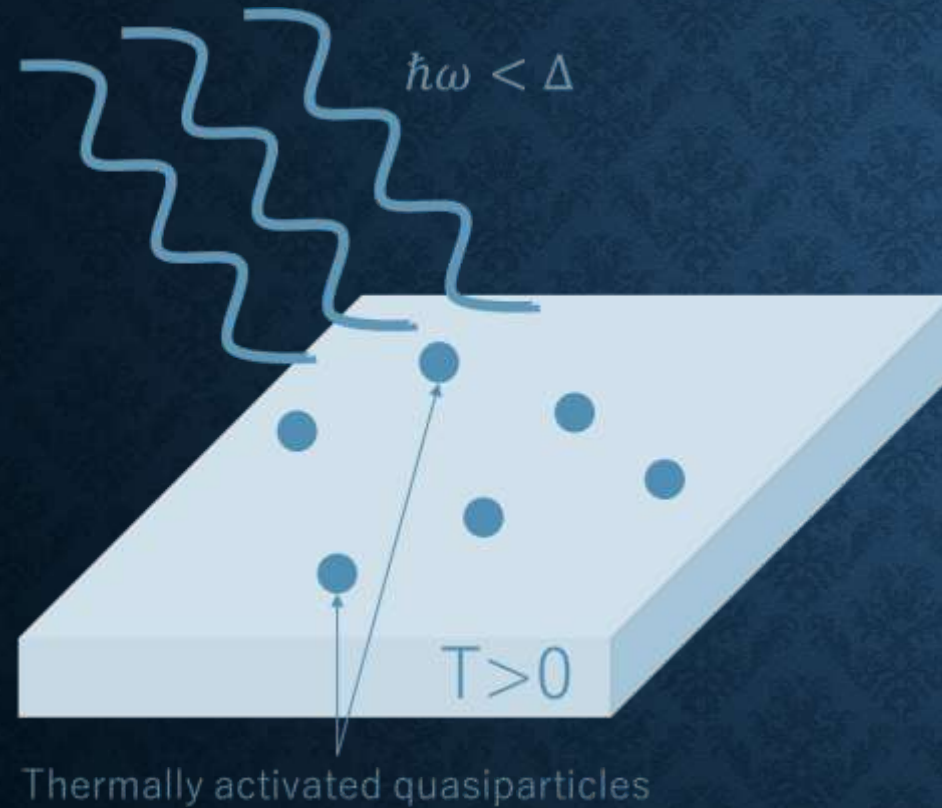
Surface resistance $\propto \frac{1}{Q_0}$



Surface resistance $\propto \frac{1}{Q_0}$

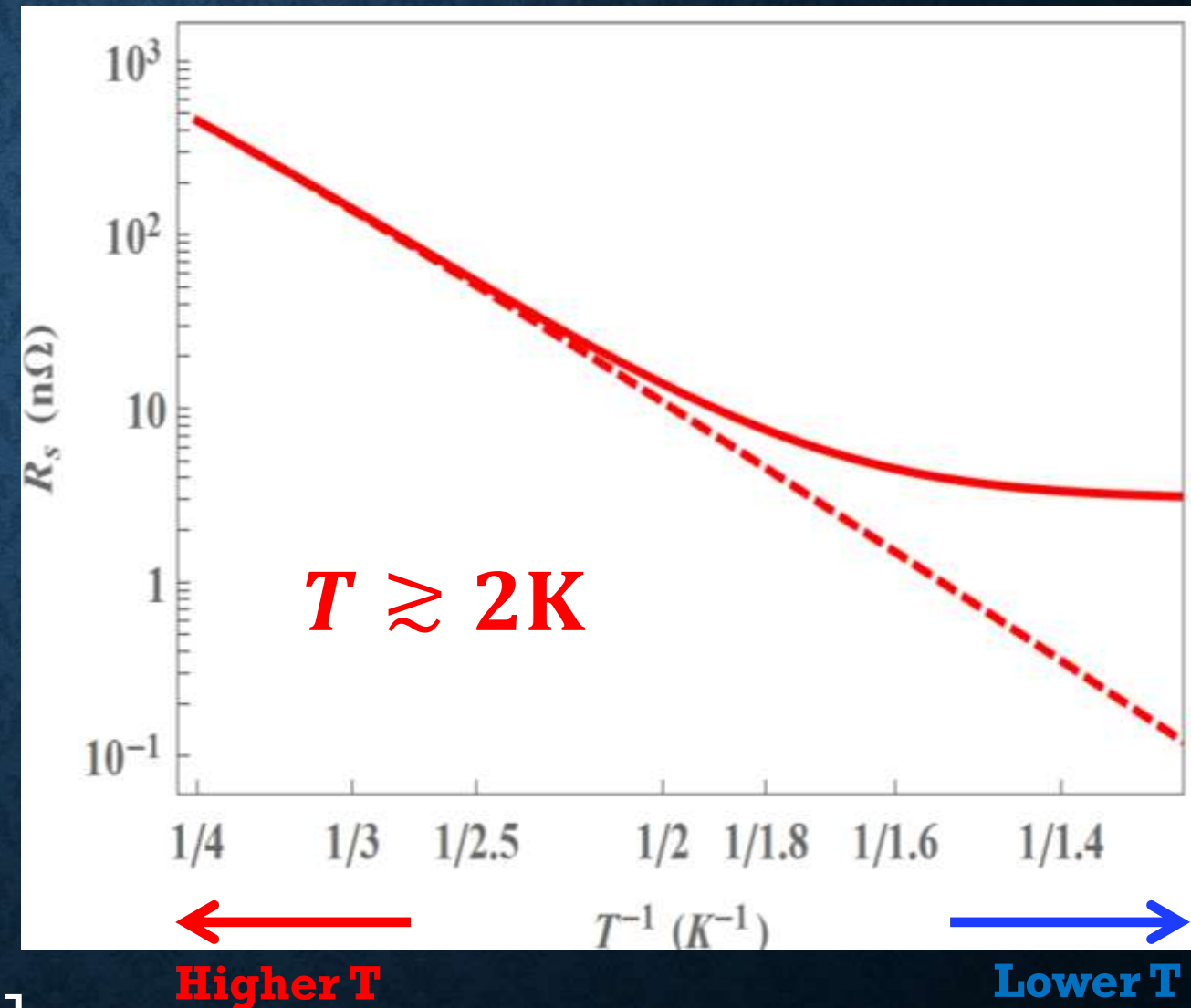


At a higher T ($\gtrsim 2\text{K}$)



The contribution from **thermally activated quasiparticles** decreases exponentially [$\propto \exp(-\Delta/kT)$].

Surface resistance $\propto \frac{1}{Q_0}$



More on thermal quasiparticle contributions

$$Q_0 = \frac{G}{R_s}$$

$G(\sim 100\Omega)$
Is determined by
cavity design
($G = 270\Omega$ for Tesla shape)

$$R_s = \frac{1}{2} \mu_0^2 \omega^2 \lambda^3 \sigma_1$$

More on thermal quasiparticle contributions

$$Q_0 = \frac{G}{R_s}$$

$G(\sim 100\Omega)$
Is determined by
cavity design
($G = 270\Omega$ for Tesla shape)

$$R_s = \frac{1}{2} \mu_0^2 \omega^2 \lambda^3 \sigma_1$$

$$\sigma_1 \sim \sigma_n \int_{\Delta}^{\infty} N(\epsilon)N(\epsilon + \hbar\omega)e^{-\frac{\Delta}{kT}} d\epsilon$$

DOS

More on thermal quasiparticle contributions

$$Q_0 = \frac{G}{R_S}$$

$G(\sim 100\Omega)$
Is determined by
cavity design
($G = 270\Omega$ for Tesla shape)

$$R_S = \frac{1}{2} \mu_0^2 \omega^2 \lambda^3 \sigma_1$$

$$\sigma_1 \sim \sigma_n \int_{\Delta}^{\infty} N(\epsilon) N(\epsilon + \hbar\omega) e^{-\frac{\Delta}{kT}} d\epsilon$$

DOS

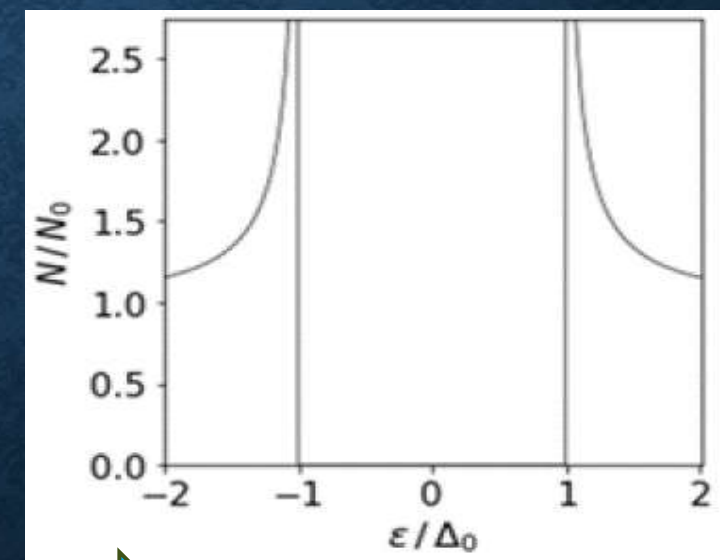
Ideal case



$\hbar\omega$
($\ll \Delta$)



**Ideal BCS
superconductor**



**Ideal
Quasiparticle
DOS**

$$\frac{N(\epsilon)}{N_0} = Re \frac{\epsilon}{\sqrt{\epsilon^2 - \Delta^2}}$$

**Mattis-Bardeen
formula**

$$\sigma_1 = \sigma_n \frac{2\Delta}{kT} \ln \frac{CkT}{\hbar\omega} e^{-\frac{\Delta}{kT}}$$

More on thermal quasiparticle contributions (2)

$$Q_0 = \frac{G}{R_S}$$

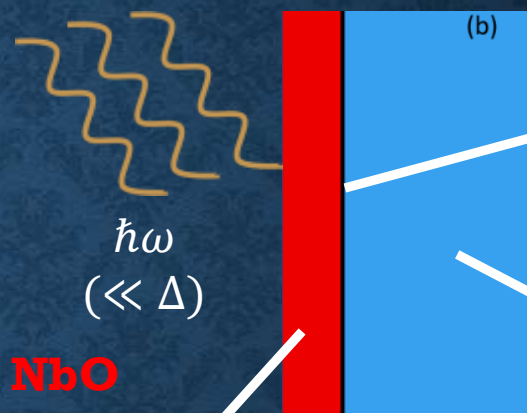
$G(\sim 100\Omega)$
Is determined by
cavity design
($G = 270\Omega$ for Tesla shape)

$$R_S = \frac{1}{2} \mu_0^2 \omega^2 \lambda^3 \sigma_1$$

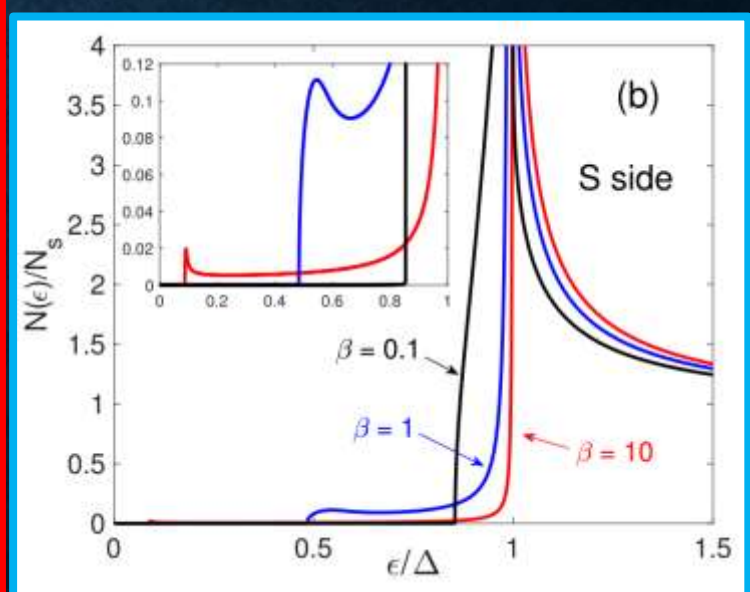
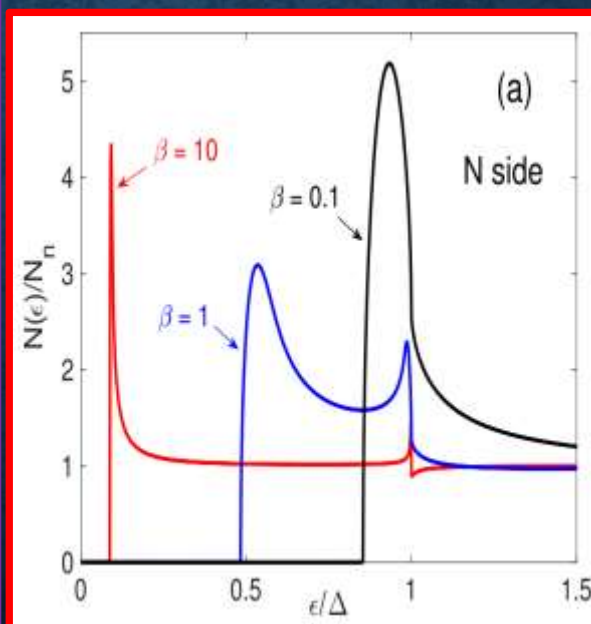
$$\sigma_1 \sim \sigma_n \int_{\Delta}^{\infty} N(\epsilon) N(\epsilon + \hbar\omega) e^{-\frac{\Delta}{kT}} d\epsilon$$

DOS

More realistic case

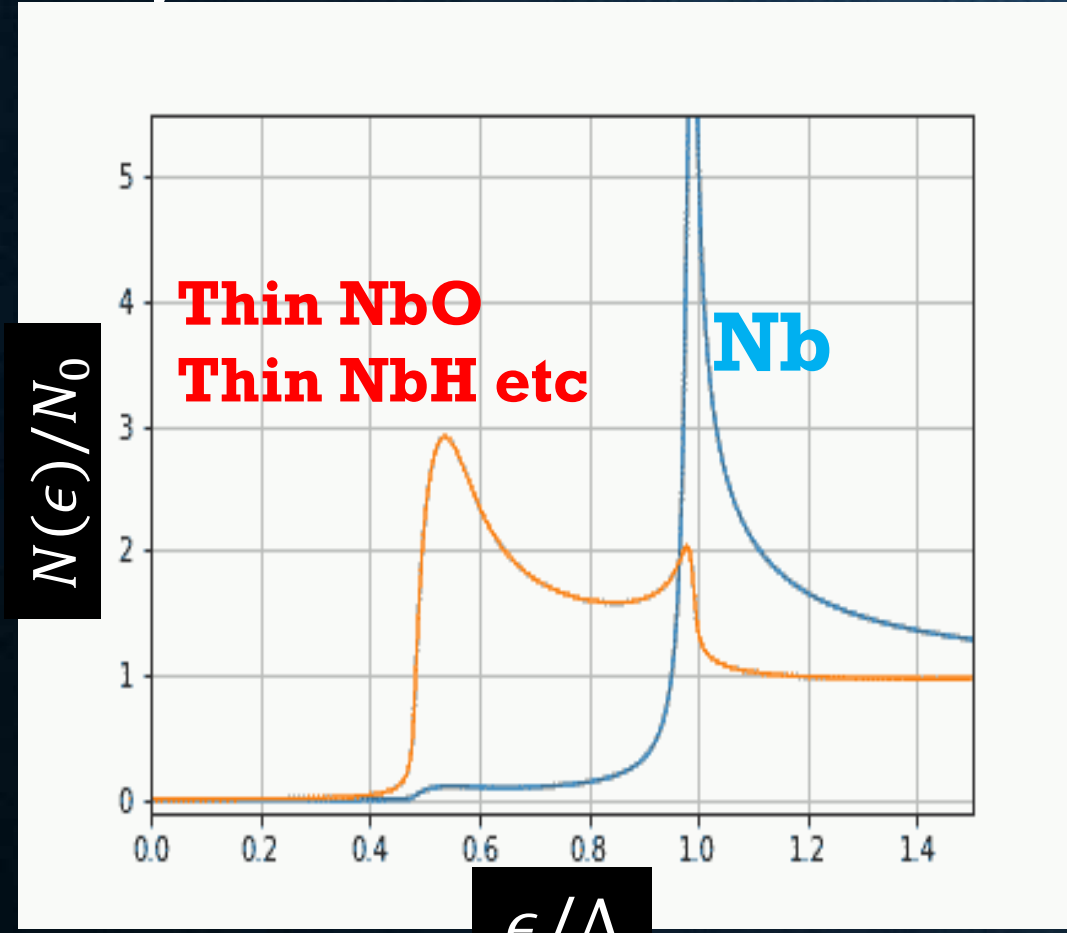


Proximity effect
at the interface



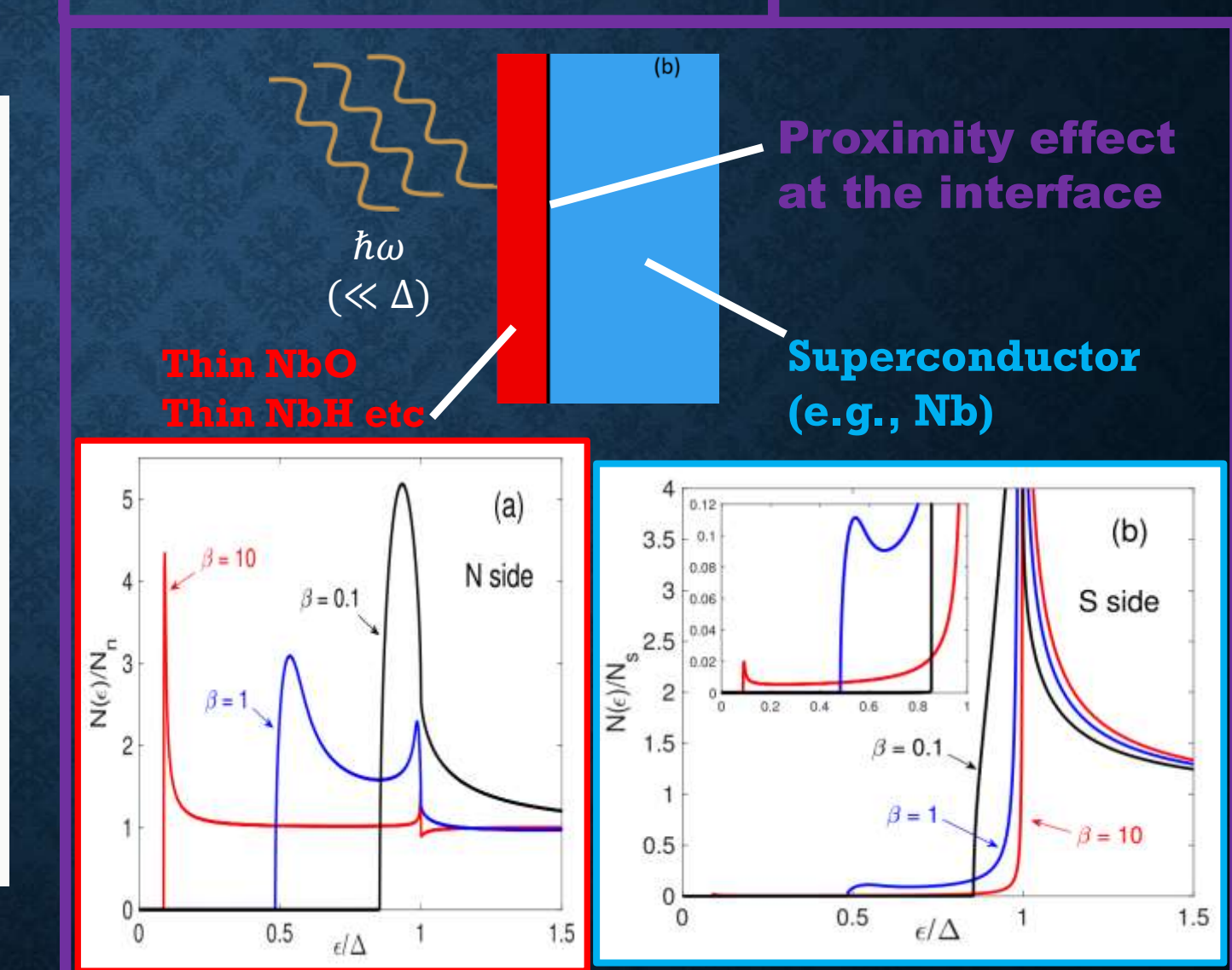
More on thermal quasiparticle contributions (3)

Moreover, when the microwave amplitude is large, DOSs oscillates in sync with the microwave field.



T Kubo and A Gurevich,
Physical Review B 100, 064522 (2019)

More realistic case

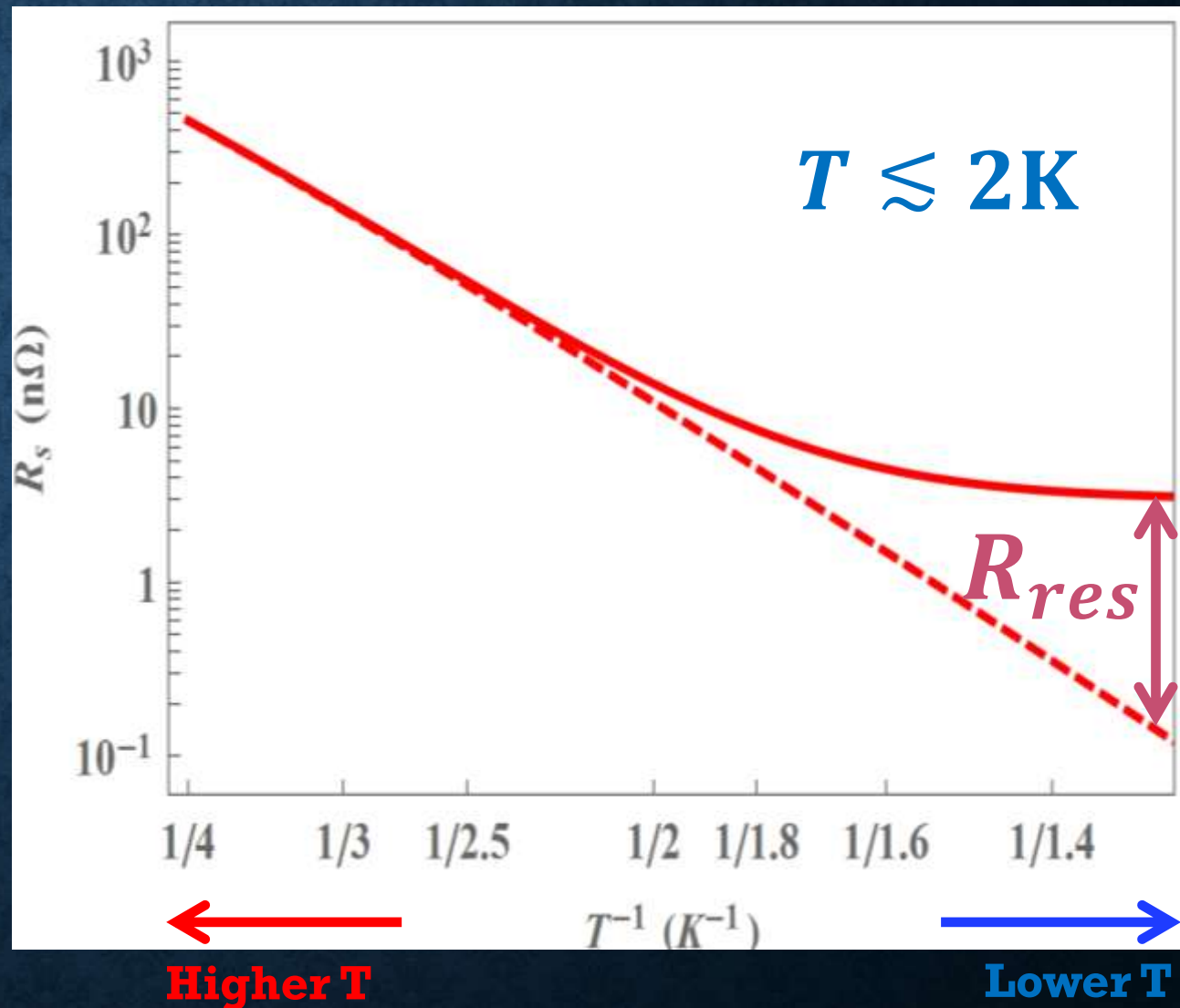


A Gurevich and T Kubo, Physical Review B 96, 184515 (2017)

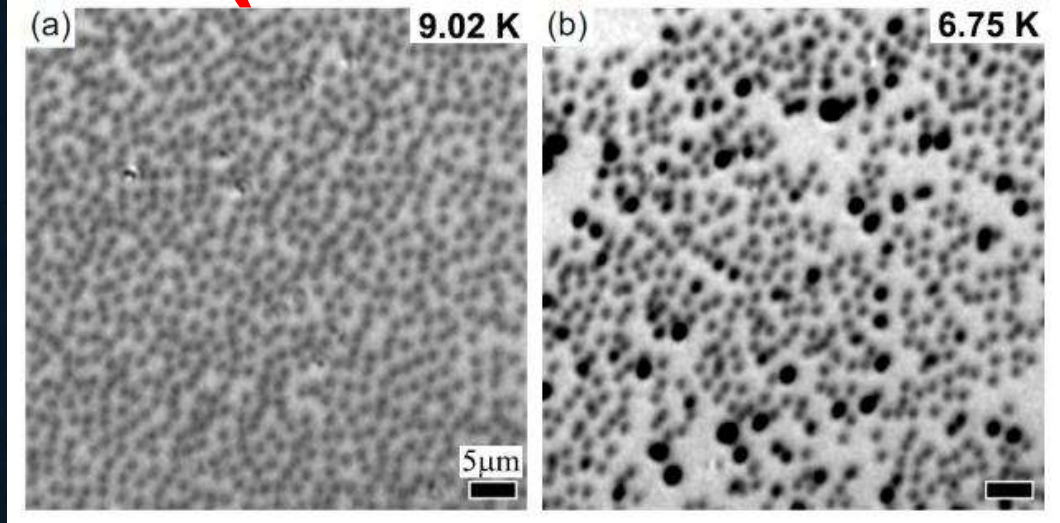
At a lower T ($\lesssim 2\text{K}$)

The quasiparticle contribution $R_s \sim e^{-\frac{\Delta}{k_B T}}$ is exponentially suppressed (dashed curve), but **other mechanisms can dominate at low temperatures.**

Surface resistance $\propto \frac{1}{Q_0}$



Vortices (dominant cause of R_{res} in accelerator cavities)



Videos of vortex dynamics in cavity-grade Nb can be found in
Ooi et al., PRB 111, 094519 (2025)

Microwave-driven vortex dynamics cause dissipation, which is only weakly dependent on temperature, leading to an elevated surface resistance: R_{res}

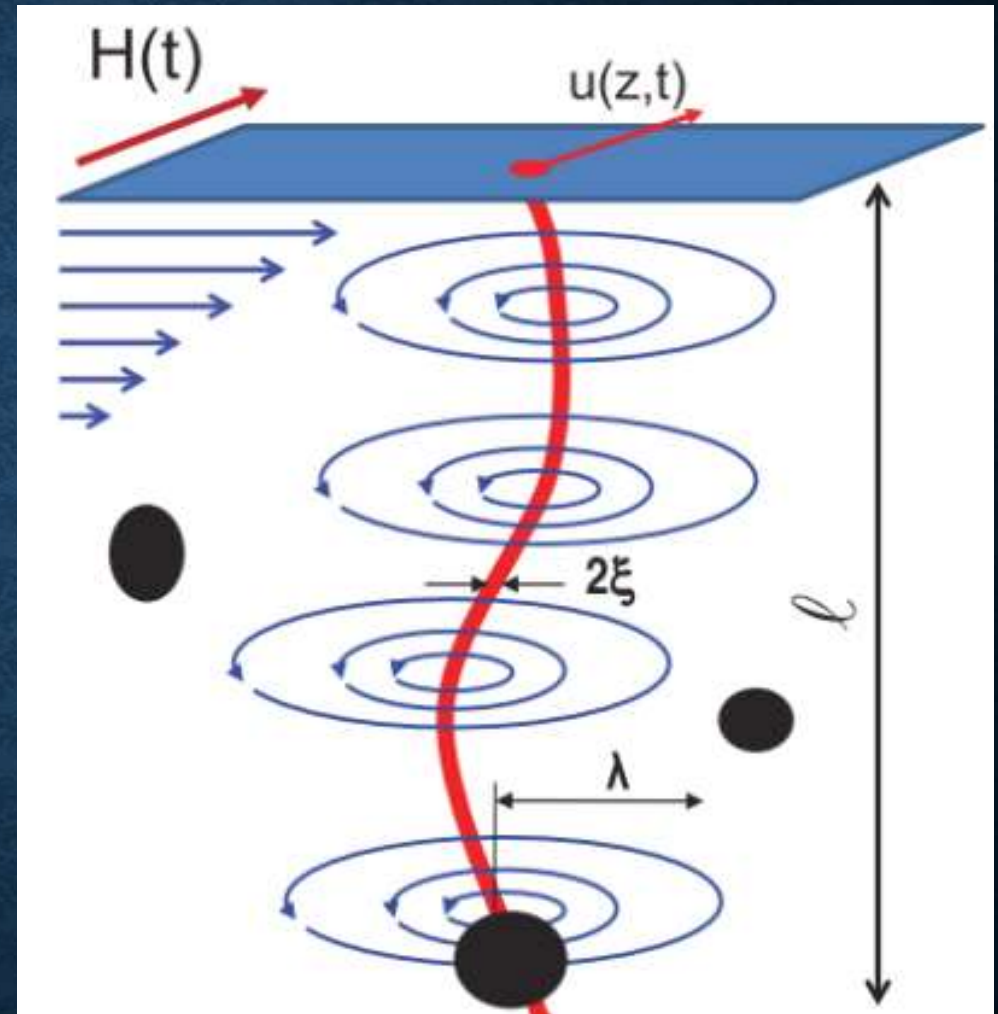
See also,

A. Romanenko et al., Appl. Phys. Lett. 105, 234103 (2014).

S. Huang et al., Phys. Rev. Accelerators and Beams 19, 082001 (2016).

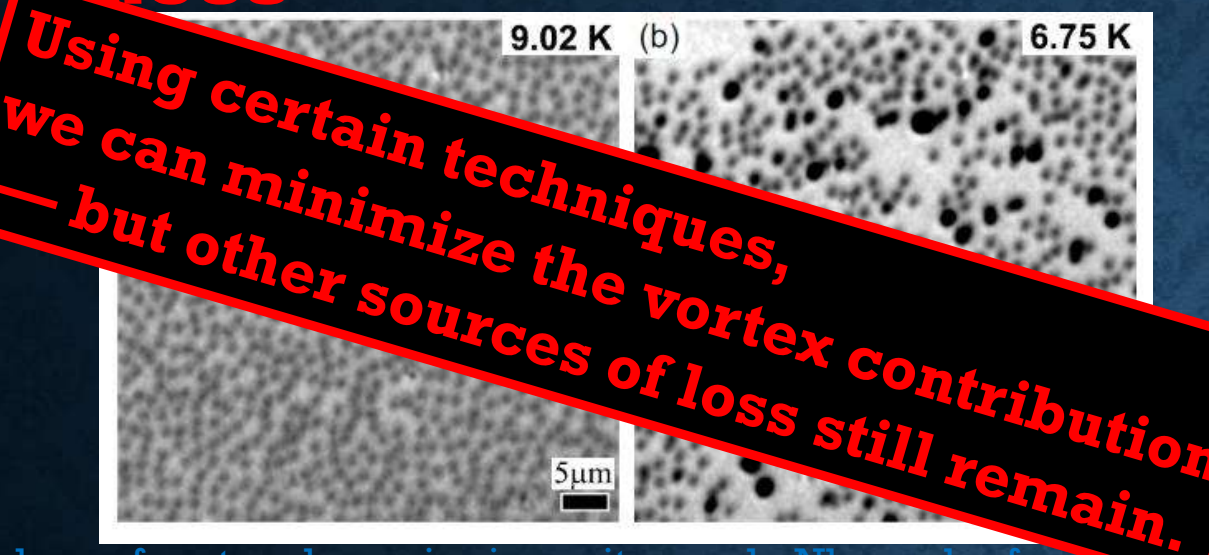
S. Posen et al., J. Appl. Phys. 119, 213903 (2016).

S. Ooi et al., Physical Review B 104, 064504 (2021)



A. Gurevich and G. Ciovati, PRB 87, 054502 (2013)

Vortices

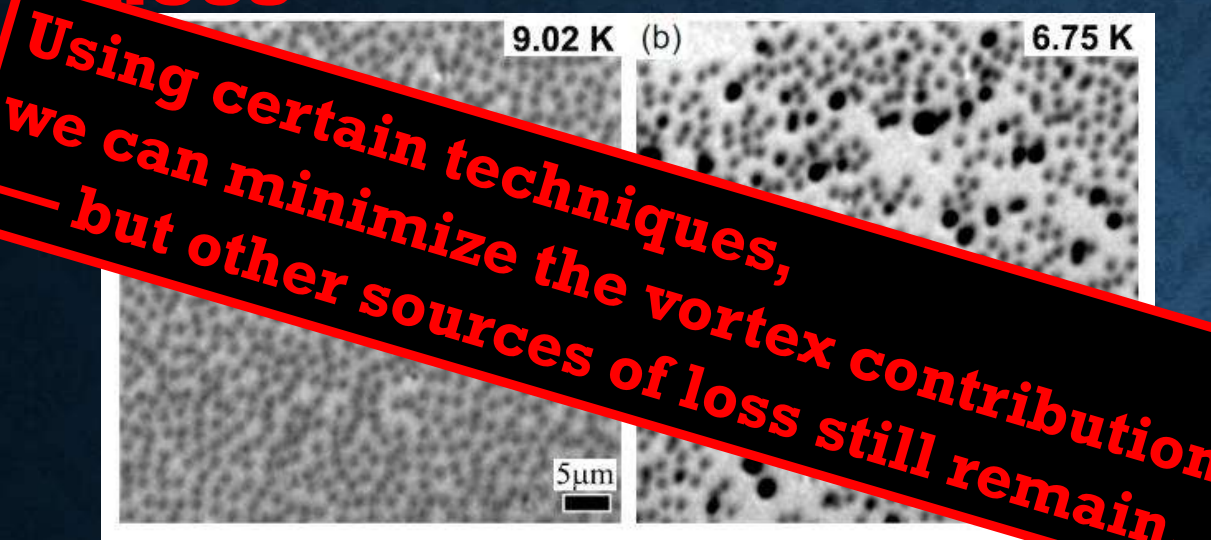


*Using certain techniques,
we can minimize the vortex contribution
— but other sources of loss still remain.*

Videos of vortex dynamics in cavity-grade Nb can be found [here](#).

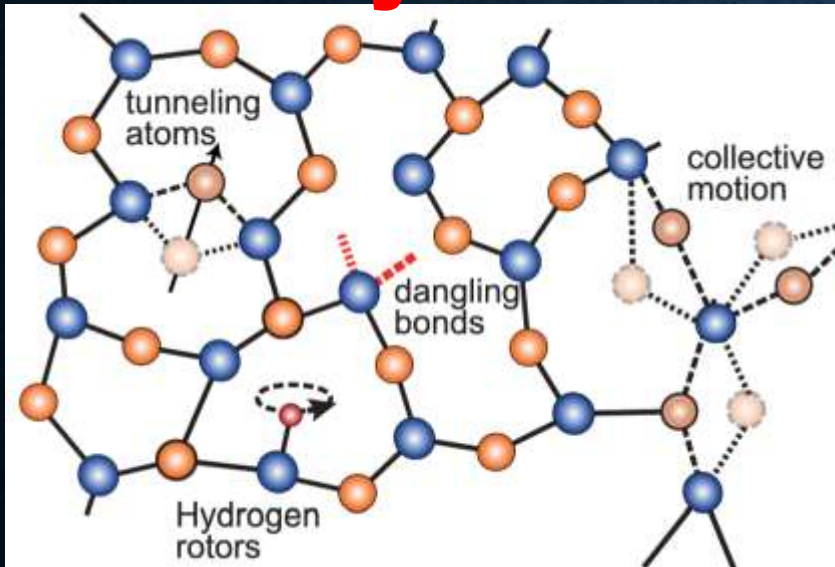
Ooi et al., PRB 111, 094519 (2025)

Vortices

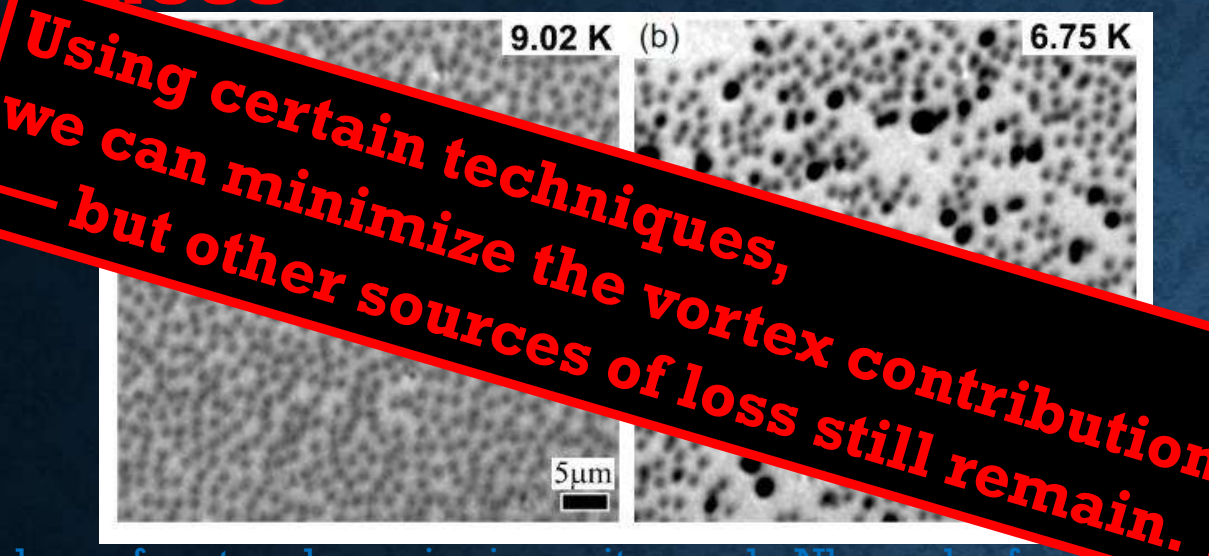


Videos of vortex dynamics in cavity-grade Nb can be found in
Ooi et al., PRB 111, 094519 (2025)

Two-level system defects

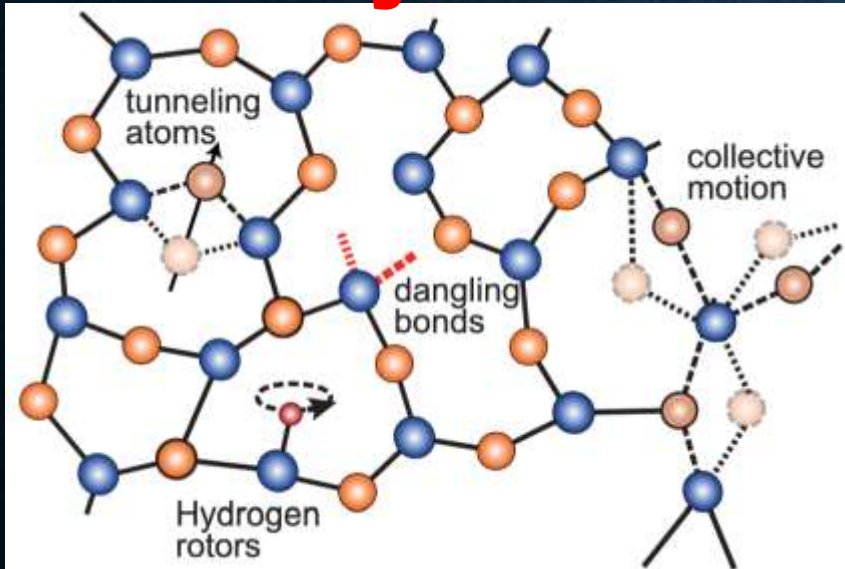


Vortices



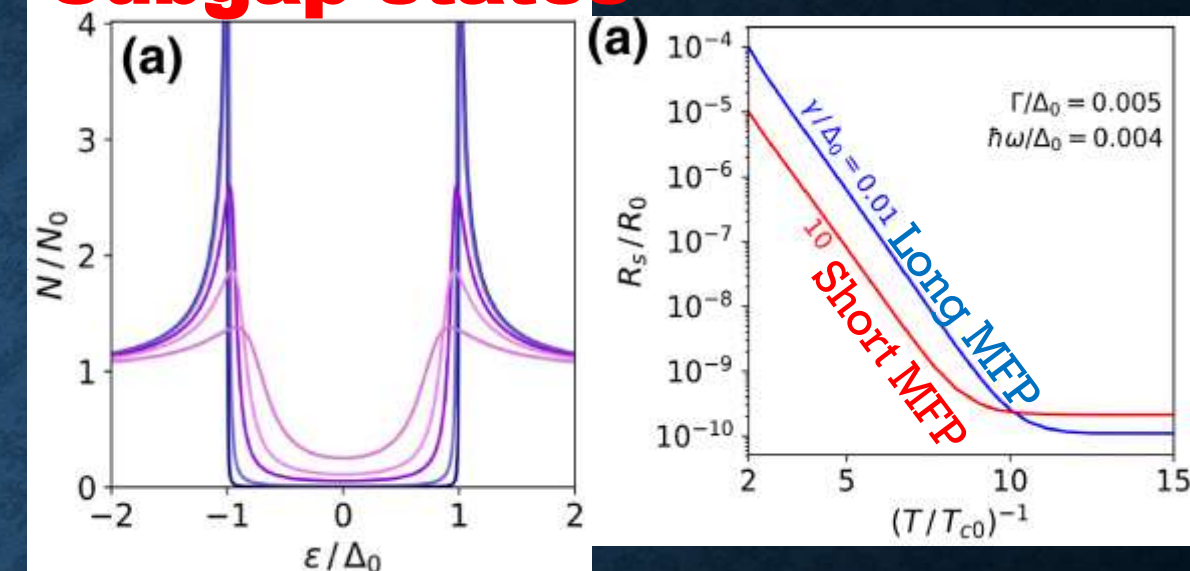
Videos of vortex dynamics in cavity-grade Nb can be found in
Ooi et al., PRB 111, 094519 (2025)

Two-level system defects



Müller et al Rep. Prog. Phys. 82, 124501 (2019)

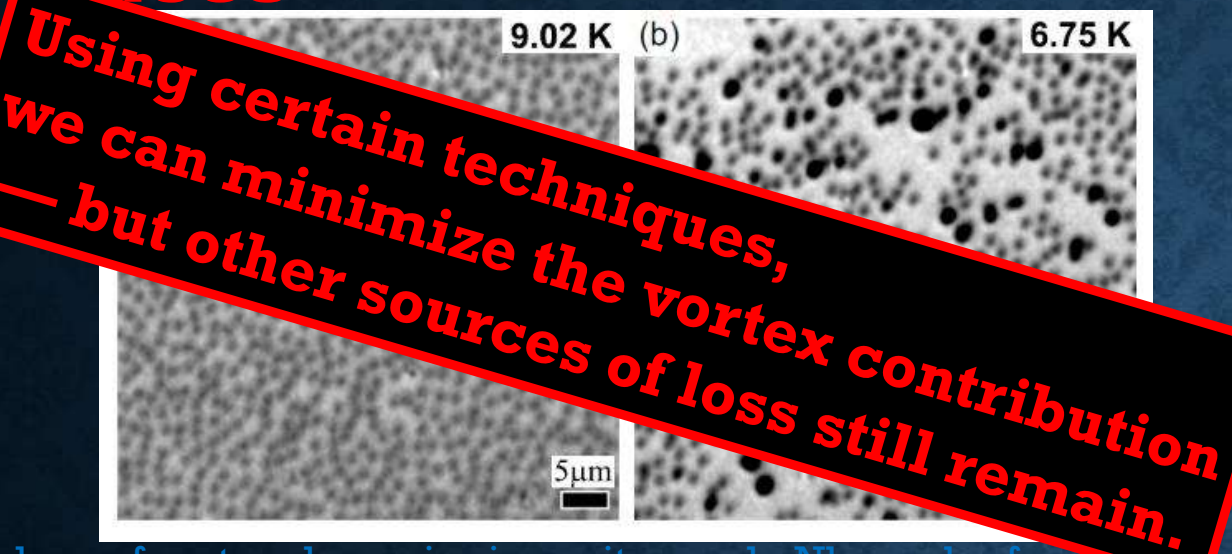
Subgap states



T. Kubo, Phys. Rev. Applied 17, 014018 (2022)

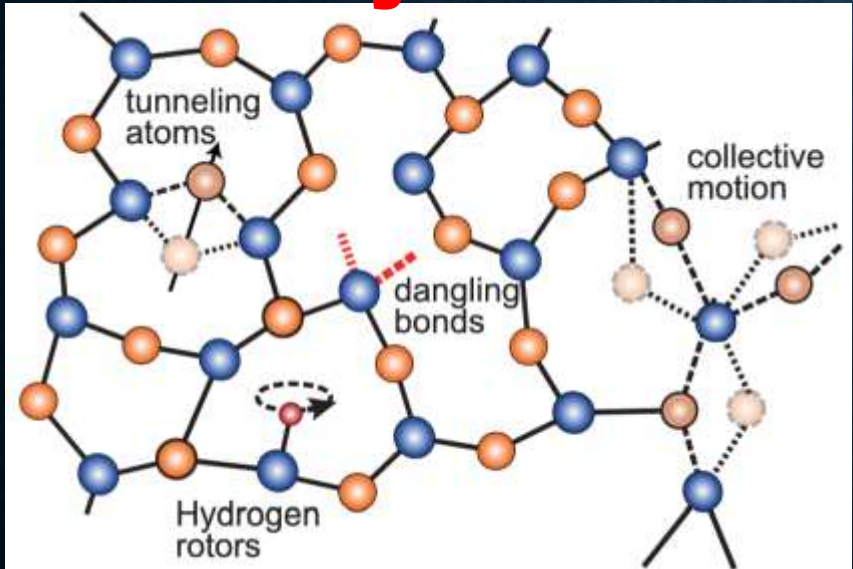
A Gurevich and T Kubo, Physical Review B 96, 184515 (2017)

Vertices



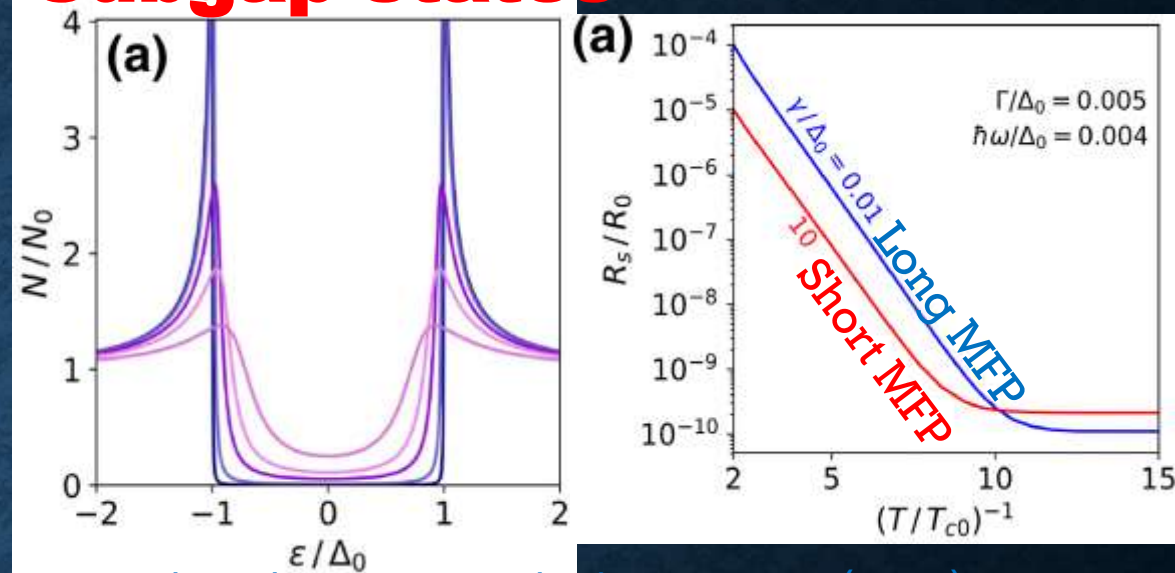
Videos of vortex dynamics in cavity-grade Nb can be found in
Ooi et al., PRB 111, 094519 (2025)

Two-level system defects



Müller et al Rep. Prog. Phys. 82, 124501 (2019)

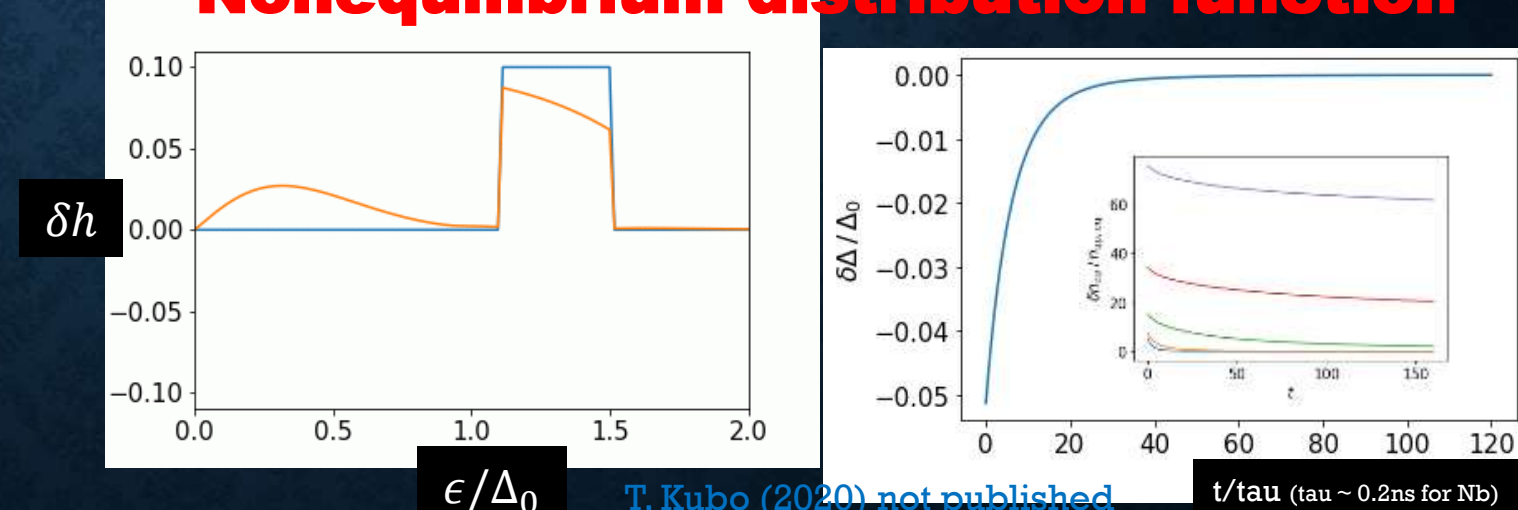
Subgap states



T. Kubo, Phys. Rev. Applied 17, 014018 (2022)

A Gurevich and T Kubo, Physical Review B 96, 184515 (2017)

Nonequilibrium quasi particles and Nonequilibrium distribution function



ϵ/Δ_0

T. Kubo (2020) not published

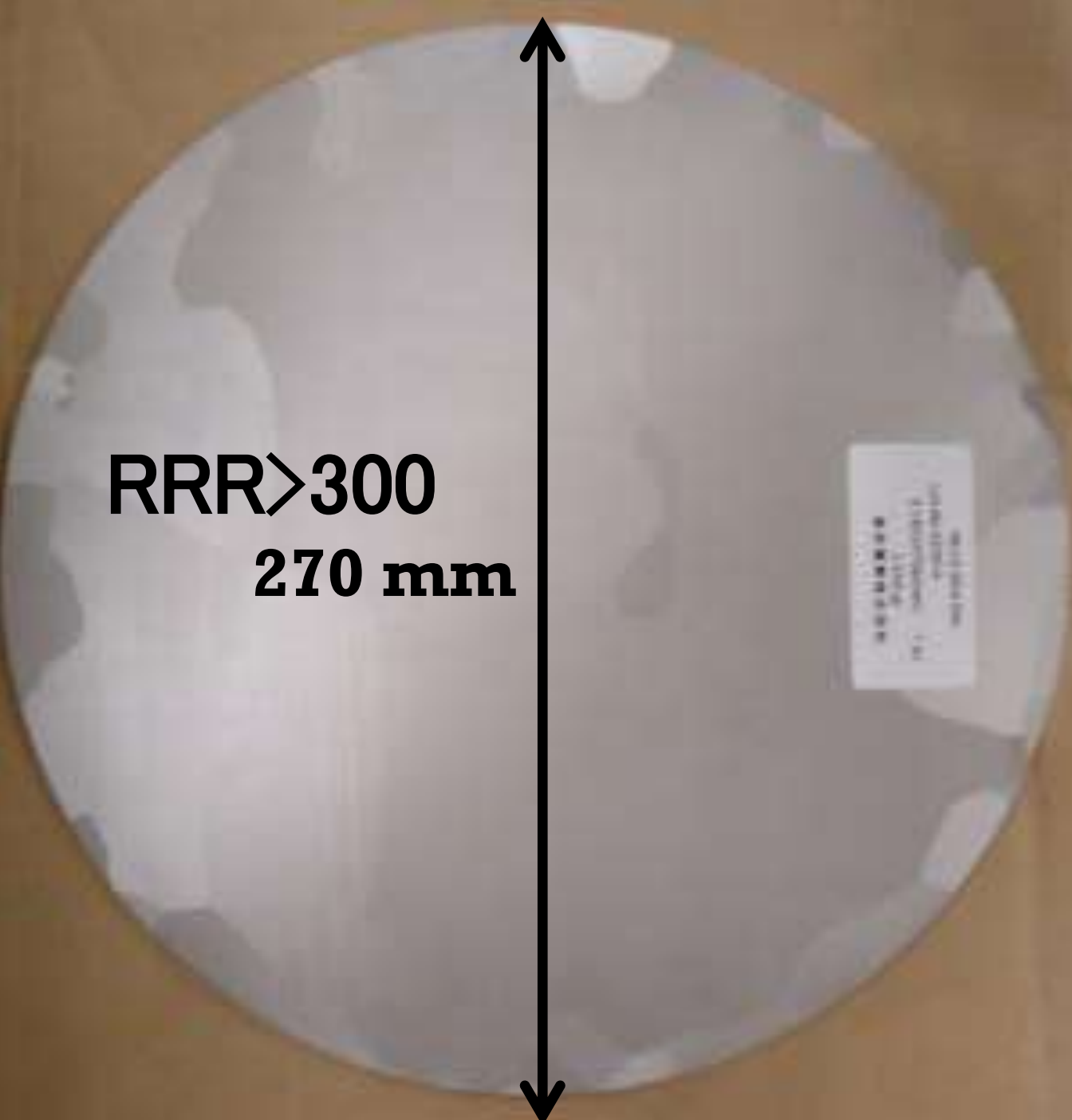
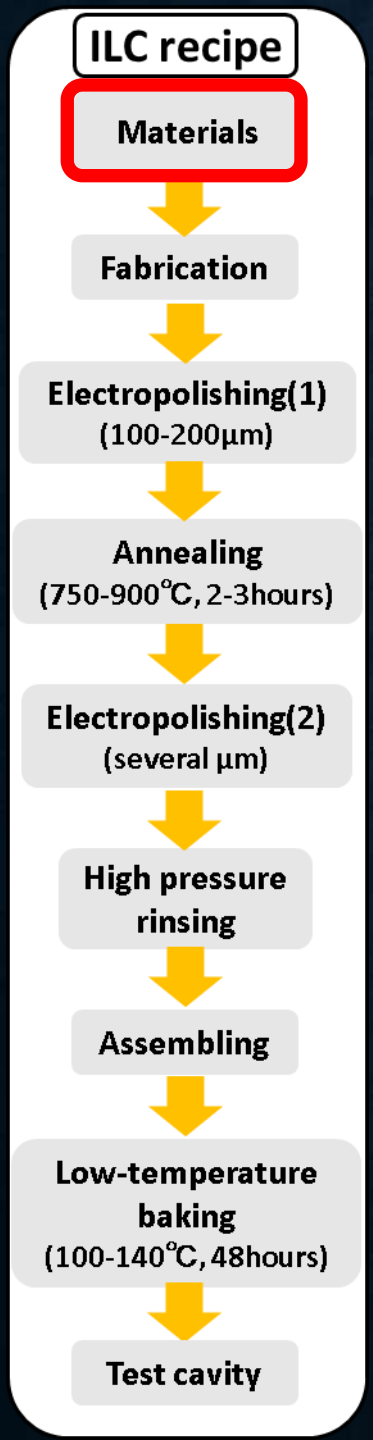
t/τ_a ($\tau_\text{a} \sim 0.2\text{ns}$ for Nb)

In such a seemingly complex situation,
how do accelerator researchers extract
high cavity performance?

**Trial and error
over several decades!**



Nb cavity technology for accelerators: Classical ILC recipe as a representative example



High purity Nb

ILC recipe

Materials

Fabrication

Electropolishing(1)
(100-200 μ m)

Annealing
(750-900°C, 2-3hours)

Electropolishing(2)
(several μ m)

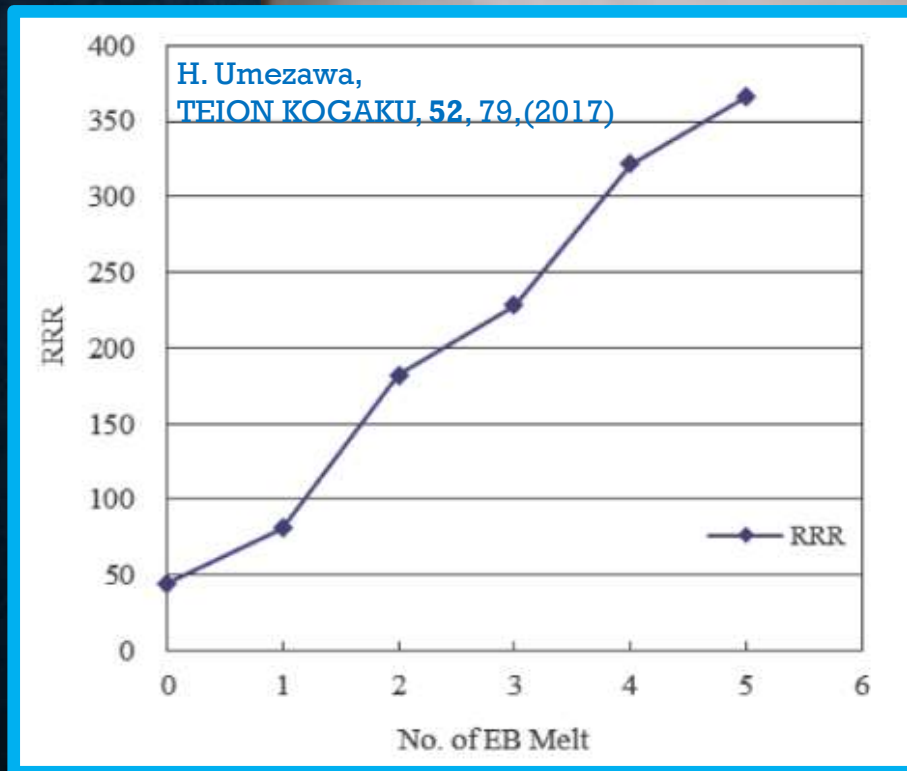
High pressure
rinsing

Assembling

Low-temperature
baking
(100-140°C, 48hours)

Test cavity

RRR>300



Pure Nb has the highest H_{c1} and a good thermal conductivity

See also a review article:
T. Kubo, Jpn. J. Appl. Phys. 64, 018002 (2025)

ILC recipe

Materials

Fabrication

Electropolishing(1)
(100-200 μm)

Annealing
(750-900°C, 2-3hours)

Electropolishing(2)
(several μm)

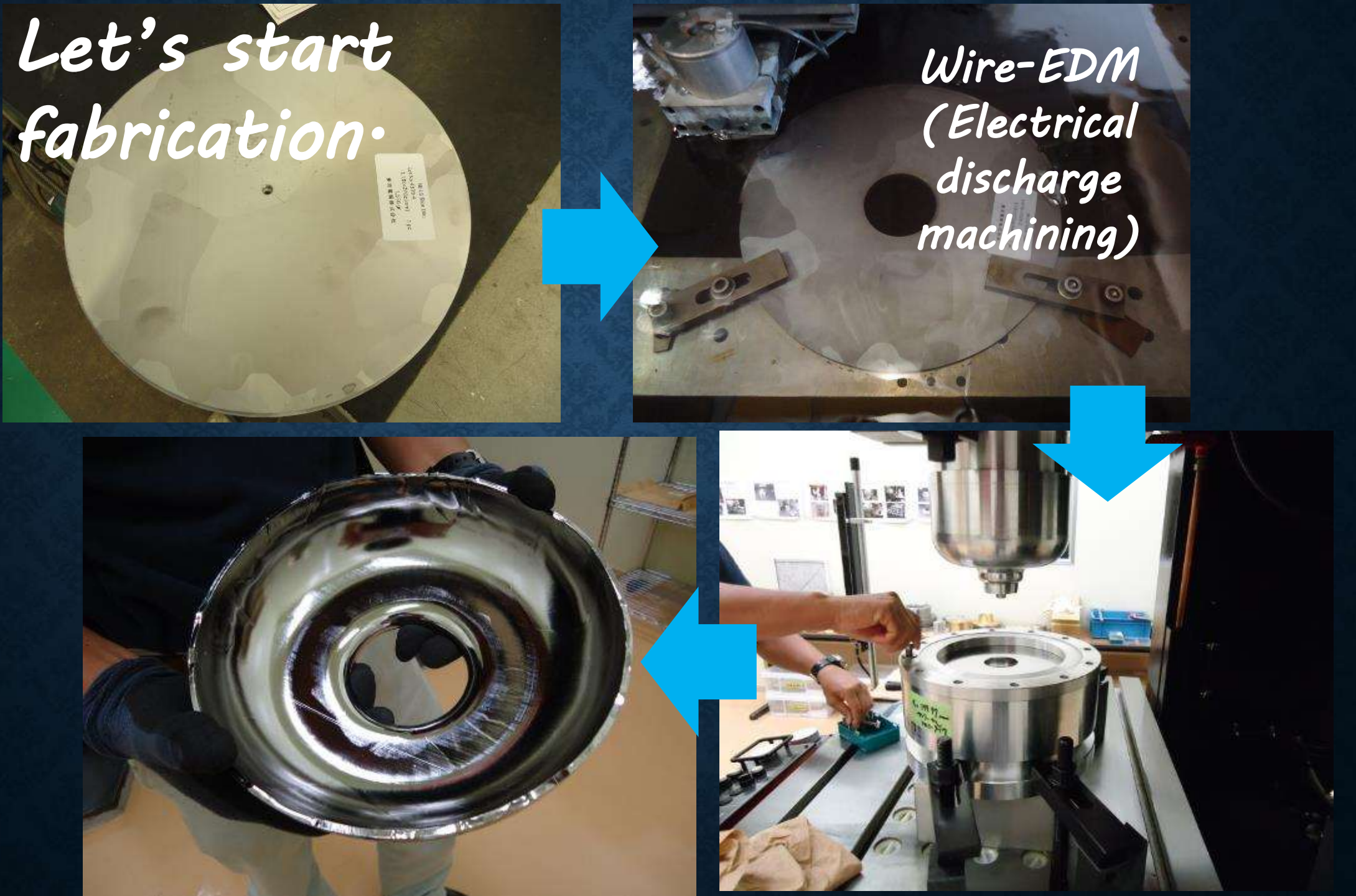
High pressure
rinsing

Assembling

Low-temperature
baking
(100-140°C, 48hours)

Test cavity

Let's start fabrication:



ILC recipe

Materials

Fabrication

Electropolishing(1)
(100-200 μm)

Annealing
(750-900°C, 2-3hours)

Electropolishing(2)
(several μm)

High pressure
rinsing

Assembling

Low-temperature
baking
(100-140°C, 48hours)

Test cavity



Electron beam welding
Cavity material quality is maintained



ILC recipe

Materials

Fabrication

Electropolishing(1)
(100-200 μm)

Annealing
(750-900°C, 2-3hours)

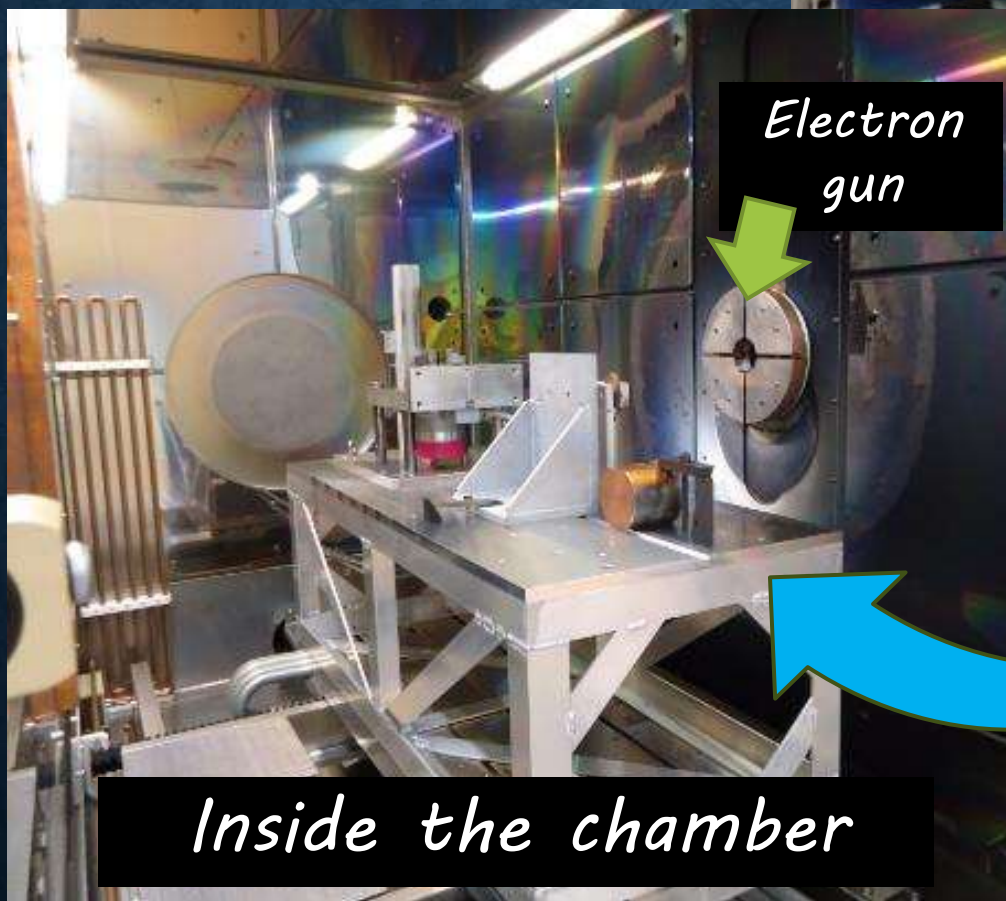
Electropolishing(2)
(several μm)

High pressure
rinsing

Assembling

Low-temperature
baking
(100-140°C, 48hours)

Test cavity



Inside the chamber

ILC recipe

Materials

Fabrication

Electropolishing(1)
(100-200 μm)

Annealing
(750-900°C, 2-3hours)

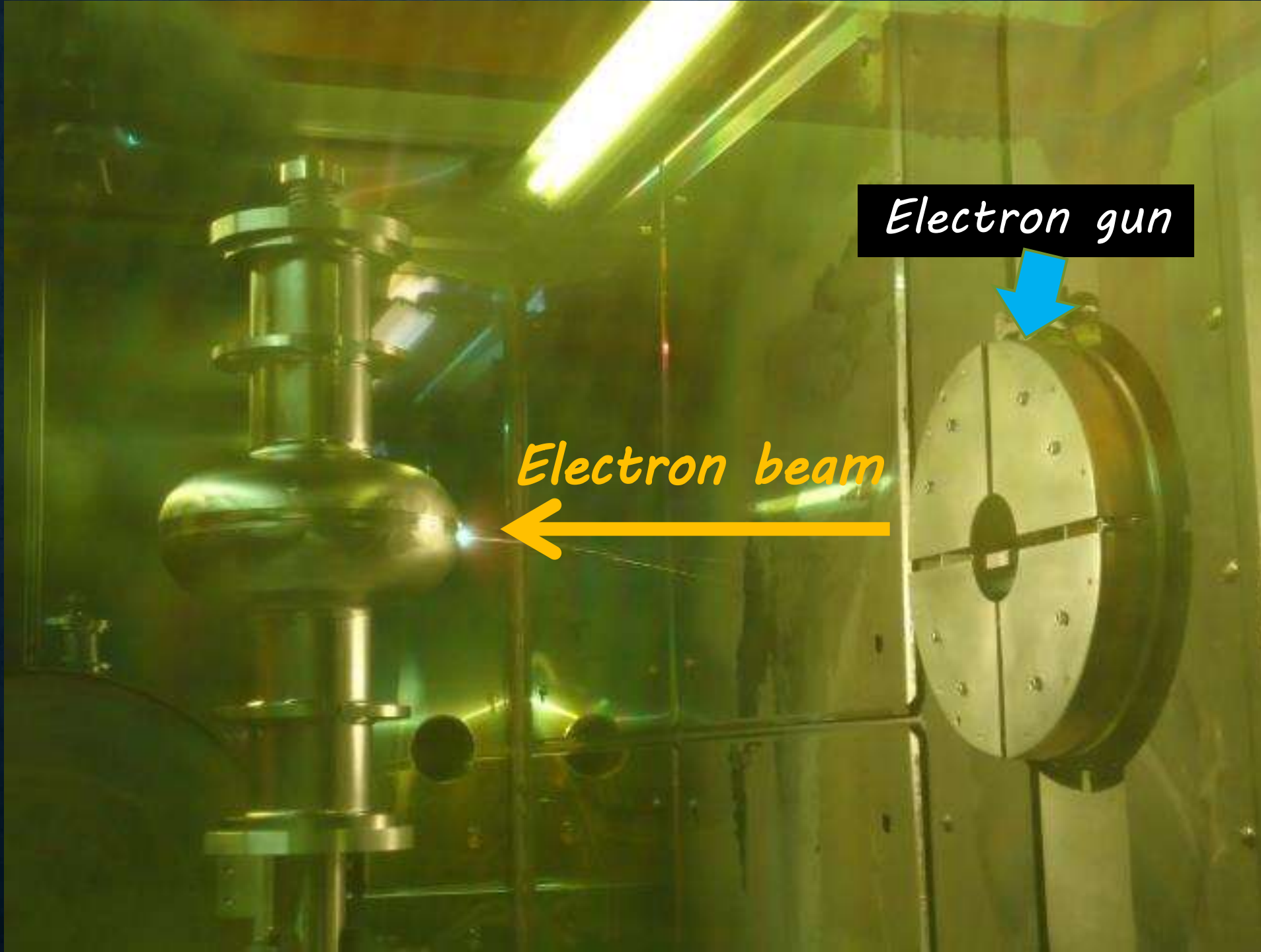
Electropolishing(2)
(several μm)

High pressure
rinsing

Assembling

Low-temperature
baking
(100-140°C, 48hours)

Test cavity



ILC recipe

Materials

Fabrication

Electropolishing(1)
(100-200 μm)

Annealing
(750-900°C, 2-3hours)

Electropolishing(2)
(several μm)

High pressure
rinsing

Assembling

Low-temperature
baking
(100-140°C, 48hours)

Test cavity



ILC recipe

Materials



Fabrication



Electropolishing(1)
(100-200 μ m)



Annealing
(750-900°C, 2-3hours)



Electropolishing(2)
(several μ m)



High pressure
rinsing



Assembling



Low-temperature
baking
(100-140°C, 48hours)



Test cavity

Electropolishing (EP)

- The electrolyte is a mixture of (9:1) sulfuric acid and hydrofluoric acid (HF).
- A DC voltage is applied with Nb as the anode and aluminum as the cathode.
- Niobium is oxidized to form Nb_2O_5 .
- This oxide layer is dissolved and polished away by HF present in the electrolyte.



ILC recipe

Materials



Fabrication



Electropolishing(1)
(100-200 μ m)



Annealing
(750-900°C, 2-3hours)



Electropolishing(2)
(several μ m)



High pressure
rinsing



Assembling



Low-temperature
baking
(100-140°C, 48hours)



Test cavity

Electropolishing (EP)

- The electrolyte is a mixture of (9:1) sulfuric acid and hydrofluoric acid (HF).
- A DC voltage is applied with Nb as the anode and aluminum as the cathode.
- Niobium is oxidized to form Nb_2O_5 .
- This oxide layer is dissolved and polished away by HF present in the electrolyte.



ILC recipe

Materials



Fabrication



Electropolishing(1)
(100-200μm)



Annealing
(750-900°C, 2-3hours)



Electropolishing(2)
(several μm)



High pressure
rinsing



Assembling



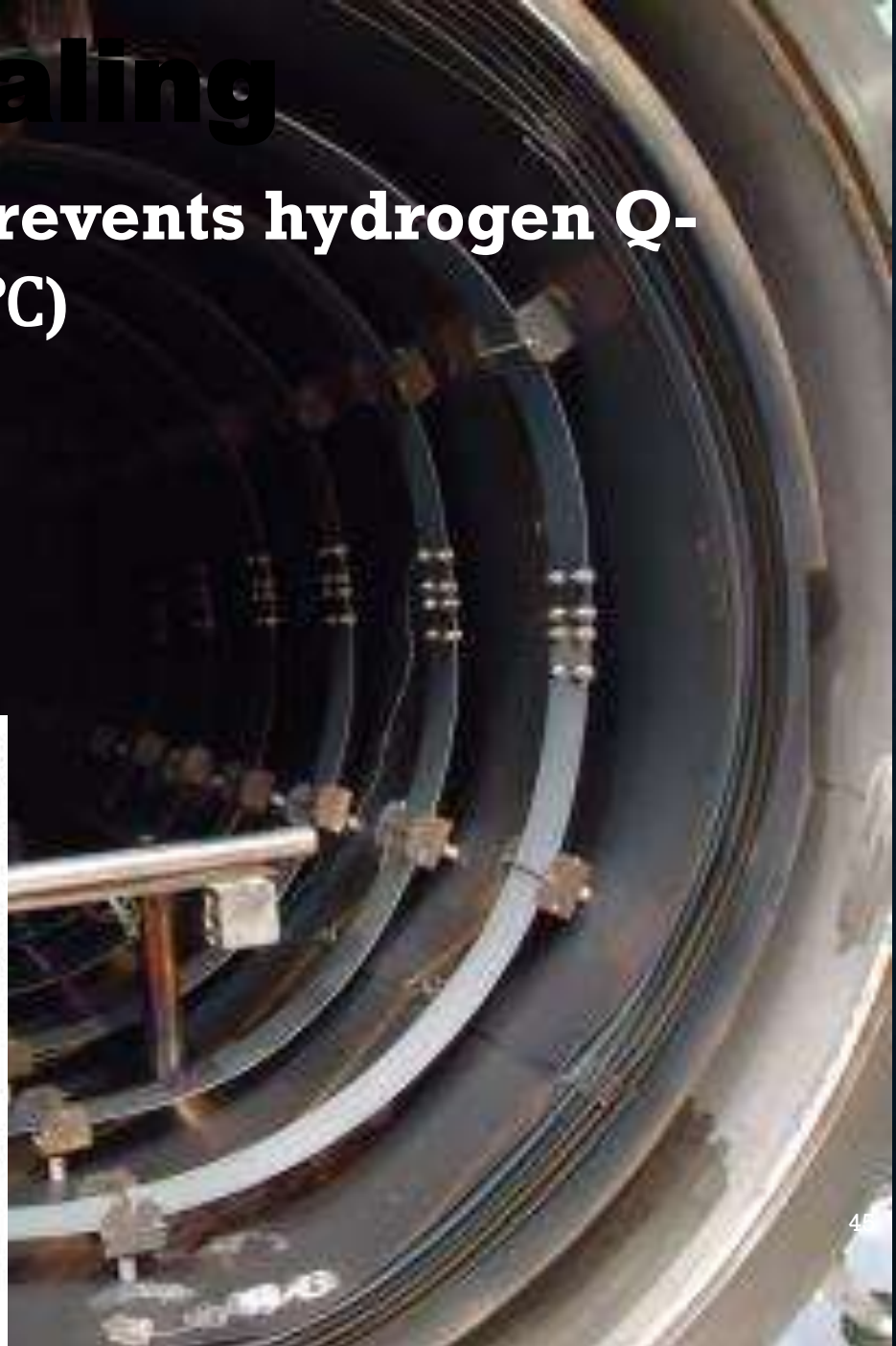
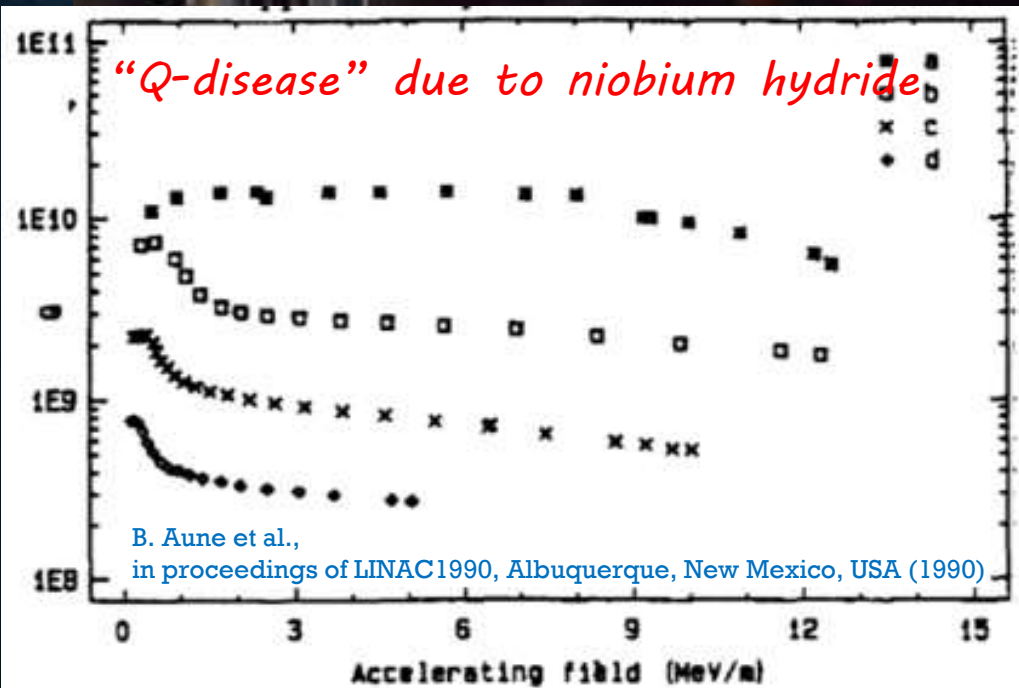
Low-temperature
baking
(100-140°C, 48hours)



Test cavity

Annealing

- To degas hydrogen — prevents hydrogen Q-disease (requires >700 °C)



ILC recipe

Materials



Fabrication



Electropolishing(1)
(100-200μm)



Annealing
(750-900°C, 2-3hours)



Electropolishing(2)
(several μm)



High pressure
rinsing



Assembling



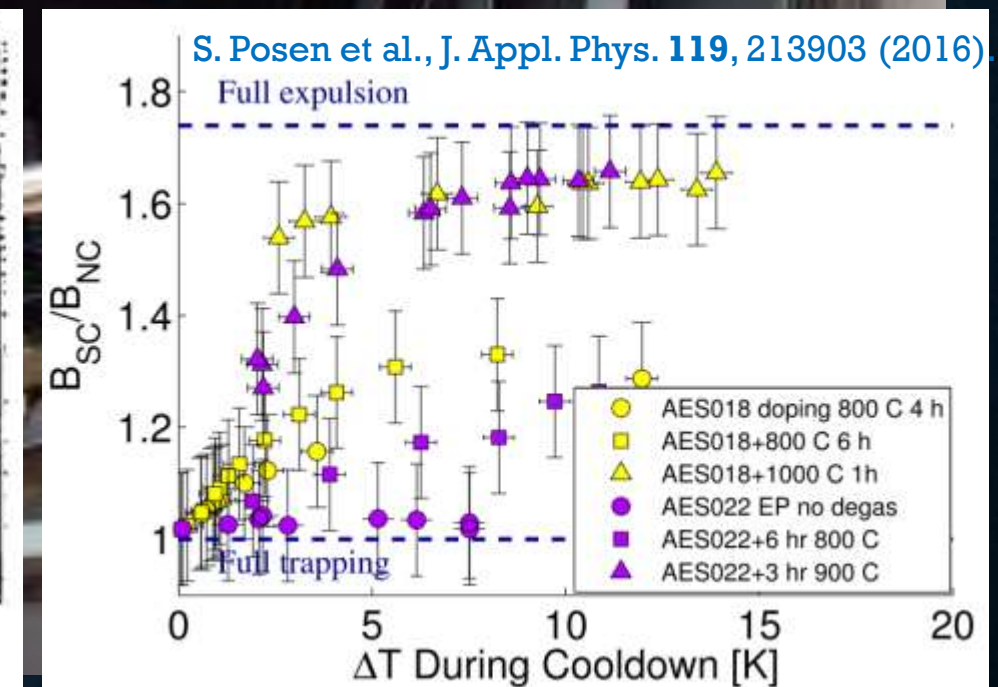
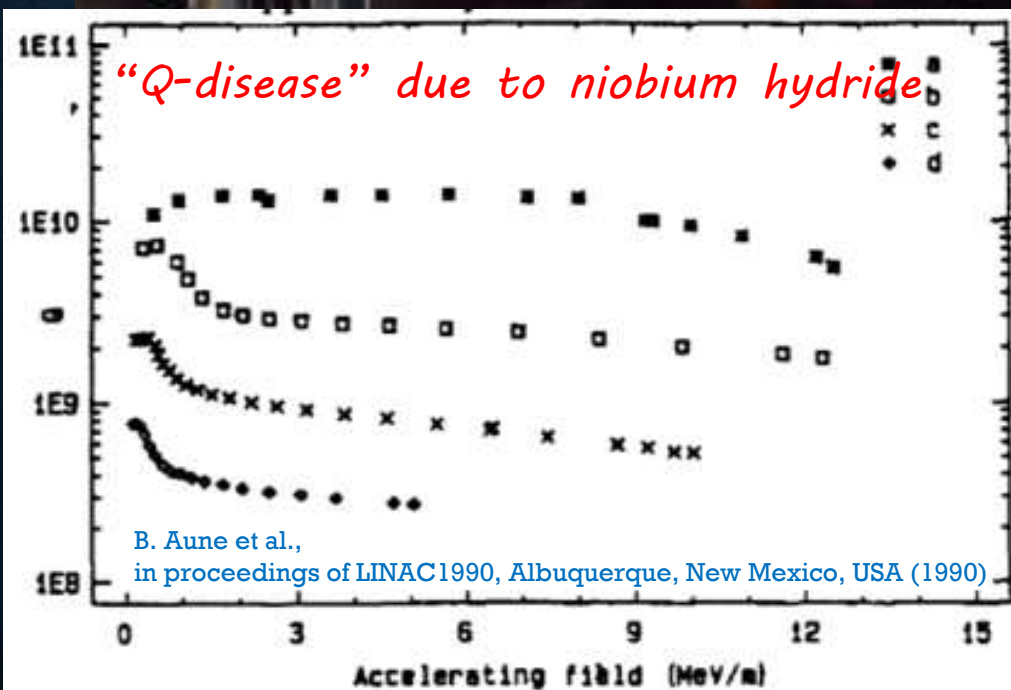
Low-temperature
baking
(100-140°C, 48hours)



Test cavity

Annealing

- To degas hydrogen — prevents hydrogen Q-disease (requires >700 °C)
- To reduce pinning centers — minimizes trapped flux (requires ~900 °C)



ILC recipe

Materials



Fabrication



Electropolishing(1)
(100-200 μ m)



Annealing
(750-900°C, 2-3hours)



Electropolishing(2)
(several μ m)



High pressure
rinsing



Assembling



Low-temperature
baking
(100-140°C, 48hours)



Test cavity

A second EP step, removing only a few microns.



ILC recipe

Materials



Fabrication



Electropolishing(1)
(100-200 μ m)



Annealing
(750-900°C, 2-3hours)



Electropolishing(2)
(several μ m)



High pressure
rinsing



Assembling

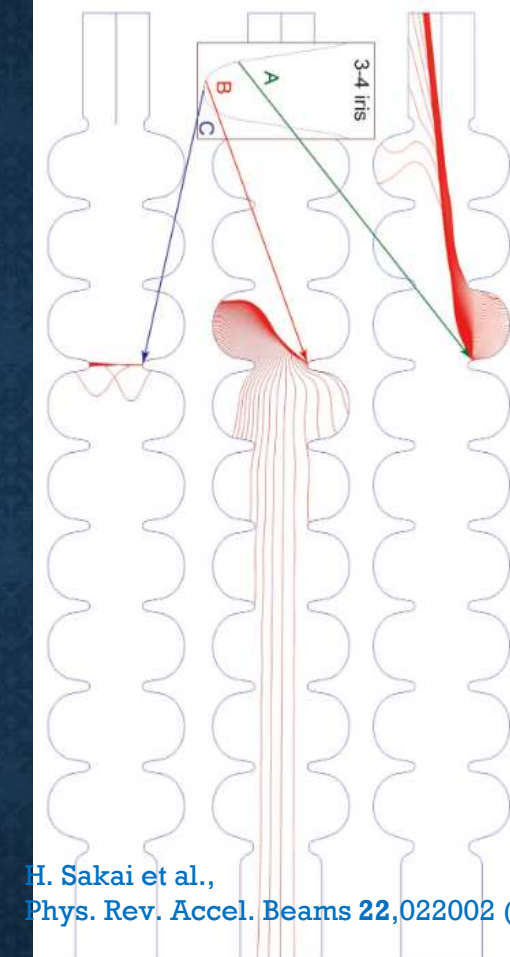
Low-temperature
baking
(100-140°C, 48hours)



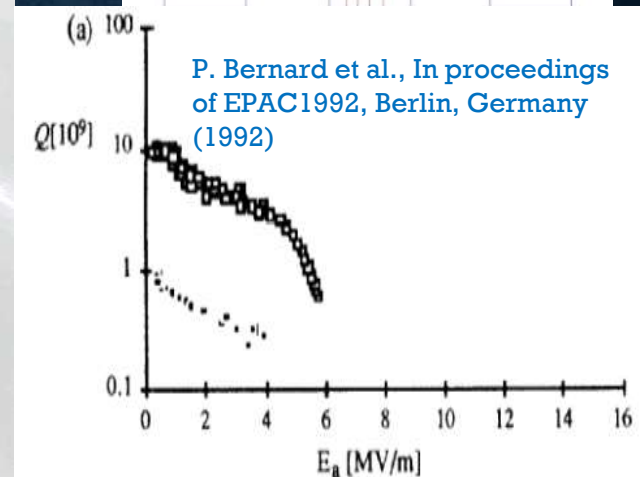
Test cavity



Courtesy of Mathieu Omet (KEK)



H. Sakai et al.,
Phys. Rev. Accel. Beams 22, 022002 (2019)



ILC recipe

Materials



Fabrication



Electropolishing(1)
(100-200μm)



Annealing
(750-900°C, 2-3hours)



Electropolishing(2)
(several μm)



High pressure
rinsing



Assembling



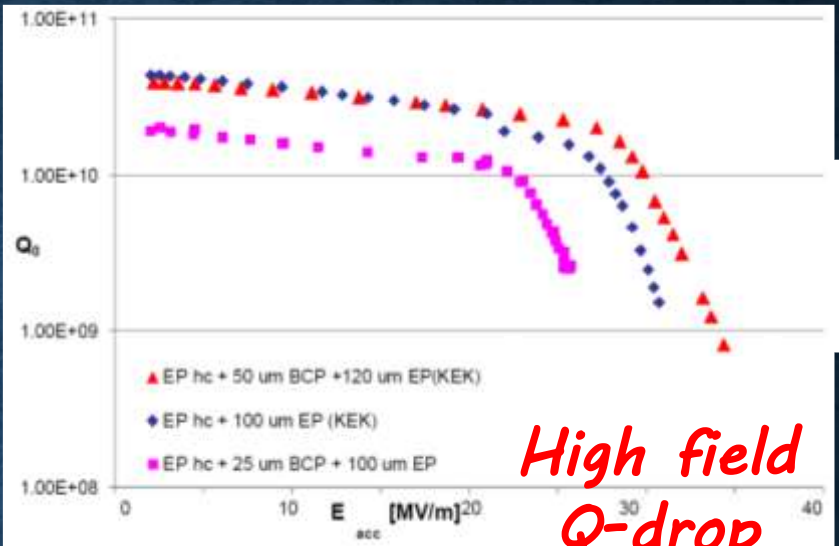
Low-temperature
baking
(100-140°C, 48hours)

Test cavity

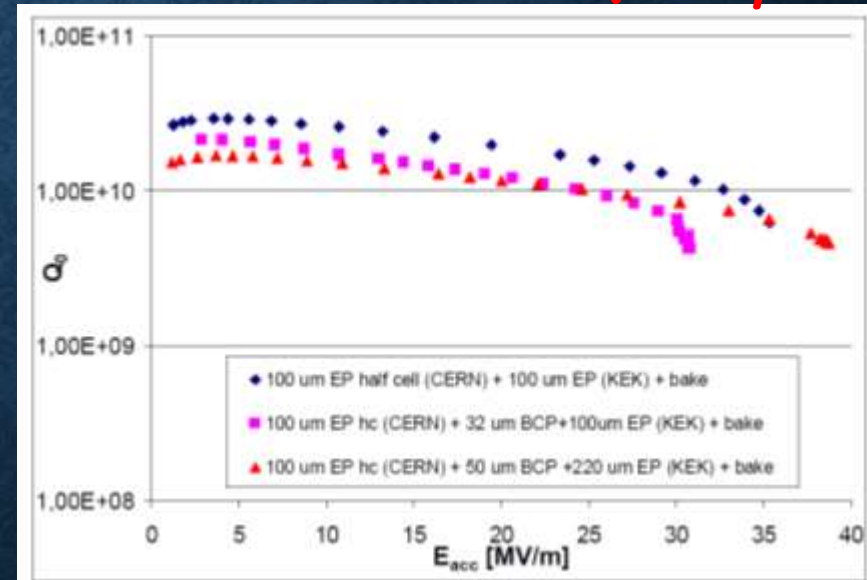
120°C—48h bake



Courtesy of Mathieu Omet (KEK)



High field
Q-drop

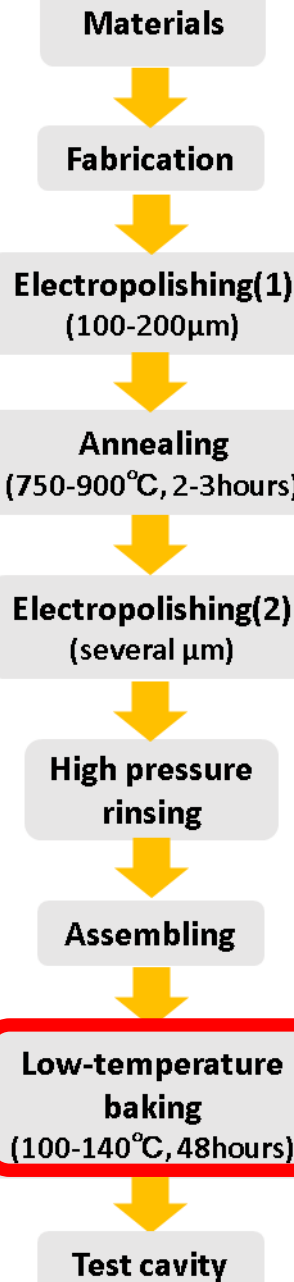


Spatial variation of the mean free path on the scale of the penetration depth suppresses the surface current, thereby increasing the maximum achievable field.

T. Kubo, Supercond. Sci. and Technol. 30, 023001 (2017); Sci. and Technol. 34, 045006 (2021)

V. Ngampruetikorn and J. A. Sauls, Phys. Rev. Research 1, 012015(R) (2019)

120°C—48h bake



Labs in Japan and the US traditionally applied a 100°C bake to remove residual water after high-pressure rinsing. In contrast, labs in Germany and France did not adopt this step — and continued to suffer from the so-called Q-drop.

At the time, the reason was unknown, and the phenomenon was even nicknamed the "European disease." It wasn't until the late 1990s that the community realized the low-temperature bake was the key. This is a prime example of the serendipitous discoveries that have accumulated over the past few decades.



Courtesy of Mathieu Omet (KEK)



Spatial variation of the mean free path on the scale of the penetration depth suppresses the surface current, thereby increasing the maximum achievable field.

ILC recipe

Materials



Fabrication



Electropolishing(1)
(100-200 μ m)



Annealing
(750-900°C, 2-3hours)



Electropolishing(2)
(several μ m)



High pressure
rinsing



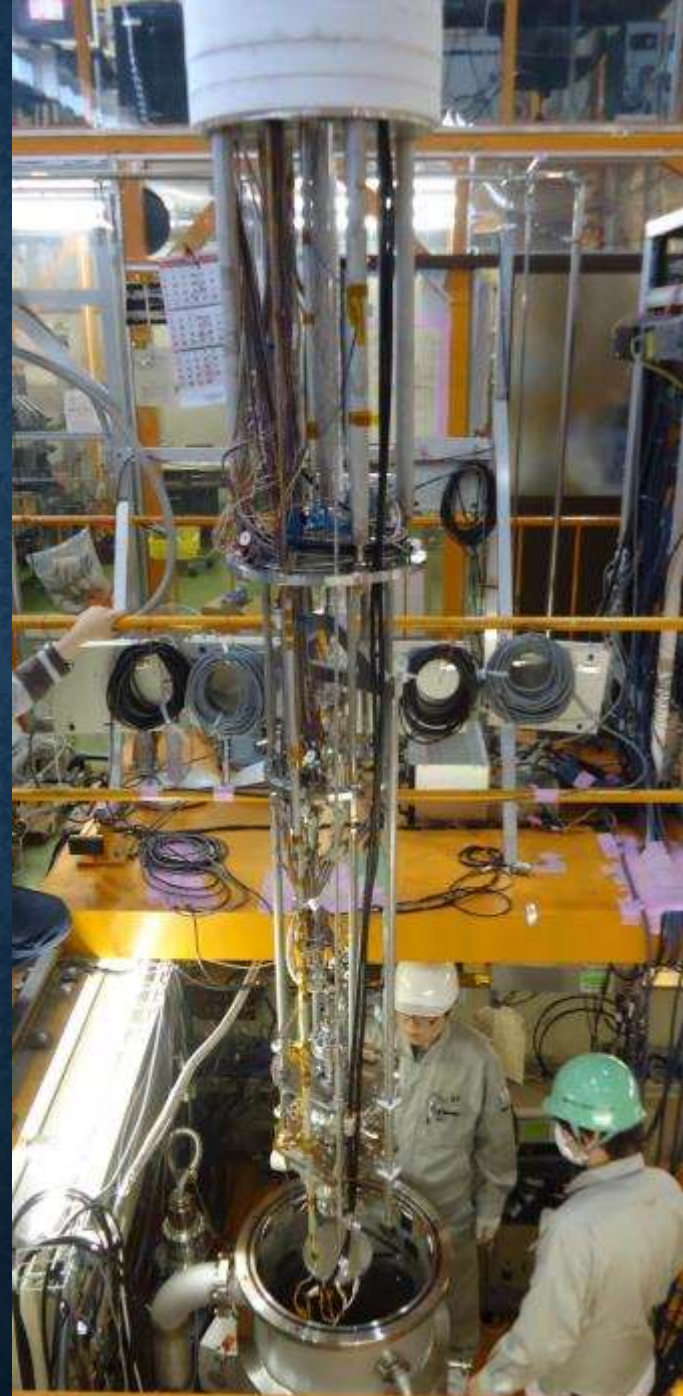
Assembling



Low-temperature
baking
(100-140°C, 48hours)



Test cavity



ILC recipe

Materials



Fabrication



Electropolishing(1)
(100-200 μ m)



Annealing
(750-900°C, 2-3hours)



Electropolishing(2)
(several μ m)



High pressure
rinsing

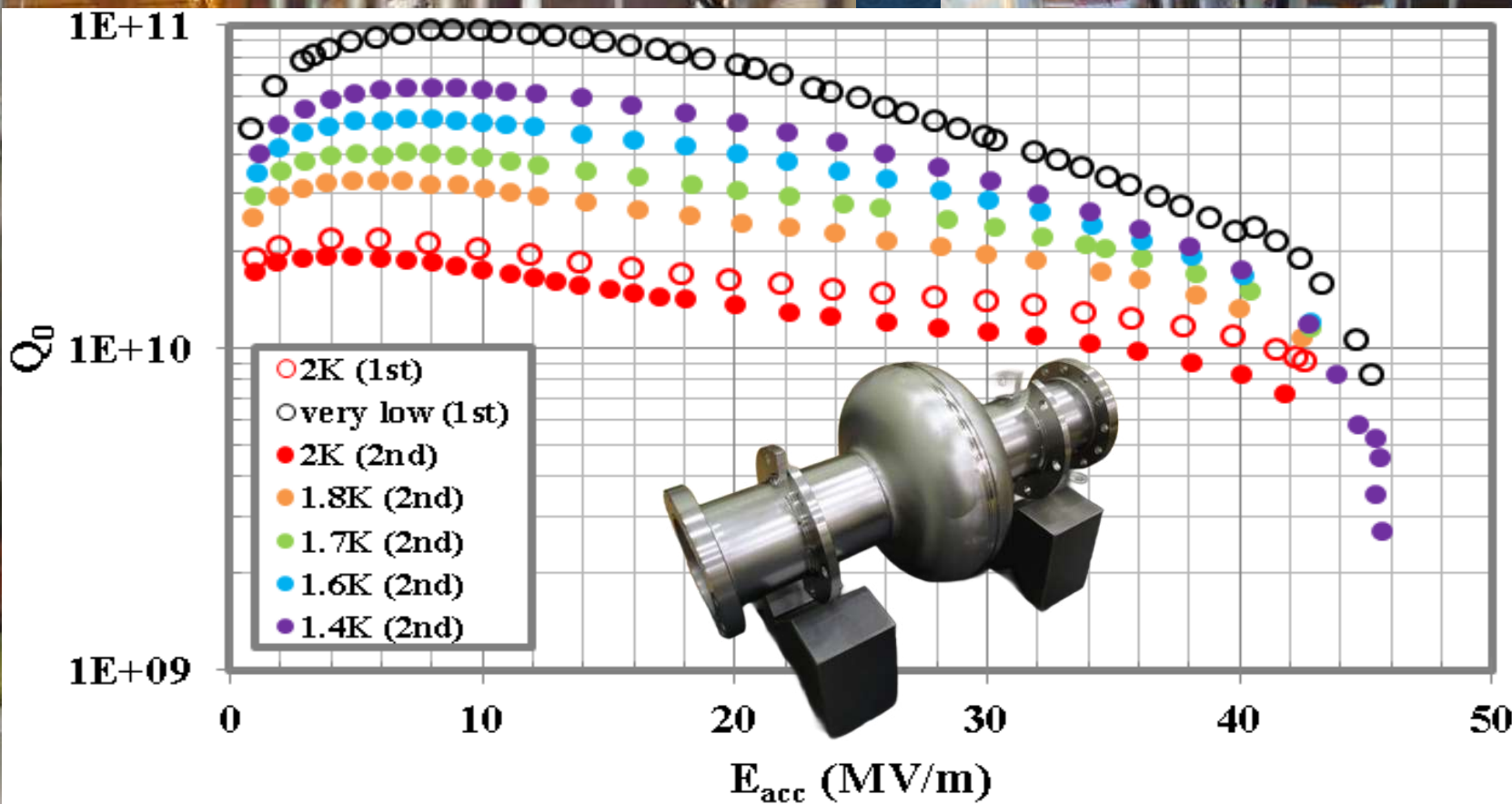


Assembling



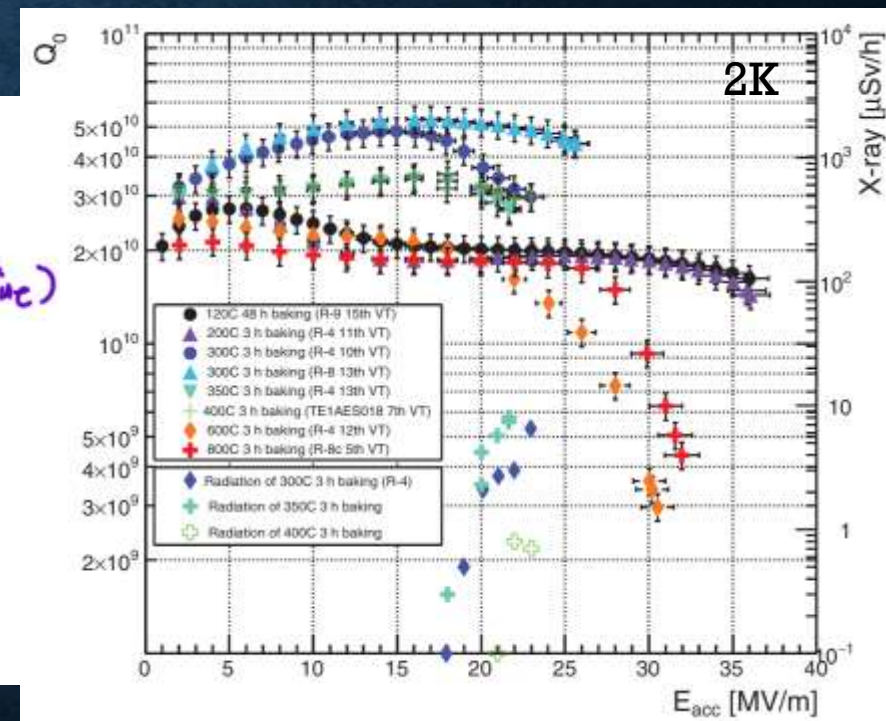
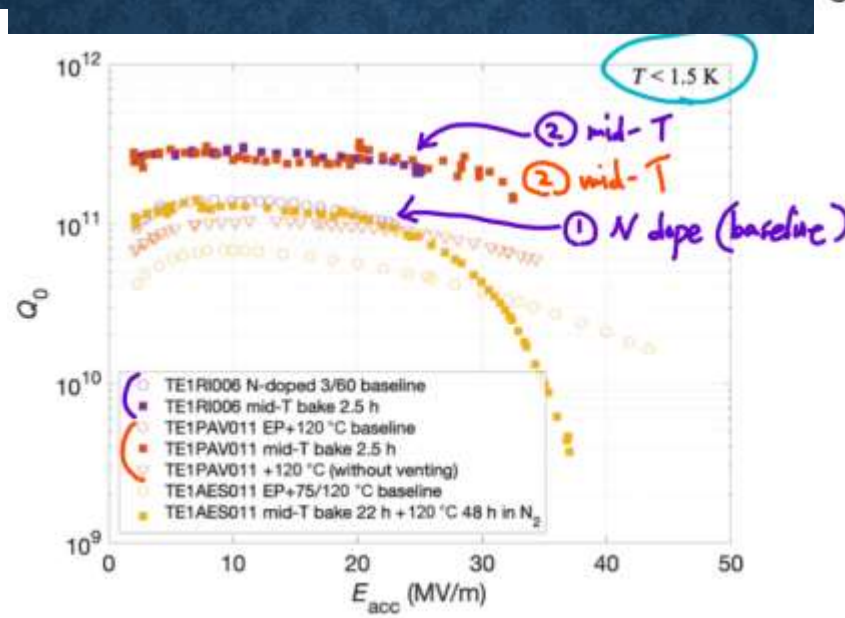
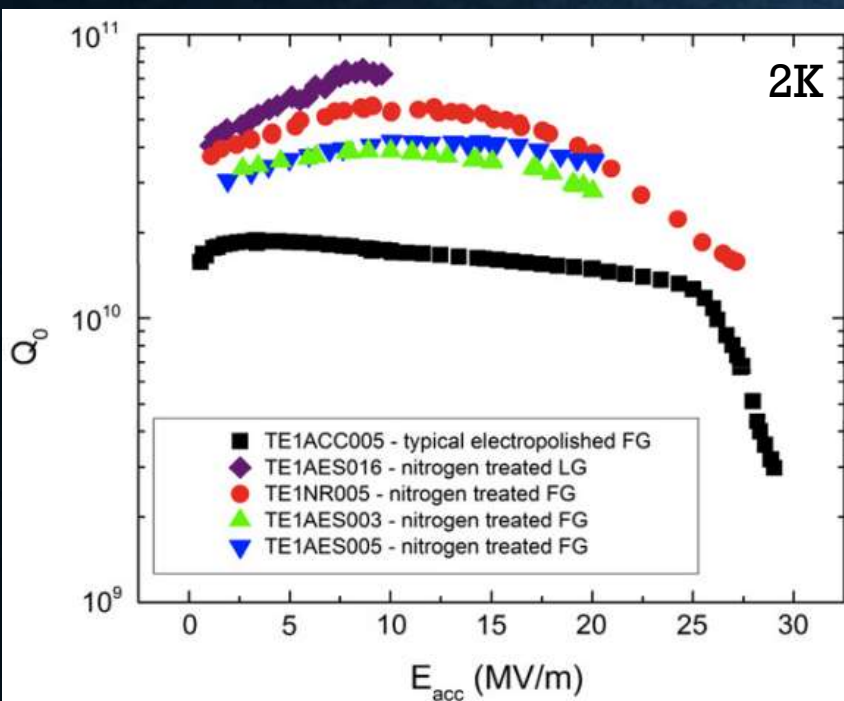
Low-temperature
baking
(100-140°C, 48hours)

Test cavity



Many modern recipes exist: N-doping, N-infusion, two-step bake, mid-T in situ/furnace bakes, etc.

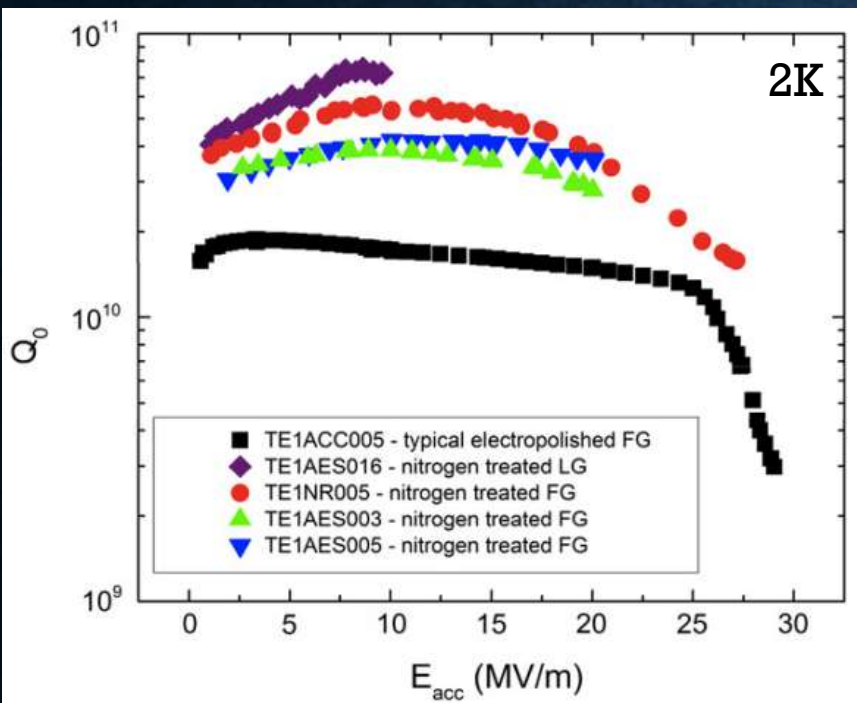
They are all variants of the classical recipe, with some steps replaced or modified.



S. Posen et al.,
Phys. Rev. Applied 13, 014024 (2020)

An example of other recipes: nitrogen doping

A. Grassellino et al.,
Supercond. Sci. Technol. **26**, 102001 (2013)



The physics behind superconducting RF cavities is highly complex and not yet fully understood.

Sometimes,
even a small change can lead to a major breakthrough.

Materials



Fabrication

Electropolishing(1)
(100-200μm)Annealing
(750-900°C, 2-3hours)Electropolishing(2)
(several μm)High pressure
rinsing

Assembling

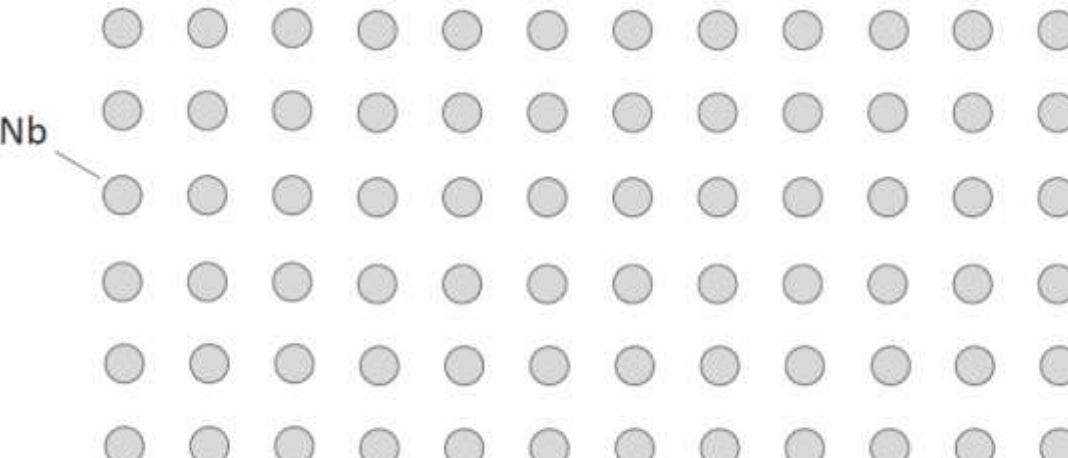
low-temperature
baking
(100-140°C, 48hours)

Test cavity

N-doping treatment

800C UHV,
3 hours800C N₂
injection
p=25mTorr800C N₂, 2
minutes800C UHV,
6 minutesUHV
cooling

5 um EP



~~IC recipe~~

N doping

Materials



Fabrication



Electropolishing(1)
(100-200 μ m)



Annealing
(750-900°C, 2-3 hours)



Electropolishing(2)
(several μ m)



High pressure
rinsing



Assembling



~~low-temperature
baking~~
(100-140°C, 4 hours)

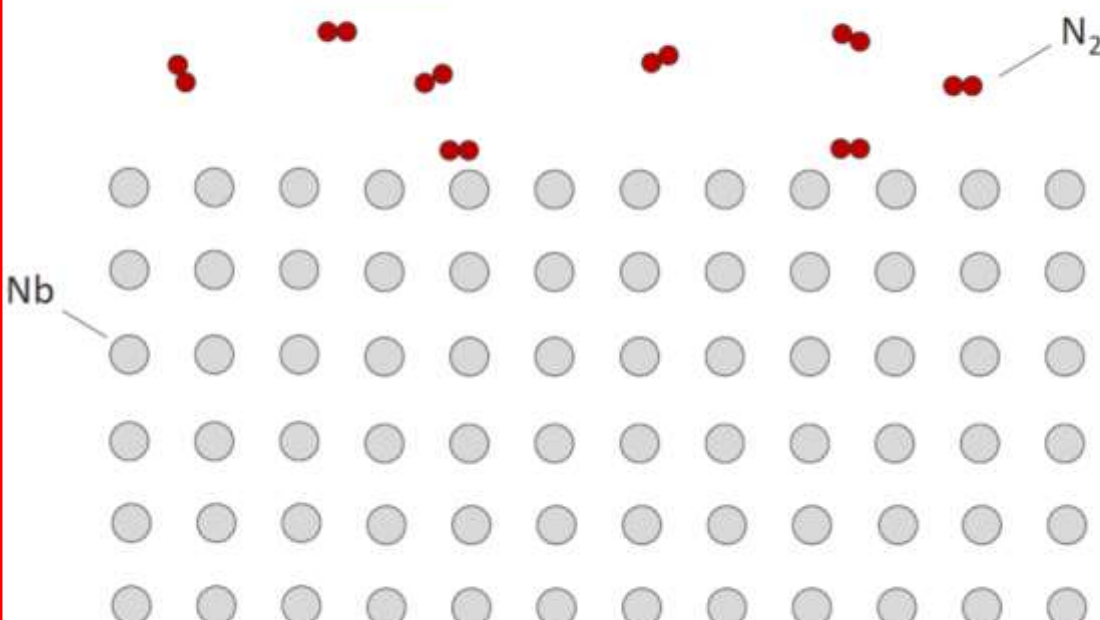


Test cavity

Inject N₂ gas
(~Pa)
at 800°C
for 2 minutes

Insert additional step

N-doping treatment



Materials



Fabrication

Electropolishing(1)
(100-200μm)Annealing
(750-900°C, 2-3 hours)Electropolishing(2)
(several μm)

High pressure rinsing



Assembling

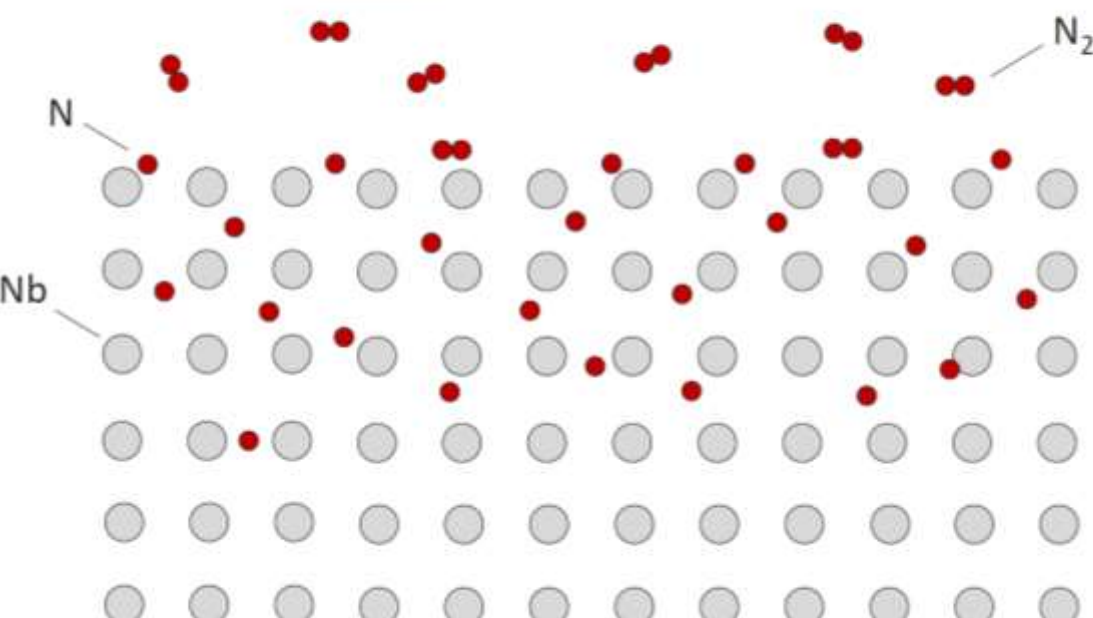
low-temperature baking
(100-140°C, 4-8 hours)

Test cavity

Inject N₂ gas (~Pa)
at 800°C
for 2 minutes

Insert additional step

N-doping treatment (example: the “2/6 recipe”)



~~IC recipe~~

N doping

Materials



Fabrication



Electropolishing(1)
(100-200 μ m)



Annealing
(750-900°C, 2-3 hours)



Electropolishing(2)
(several μ m)



High pressure
rinsing



Assembling



~~low-temperature
baking~~
(100-140°C, 4 hours)

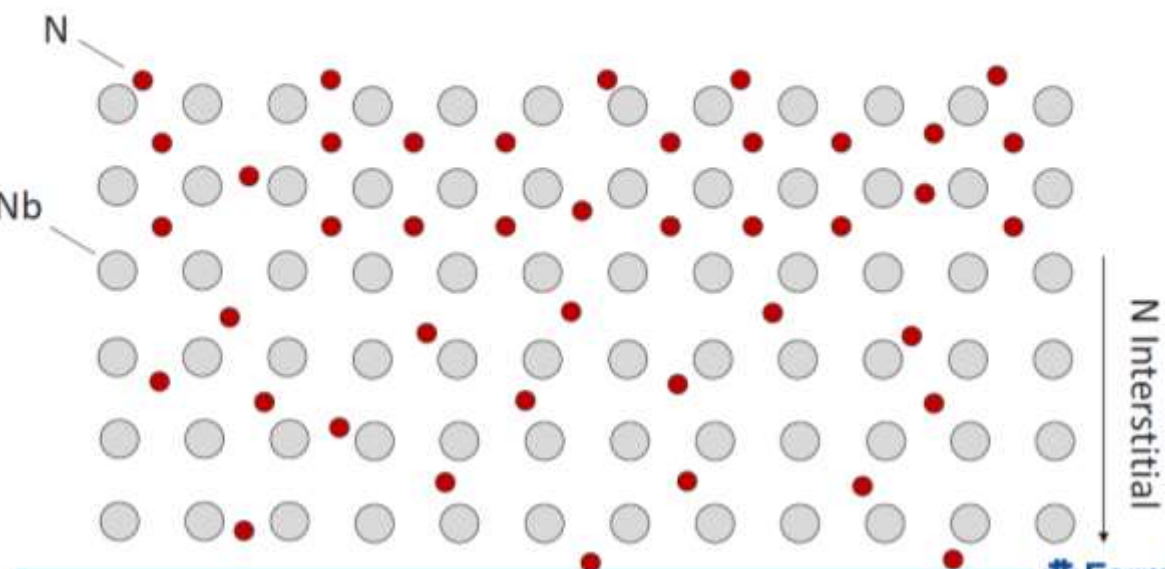
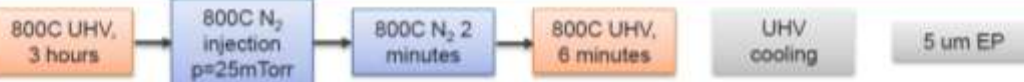


Test cavity

Inject N₂ gas
(~Pa)
at 800°C
for 2 minutes

Insert additional step

N-doping treatment (example: the “2/6 recipe”)



Fermilab

~~IC recipe~~

N doping

Materials

Fabrication

Electropolishing(1)
(100-200 μ m)

Annealing
(750-900°C, 2-3 hours)

Electropolishing(2)
(several μ m)

High pressure
rinsing

Assembling

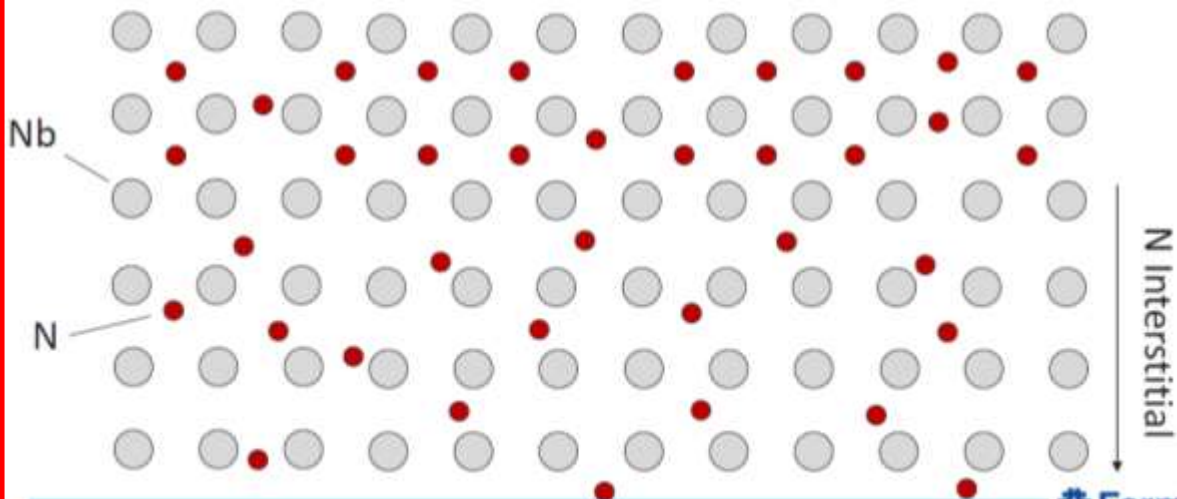
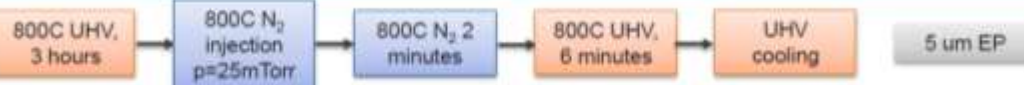
~~low-temperature
baking~~
(100-140°C, 4 hours)

Test cavity

Insert additional step

Inject N₂ gas
(~Pa)
at 800°C
for 2 minutes

N-doping treatment (example: the “2/6 recipe”)



Materials



Fabrication

Electropolishing(1)
(100-200μm)Annealing
(750-900°C, 2-3hours)Electropolishing(2)
(several μm)

High pressure rinsing



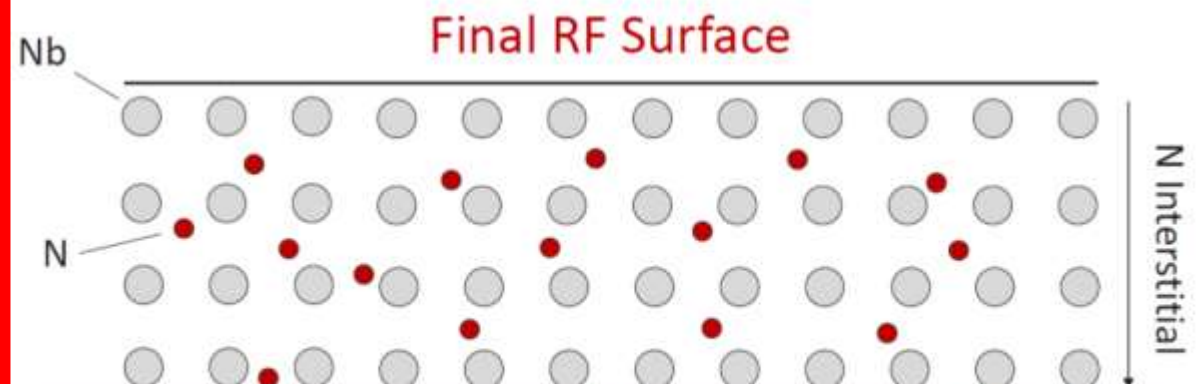
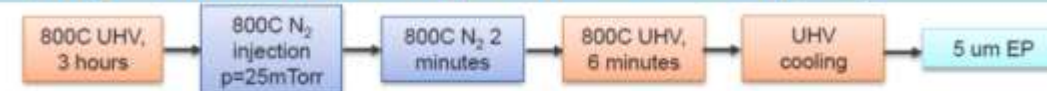
Assembling

low-temperature
baking
(100-140°C, 48hours)

Test cavity

Electropolish by 5-7μm

N-doping treatment (example: the “2/6 recipe”)



~~ILC recipe~~

N doping

Materials



Fabrication



Electropolishing(1)
(100-200 μ m)



Annealing
(750-900°C, 2-3hours)



Electropolishing(2)
(several μ m)



High pressure
rinsing



Assembling

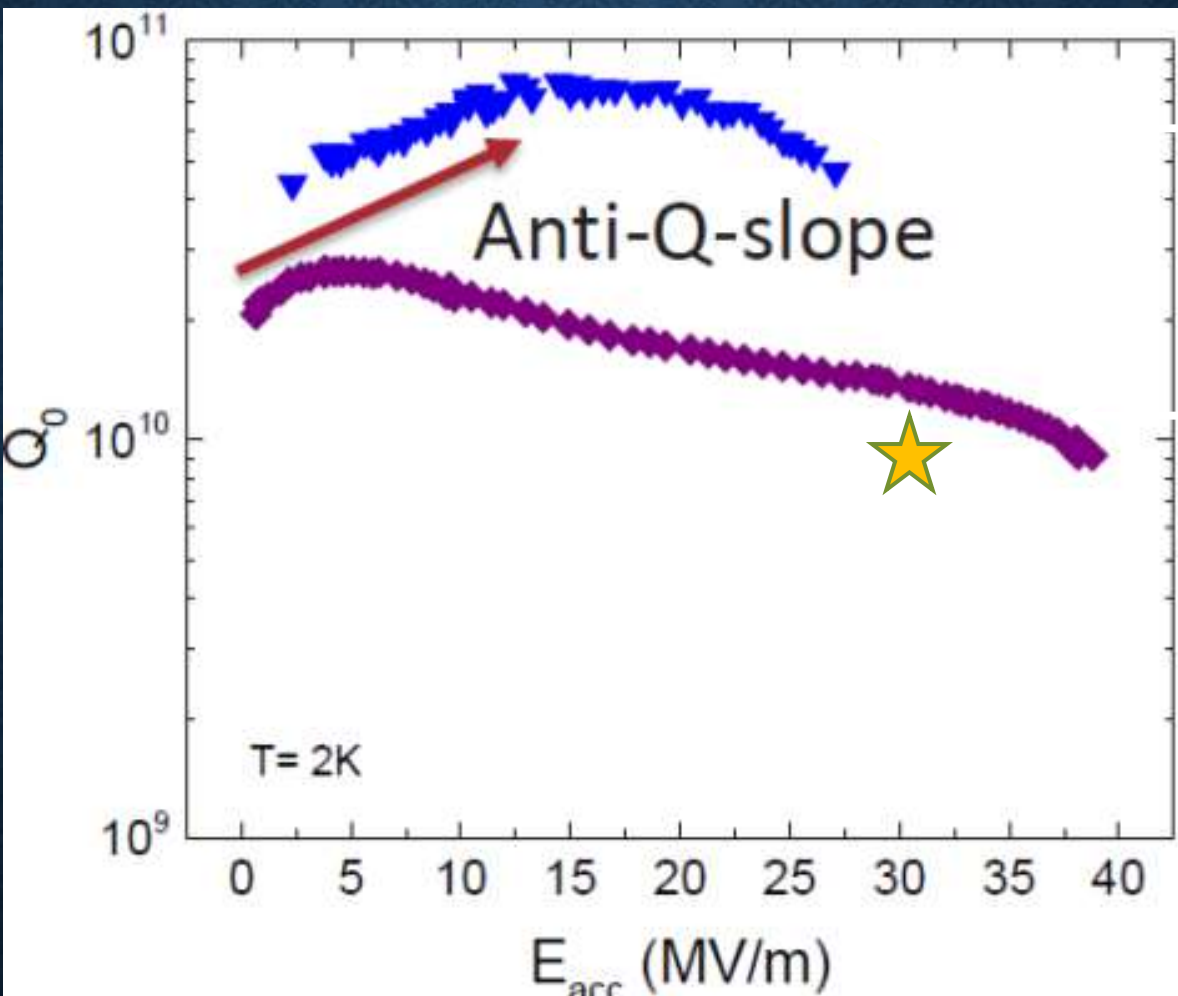


low-temperature
baking
(100-140°C, 4-5hours)



Test cavity

Then we obtain a higher Q

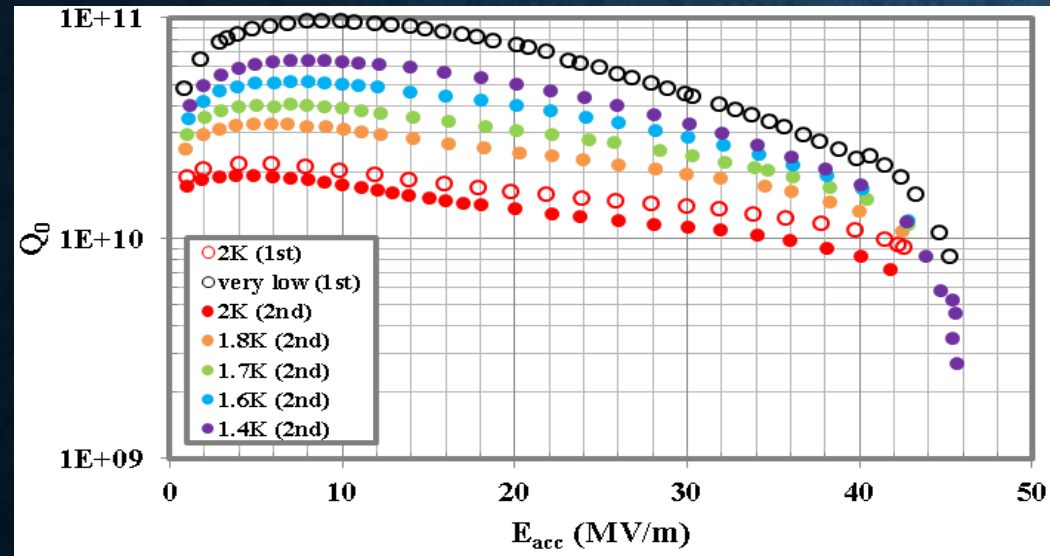


N dope

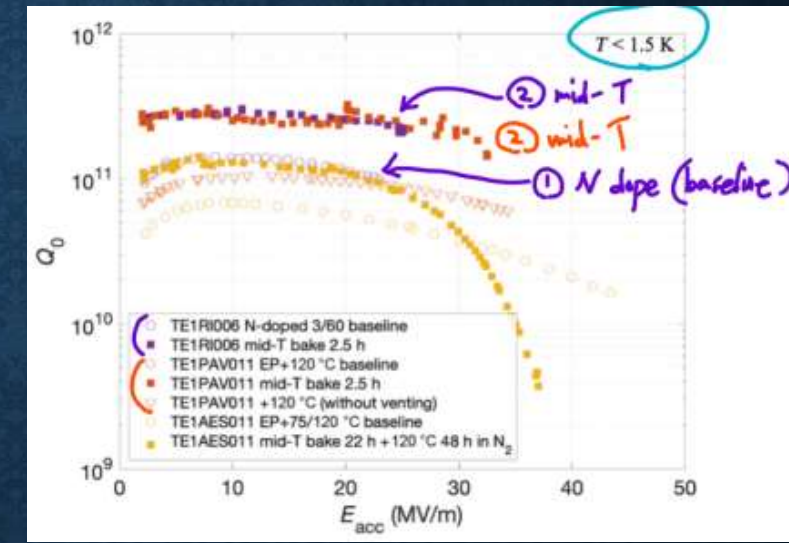
ILC recipe

A. Grassellino et al, Supercond. Sci. Technol. **26** 102001 (2013)

The accelerator community can build the best cavities on the planet — achieving $Q > 10^{11}$.



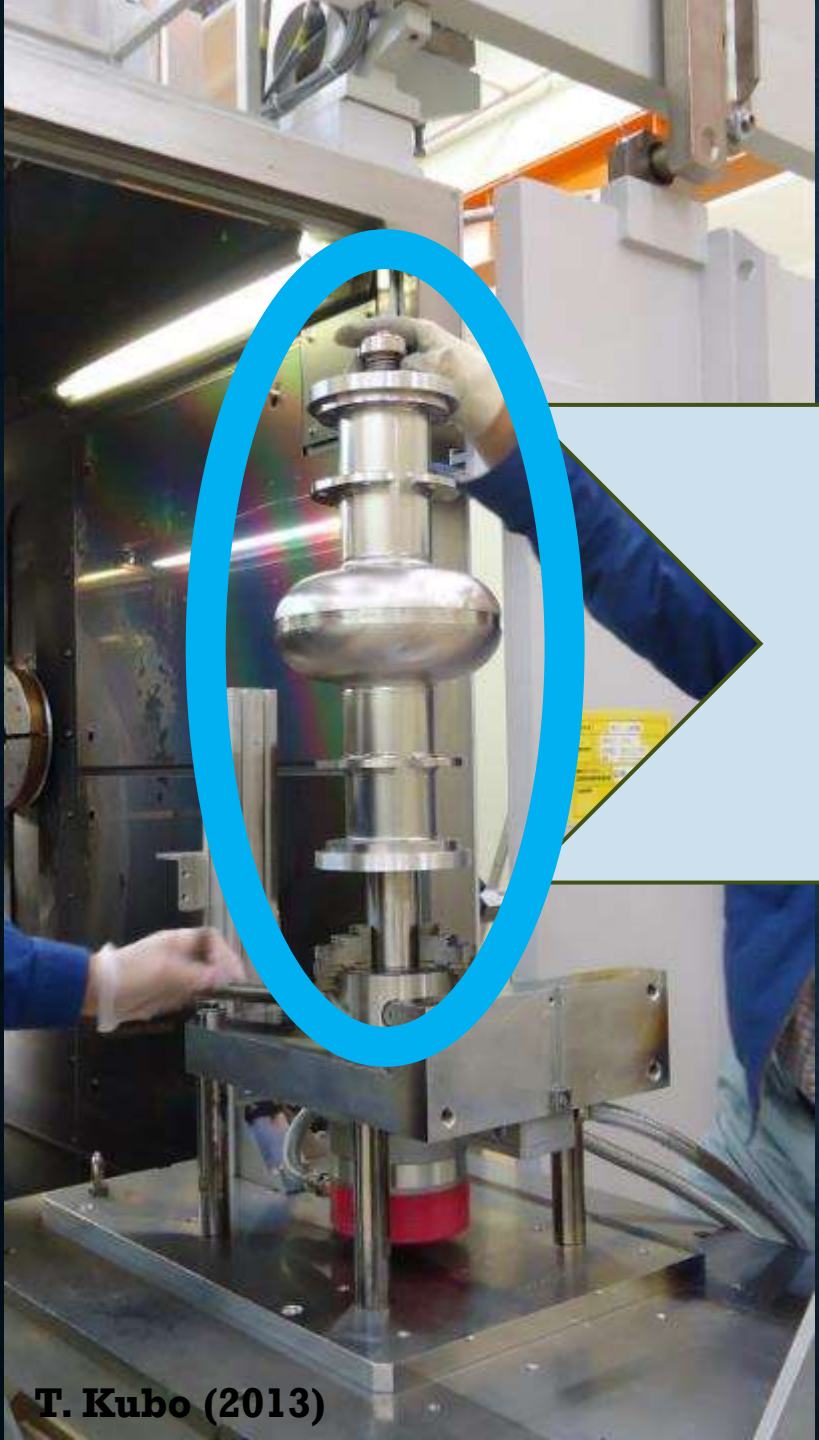
T Kubo et al., In-house production of a large-grain single-cell cavity at cavity fabrication facility and results of performance tests, IPAC2014, Dresden, Germany, WEPRI022, p.2519



S. Posen et al.,
Phys. Rev. Applied 13, 014024 (2020)

So why not make use of this technology in other applications?

Toward the Quantum Regime



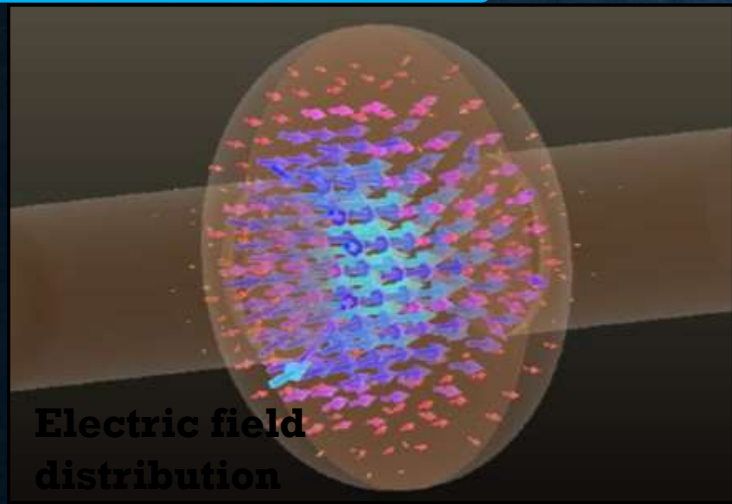
T. Kubo (2013)



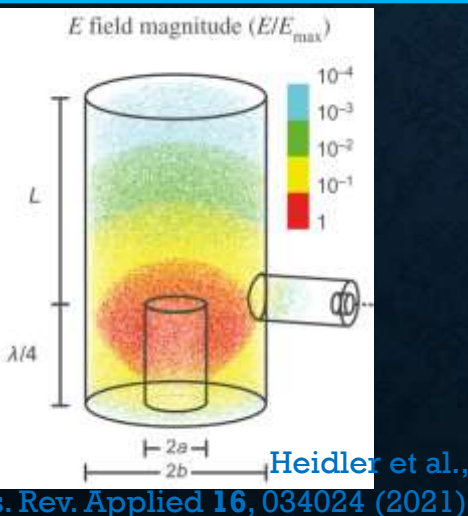
T. Kubo (2024)

The biggest differences between cavities for accelerators and those for quantum applications

Accelerators

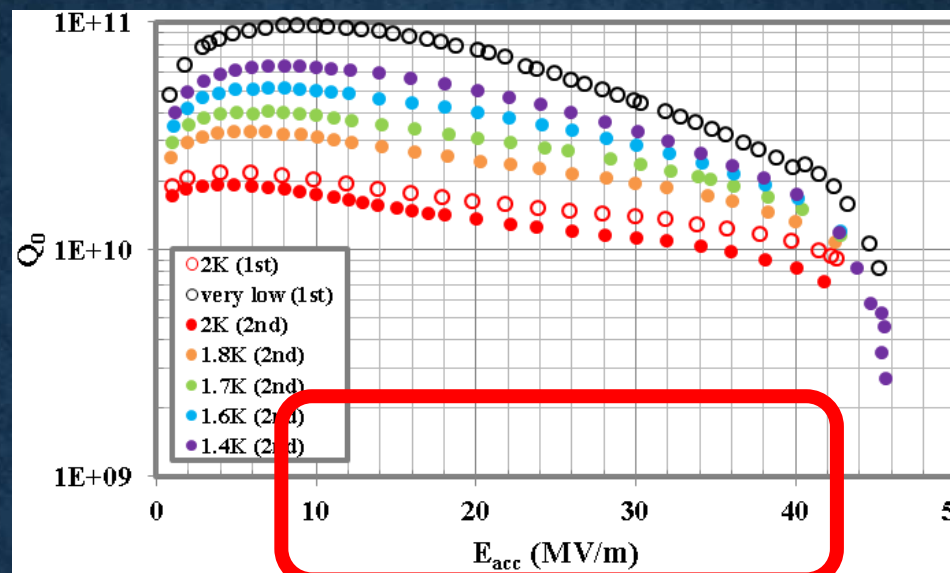
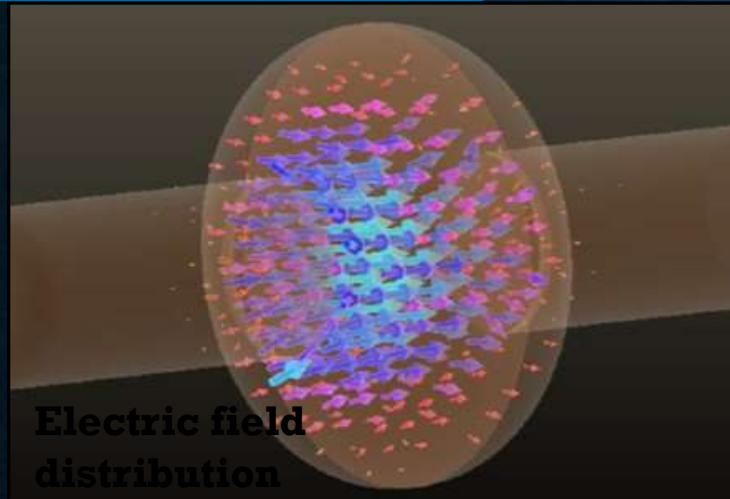


Quantum computing



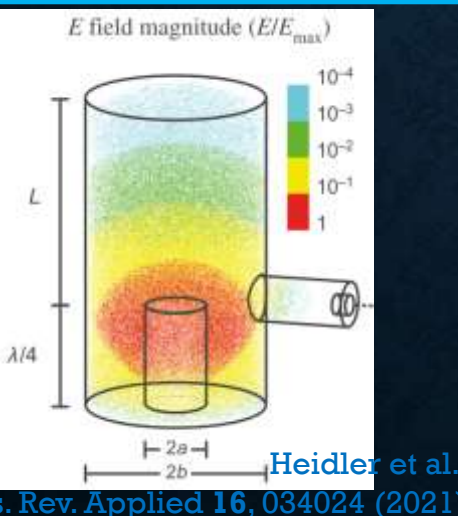
The biggest differences between cavities for accelerators and those for quantum applications

Accelerators

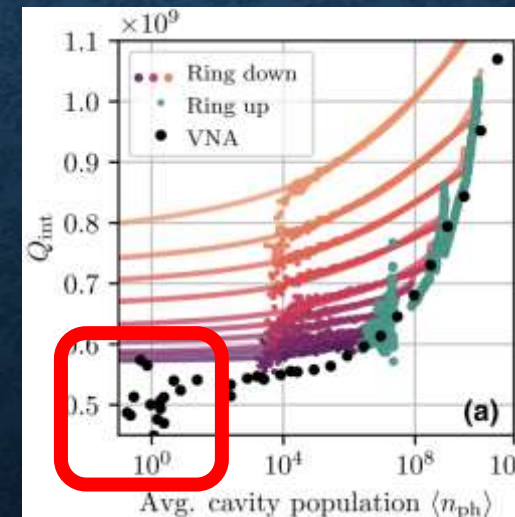


photon number $\langle n \rangle \sim 10^{25}$

Quantum computing



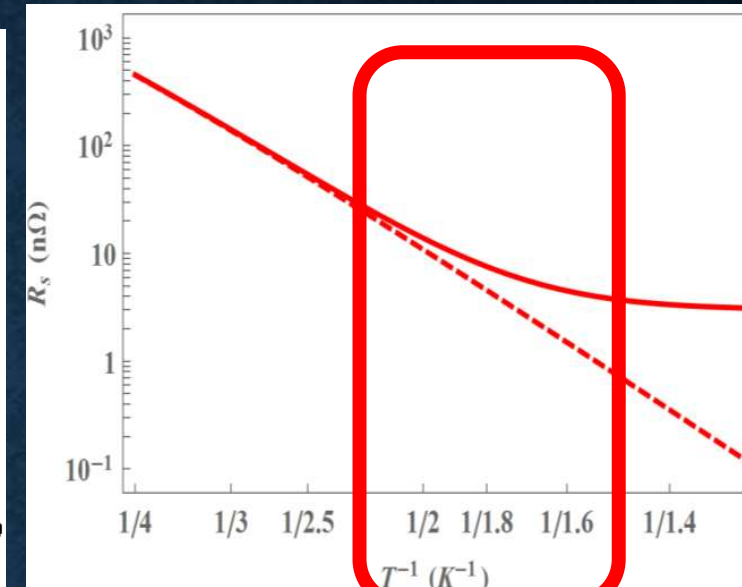
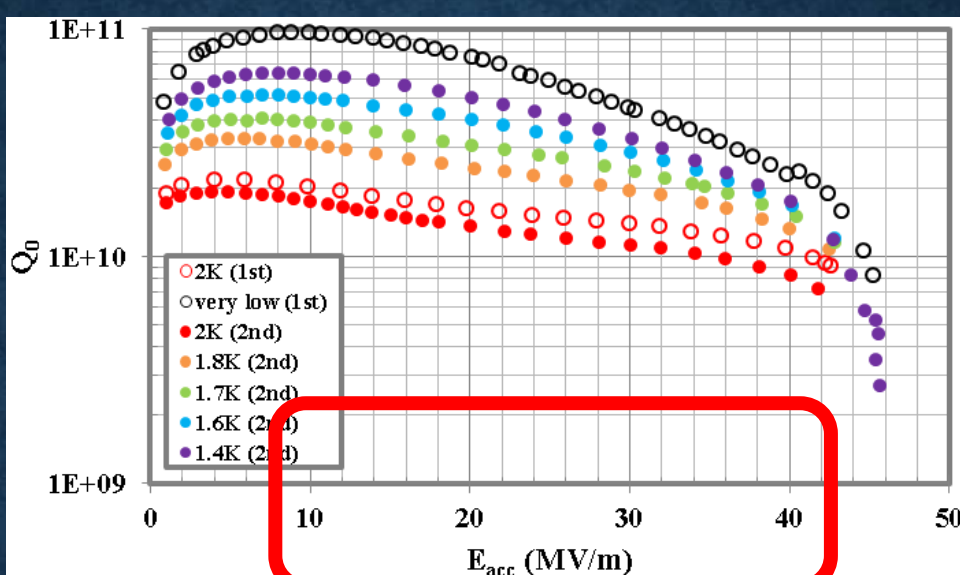
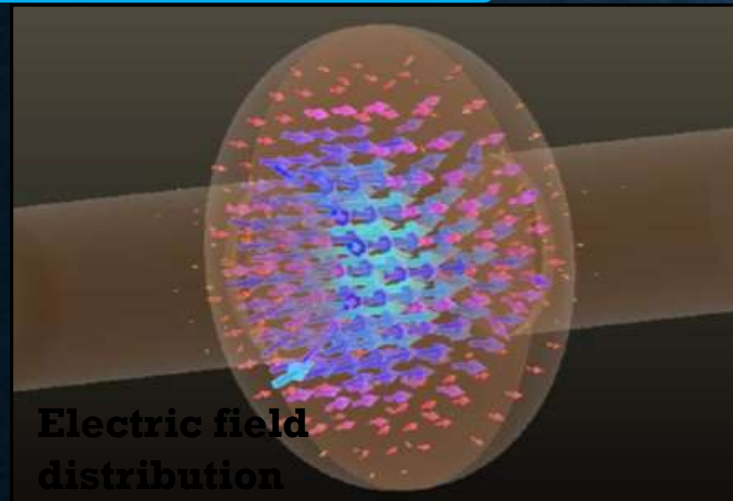
Heidler et al.,
Phys. Rev. Applied 16, 034024 (2021)



photon number $\langle n \rangle \sim 1$

The biggest differences between cavities for accelerators and those for quantum applications

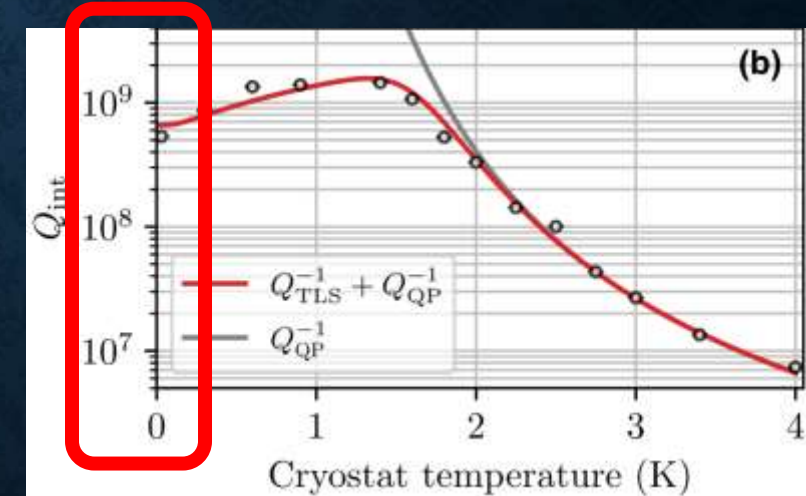
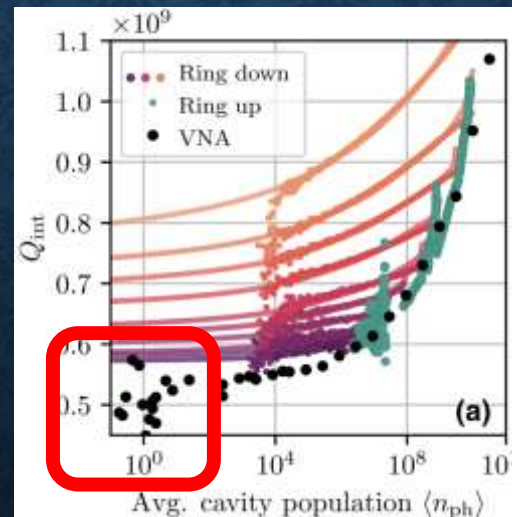
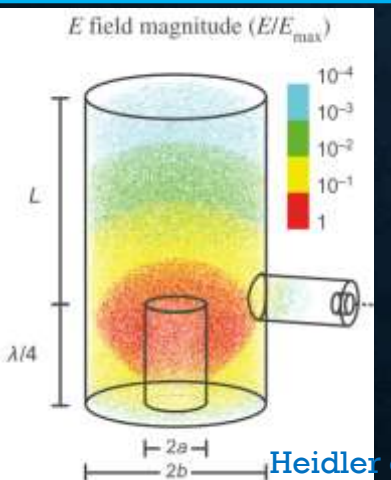
Accelerators



photon number $\langle n \rangle \sim 10^{25}$

$T \simeq 2$ K

Quantum computing



photon number $\langle n \rangle \sim 1$

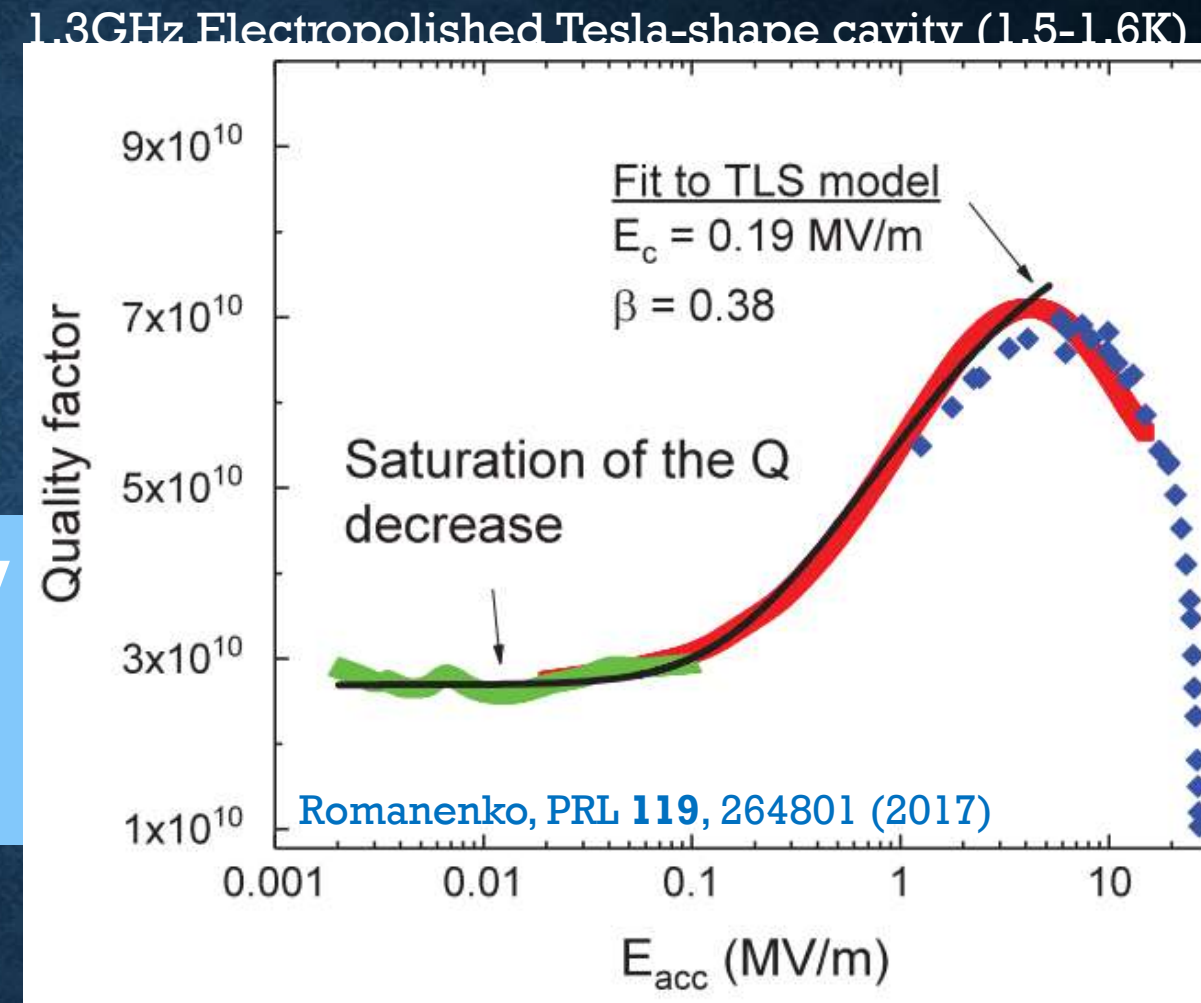
$T \simeq 20$ mK

**Can accelerator technology
deliver high Q even at
Quantum regime?**

**Can accelerator technology
deliver high Q even at
Quantum regime?**

YES

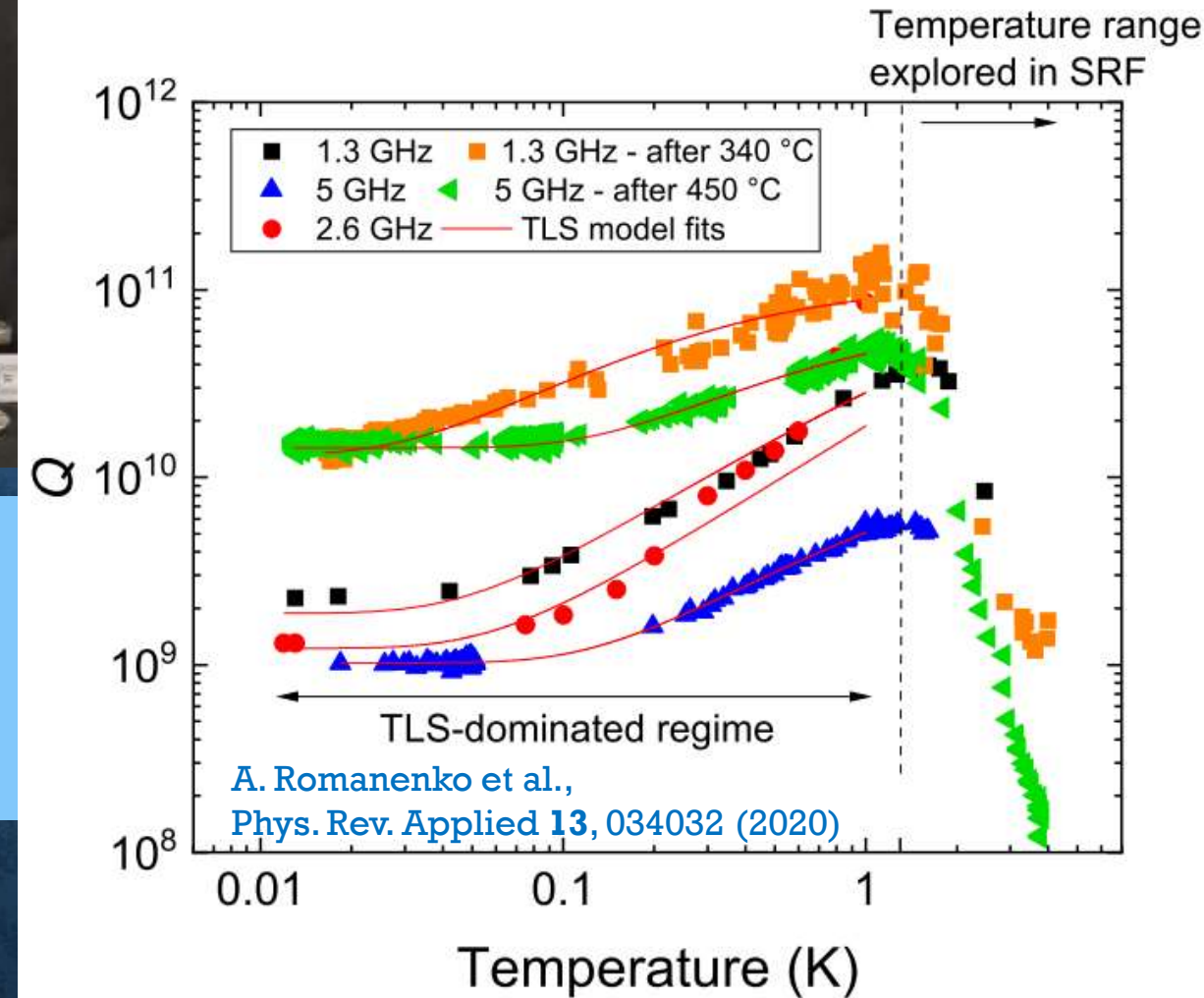
**Can accelerator technology
deliver high Q even at
Quantum regime?**



**The degradation of Q at low fields saturates
at $E_{\text{acc}} \lesssim 0.1 \text{ MV/m}$ (photon number $\langle n \rangle \lesssim 10^{20}$)**

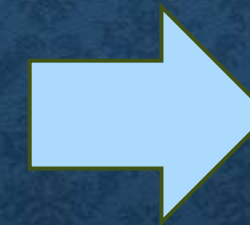
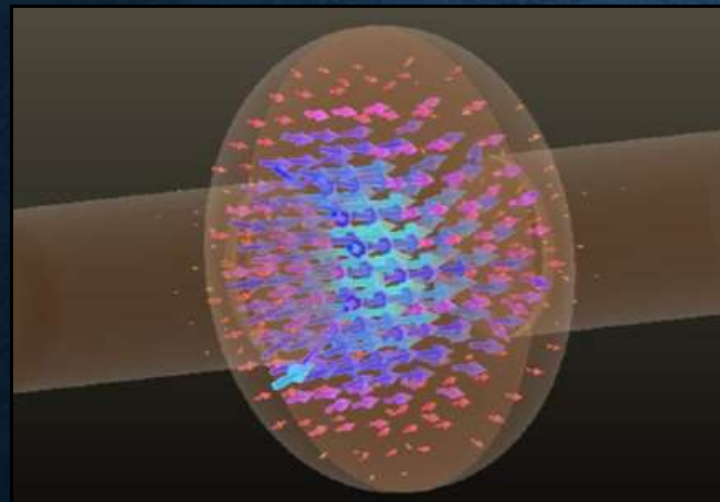


Can accelerator technology deliver high Q even at Quantum regime?

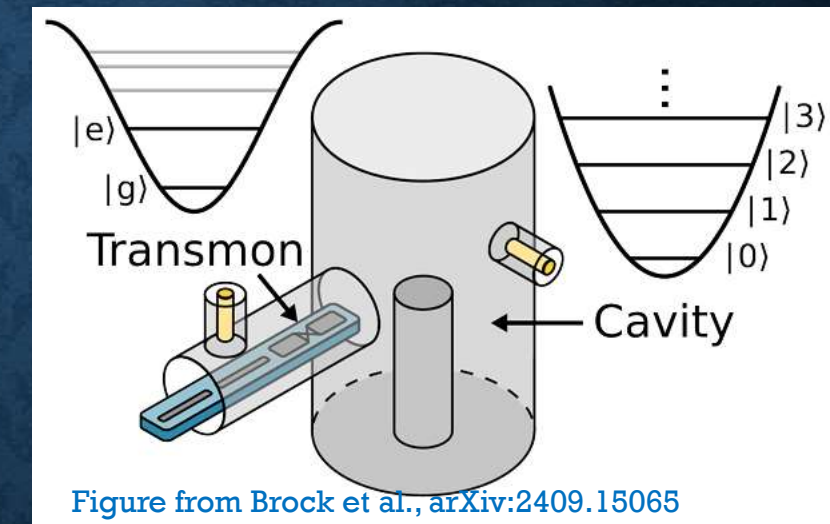


**Q degrades at low temperature,
but remains very high.**

Accelerator cavity

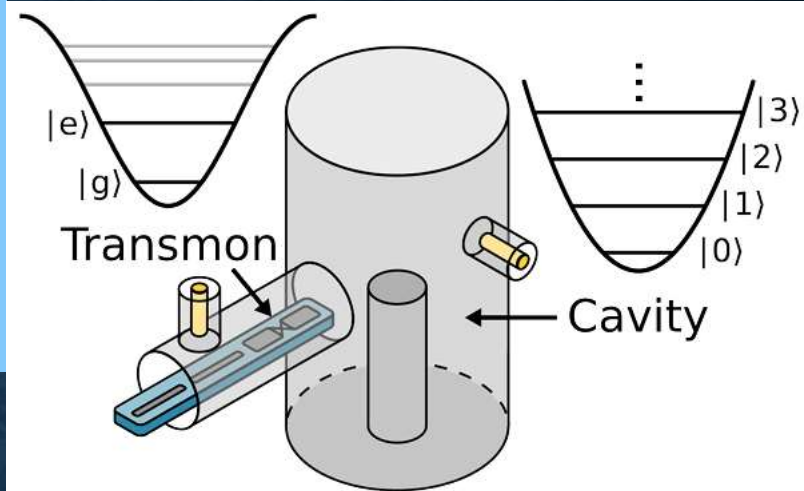


Quantum memory cavity for quantum computing



High-Q superconducting cavities allow us to store quantum information redundantly, enabling bosonic error correction.

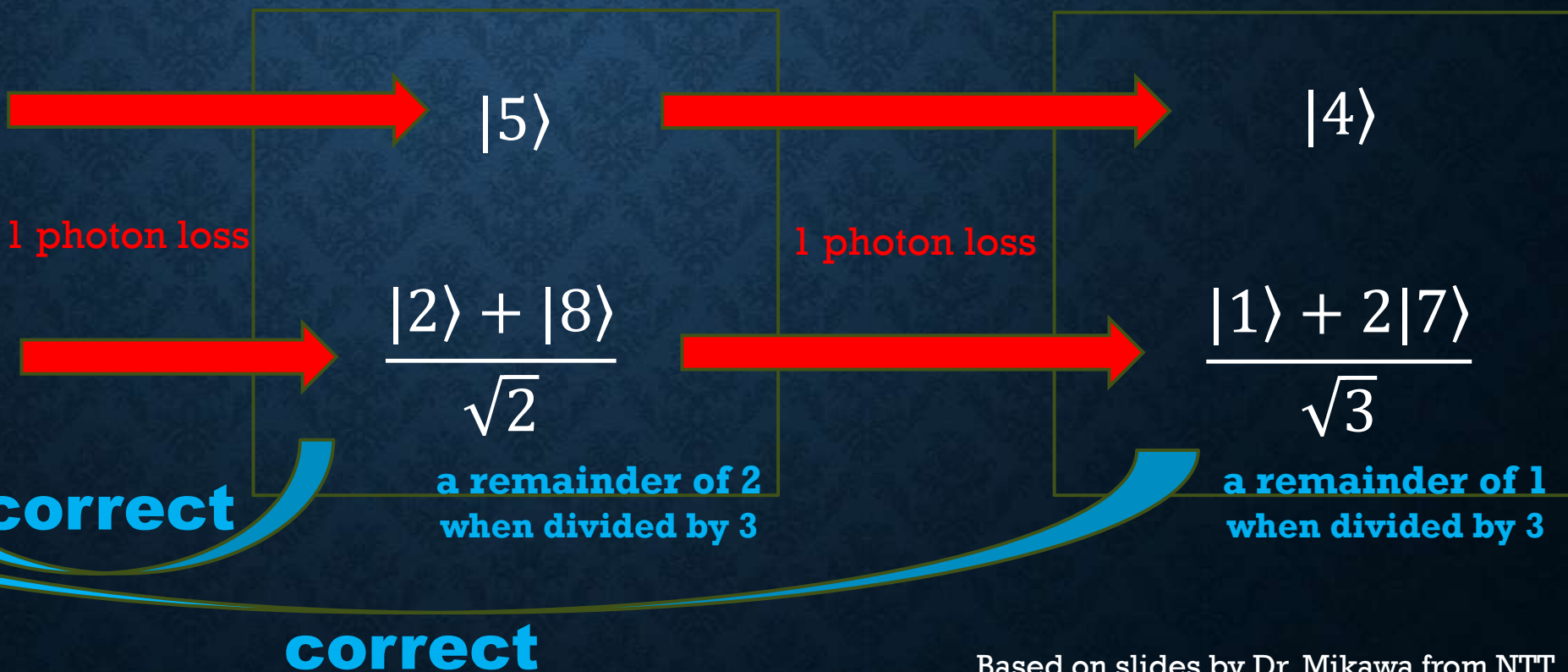
Figure from Brock et al., arXiv:2409.15065



Known to reduce the required number of qubits by one to two orders of magnitude.

e.g. binomial code

$$|0\rangle_L = \frac{|0\rangle + \sqrt{3}|6\rangle}{2}$$



$$|1\rangle_L = \frac{\sqrt{3}|3\rangle + |9\rangle}{2}$$

correct

a remainder of 2
when divided by 3

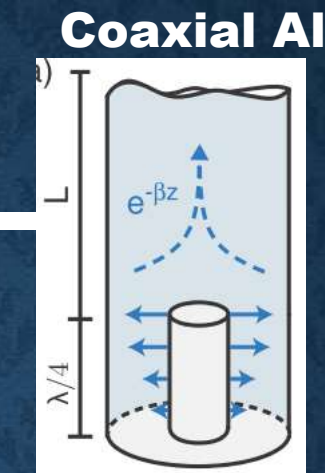
a remainder of 1
when divided by 3

correct

Based on slides by Dr. Mikawa from NTT

3D coaxial cavity progress

- Reagor et al., Phys. Rev. B **94**, 014506 (2016)
Aluminum,
4.25GHz, $Q = 7 \times 10^7$ ($\langle n \rangle \sim 1$)

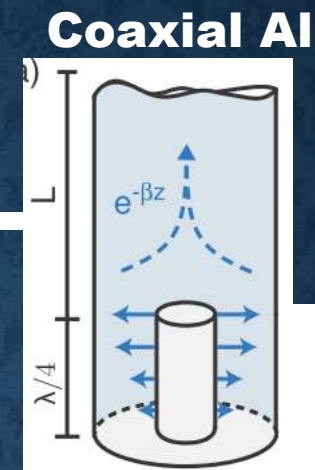


3D coaxial cavity progress

- Reagor et al., Phys. Rev. B **94**, 014506 (2016)

Aluminum,

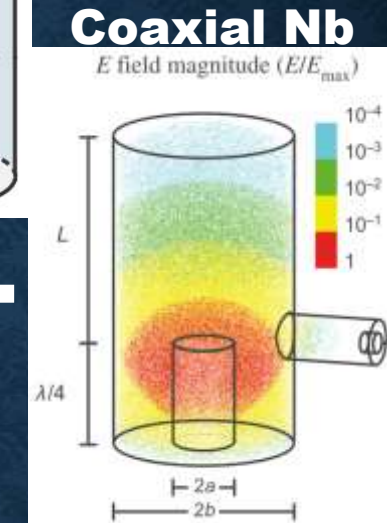
4.25GHz, $Q = 7 \times 10^7$ ($\langle n \rangle \sim 1$)



- Heidler et al., Phys. Rev. Applied **16**, 034024 (2021)

Niobium (1:1:1 buffered chemical polishing at 0-5°C),

7.9GHz, $Q = 5 \times 10^8$ ($\langle n \rangle \sim 1$)



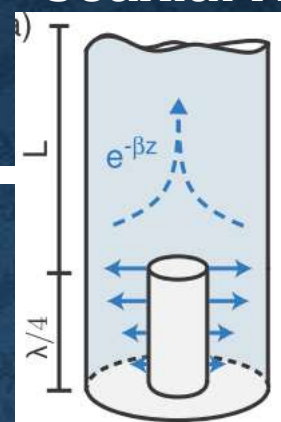
3D coaxial cavity progress

- Reagor et al., Phys. Rev. B **94**, 014506 (2016)

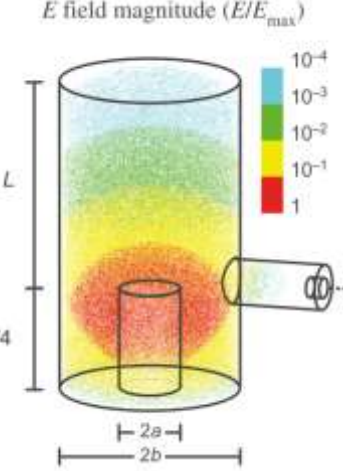
Aluminum,

4.25GHz, $Q = 7 \times 10^7$ ($\langle n \rangle \sim 1$)

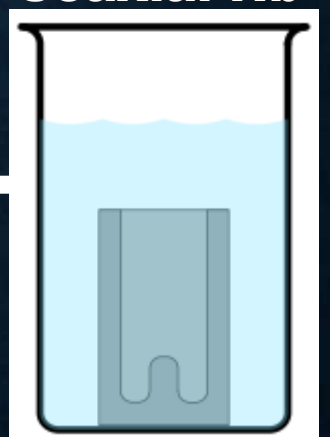
Coaxial Al



Coaxial Nb



Coaxial Nb



- Heidler et al., Phys. Rev. Applied **16**, 034024 (2021)

Niobium (1:1:1 buffered chemical polishing at 0-5°C),

7.9GHz, $Q = 5 \times 10^8$ ($\langle n \rangle \sim 1$)

- Oriani et al., Phys. Rev. Applied **24**, 044080 (2025)

Niobium (1:1:2 water buffered chemical polishing below 10°C),

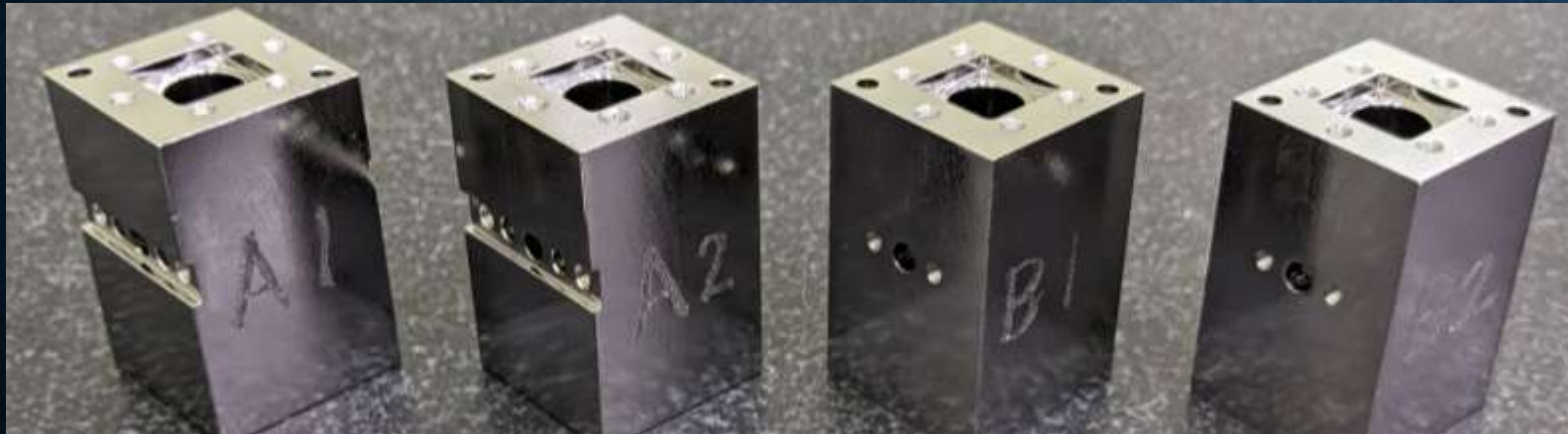
6.5GHz, $Q = 1.4 \times 10^9$ ($\langle n \rangle \sim 1$)



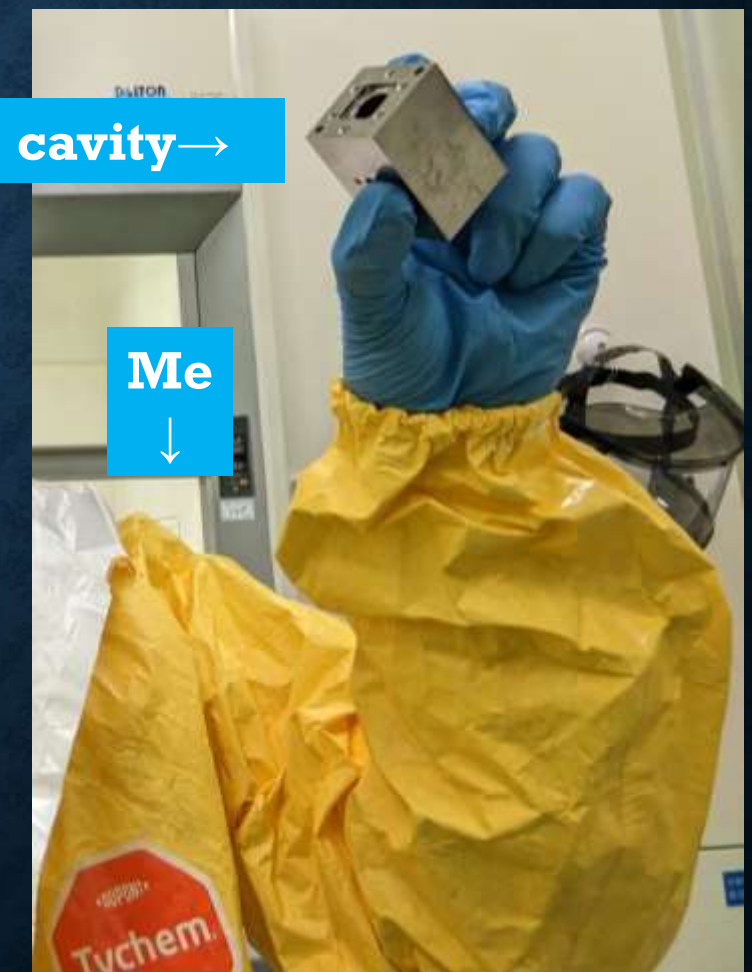
The world record (as of 2024)

Let's break the world record

Nb coaxial cavity of **KEK-NTT** collaboration



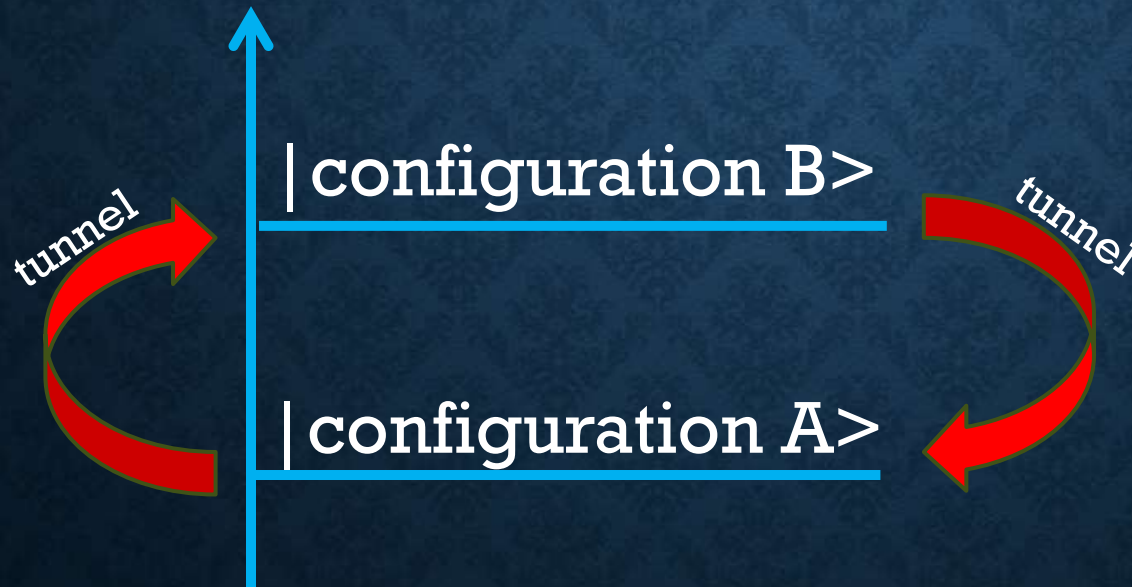
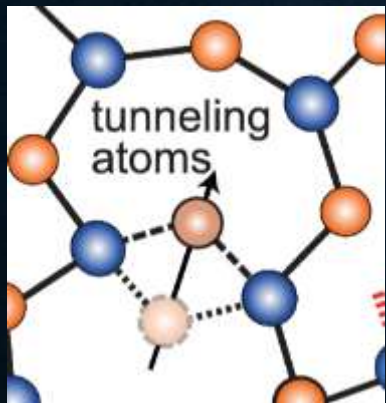
cavity→



The greatest enemy of SRF technology in quantum applications is the TLS defect.

Most amorphous solids show universal behavior at temperatures below a few kelvin.
This behavior can be explained by the well-established “*standard tunneling model*”.

Two-level system (TLS) defects



See also a review paper:

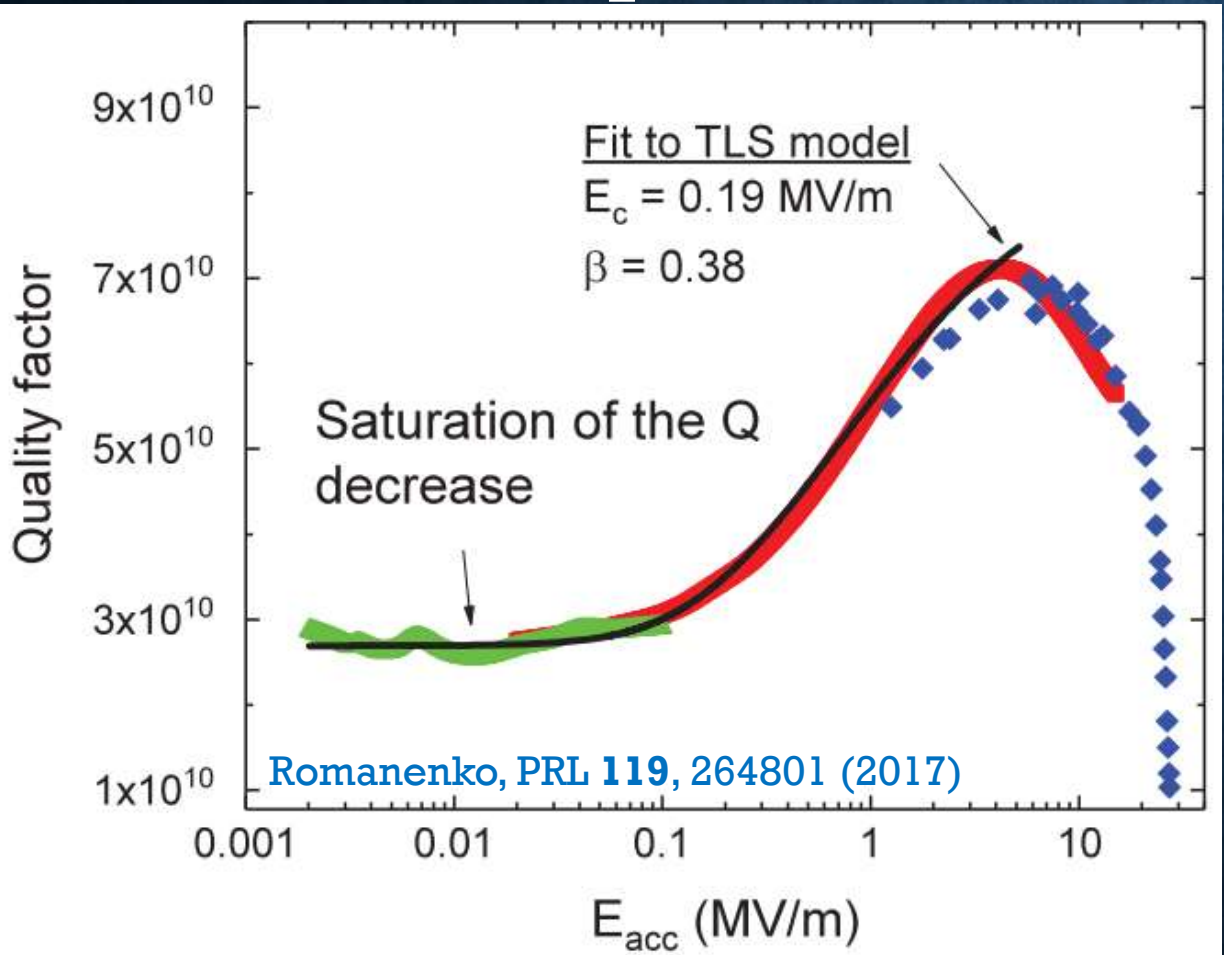
Müller et al Rep. Prog. Phys. **82**, 124501 (2019)

The dipoles formed in this way couple to the electric field and cause dielectric loss.

$$\frac{1}{Q_{\text{int}}(\bar{n})} = F \delta_{\text{TLS}}^0 \frac{\tanh\left(\frac{hf_r}{2kT}\right)}{\sqrt{1 + \left(\frac{\bar{n}}{n_c}\right)^\beta}} + \frac{1}{Q_{\text{res}}},$$

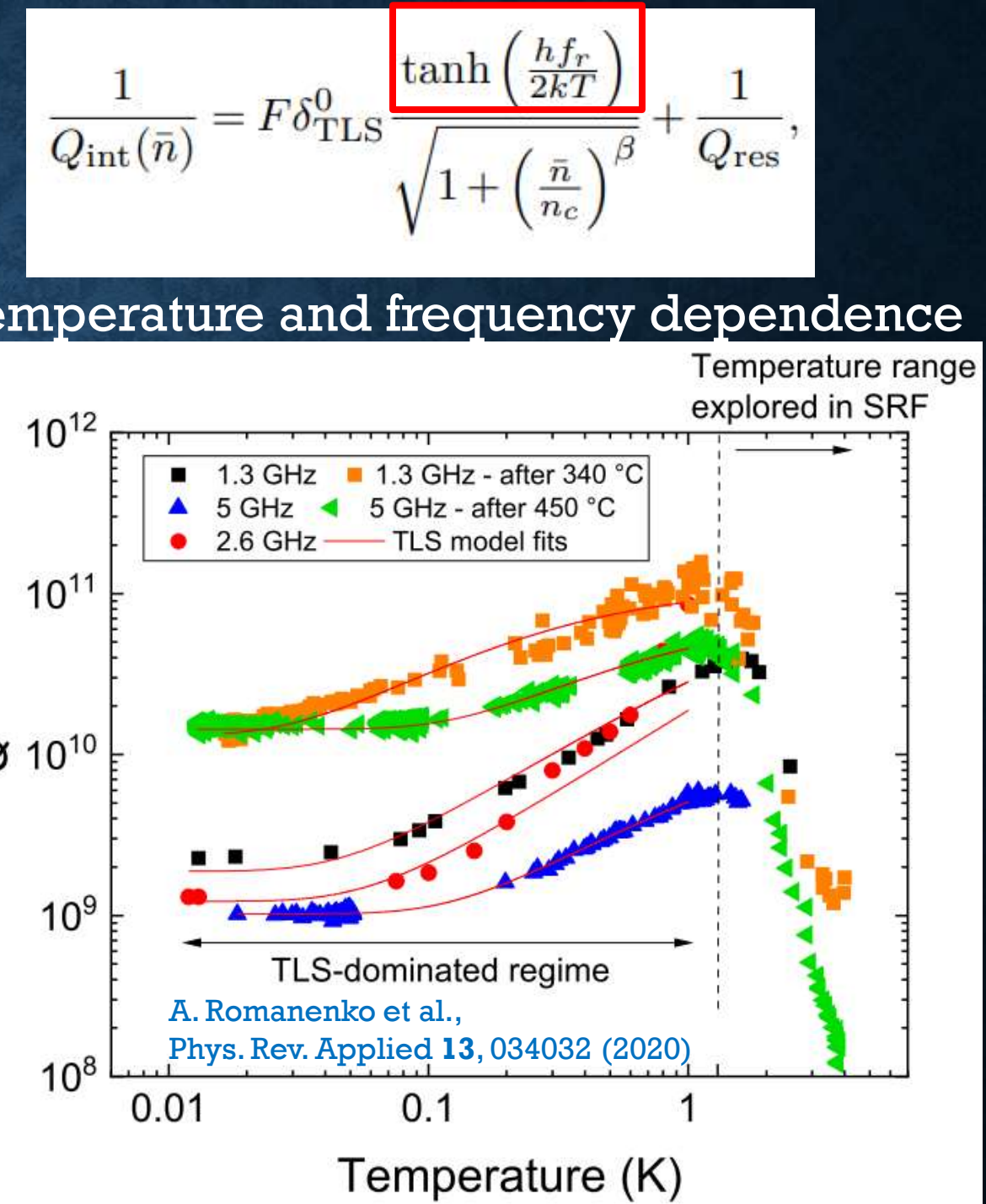
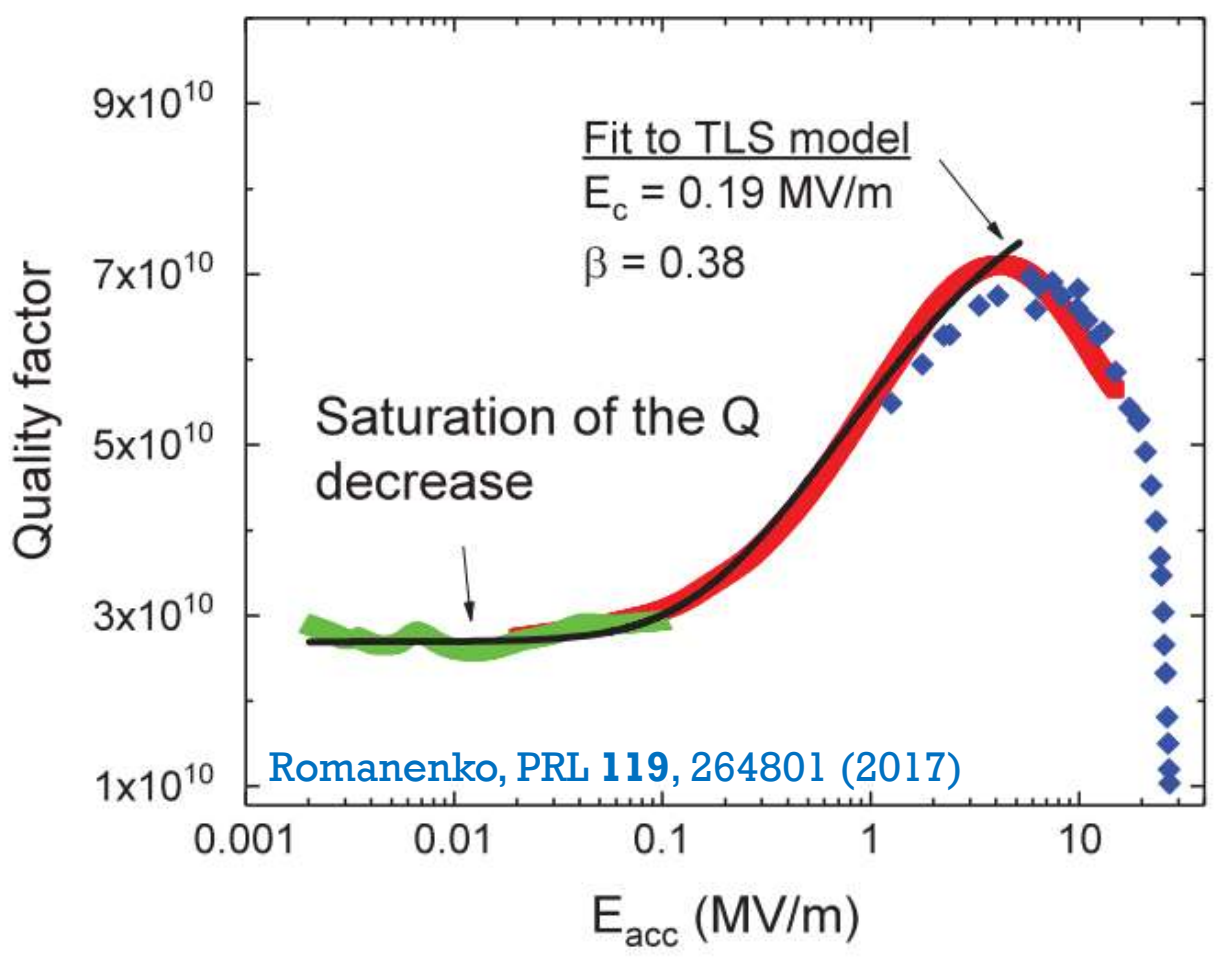
$$\frac{1}{Q_{\text{int}}(\bar{n})} = F \delta_{\text{TLS}}^0 \frac{\tanh\left(\frac{hf_r}{2kT}\right)}{\sqrt{1 + \left(\frac{\bar{n}}{n_c}\right)^\beta}} + \frac{1}{Q_{\text{res}}},$$

Field dependence

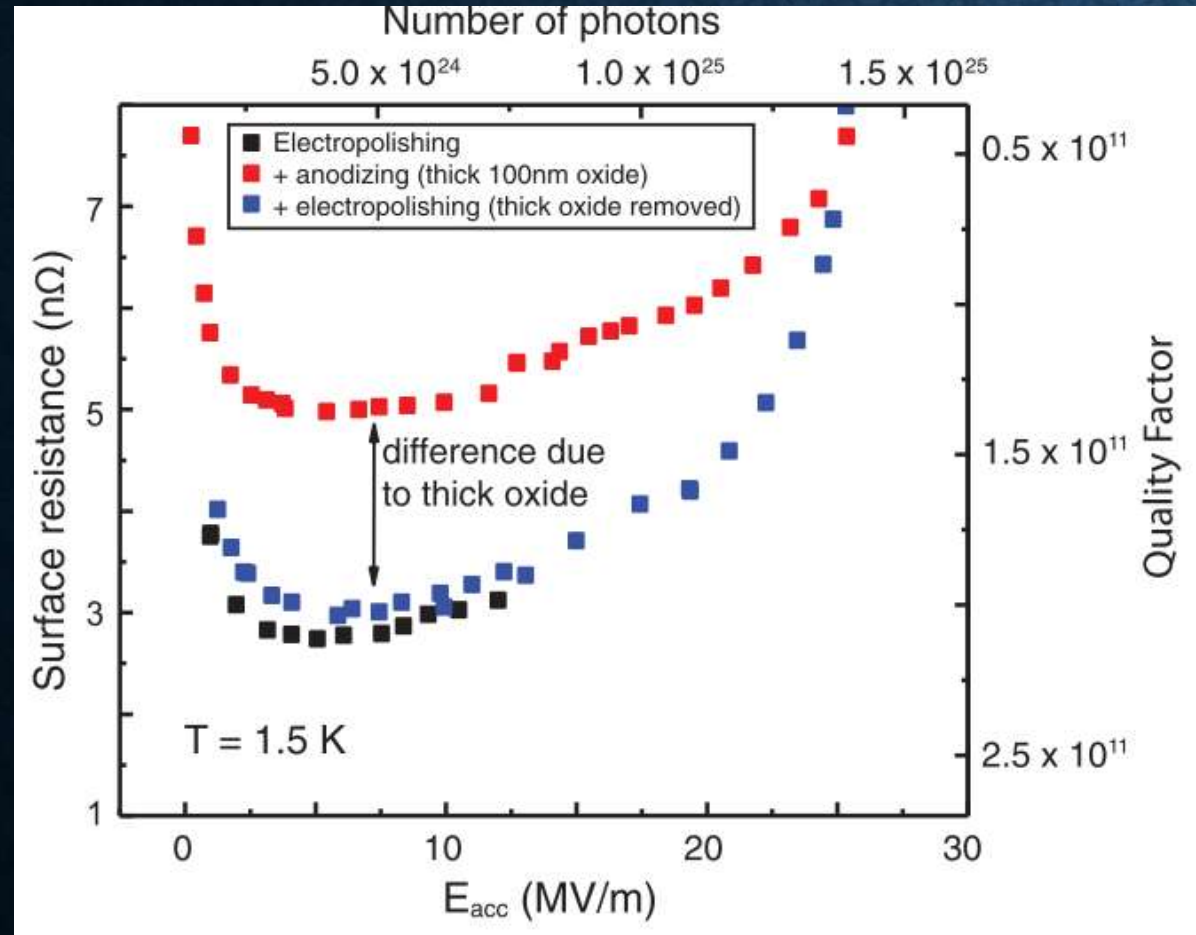


$$\frac{1}{Q_{\text{int}}(\bar{n})} = F\delta_{\text{TLS}}^0 \frac{\tanh\left(\frac{hf_r}{2kT}\right)}{\sqrt{1 + \left(\frac{\bar{n}}{n_c}\right)^\beta}} + \frac{1}{Q_{\text{res}}},$$

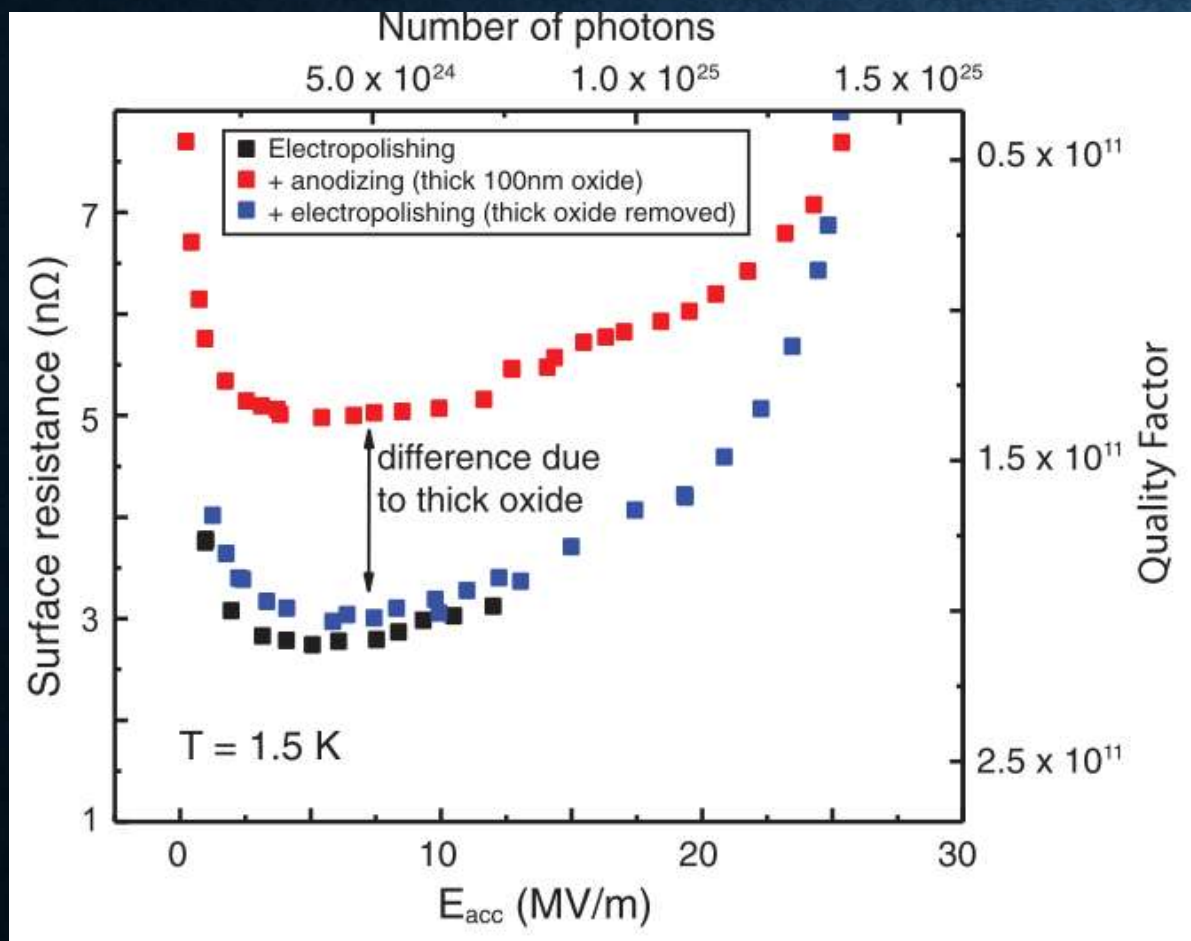
Field dependence



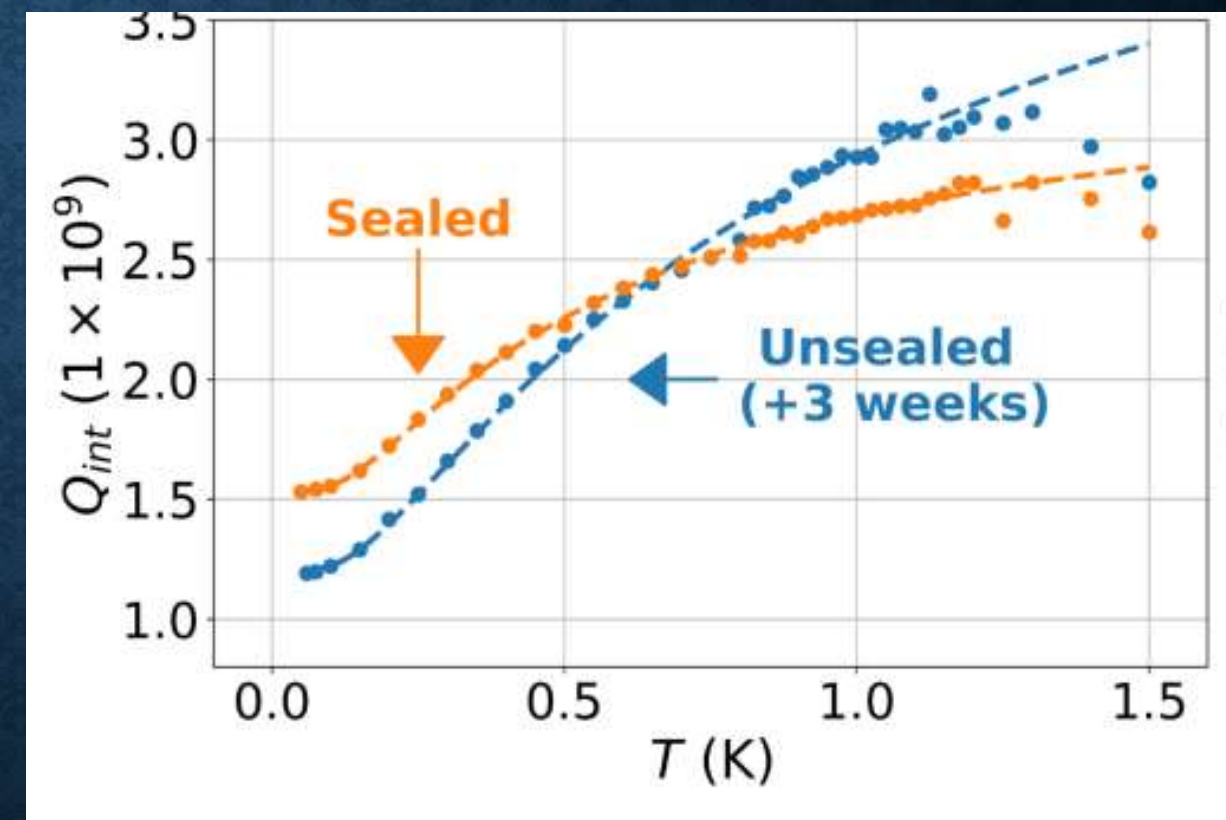
TLSS live in the oxide layer on the inner surface of the niobium cavity.



TLSS live in the oxide layer on the inner surface of the niobium cavity.
The oxide inevitably regrows after any surface treatment.
Whether TLSSs can be reduced by surface treatment is not obvious.



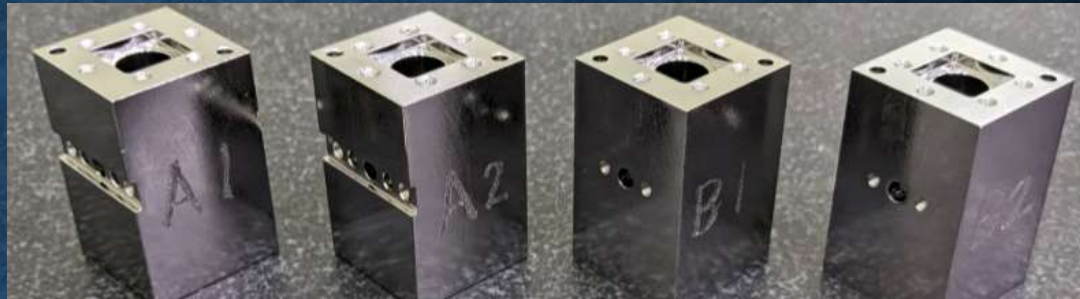
Romanenko, PRL 119, 264801 (2017)



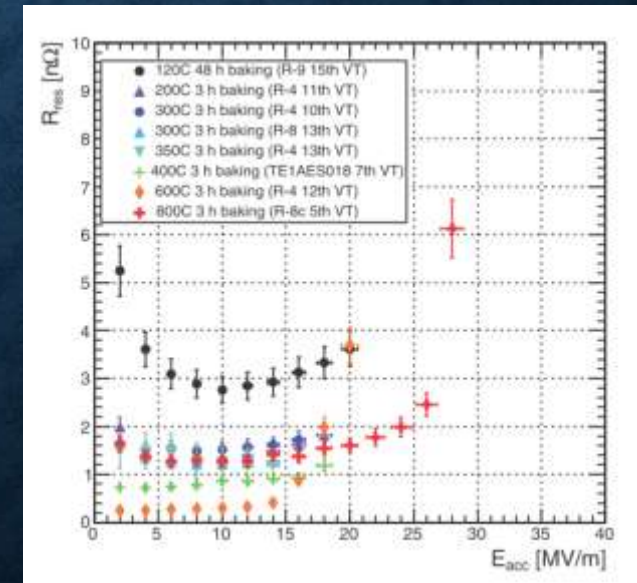
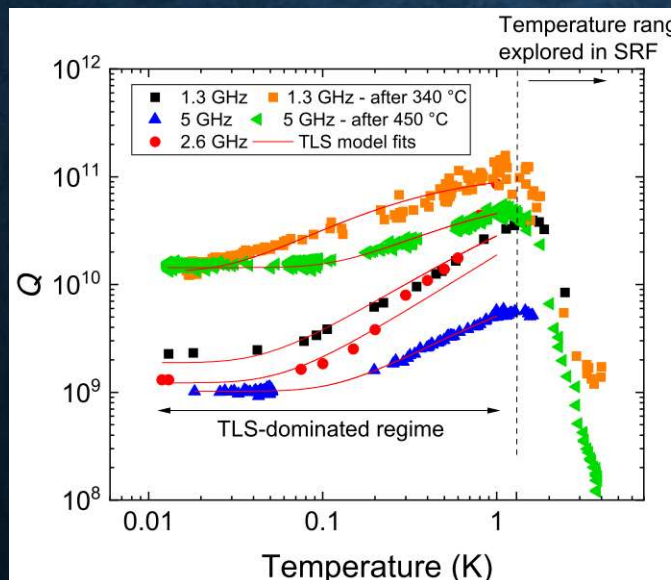
Oriani et al., arXiv:2403.00286

We applied accelerator-type surface treatments to the quantum cavity, while omitting processes intended for high-gradient operation.

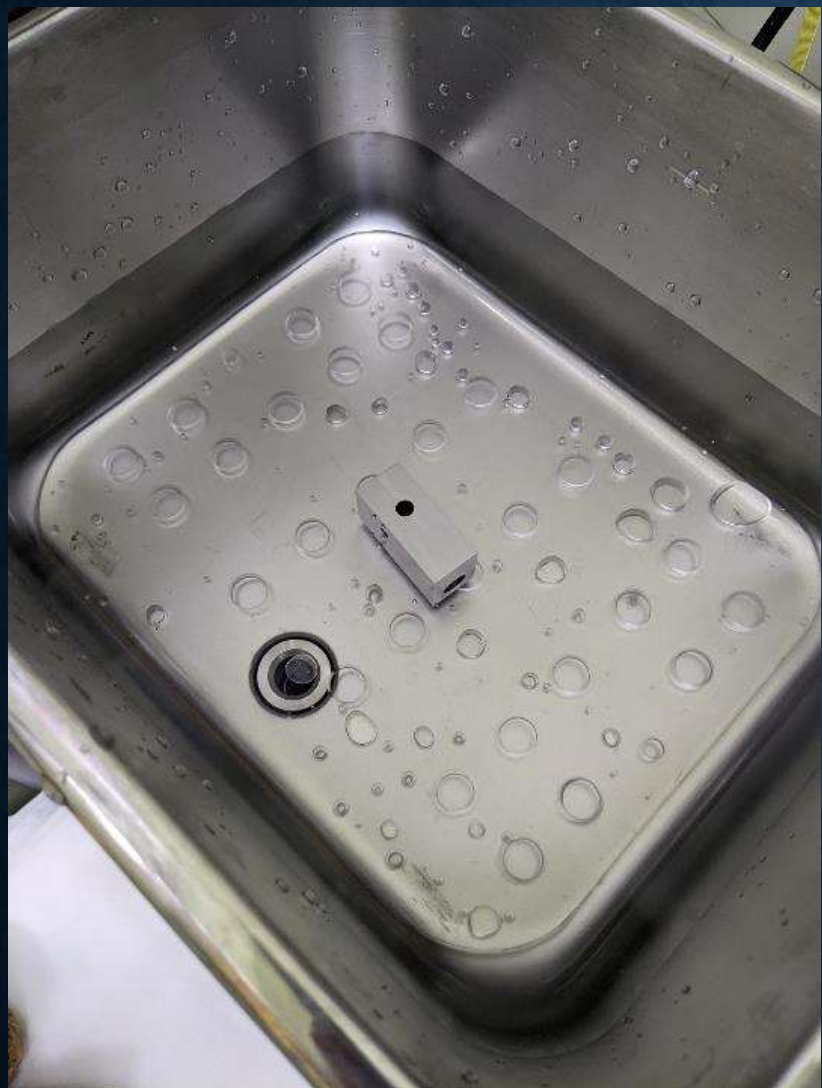
1. Removal of approximately $100\ \mu\text{m}$ of material from the inner surface using buffered chemical polishing (BCP) at room temperature ($\gtrsim 20^\circ\text{C}$).
2. Baking the cavity in a vacuum furnace at 900°C for 3 hours (high-T bake).
3. Light BCP ("BCP flush") to remove a few additional micrometers of material.
4. Additional treatment for surface optimization



Prior work suggests a possible route: despite inevitable regrowth, a **mid-temperature bake** that disrupts the oxide may help.



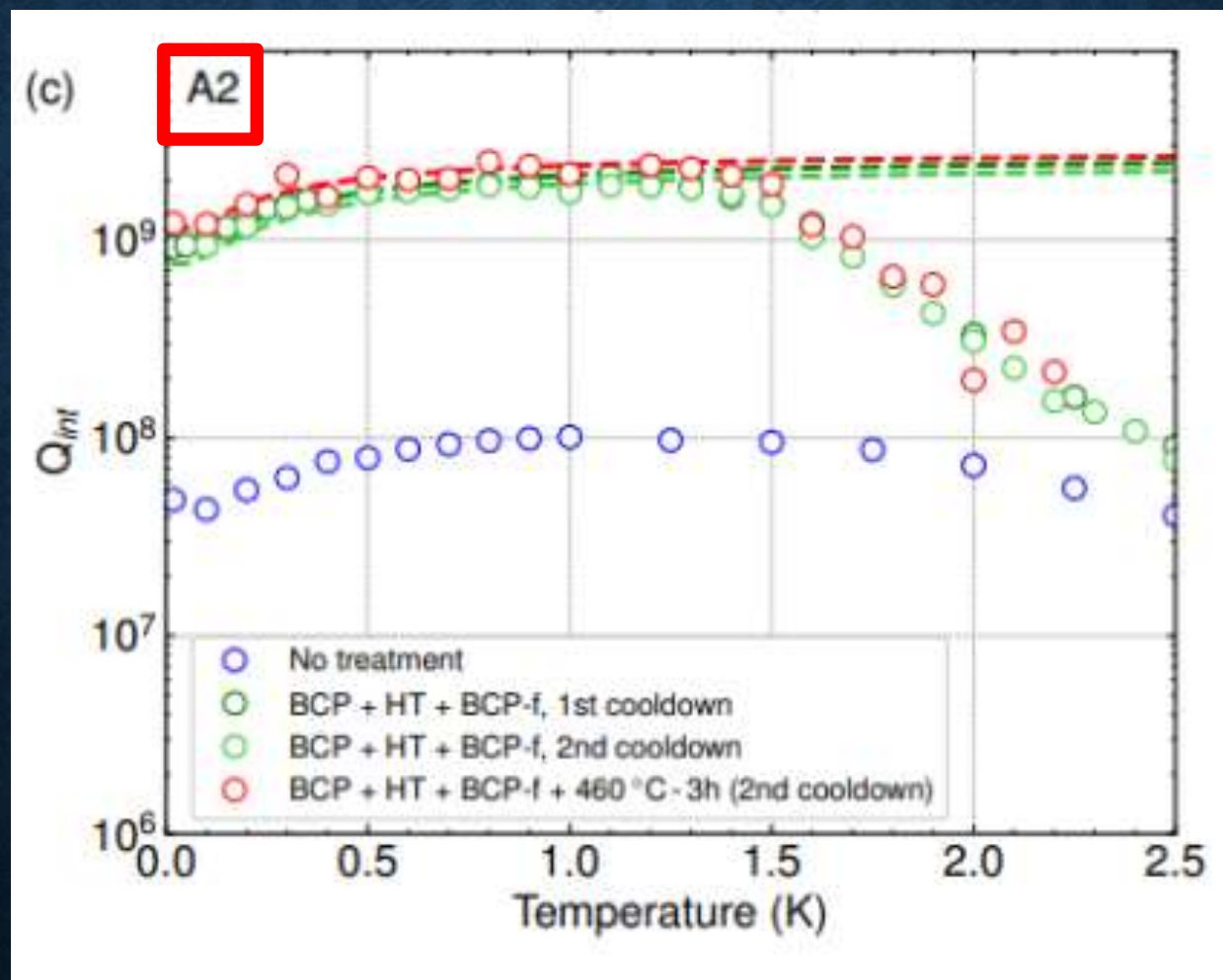
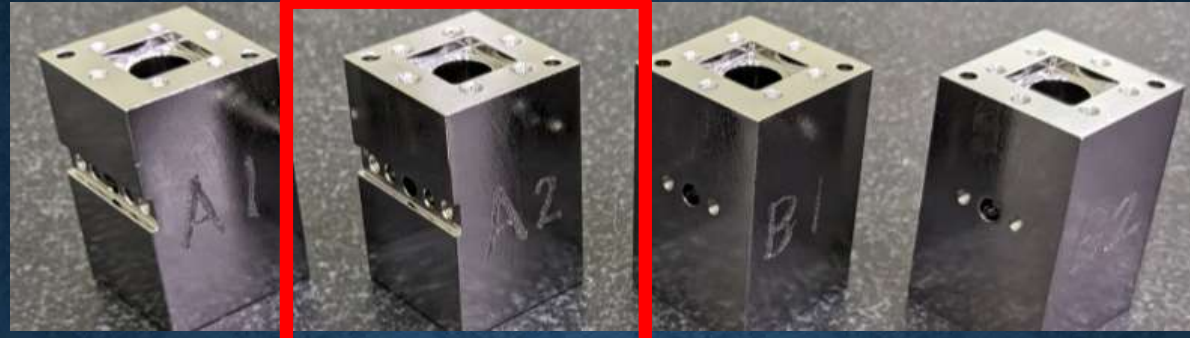
Ultrasonic cleansing



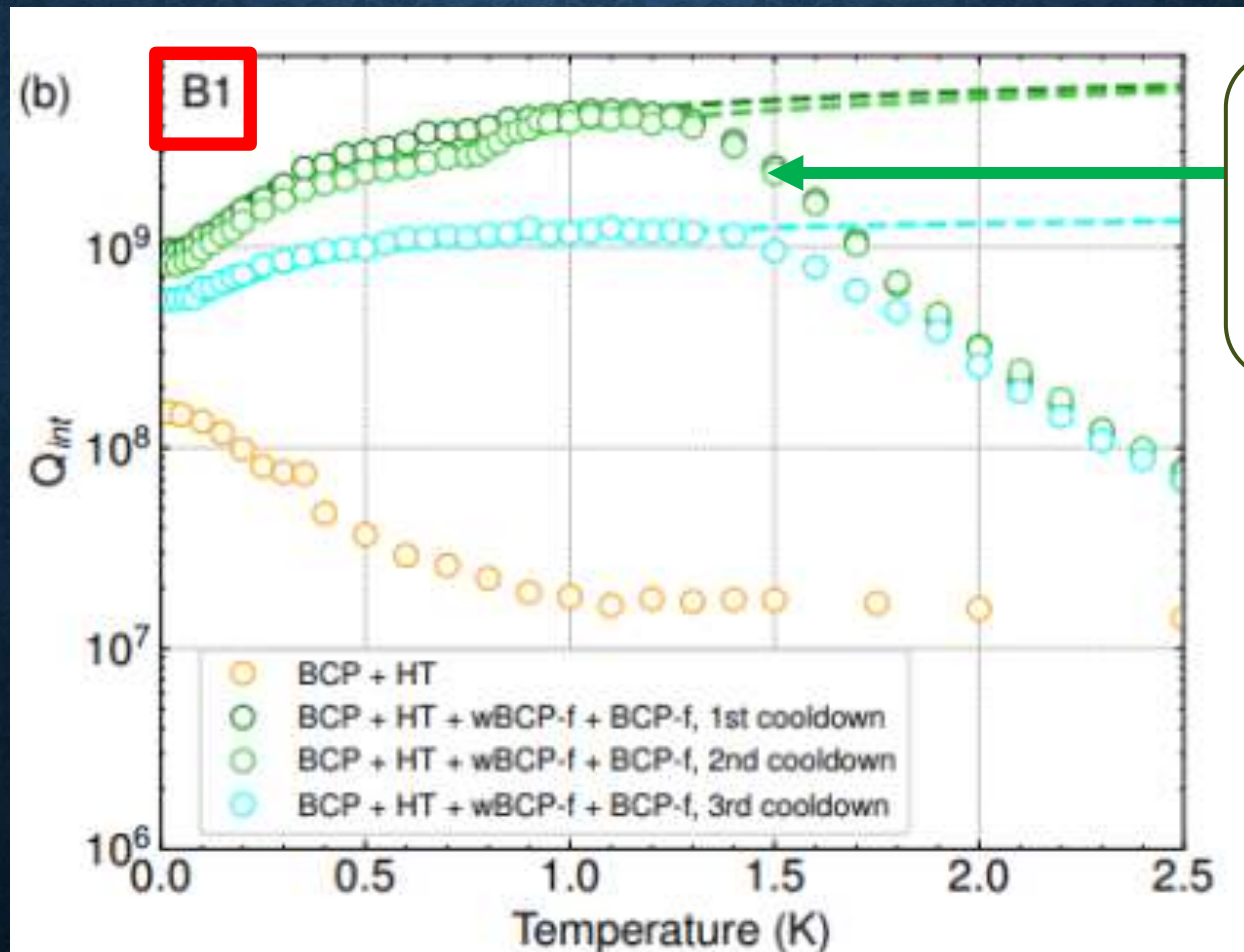
Buffered Chemical Polishing (BCP)



comparable to
the world record→

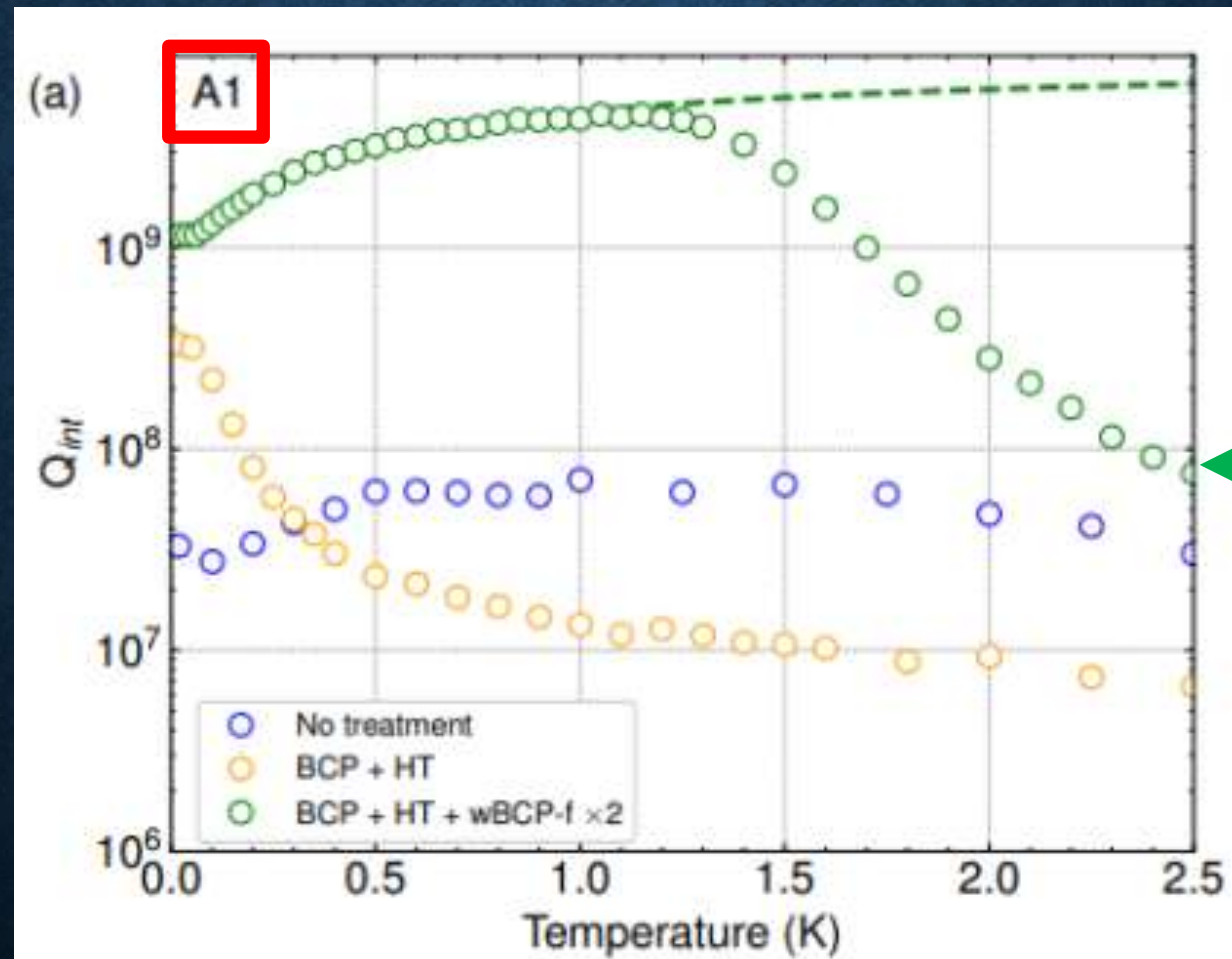


comparable to
the world record→

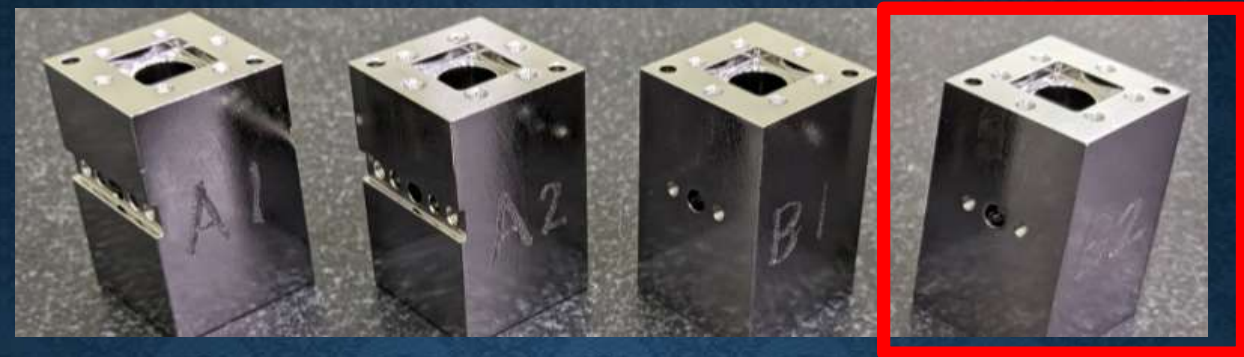


Room temperature
wBCP (1:1:1) flush
vBCP=water buffered CP

comparable to
the world record→

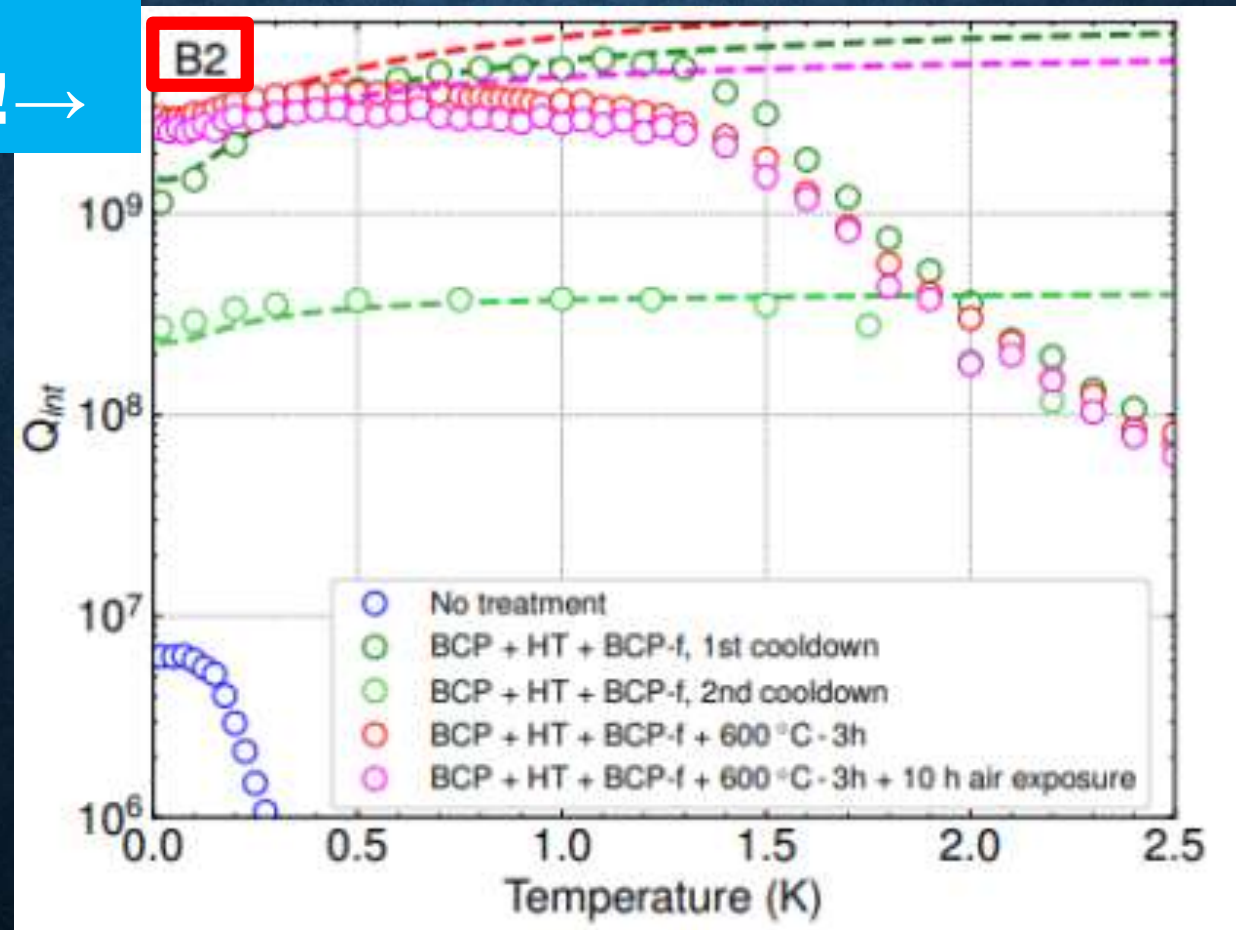


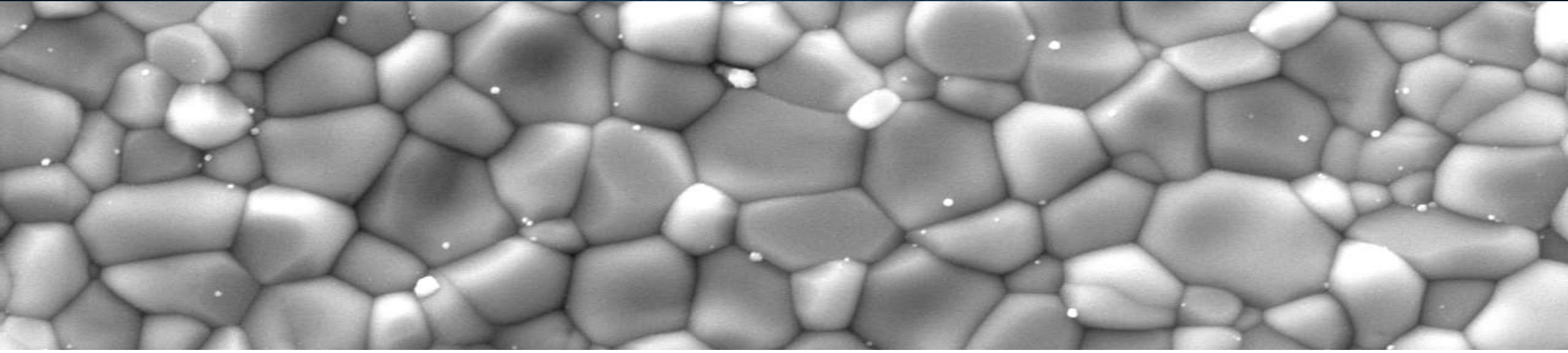
← Cold (5°C)
wBCP (1:1:2) flush
wBCP=water buffered CP



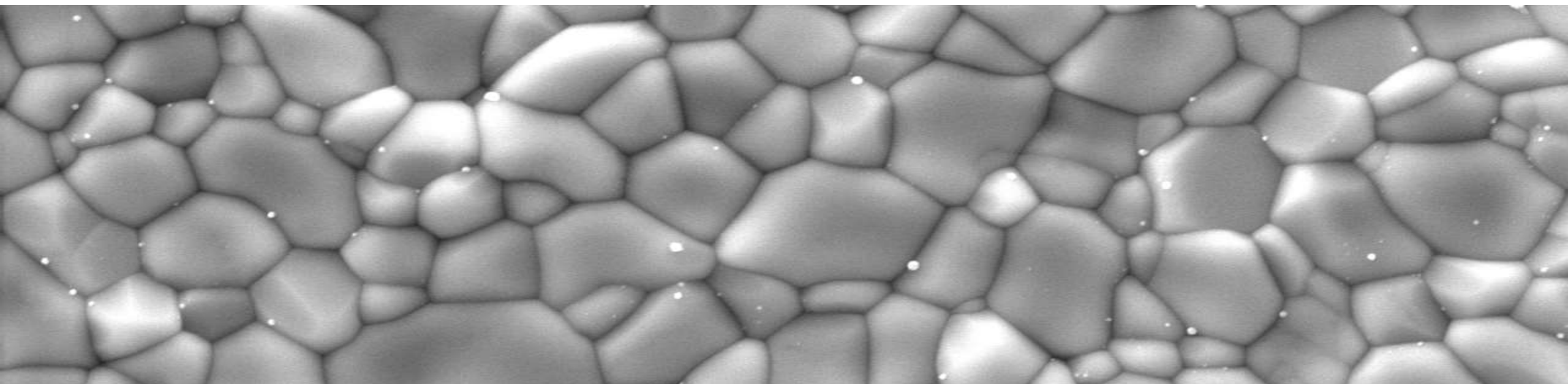
We broke
the world record!!! →

Corresponding to
photon lifetime of ~0.1 sec.





Nb₃Sn cavity



SU70 15.0kV 15.2mm x7.00k SE(M)

Courtesy of Hayato Ito (KEK)

5.00um

Thanks to its higher T_c ,
 Nb_3Sn achieves $Q(4\text{ K})$
comparable to Nb at 2 K.

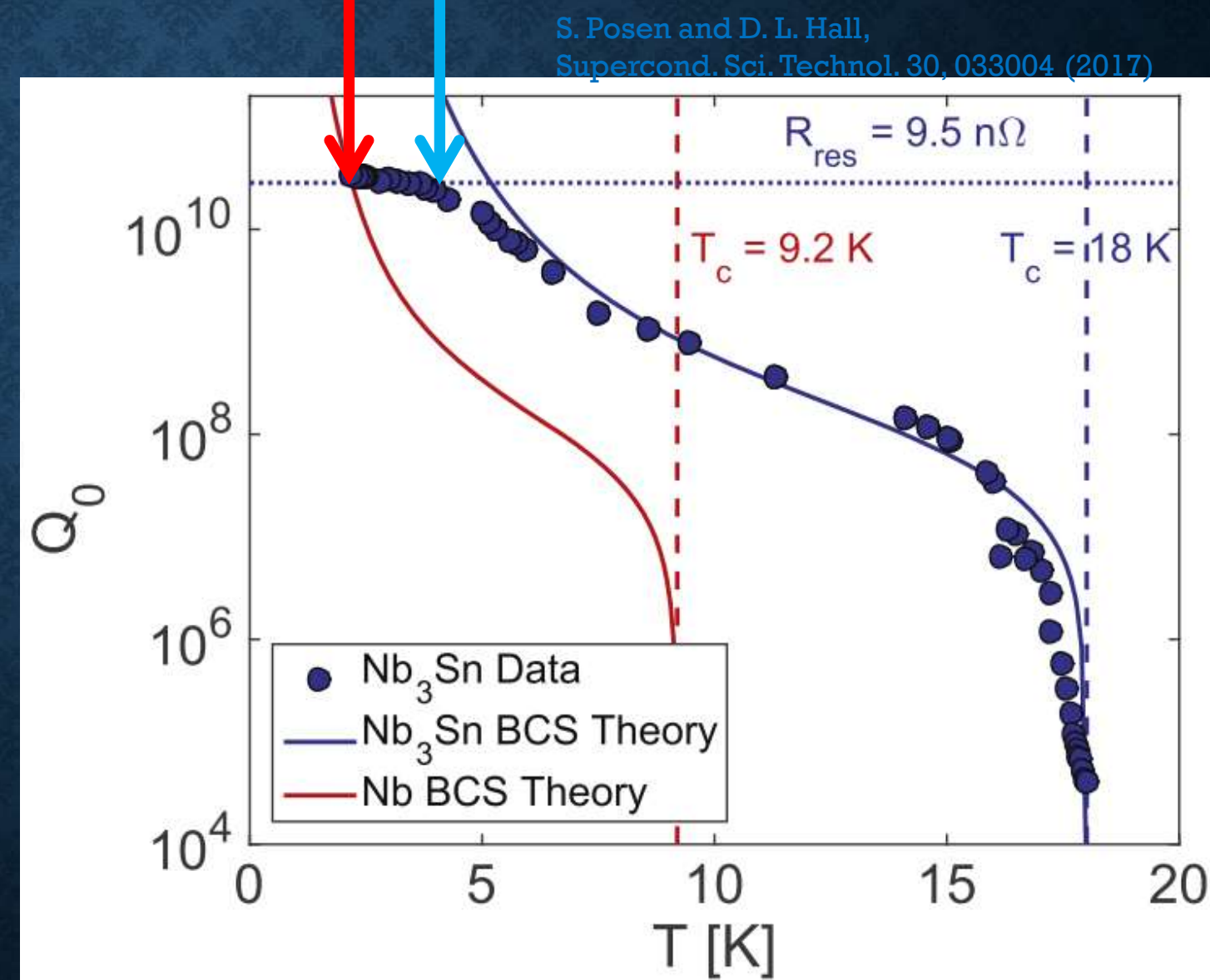
Note that cryogenic efficiency at 4 K is approximately 3 to 4 times higher than at 2 K.



**4 K Accelerator Operation
with Cryocoolers**

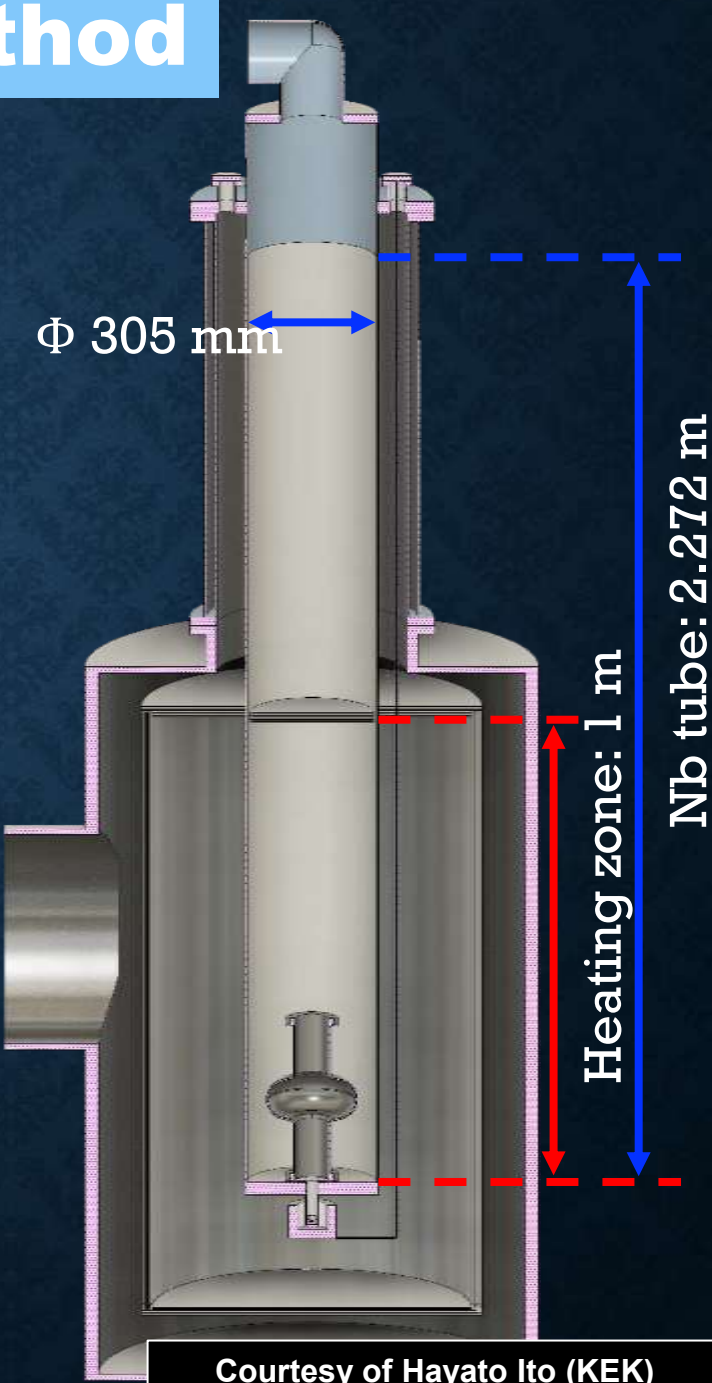
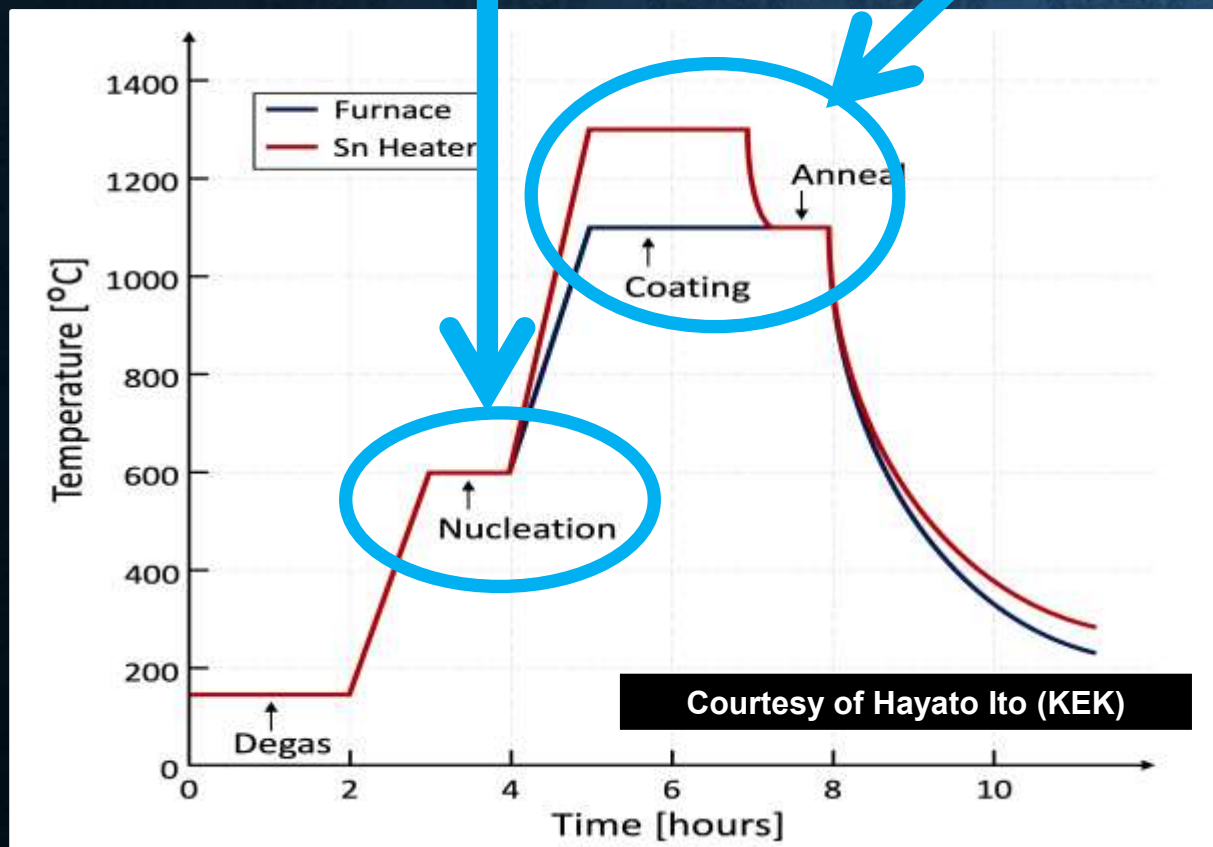
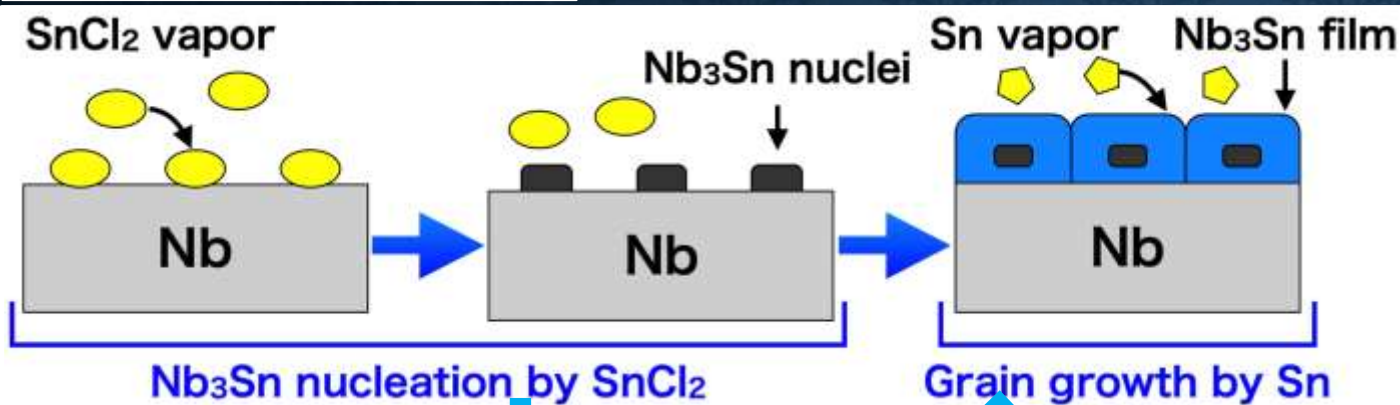
**$Q(\text{Nb}) \sim 10^{10}$
at 2 K**

**$Q(\text{Nb}_3\text{Sn}) \sim 10^{10}$
at 4 K**

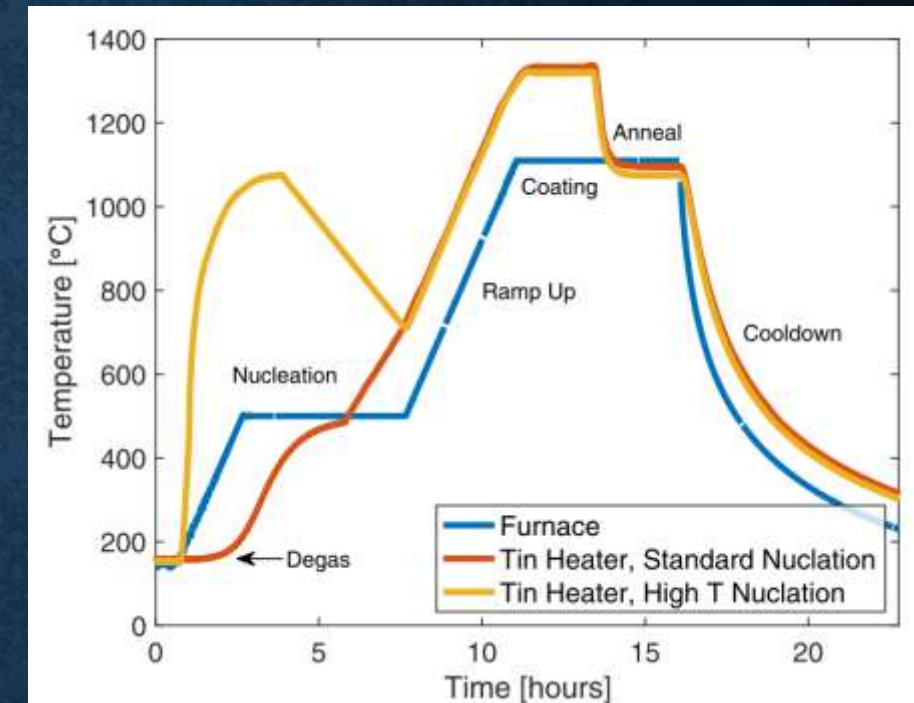
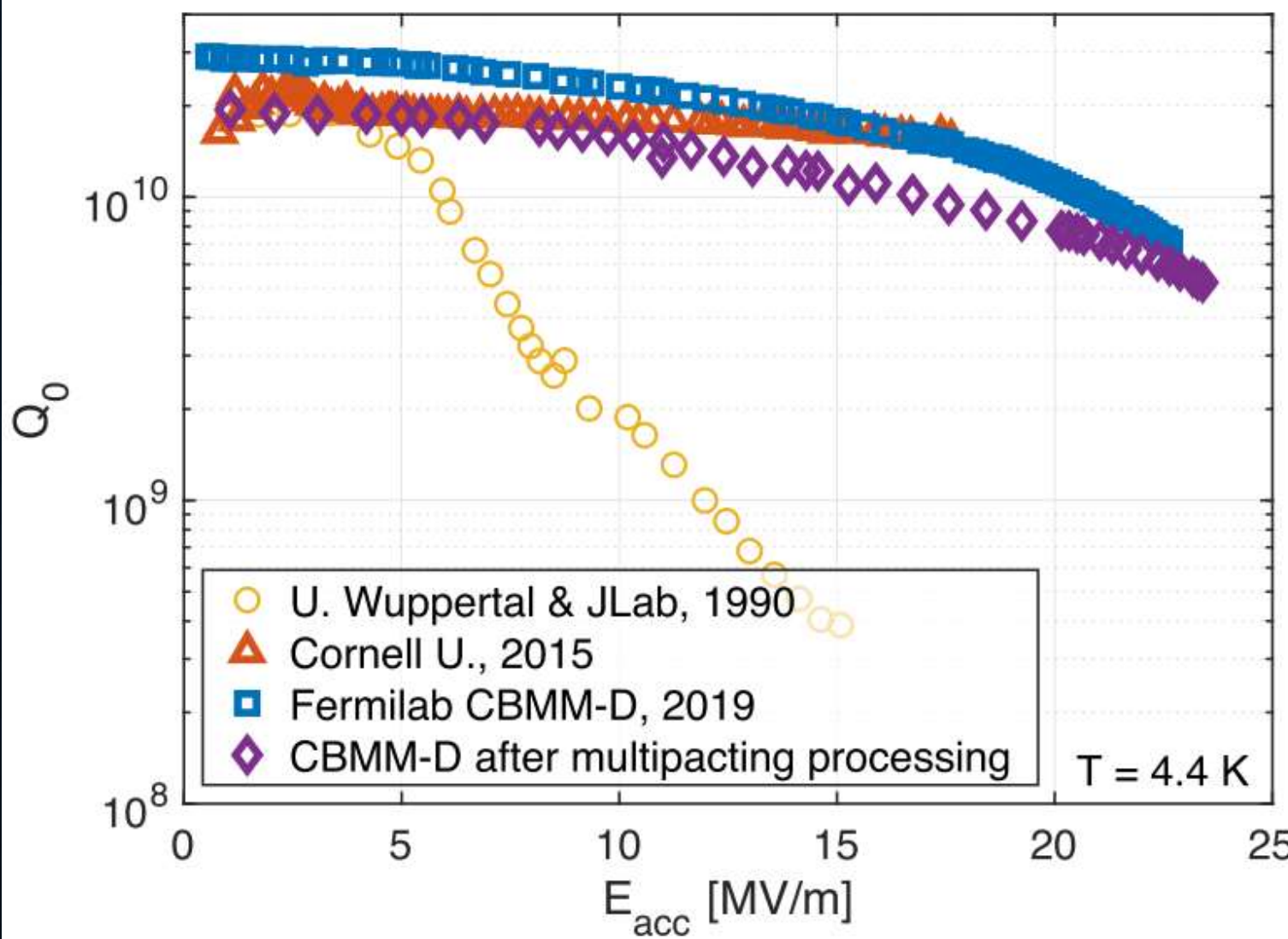


Vapor diffusion method

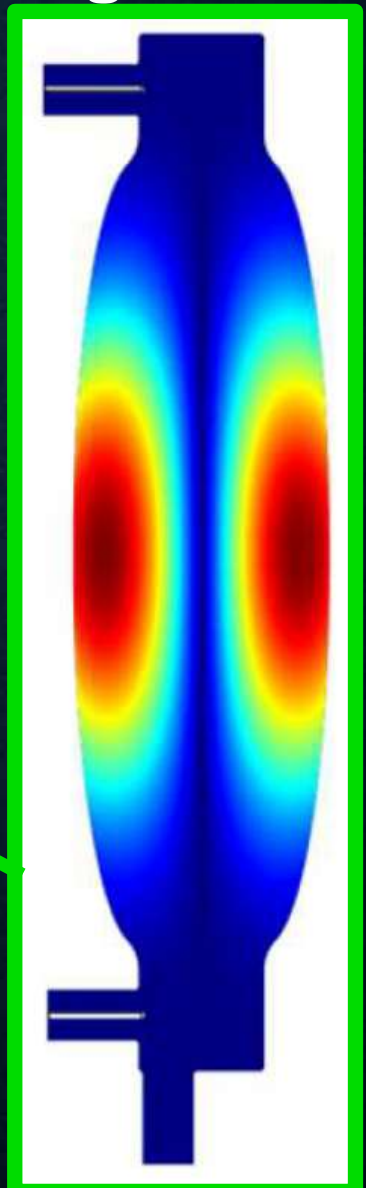
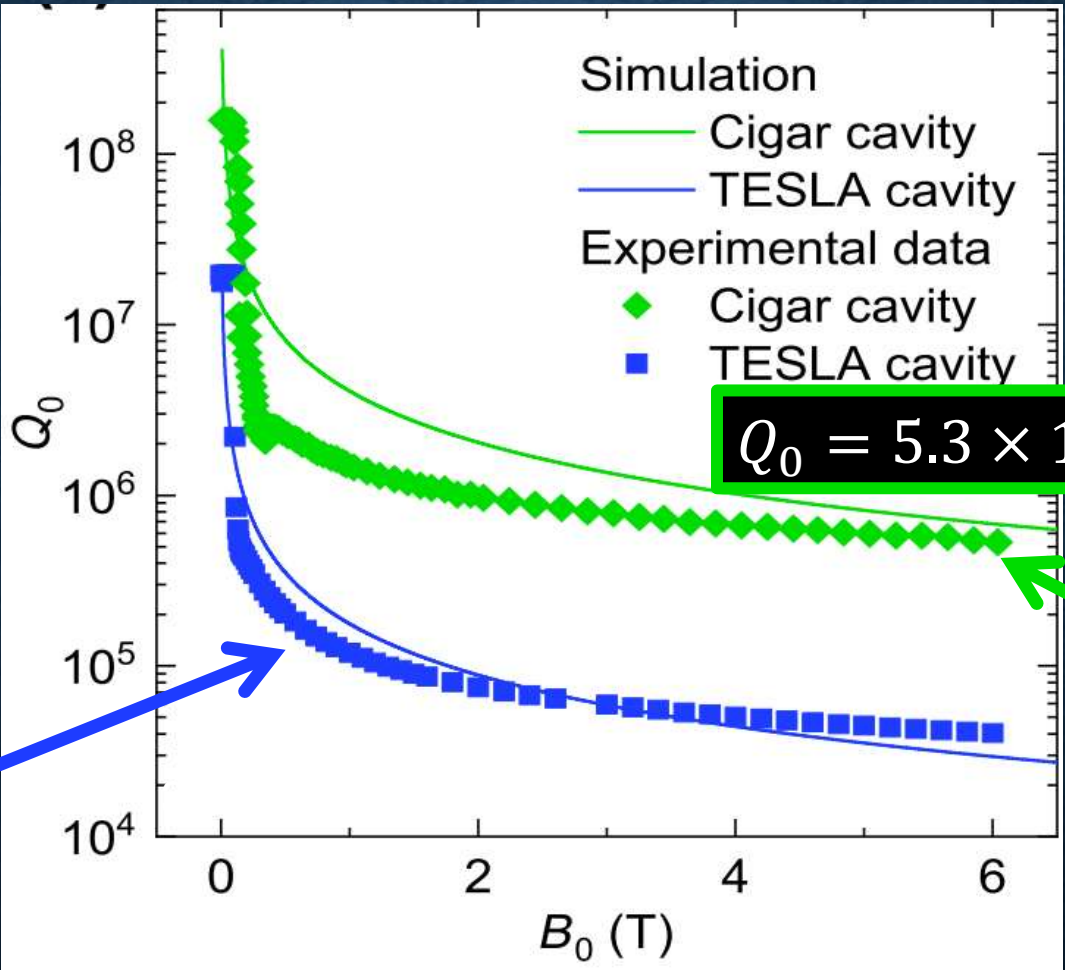
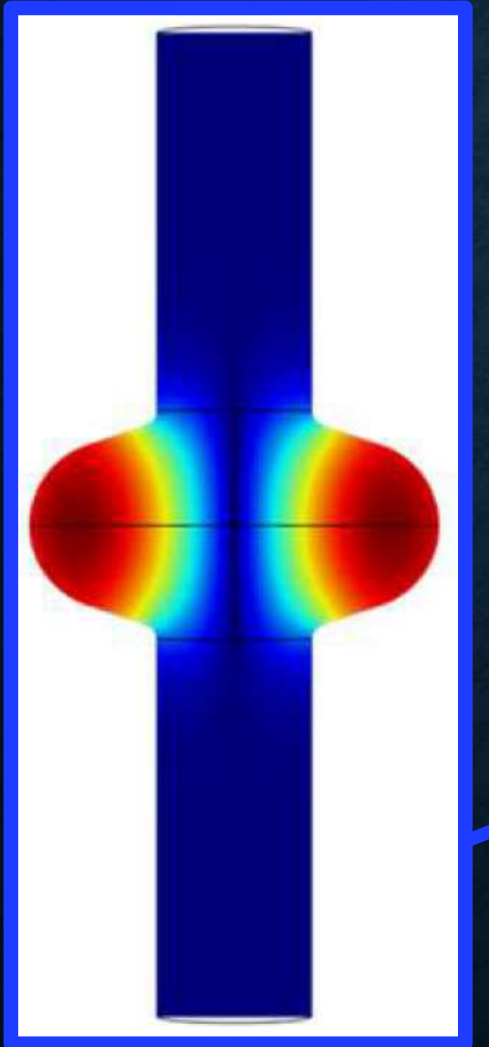
Courtesy of Hayato Ito (KEK)



The best Nb₃Sn cavity ever

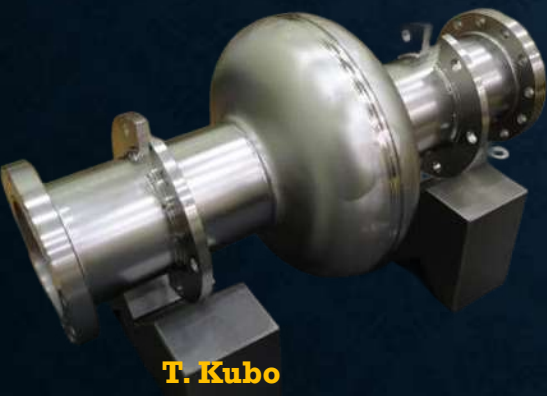


Nb₃Sn has a much higher H_{c2} than Nb, allowing it to remain superconducting in the vortex state under strong DC magnetic fields. This makes it a promising material for cavities operated in magnetic fields — for example, in axion dark matter searches.

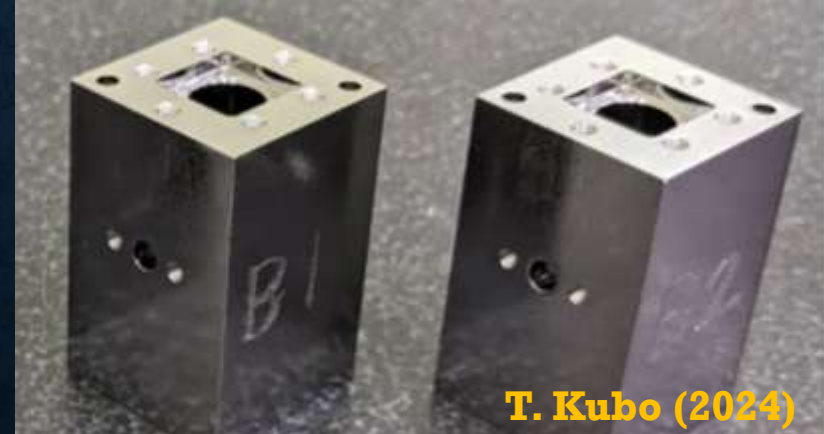


Summary up to this point

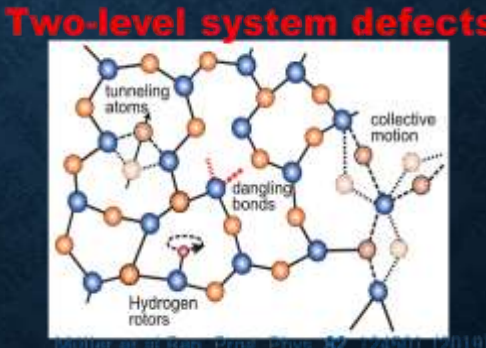
- Decades of trial and error in the accelerator community have led to the development and accumulation of a wide range of techniques and knowledge — enabling us to build the best superconducting cavities on the planet.
- Today, efforts to apply this expertise to quantum technologies are underway worldwide, including at KEK.
- Collaborations with quantum researchers give us access to ultra-low temperatures and fields — an unexplored regime for the accelerator community. These conditions may shed light on R_{res} , nonlinear R_s , nonequilibrium quasiparticles, subgap states, and more — insights that could help improve cavity performance in the long term.



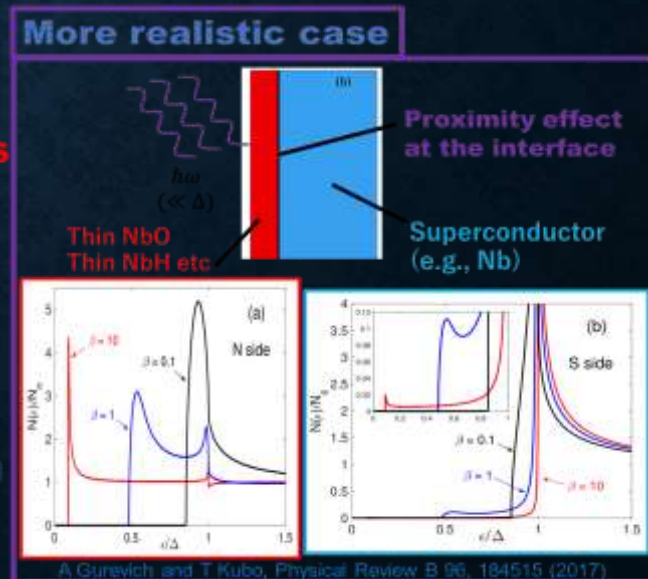
Nb accelerator cavity



Nb cavities for quantum computing



Moller et al. Rep. Prog. Phys. 82, 124501 (2019)



A. Gurevich and T. Kubo, Physical Review B 96, 184515 (2017)

The intersection of cutting-edge condensed matter physics and superconducting resonators

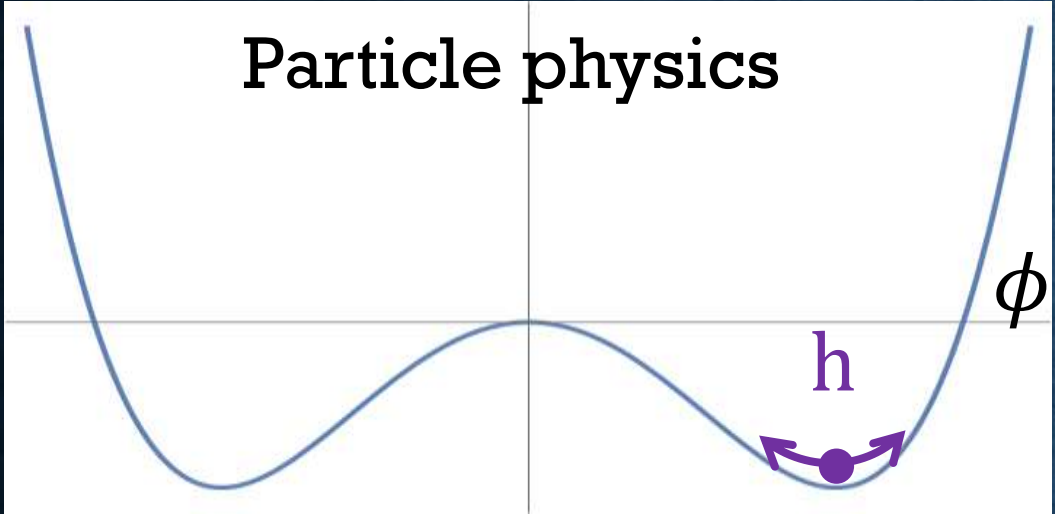
The Higgs Mode

This part is based on the following 3 papers

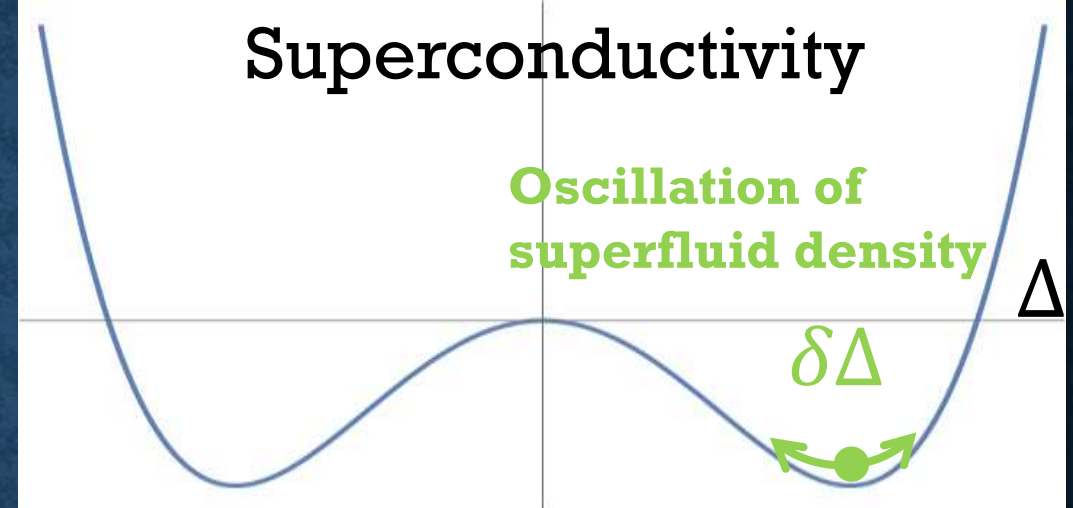
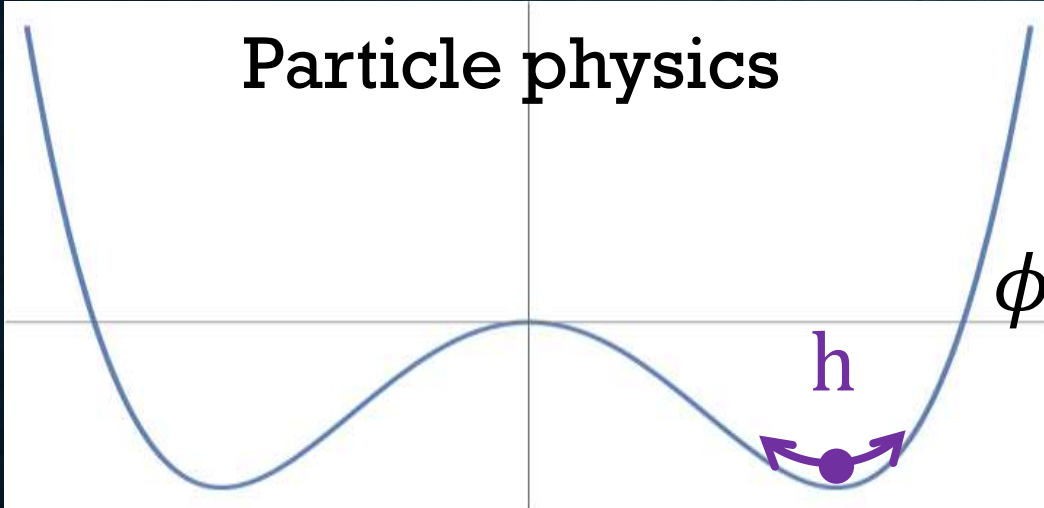
- T. Kubo, Phys. Rev. Applied **22**, 044042 (2024)
- T. Kubo, Phys. Rev. Applied **23**, 054091 (2025)
- T. Kubo, arXiv:2509.09766 (Published soon in a journal)

DOI: <https://doi.org/10.1103/PhysRevApplied.22.044042>
DOI: <https://doi.org/10.1103/PhysRevApplied.23.054091>
DOI: <https://doi.org/10.48550/arXiv.2509.09766>

Higgs?



Higgs?



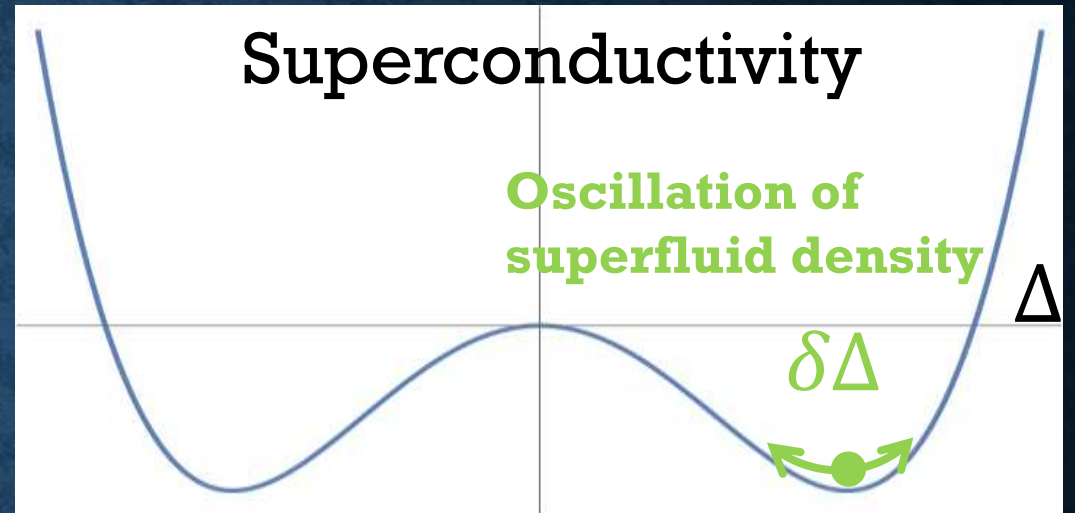
Higgs?

- The Higgs mode in superconductivity is an $\mathcal{O}(A^2)$ effect. It does not appear in standard linear-response theories such as Mattis–Bardeen theory, but it does emerge in nonlinear response:

$$\delta\Delta \propto A^2$$

Nonlinear correction
to the current density

$$\delta J \sim A\delta\Delta \propto A^3 = A_0^3 \cos^3 \omega t$$



Higgs?

- The Higgs mode in superconductivity is an $\mathcal{O}(A^2)$ effect. It does not appear in standard linear-response theories such as Mattis–Bardeen theory, but it does emerge in nonlinear response:

$$\delta\Delta \propto A^2$$

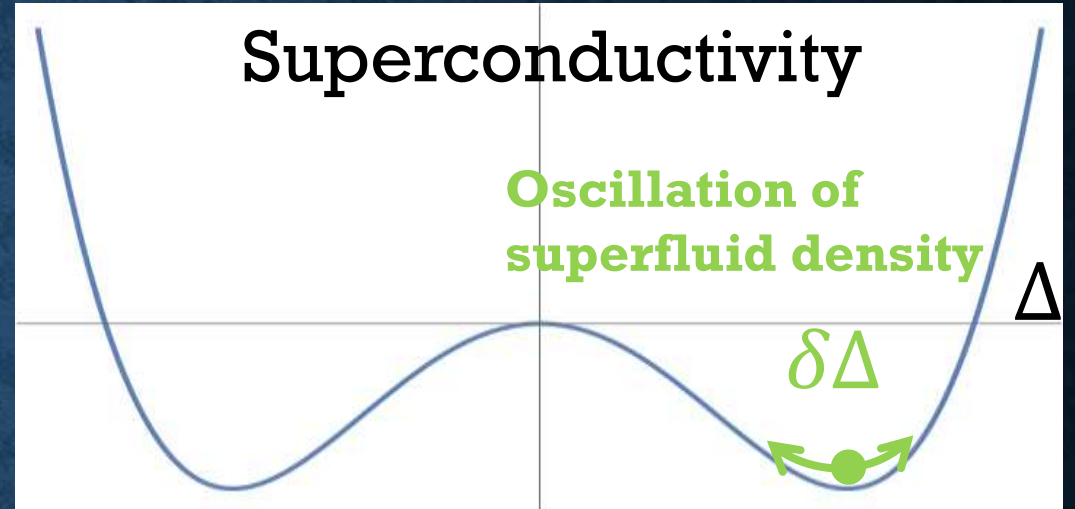
Nonlinear correction
to the current density

$$\delta J \sim A\delta\Delta \propto A^3 = A_0^3 \cos^3 \omega t$$

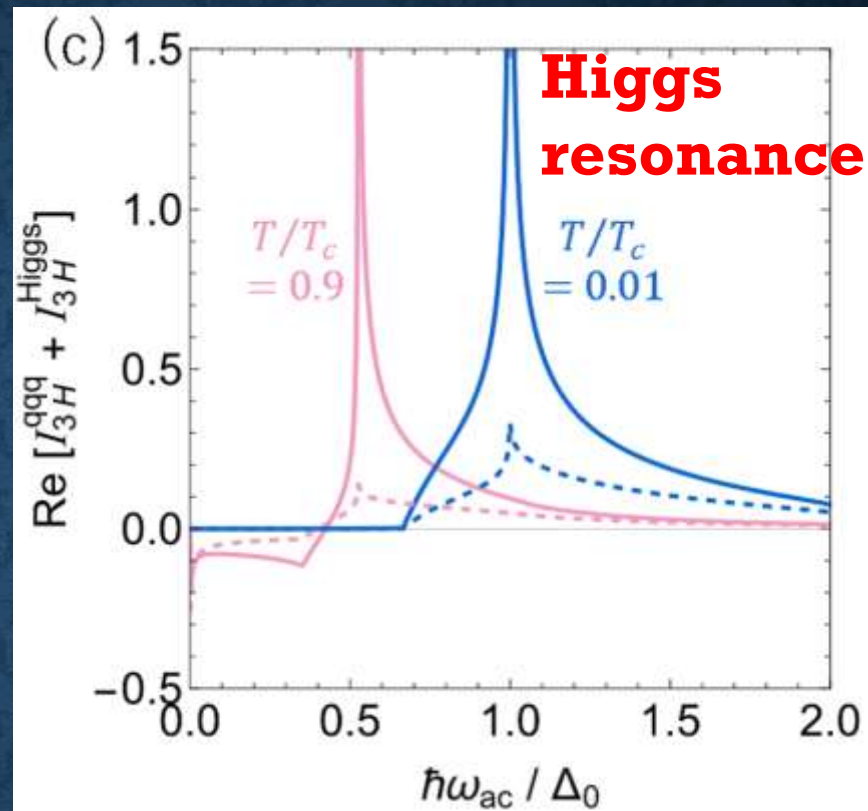
$$\sim \mathcal{O}(A_0^3) \cos \omega t + \mathcal{O}(A_0^3) \cos 3\omega t$$

First harmonic

Third harmonic



Higgs?



$$\delta J \sim A \delta \Delta \propto A^3 = A_0^3 \cos^3 \omega t$$

$$\sim \mathcal{O}(A_0^3) \cos \omega t + \mathcal{O}(A_0^3) \cos 3\omega t$$

↓

First harmonic

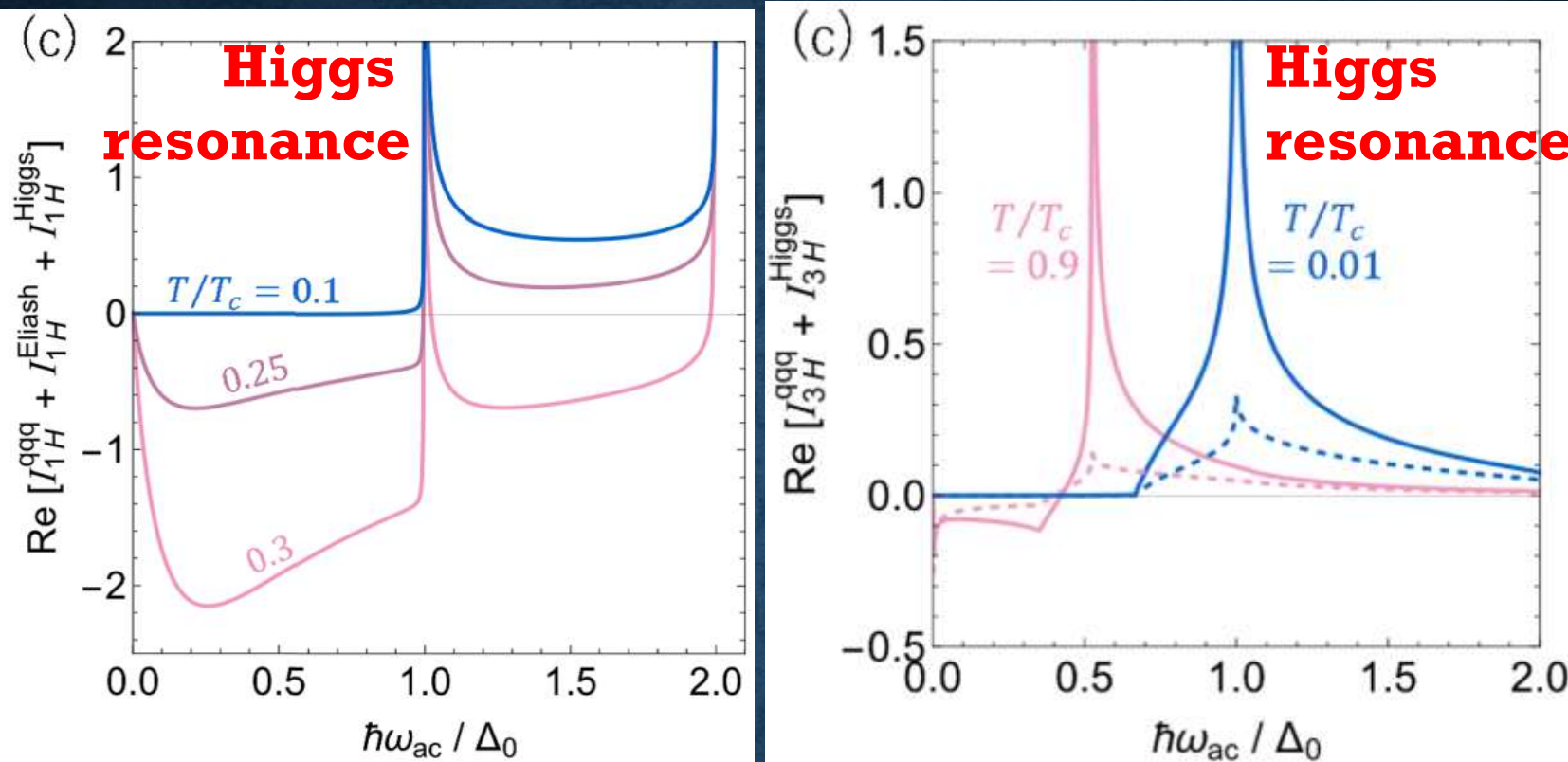
↓

Third harmonic



As for the 3rd harmonic response, see also, M. Silaev, Phys. Rev. B **99**, 224511 (2019);
P. Derendorf et al., Phys. Rev. B **109**, 024510 (2024)

Higgs?



$$\delta J \sim A \delta \Delta \propto A^3 = A_0^3 \cos^3 \omega t$$

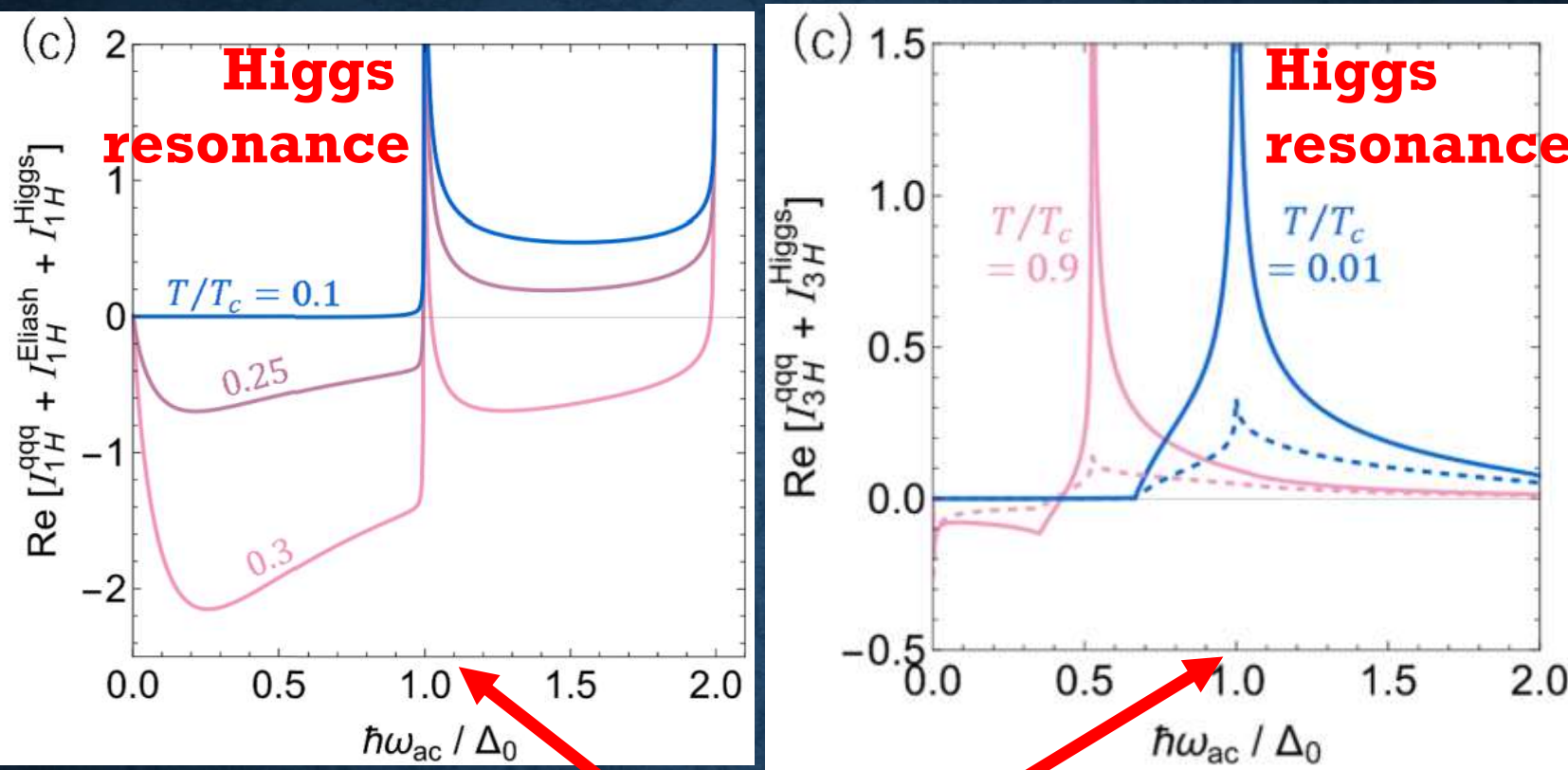
$$\sim \mathcal{O}(A_0^3) \cos \omega t + \mathcal{O}(A_0^3) \cos 3\omega t$$

First harmonic

Third harmonic

As for the 3rd harmonic response, see also, M. Silaev, Phys. Rev. B **99**, 224511 (2019);
P. Derendorf et al., Phys. Rev. B **109**, 024510 (2024)

Higgs?



$\Delta_0/h = 360\text{GHz}$ (Nb) higher than typical frequencies of SC devices
 $\Delta_0/h = 44\text{ GHz}$ (Al)
 $\Delta_0/h = 18\text{ GHz}$ (Ti) Accessible?

As for the 3rd harmonic response, see also, M. Silaev, Phys. Rev. B **99**, 224511 (2019);
P. Derendorf et al., Phys. Rev. B **109**, 024510 (2024)

Higgs?

Another way of exciting Higgs mode: **dc + ac**

A. Moor et al., Phys. Rev. Lett. **118**, 047001 (2017)
T. Jujo, J. Phys. Soc. Jpn. **91**, 074711 (2022)
T. Kubo, Phys. Rev. Applied **22**, 044042 (2024)
T. Kubo, Phys. Rev. Applied **23**, 054091 (2025)

$$\delta\Delta \propto A^2 \quad \xrightarrow{\hspace{1cm}} \quad \delta\Delta \propto (A_{dc} + A)^2$$

Higgs?

Another way of exciting Higgs mode: **dc + ac**

A. Moor et al., Phys. Rev. Lett. **118**, 047001 (2017)
T. Jujo, J. Phys. Soc. Jpn. **91**, 074711 (2022)
T. Kubo, Phys. Rev. Applied **22**, 044042 (2024)
T. Kubo, Phys. Rev. Applied **23**, 054091 (2025)

$$\delta\Delta \propto A^2 \quad \xrightarrow{\hspace{1cm}} \quad \delta\Delta \propto (A_{dc} + A)^2 \supset A_{dc} \cdot A + \mathcal{O}(A^2)$$

Higgs?

Another way of exciting Higgs mode: **dc + ac**

A. Moor et al., Phys. Rev. Lett. **118**, 047001 (2017)
T. Jujo, J. Phys. Soc. Jpn. **91**, 074711 (2022)
T. Kubo, Phys. Rev. Applied **22**, 044042 (2024)
T. Kubo, Phys. Rev. Applied **23**, 054091 (2025)

$$\delta\Delta \propto A^2 \quad \xrightarrow{\hspace{1cm}} \quad \delta\Delta \propto (A_{dc} + A)^2 \supset A_{dc} \cdot A + \mathcal{O}(A^2)$$

↓ ↓

**Linear
response**

**Nonlinear
response**

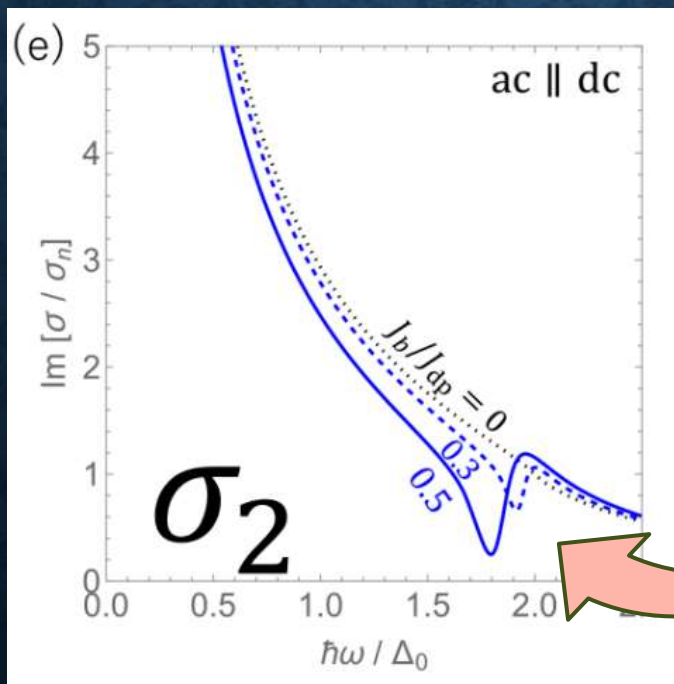
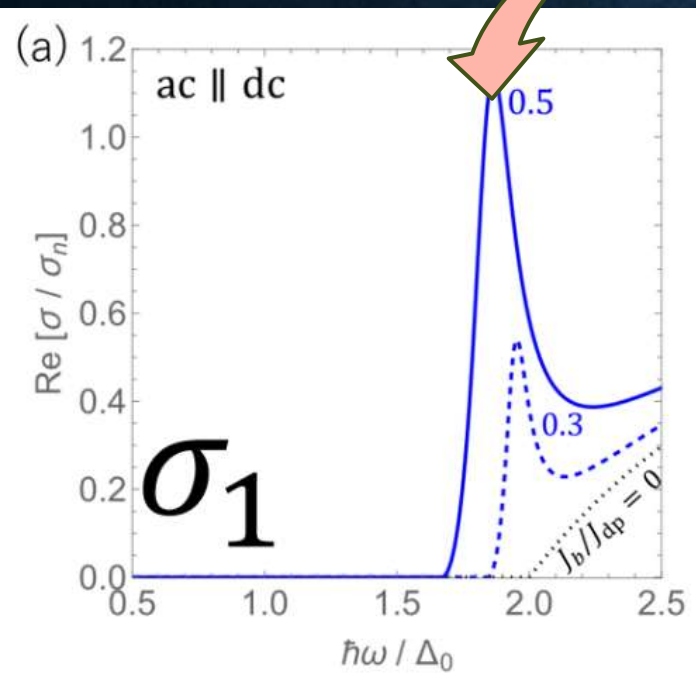
Higgs?

Another way of exciting Higgs mode: dc + ac

A. Moor et al., Phys. Rev. Lett. **118**, 047001 (2017)
T. Jujo, J. Phys. Soc. Jpn. **91**, 074711 (2022)
T. Kubo, Phys. Rev. Applied **22**, 044042 (2024)
T. Kubo, Phys. Rev. Applied **23**, 054091 (2025)

$$\delta\Delta \propto A^2 \quad \xrightarrow{\text{Large } A} \quad \delta\Delta \propto (A_{dc} + A)^2 \supset A_{dc} \cdot A + \mathcal{O}(A^2)$$

T. Kubo,
Phys. Rev. Applied **23**, 054091 (2025)



Linear
response

Nonlinear
response

$2\Delta_0/h = 720\text{GHz (Nb)}$
 $2\Delta_0/h = 88\text{ GHz}_{\text{Z}_5} (\text{Al})$
 $2\Delta_0/h = 36\text{ GHz} (\text{Ti})$

These are the hallmarks of the Higgs mode, which appear at frequencies around Δ , far higher than those of typical superconducting devices.

These are the hallmarks of the Higgs mode, which appear at frequencies around Δ , far higher than those of typical superconducting devices.

However, its low-frequency tail still plays an important and nontrivial role in superconducting devices.

These are the hallmarks of the Higgs mode, which appear at frequencies around Δ , far higher than those of typical superconducting devices.

However, its low-frequency tail still plays an important and nontrivial role in superconducting devices.

Some effects of the Higgs mode have, in fact, already manifested themselves, although they have not been recognized as such. A representative example is the **current-dependent kinetic inductance**.

(1)



Only weak ac

Outline

Outline

(1)



Only weak ac

(2)



Only dc current

Outline

(1)



Only weak ac

(2)



Only dc current

(3)

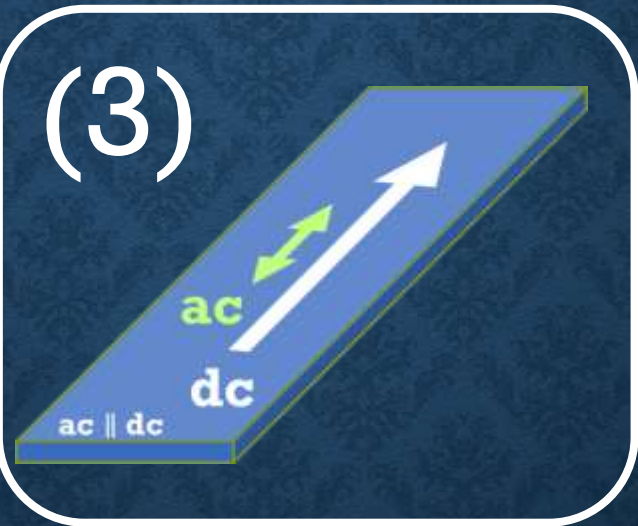
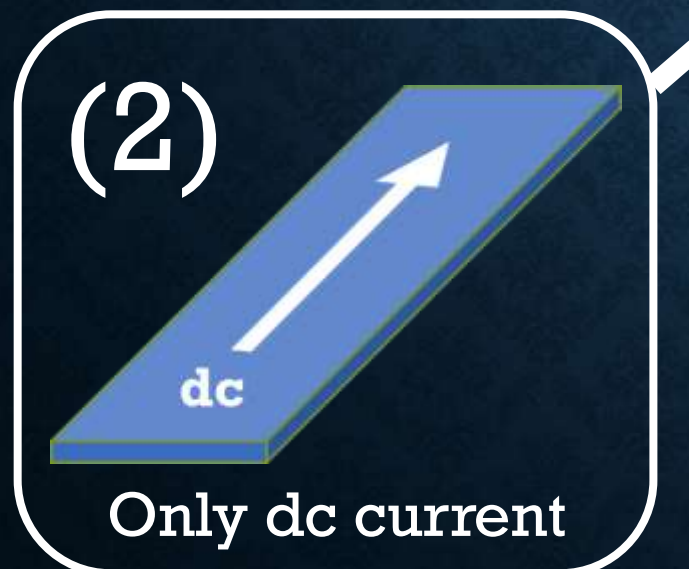
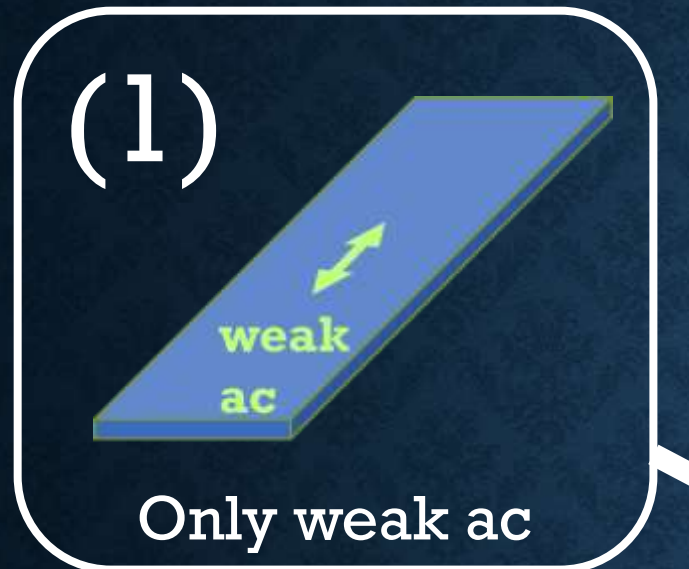


ac + dc

Semi-phenomenological
approach

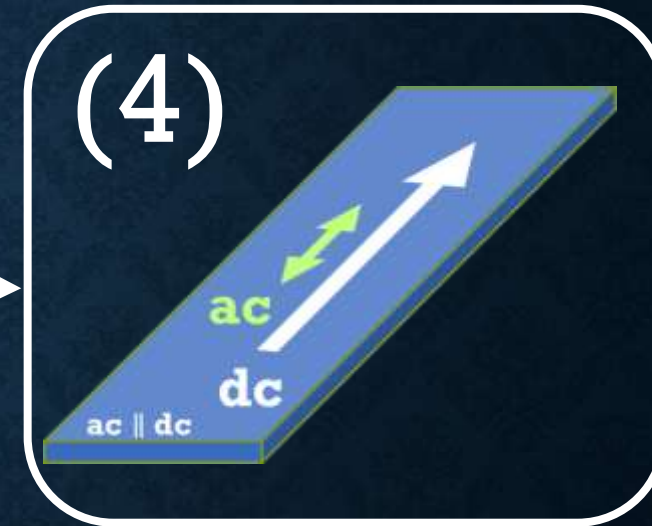
- S. M. Anlage et al., IEEE Trans. Magn. **25**, 1388 (1989).
- J. R. Clem and V. G. Kogan, Phys. Rev. B **86**, 174521 (2012).
- T. Kubo, Phys. Rev. Research **2**, 033203 (2020).

Outline



ac + dc
Semi-phenomenological
approach

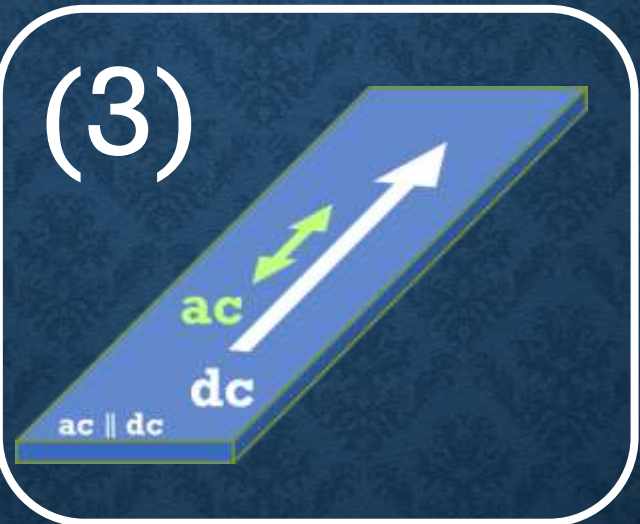
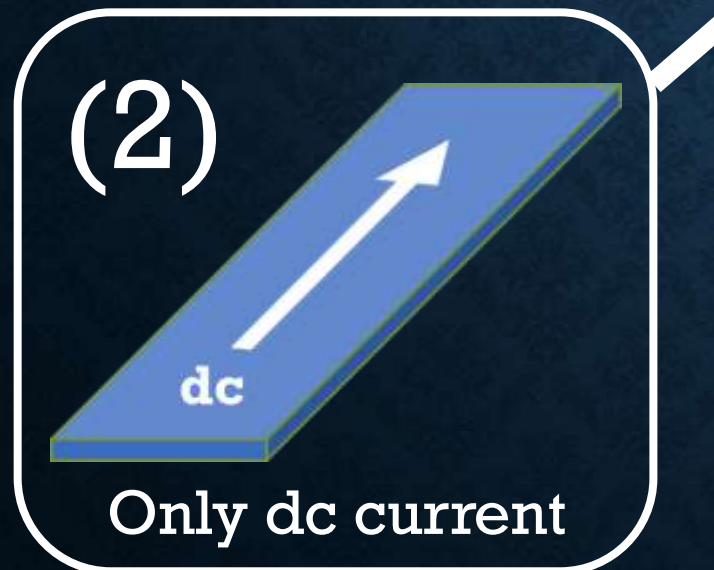
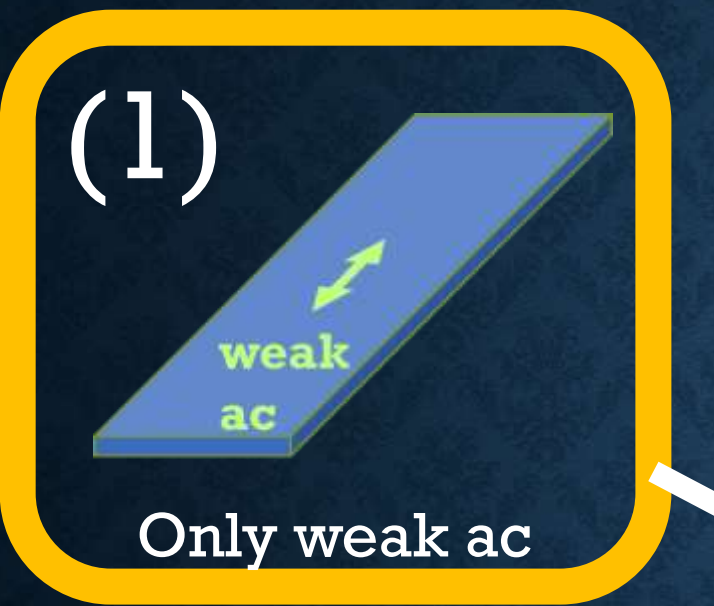
- S. M. Anlage et al., IEEE Trans. Magn. **25**, 1388 (1989).
- J. R. Clem and V. G. Kogan, Phys. Rev. B **86**, 174521 (2012).
- T. Kubo, Phys. Rev. Research **2**, 033203 (2020).



ac + dc
Microscopic
nonequilibrium
superconductivity₁₁₂

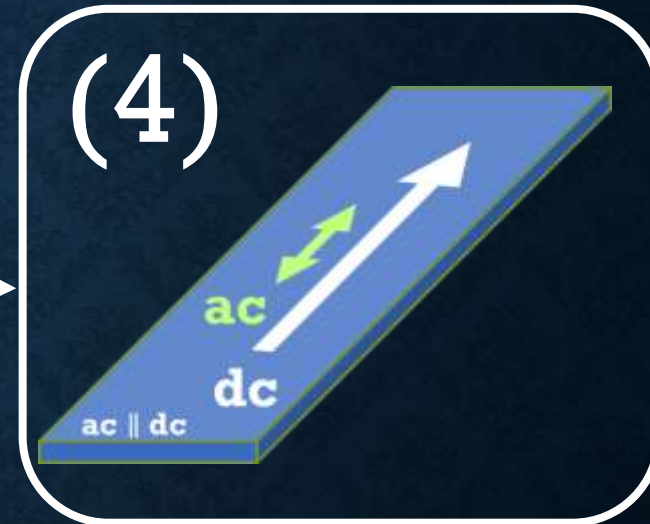
- T. Kubo, Phys. Rev. Applied **22**, 044042 (2024)
- T. Kubo, Phys. Rev. Applied **23**, 054091 (2025)

Outline



Semi-phenomenological
approach

- S. M. Anlage et al., IEEE Trans. Magn. **25**, 1388 (1989).
- J. R. Clem and V. G. Kogan, Phys. Rev. B **86**, 174521 (2012).
- T. Kubo, Phys. Rev. Research **2**, 033203 (2020).



Microscopic
nonequilibrium
superconductivity₁₁₃

- T. Kubo, Phys. Rev. Applied **22**, 044042 (2024)
- T. Kubo, Phys. Rev. Applied **23**, 054091 (2025)

Kinetic inductance under an AC perturbation (no DC current)



The kinetic inductivity is defined by

$$L_k \frac{dJ_s}{dt} = E$$

Kinetic inductance under an AC perturbation (no DC current)

weak
ac

The kinetic inductivity is defined by

$$L_k \frac{dJ_s}{dt} = E$$

or

$$L_k = \frac{E}{\dot{J}_s} = - \frac{\dot{A}}{\dot{J}_s}$$

Kinetic inductance under an AC perturbation (no DC current)

weak
ac

The kinetic inductivity is defined by

$$L_k \frac{dJ_s}{dt} = E$$

or

$$L_k = \frac{E}{\dot{J}_s} = - \frac{\dot{A}}{\dot{J}_s}$$

London eq.

$$J_s = - \frac{A}{\mu_0 \lambda^2}$$
$$d\lambda/dt = 0$$



Kinetic inductance under an AC perturbation (no DC current)

weak
ac

The kinetic inductivity is defined by

$$L_k \frac{dJ_s}{dt} = E$$

or

$$L_k = \frac{E}{\dot{J}_s} = - \frac{\dot{A}}{\dot{J}_s}$$

London eq.

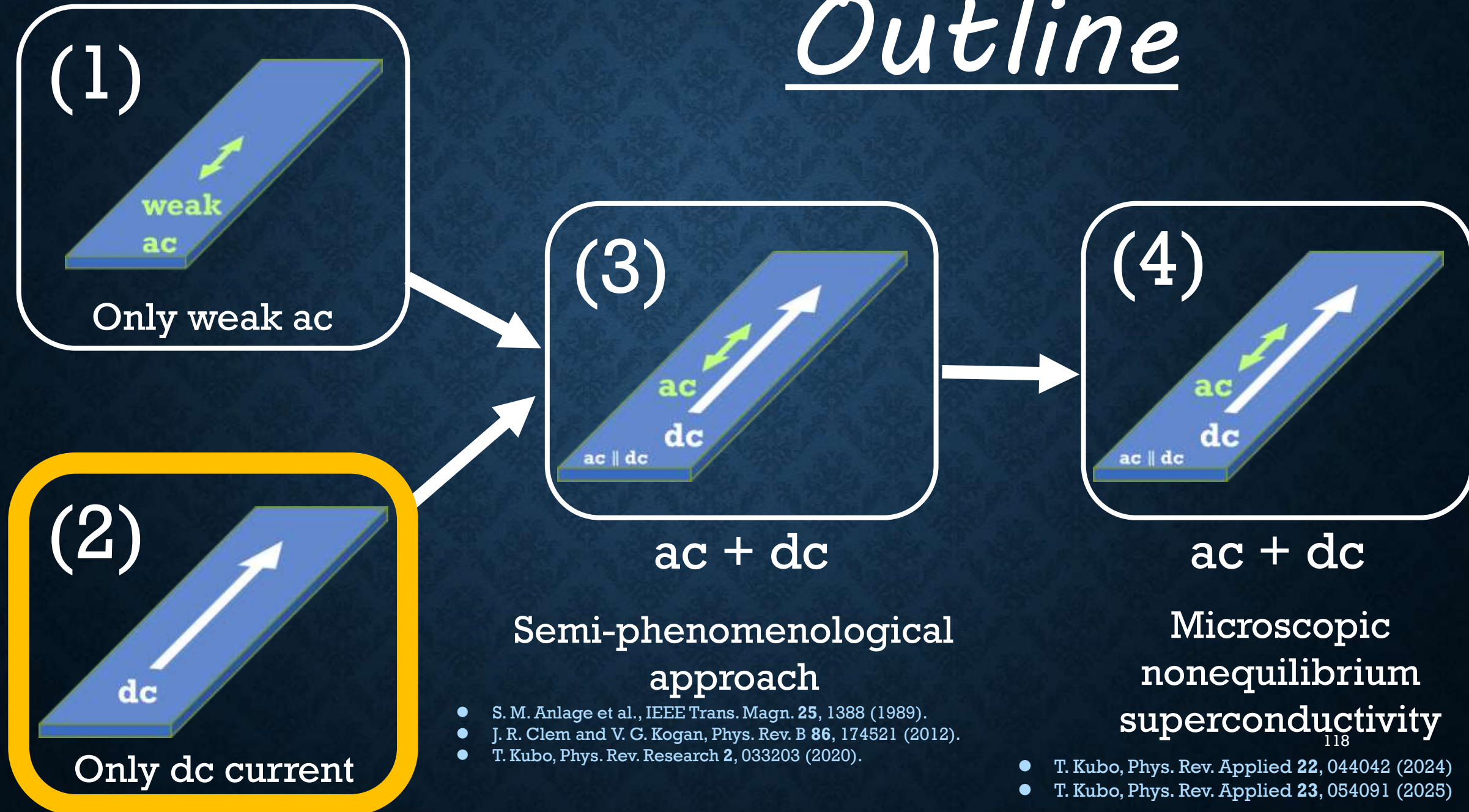
$$J_s = - \frac{A}{\mu_0 \lambda^2}$$
$$d\lambda/dt = 0$$

Very well-known result

$$L_k = \mu_0 \lambda^2 \propto \frac{1}{n_s}$$

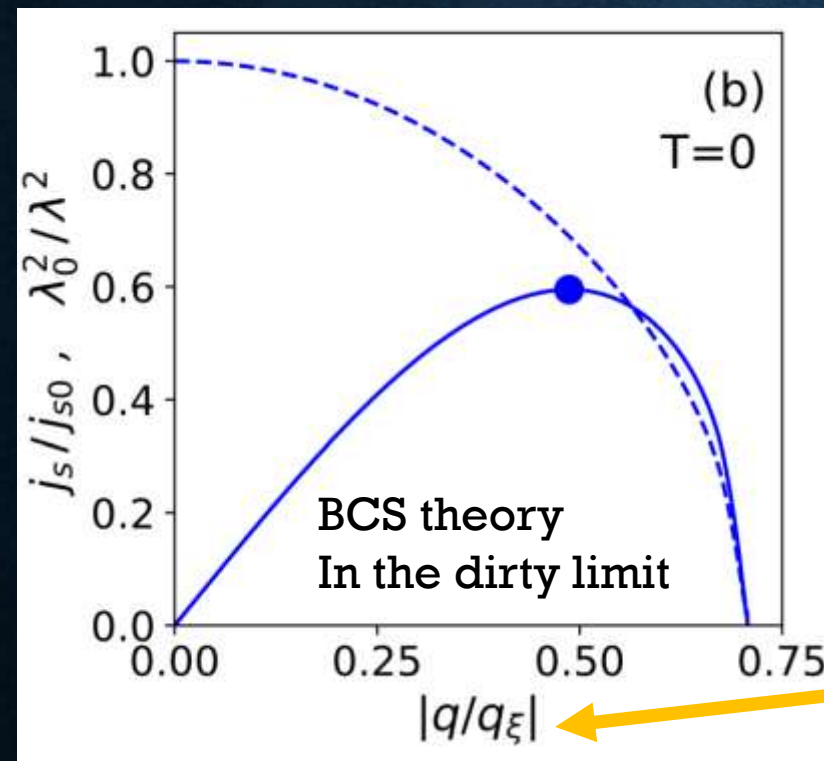
This basic result already implies that an oscillation of the superfluid density n_s (i.e., the Higgs mode) can influence the kinetic inductance.

Outline





Next, we consider **only a dc current**.
This case is also well understood from decades ago.



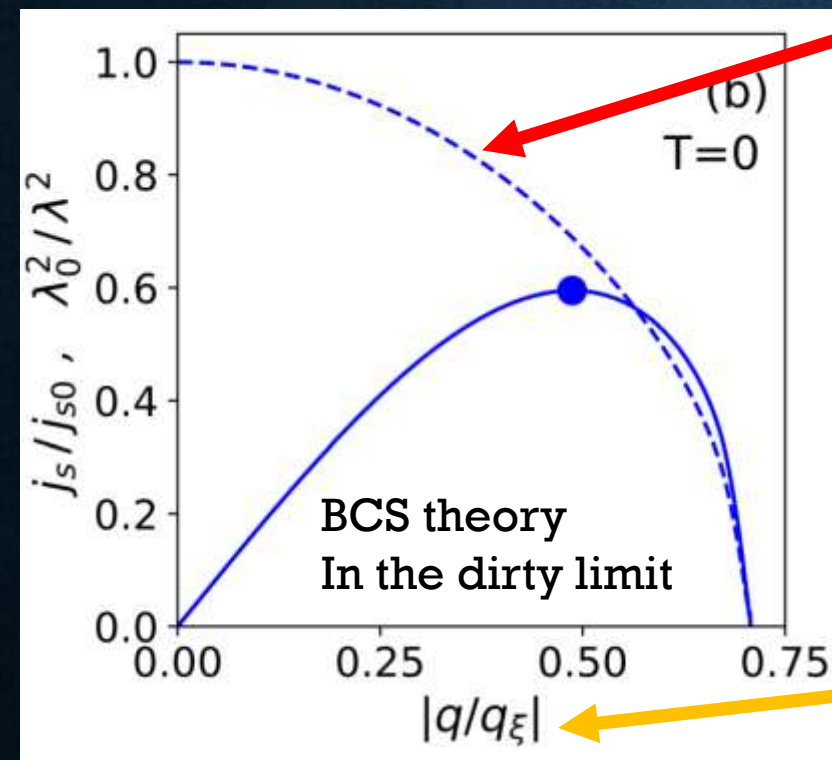
q (superfluid momentum)

See, e.g.,

T. Kubo, Phys. Rev. Research 2, 033203 (2020)



Next, we consider **only a dc current**.
This case is also well understood from decades ago.



$$n_s \propto \lambda^{-2} \text{ (superfluid density)}$$

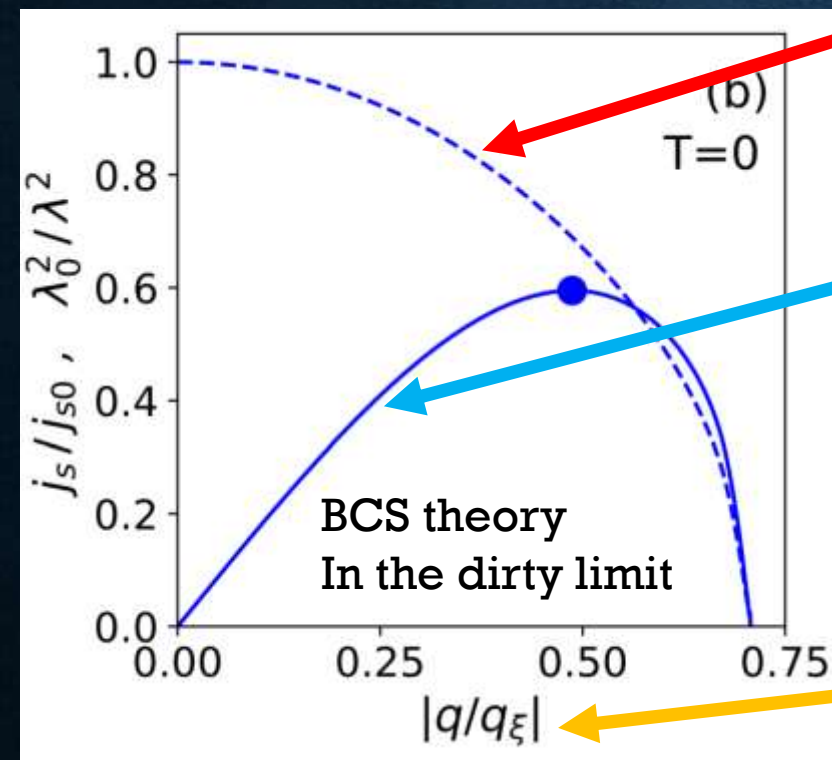
q (superfluid momentum)

See, e.g.,

T. Kubo, Phys. Rev. Research 2, 033203 (2020)



Next, we consider **only a dc current**.
This case is also well understood from decades ago.



$$n_s \propto \lambda^{-2} \text{ (superfluid density)}$$

$$J \sim n_s q \text{ (current density)}$$

the maximum value ● is called the depairing current

$$q \text{ (superfluid momentum)}$$

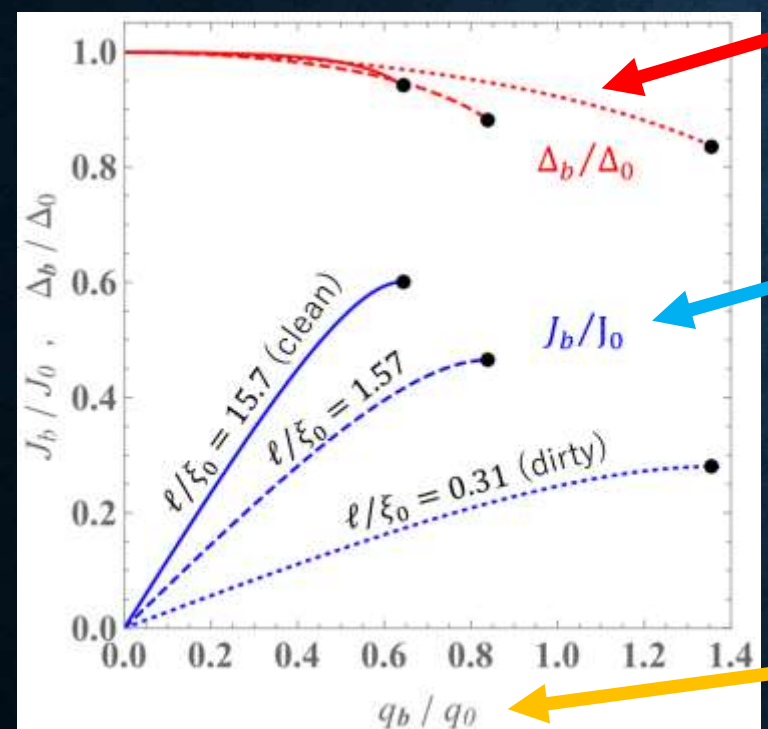
See, e.g.,

T. Kubo, Phys. Rev. Research 2, 033203 (2020)



Next, we consider **only a dc current**.
This case is also well understood from decades ago.

Δ (pair potential)



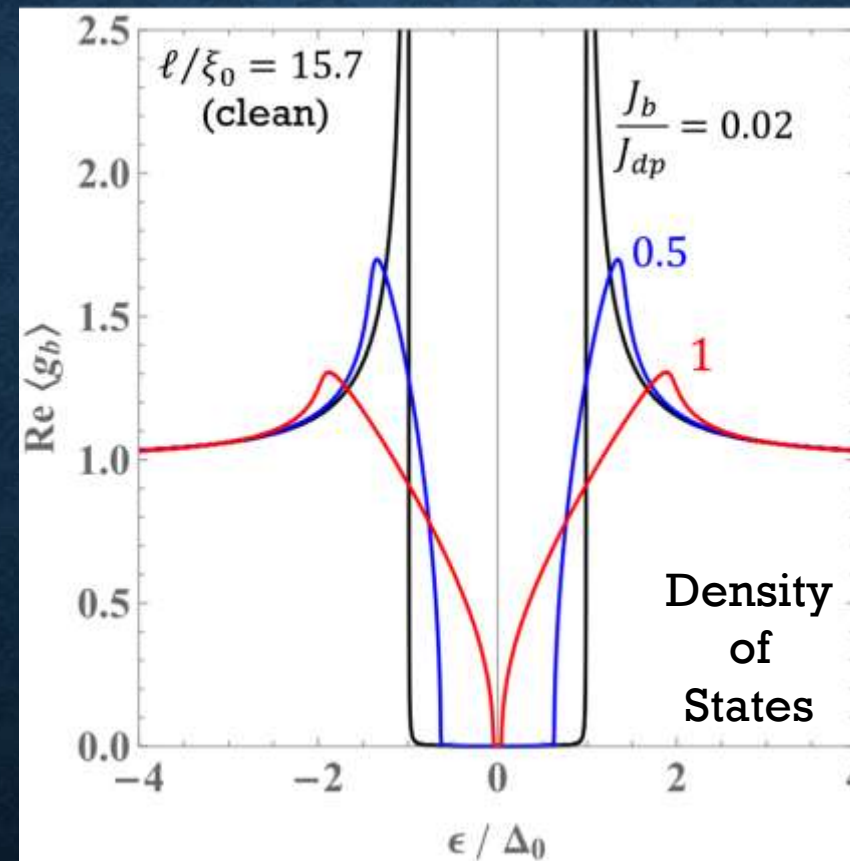
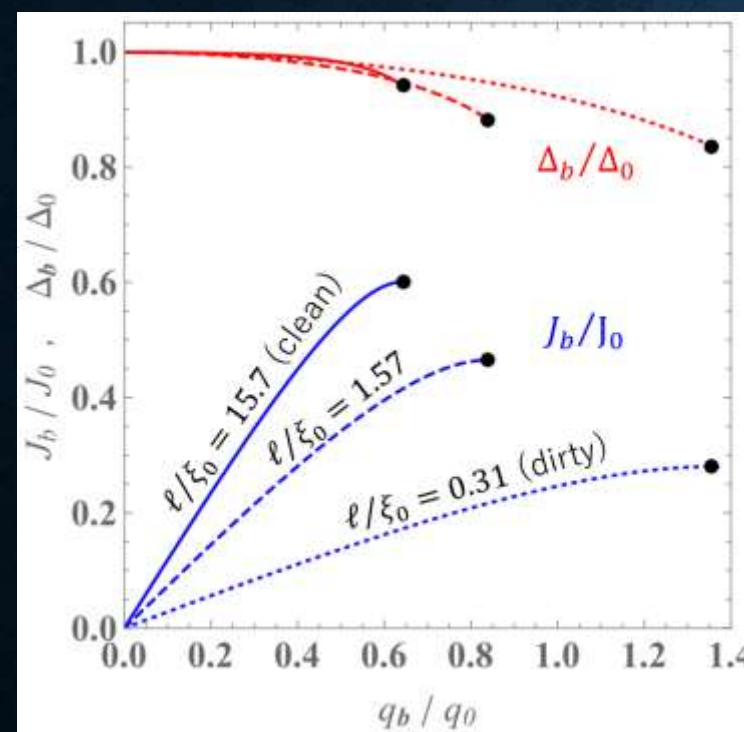
$J \sim n_s q$ (current density)

the maximum value ● is called the depairing current

q (superfluid momentum)

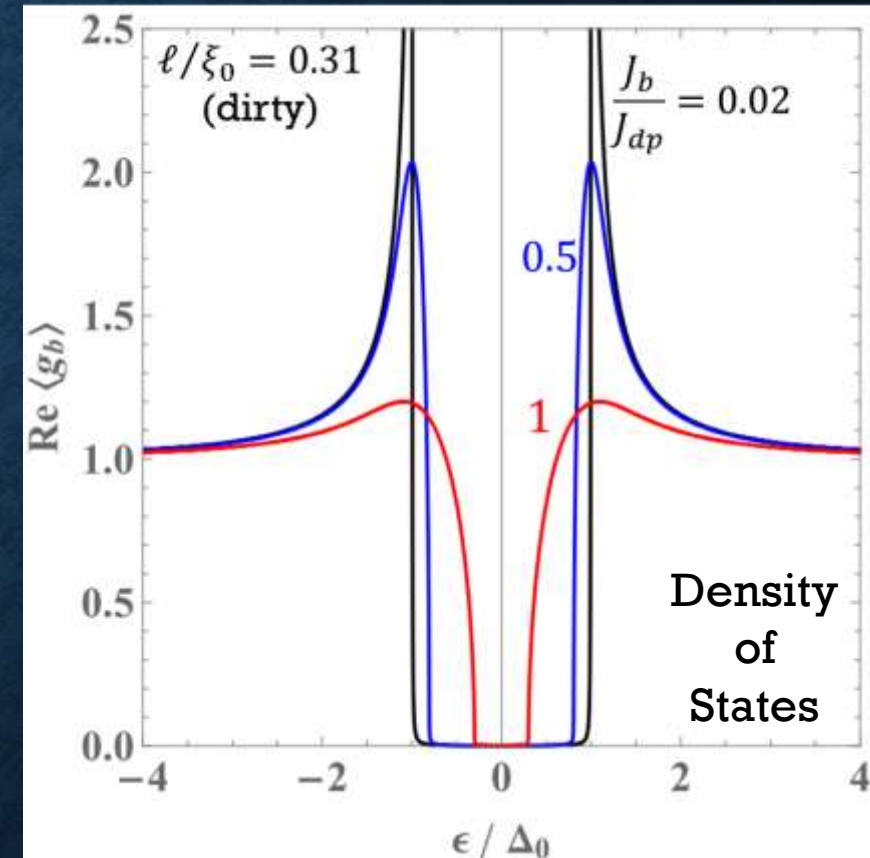
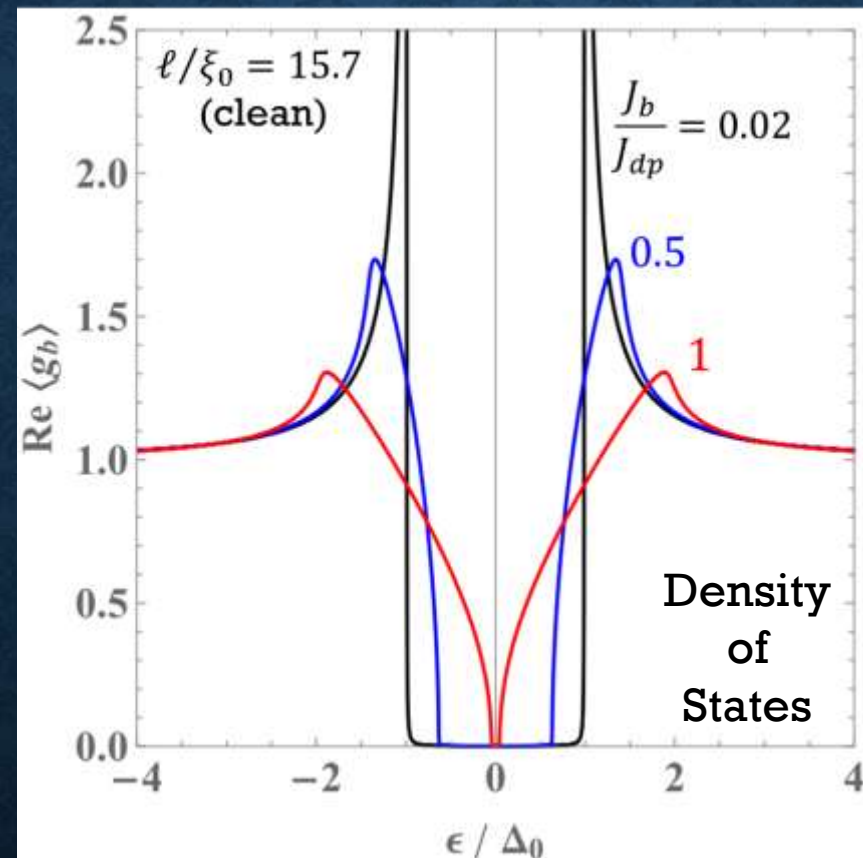
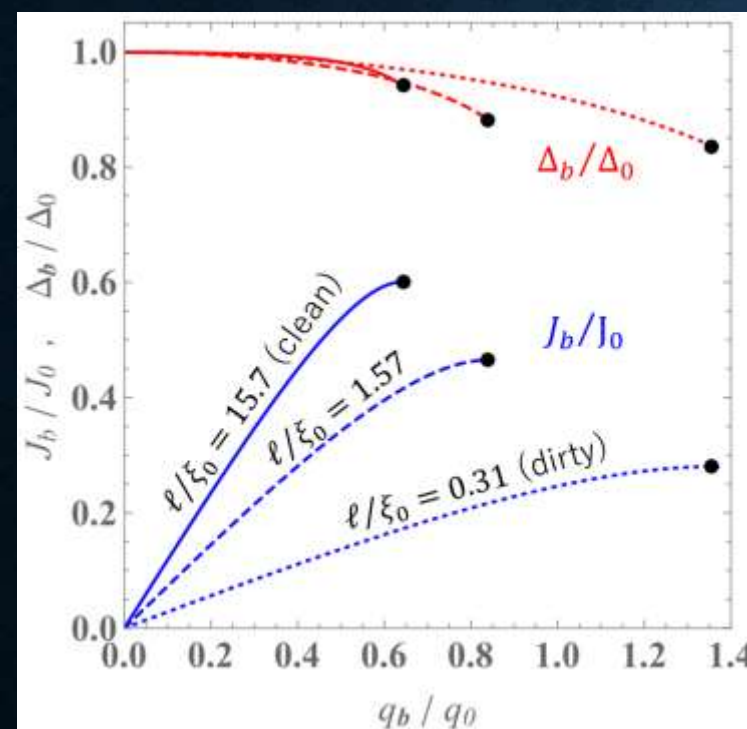


Next, we consider **only a dc current**.
This case is also well understood from decades ago.

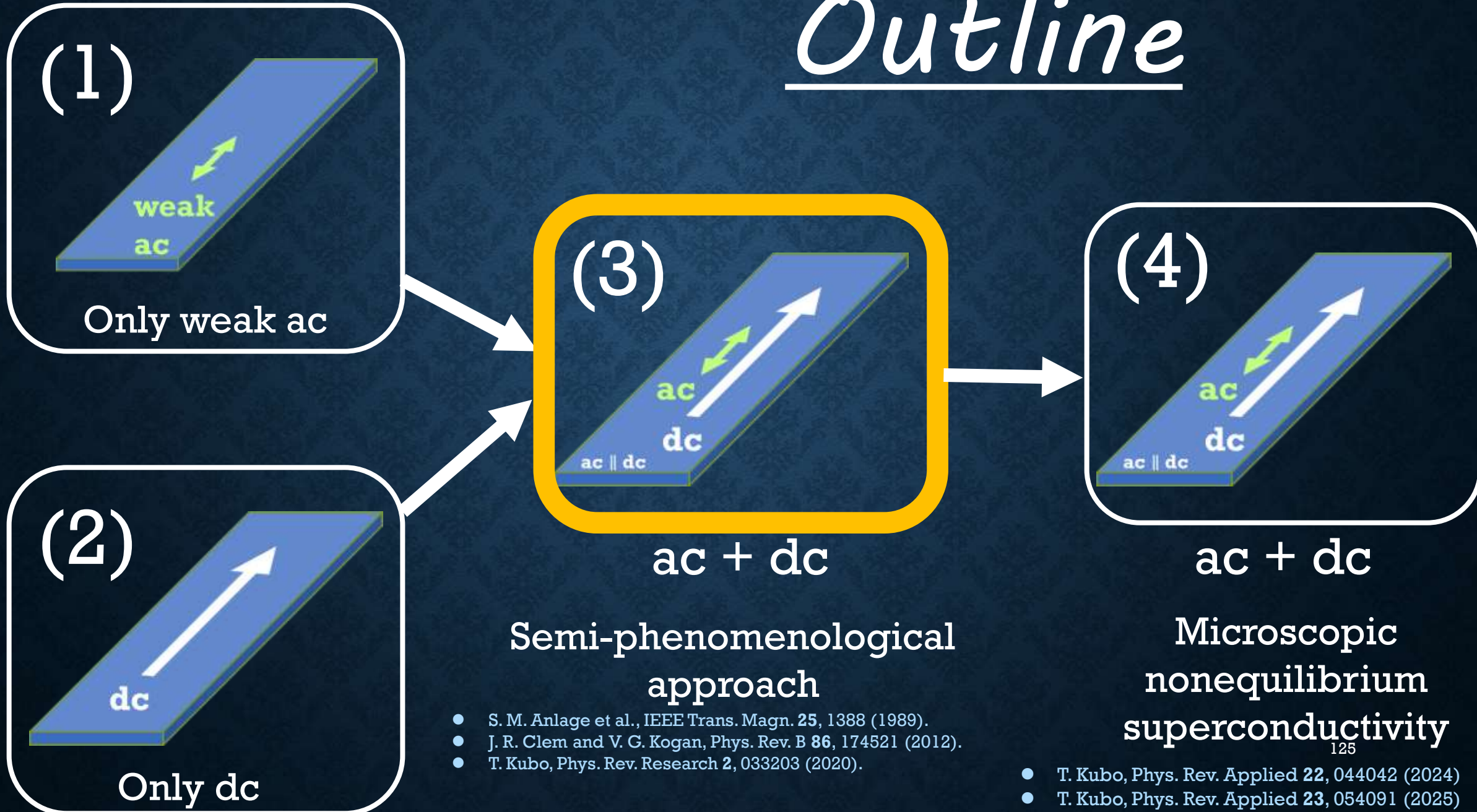


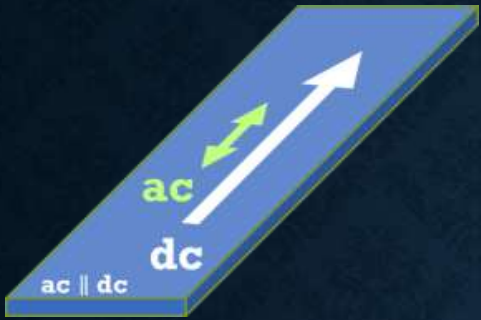


Next, we consider **only a dc current**.
This case is also well understood from decades ago.



Outline





Let us go back to the definition of L_k .

We soon find that it is more complicated than expected.

$$L_k \frac{dJ_s}{dt} = E$$



$$J_s \propto n_s q$$
$$\frac{dJ_s}{dt} \propto n_s q + n_s \dot{q}$$



Let us go back to the definition of L_k .
We soon find that it is more complicated than expected.

- S. M. Anlage et al., IEEE Trans. Magn. **25**, 1388 (1989).
- J. R. Clem and V. G. Kogan, Phys. Rev. B **86**, 174521 (2012).
- T. Kubo, Physical Review Research **2**, 033203 (2020).

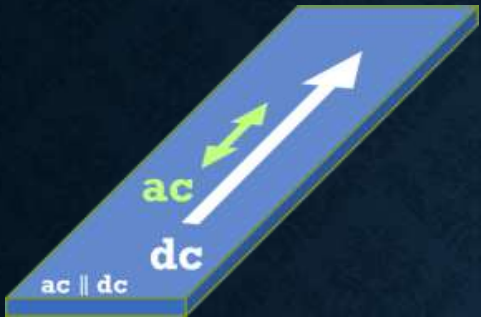
$$L_k \frac{dJ_s}{dt} = E$$



$$\boxed{\begin{aligned} J_s &\propto n_s q \\ \frac{dJ_s}{dt} &\propto \dot{n}_s q + n_s \dot{q} \end{aligned}}$$

$$\boxed{L_k = \mu_0 \lambda_0^2 \frac{\dot{q}}{\frac{\dot{n}_s}{n_{s0}} q + \frac{n_s}{n_{s0}} \dot{q}}}$$

$$n_{s0} := n_s(q = 0, T = 0)$$



Let us go back to the definition of L_k .
We soon find that it is more complicated than expected.

- S. M. Anlage et al., IEEE Trans. Magn. **25**, 1388 (1989).
- J. R. Clem and V. G. Kogan, Phys. Rev. B **86**, 174521 (2012).
- T. Kubo, Physical Review Research **2**, 033203 (2020).

$$L_k \frac{dJ_s}{dt} = E$$

→

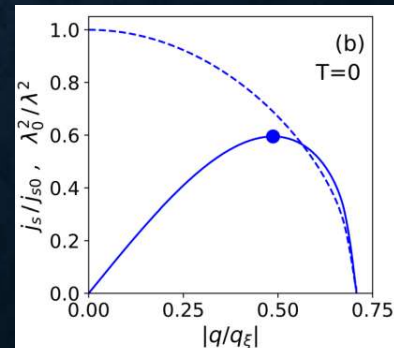
$$J_s \propto n_s q$$

$$\frac{dJ_s}{dt} \propto \dot{n}_s q + n_s \dot{q}$$

$$n_{s0} := n_s(q = 0, T = 0)$$

$$L_k = \mu_0 \lambda_0^2 \frac{\dot{q}}{\frac{\dot{n}_s}{n_{s0}} q + \boxed{\frac{n_s}{n_{s0}} \dot{q}}}$$

This part can be calculated from the equilibrium theory:
the BCS theory





Let us go back to the definition of L_k .
We soon find that it is more complicated than expected.

- S. M. Anlage et al., IEEE Trans. Magn. **25**, 1388 (1989).
- J. R. Clem and V. G. Kogan, Phys. Rev. B **86**, 174521 (2012).
- T. Kubo, Physical Review Research **2**, 033203 (2020).

$$L_k \frac{dJ_s}{dt} = E$$

\rightarrow

$J_s \propto n_s q$
 $\frac{dJ_s}{dt} \propto n_s q + n_s \dot{q}$

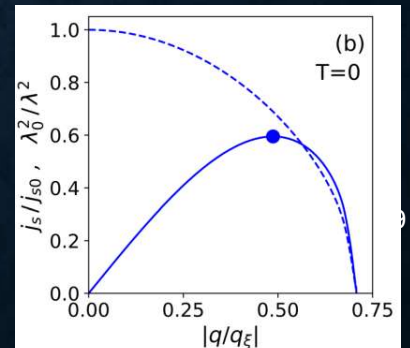
$$n_{s0} := n_s(q = 0, T = 0)$$

This looks very much like a nonequilibrium situation.

$$L_k = \mu_0 \lambda_0^2 \left[\frac{\dot{n}_s}{n_{s0}} q + \frac{n_s}{n_{s0}} \dot{q} \right]$$

Dynamics of superfluid density!

This part can be calculated from the equilibrium theory:
the BCS theory



Semi-phenomenological approach

- S. M. Anlage et al., IEEE Trans. Magn. **25**, 1388 (1989).
- J. R. Clem and V. G. Kogan, Phys. Rev. B **86**, 174521 (2012).
- T. Kubo, Physical Review Research **2**, 033203 (2020).

$$L_k = \mu_0 \lambda_0^2 \frac{\dot{q}}{\frac{n_s}{n_{s0}} q + \frac{n_s}{n_{s0}} \dot{q}}$$

To circumvent the complexity of the nonequilibrium problem, previous studies introduced the following simplifying assumptions.

Semi-phenomenological approach

- S. M. Anlage et al., IEEE Trans. Magn. **25**, 1388 (1989).
- J. R. Clem and V. G. Kogan, Phys. Rev. B **86**, 174521 (2012).
- T. Kubo, Physical Review Research **2**, 033203 (2020).

$$L_k = \mu_0 \lambda_0^2 \frac{\dot{q}}{\frac{n_s}{n_{s0}} q + \frac{n_s}{n_{s0}} \dot{q}}$$



Assumption about
 n_s dynamics

To circumvent the complexity of the nonequilibrium problem, previous studies introduced the following simplifying assumptions.

Fast experiment (Frozen n_s): $\dot{n}_s = 0$

$$L_k = \mu_0 \lambda_0^2 \frac{\dot{q}}{\frac{n_s}{n_{s0}} q + \frac{n_s}{n_{s0}} \dot{q}} \rightarrow \mu_0 \lambda_0^2 \frac{1}{\frac{n_s(q)}{n_{s0}}} = \mu_0 \lambda^2(q)$$

Semi-phenomenological approach

- S. M. Anlage et al., IEEE Trans. Magn. **25**, 1388 (1989).
- J. R. Clem and V. G. Kogan, Phys. Rev. B **86**, 174521 (2012).
- T. Kubo, Physical Review Research **2**, 033203 (2020).

$$L_k = \mu_0 \lambda_0^2 \frac{\dot{q}}{\frac{n_s}{n_{s0}} q + \frac{n_s}{n_{s0}} \dot{q}}$$



Assumption about
 n_s dynamics

To circumvent the complexity of the nonequilibrium problem, previous studies introduced the following simplifying assumptions.

Fast experiment (Frozen n_s): $\dot{n}_s = 0$

$$L_k = \mu_0 \lambda_0^2 \frac{\dot{q}}{\frac{n_s}{n_{s0}} q + \frac{n_s}{n_{s0}} \dot{q}} \rightarrow \mu_0 \lambda_0^2 \frac{1}{\frac{n_s(q)}{n_{s0}}} = \mu_0 \lambda^2(q)$$



GL theory
or
BCS theory

Semi-phenomenological approach

- S. M. Anlage et al., IEEE Trans. Magn. **25**, 1388 (1989).
- J. R. Clem and V. G. Kogan, Phys. Rev. B **86**, 174521 (2012).
- T. Kubo, Physical Review Research **2**, 033203 (2020).

$$L_k = \mu_0 \lambda_0^2 \frac{\dot{q}}{\frac{n_s}{n_{s0}} q + \frac{n_s}{n_{s0}} \dot{q}}$$



Assumption about
 n_s dynamics

To circumvent the complexity of the nonequilibrium problem, previous studies introduced the following simplifying assumptions.

Fast experiment (Frozen n_s): $\dot{n}_s = 0$

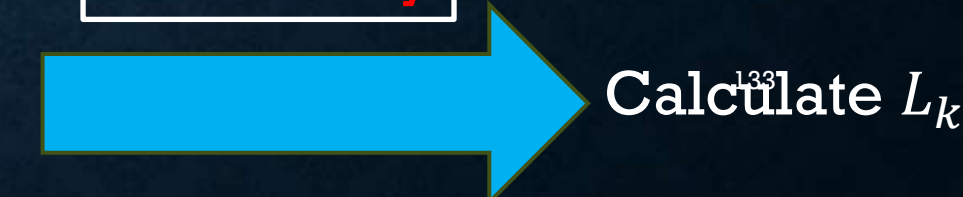
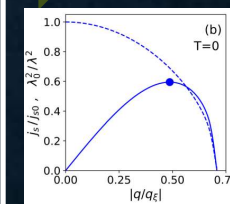
$$L_k = \mu_0 \lambda_0^2 \frac{\dot{q}}{\frac{\dot{n}_s}{n_{s0}} q + \frac{n_s}{n_{s0}} \dot{q}} \rightarrow \mu_0 \lambda_0^2 \frac{1}{\frac{n_s(q)}{n_{s0}}} = \mu_0 \lambda^2(q)$$

Slow experiment (oscillating n_s): $\dot{n}_s = (dn_s/dq)\dot{q}$

$$L_k = \mu_0 \lambda_0^2 \frac{\dot{q}}{\frac{\dot{n}_s}{n_{s0}} q + \frac{n_s}{n_{s0}} \dot{q}} \rightarrow \mu_0 \lambda_0^2 \frac{1}{(1 + q \partial_q) \frac{n_s(q)}{n_{s0}}}$$



GL theory
or
BCS theory



We can calculate L_k for **any dc bias current**.

We can calculate L_k for **any dc bias current**. However, here we focus on the small-bias regime ($J_b/J_{dp} \ll 1$), where the coefficient C in the following expansion can be determined analytically.

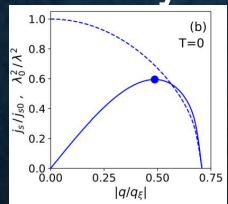
$$L_k(J_b) = L_k(0) \left\{ 1 + \textcolor{red}{C} \left(\frac{J_b}{J_{dp}} \right)^2 + \dots \right\}$$

We can calculate L_k for **any dc bias current**. However, here we focus on the small-bias regime ($J_b/J_{dp} \ll 1$), where the coefficient C in the following expansion can be determined analytically.

$$L_k(J_b) = L_k(0) \left\{ 1 + \textcolor{red}{C} \left(\frac{J_b}{J_{dp}} \right)^2 + \dots \right\}$$

Fast experiment
(Frozen n_s)

BCS theory in
the dirty limit



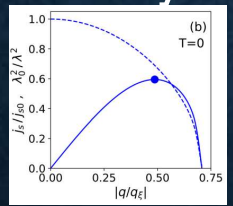
$$C(T \rightarrow 0) = \frac{(3\pi^2 + 16)s_d}{12\pi} \left(\Delta_d - \frac{4s_d}{3\pi} \right)^2 = \boxed{0.136}$$

We can calculate L_k for **any dc bias current**. However, here we focus on the small-bias regime ($J_b/J_{dp} \ll 1$), where the coefficient C in the following expansion can be determined analytically.

$$L_k(J_b) = L_k(0) \left\{ 1 + \textcolor{red}{C} \left(\frac{J_b}{J_{dp}} \right)^2 + \dots \right\}$$

Fast experiment
(Frozen n_s)

BCS theory in
the dirty limit



Slow experiment
(Oscillating n_s)

BCS theory in
the dirty limit

$$C(T \rightarrow 0) = \frac{(3\pi^2 + 16)s_d}{12\pi} \left(\Delta_d - \frac{4s_d}{3\pi} \right)^2 = \boxed{0.136}$$

$$C(T \rightarrow 0) = \frac{(3\pi^2 + 16)s_d}{4\pi} \left(\Delta_d - \frac{4s_d}{3\pi} \right)^2 = \boxed{0.409}$$

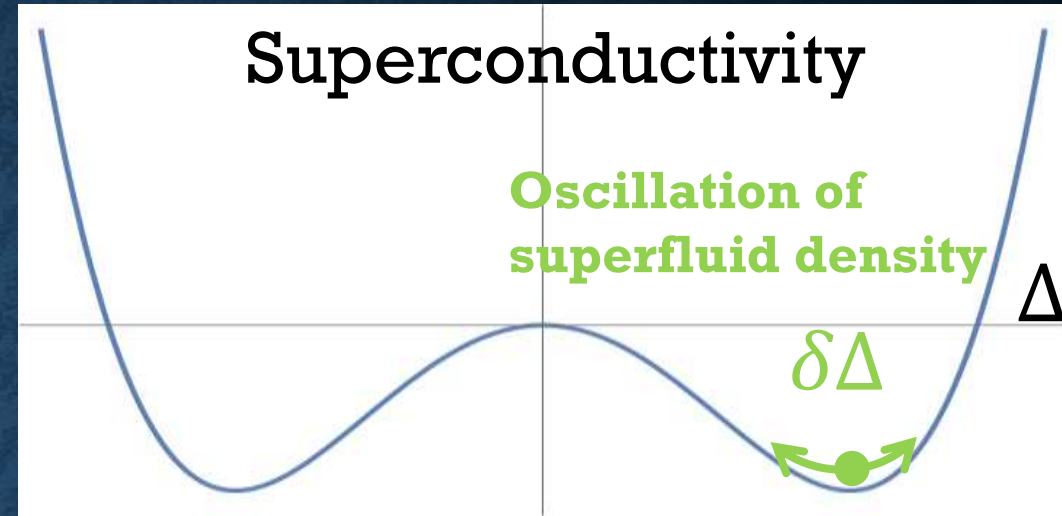
$$\Delta_d = e^{-\pi\zeta_d/4}$$

$$s_d = \Delta_d \zeta_d$$

$$\zeta_d = \frac{2}{\pi} + \frac{3\pi}{8} - \sqrt{\left(\frac{2}{\pi} + \frac{3\pi}{8}\right)^2 - 1} \simeq 0.300$$

137

Here, let us recall that the Higgs mode essentially represents an oscillation of the superfluid density n_s .

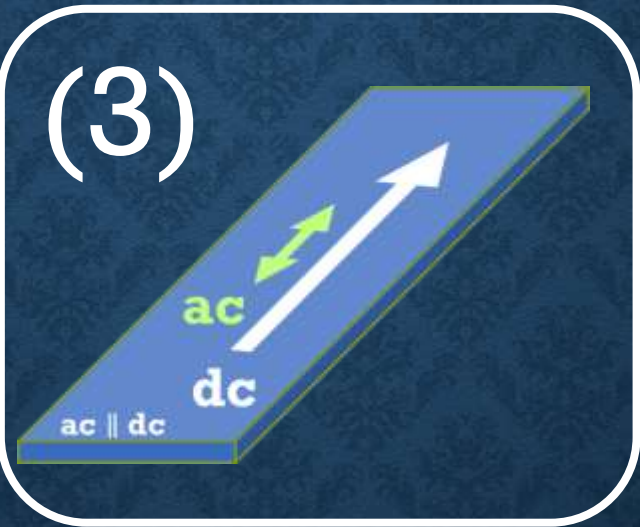
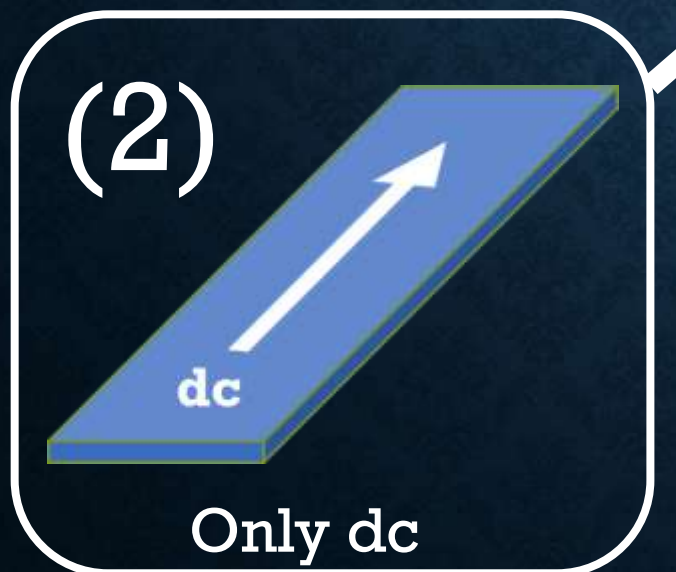
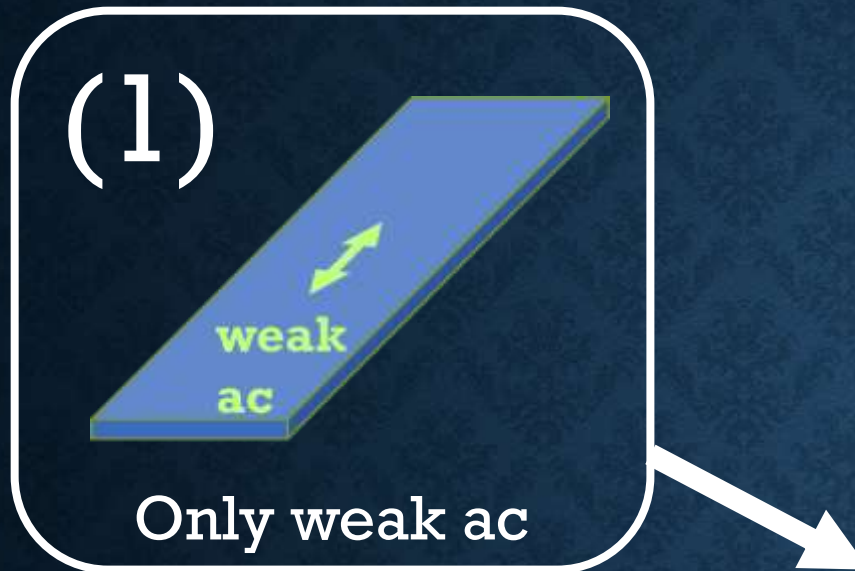


Then,

does the decades-old assumption of “frozen” and “oscillating” n_s correspond to calculations that **neglect** and **include** the **Higgs-mode** effect, respectively?

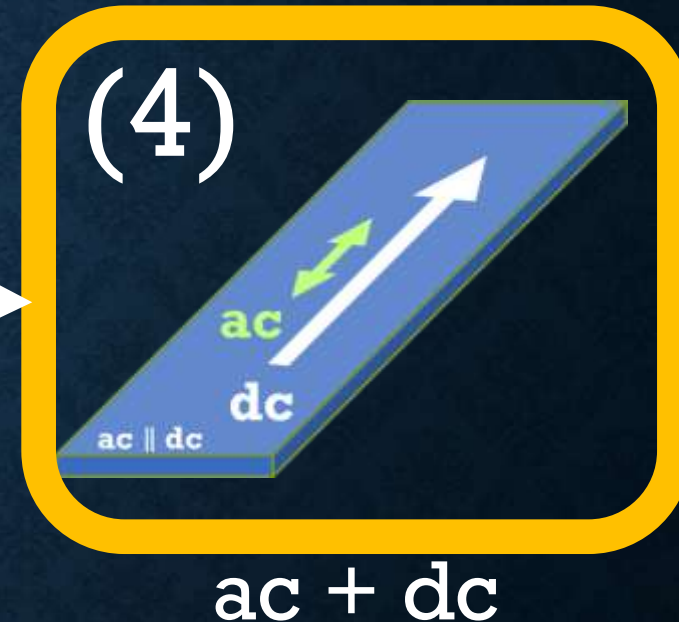
Does the difference between **C=0.136** and **C=0.409** arise from the Higgs mode?

Outline



Semi-phenomenological
approach

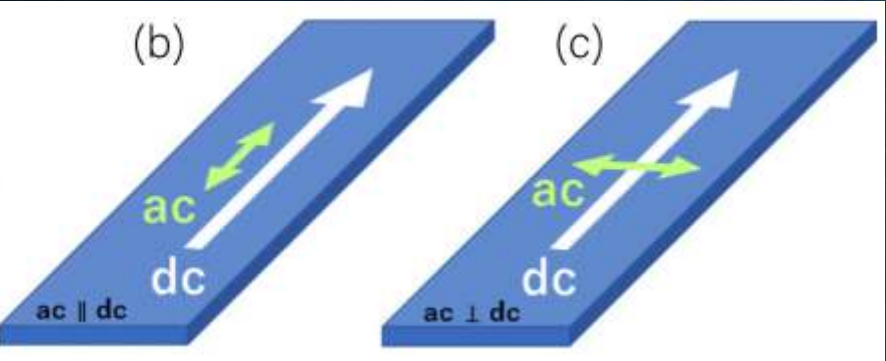
- J. R. Clem and V. G. Kogan, Phys. Rev. B **86**, 174521 (2012).
- T. Kubo, Phys. Rev. Research **2**, 033203 (2020).



**Microscopic
nonequilibrium
superconductivity**

139

- T. Kubo, Phys. Rev. Applied **22**, 044042 (2024)
- T. Kubo, Phys. Rev. Applied **23**, 054091 (2025)



In this case, we need to use the microscopic theory of **nonequilibrium** superconductivity.



- A. Moor et al., Phys. Rev. Lett. **118**, 047001 (2017)
T. Jujo, J. Phys. Soc. Jpn. **91**, 074711 (2022)
T. Kubo, Phys. Rev. Applied **22**, 044042 (2024)
T. Kubo, Phys. Rev. Applied **23**, 054091 (2025)

- **The Keldysh-Eilenberger theory** is a microscopic theory of **nonequilibrium** superconductivity. It is applicable at any temperature ($0 \leq T \leq T_c$) and for arbitrary mean free path. In this sense, it serves as the “*theory of everything for conventional superconductivity*”.
T. Kubo, Phys. Rev. Applied **22**, 044042 (2024)
- **The Keldysh-Usadel theory** represents the dirty-limit reduction of the Keldysh-Eilenberger theory of nonequilibrium superconductivity, applicable at any T ($0 \leq T \leq T_c$).¹⁴⁰
T. Kubo, Phys. Rev. Applied **23**, 054091 (2025)

Keldysh–Usadel Equation: DC Current with AC Perturbation

T. Kubo, Phys. Rev. Applied **23**, 054091 (2025)

$$\begin{aligned}
 & -i(s/2) [\hat{\tau}_3 \hat{g}_b^R(\epsilon_+) \hat{\tau}_3 \delta \hat{g}^K(\epsilon, \omega) - \hat{g}_b^R(\epsilon_+) \hat{\tau}_3 \delta \hat{g}^K(\epsilon, \omega) \hat{\tau}_3 \\
 & + \hat{\tau}_3 \delta \hat{g}^R(\epsilon, \omega) \hat{\tau}_3 \hat{g}_b^K(\epsilon_-) - \delta \hat{g}^R(\epsilon, \omega) \hat{\tau}_3 \hat{g}_b^K(\epsilon_-) \hat{\tau}_3 \\
 & + \hat{\tau}_3 \hat{g}_b^K(\epsilon_+) \hat{\tau}_3 \delta \hat{g}^A(\epsilon, \omega) - \hat{g}_b^K(\epsilon_+) \hat{\tau}_3 \delta \hat{g}^A(\epsilon, \omega) \hat{\tau}_3 \\
 & + \hat{\tau}_3 \delta \hat{g}^K(\epsilon, \omega) \hat{\tau}_3 \hat{g}_b^A(\epsilon_-) - \delta \hat{g}^K(\epsilon, \omega) \hat{\tau}_3 \hat{g}_b^A(\epsilon_-) \hat{\tau}_3] \\
 & - i(\delta W/2) [\hat{\tau}_3 \hat{g}_b^R(\epsilon_+) \hat{\tau}_3 \hat{g}_b^K(\epsilon_-) - \hat{g}_b^R(\epsilon_+) \hat{\tau}_3 \hat{g}_b^K(\epsilon_-) \hat{\tau}_3 \\
 & + \hat{\tau}_3 \hat{g}_b^R(\epsilon_-) \hat{\tau}_3 \hat{g}_b^K(\epsilon_-) - \hat{g}_b^R(\epsilon_+) \hat{\tau}_3 \hat{g}_b^K(\epsilon_+) \hat{\tau}_3 \\
 & + \hat{\tau}_3 \hat{g}_b^K(\epsilon_+) \hat{\tau}_3 \hat{g}_b^A(\epsilon_-) - \hat{g}_b^K(\epsilon_+) \hat{\tau}_3 \hat{g}_b^A(\epsilon_-) \hat{\tau}_3 \\
 & + \hat{\tau}_3 \hat{g}_b^K(\epsilon_-) \hat{\tau}_3 \hat{g}_b^A(\epsilon_-) - \hat{g}_b^K(\epsilon_+) \hat{\tau}_3 \hat{g}_b^A(\epsilon_+) \hat{\tau}_3] \\
 & = \epsilon_+ \hat{\tau}_3 \delta \hat{g}^K(\epsilon, \omega) - \delta \hat{g}^K(\epsilon, \omega) \hat{\tau}_3 \epsilon_- \\
 & + [\hat{\Delta}_b, \delta \hat{g}^K(\epsilon, \omega)] + \delta \hat{\Delta}(\omega) \hat{g}_b^K(\epsilon_-) - \hat{g}_b^K(\epsilon_+) \delta \hat{\Delta}(\omega). \tag{15}
 \end{aligned}$$

$$\begin{aligned}
 & -i(s/2) \{ \hat{\tau}_3 \hat{g}_b^r(\epsilon_+) \hat{\tau}_3 \delta \hat{g}^r(\epsilon, \omega) - \hat{g}_b^r(\epsilon_+) \hat{\tau}_3 \delta \hat{g}^r(\epsilon, \omega) \hat{\tau}_3 \\
 & + \hat{\tau}_3 \delta \hat{g}^r(\epsilon, \omega) \hat{\tau}_3 \hat{g}_b^r(\epsilon_-) - \delta \hat{g}^r(\epsilon, \omega) \hat{\tau}_3 \hat{g}_b^r(\epsilon_-) \hat{\tau}_3 \} \\
 & - i(\delta W/2) \{ \hat{\tau}_3 \hat{g}_b^r(\epsilon_+) \hat{\tau}_3 \hat{g}_b^r(\epsilon_-) \\
 & - \hat{g}_b^r(\epsilon_+) \hat{\tau}_3 \hat{g}_b^r(\epsilon_-) \hat{\tau}_3 + \hat{\tau}_3 \hat{g}_b^r(\epsilon_-) \hat{\tau}_3 \hat{g}_b^r(\epsilon_-) \\
 & - \hat{g}_b^r(\epsilon_+) \hat{\tau}_3 \hat{g}_b^r(\epsilon_+) \hat{\tau}_3 \} = \epsilon_+ \hat{\tau}_3 \delta \hat{g}^r(\epsilon, \omega) - \delta \hat{g}^r(\epsilon, \omega) \hat{\tau}_3 \epsilon_- \\
 & + [\hat{\Delta}_b, \delta \hat{g}^r(\epsilon, \omega)] + \delta \hat{\Delta}(\omega) \hat{g}_b^r(\epsilon_-) - \hat{g}_b^r(\epsilon_+) \delta \hat{\Delta}(\omega), \tag{13}
 \end{aligned}$$

$$\delta \Delta(\omega) = -\frac{g}{8} \int d\epsilon \text{Tr}[-i\tau_2 \delta \hat{g}^K(\epsilon, \omega)]. \tag{17}$$

Higgs
↓

We solve these equations to obtain the AC-induced **nonequilibrium corrections** ($\delta \hat{g}^{R,A,K}$ and $\delta \Delta$).

Keldysh–Usadel Equation: DC Current with AC Perturbation

T. Kubo, Phys. Rev. Applied **23**, 054091 (2025)

$$\begin{aligned}
 & -i(s/2) [\hat{\tau}_3 \hat{g}_b^R(\epsilon_+) \hat{\tau}_3 \delta \hat{g}^K(\epsilon, \omega) - \hat{g}_b^R(\epsilon_+) \hat{\tau}_3 \delta \hat{g}^K(\epsilon, \omega) \hat{\tau}_3 \\
 & + \hat{\tau}_3 \delta \hat{g}^R(\epsilon, \omega) \hat{\tau}_3 \hat{g}_b^K(\epsilon_-) - \delta \hat{g}^R(\epsilon, \omega) \hat{\tau}_3 \hat{g}_b^K(\epsilon_-) \hat{\tau}_3 \\
 & + \hat{\tau}_3 \hat{g}_b^K(\epsilon_+) \hat{\tau}_3 \delta \hat{g}^A(\epsilon, \omega) - \hat{g}_b^K(\epsilon_+) \hat{\tau}_3 \delta \hat{g}^A(\epsilon, \omega) \hat{\tau}_3 \\
 & + \hat{\tau}_3 \delta \hat{g}^K(\epsilon, \omega) \hat{\tau}_3 \hat{g}_b^A(\epsilon_-) - \delta \hat{g}^K(\epsilon, \omega) \hat{\tau}_3 \hat{g}_b^A(\epsilon_-) \hat{\tau}_3] \\
 & - i(\delta W/2) [\hat{\tau}_3 \hat{g}_b^R(\epsilon_+) \hat{\tau}_3 \hat{g}_b^K(\epsilon_-) - \hat{g}_b^R(\epsilon_+) \hat{\tau}_3 \hat{g}_b^K(\epsilon_-) \hat{\tau}_3 \\
 & + \hat{\tau}_3 \hat{g}_b^R(\epsilon_-) \hat{\tau}_3 \hat{g}_b^K(\epsilon_-) - \hat{g}_b^R(\epsilon_+) \hat{\tau}_3 \hat{g}_b^K(\epsilon_+) \hat{\tau}_3 \\
 & + \hat{\tau}_3 \hat{g}_b^K(\epsilon_+) \hat{\tau}_3 \hat{g}_b^A(\epsilon_-) - \hat{g}_b^K(\epsilon_+) \hat{\tau}_3 \hat{g}_b^A(\epsilon_-) \hat{\tau}_3 \\
 & + \hat{\tau}_3 \hat{g}_b^K(\epsilon_-) \hat{\tau}_3 \hat{g}_b^A(\epsilon_-) - \hat{g}_b^K(\epsilon_+) \hat{\tau}_3 \hat{g}_b^A(\epsilon_+) \hat{\tau}_3] \\
 & = \epsilon_+ \hat{\tau}_3 \delta \hat{g}^K(\epsilon, \omega) - \delta \hat{g}^K(\epsilon, \omega) \hat{\tau}_3 \epsilon_- \\
 & + [\hat{\Delta}_b, \delta \hat{g}^K(\epsilon, \omega)] + \delta \hat{\Delta}(\omega) \hat{g}_b^K(\epsilon_-) - \hat{g}_b^K(\epsilon_+) \delta \hat{\Delta}(\omega). \tag{15}
 \end{aligned}$$

$$\begin{aligned}
 & -i(s/2) \{ \hat{\tau}_3 \hat{g}_b^r(\epsilon_+) \hat{\tau}_3 \delta \hat{g}^r(\epsilon, \omega) - \hat{g}_b^r(\epsilon_+) \hat{\tau}_3 \delta \hat{g}^r(\epsilon, \omega) \hat{\tau}_3 \\
 & + \hat{\tau}_3 \delta \hat{g}^r(\epsilon, \omega) \hat{\tau}_3 \hat{g}_b^r(\epsilon_-) - \delta \hat{g}^r(\epsilon, \omega) \hat{\tau}_3 \hat{g}_b^r(\epsilon_-) \hat{\tau}_3 \} \\
 & - i(\delta W/2) \{ \hat{\tau}_3 \hat{g}_b^r(\epsilon_+) \hat{\tau}_3 \hat{g}_b^r(\epsilon_-) \\
 & - \hat{g}_b^r(\epsilon_+) \hat{\tau}_3 \hat{g}_b^r(\epsilon_-) \hat{\tau}_3 + \hat{\tau}_3 \hat{g}_b^r(\epsilon_-) \hat{\tau}_3 \hat{g}_b^r(\epsilon_-) \\
 & - \hat{g}_b^r(\epsilon_+) \hat{\tau}_3 \hat{g}_b^r(\epsilon_+) \hat{\tau}_3 \} = \epsilon_+ \hat{\tau}_3 \delta \hat{g}^r(\epsilon, \omega) - \delta \hat{g}^r(\epsilon, \omega) \hat{\tau}_3 \epsilon_- \\
 & + [\hat{\Delta}_b, \delta \hat{g}^r(\epsilon, \omega)] + \delta \hat{\Delta}(\omega) \hat{g}_b^r(\epsilon_-) - \hat{g}_b^r(\epsilon_+) \delta \hat{\Delta}(\omega), \tag{13}
 \end{aligned}$$

$$\delta \Delta(\omega) = -\frac{g}{8} \int d\epsilon \text{Tr}[-i\tau_2) \delta \hat{g}^K(\epsilon, \omega)]. \tag{17}$$

Higgs
↓

We solve these equations to obtain the AC-induced **nonequilibrium corrections** ($\delta \hat{g}^{R,A,K}$ and $\delta \Delta$).



To obtain the ac response,
we substitute the solutions ($\delta \hat{g}^{R,A,K}$, $\delta \Delta$) into



$$\delta \mathbf{J}(\omega) = -i \frac{\sigma_n}{e} \int d\epsilon \delta \mathbf{S}(\epsilon, \omega), \tag{18}$$

$$\begin{aligned}
 \delta \mathbf{S}(\epsilon, \omega) = & (i/16) \text{Tr} [i \mathbf{q}_b \\
 & \times \{ \hat{\tau}_3 \hat{g}_b^R(\epsilon_+) \hat{\tau}_3 \delta \hat{g}^K(\epsilon, \omega) + \hat{\tau}_3 \delta \hat{g}^R(\epsilon, \omega) \hat{\tau}_3 \hat{g}_b^K(\epsilon_-) \\
 & + \hat{\tau}_3 \hat{g}_b^K(\epsilon_+) \hat{\tau}_3 \delta \hat{g}^A(\epsilon, \omega) + \hat{\tau}_3 \delta \hat{g}^K(\epsilon, \omega) \hat{\tau}_3 \hat{g}_b^A(\epsilon_-) \} \\
 & + i \delta \mathbf{q}_\omega \{ \hat{\tau}_3 \hat{g}_b^R(\epsilon_+) \hat{\tau}_3 \hat{g}_b^K(\epsilon_-) + \hat{\tau}_3 \hat{g}_b^K(\epsilon_+) \hat{\tau}_3 \hat{g}_b^A(\epsilon_-) \}]. \tag{19}
 \end{aligned}$$

Instead of showing the rigorous algebraic calculations, we will look at schematic illustrations that represent the final results.

$$J \sim Agg + A_{dc}g\delta g$$

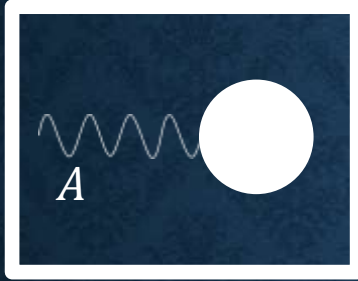


$$\delta \mathbf{J}(\omega) = -i \frac{\sigma_n}{e} \int d\epsilon \delta \mathbf{S}(\epsilon, \omega), \quad (18)$$

$$\begin{aligned} \delta \mathbf{S}(\epsilon, \omega) = & (i/16) \text{Tr} [i \mathbf{q}_b \\ & \times \{ \hat{\tau}_3 \hat{g}_b^R(\epsilon_+) \hat{\tau}_3 \delta \hat{g}^K(\epsilon, \omega) + \hat{\tau}_3 \delta \hat{g}^R(\epsilon, \omega) \hat{\tau}_3 \hat{g}_b^K(\epsilon_-) \\ & + \hat{\tau}_3 \hat{g}_b^K(\epsilon_+) \hat{\tau}_3 \delta \hat{g}^A(\epsilon, \omega) + \hat{\tau}_3 \delta \hat{g}^K(\epsilon, \omega) \hat{\tau}_3 \hat{g}_b^A(\epsilon_-) \} \\ & + i \delta \mathbf{q}_\omega \{ \hat{\tau}_3 \hat{g}_b^R(\epsilon_+) \hat{\tau}_3 \hat{g}_b^K(\epsilon_-) + \hat{\tau}_3 \hat{g}_b^K(\epsilon_+) \hat{\tau}_3 \hat{g}_b^A(\epsilon_-) \}] . \end{aligned} \quad (19)$$

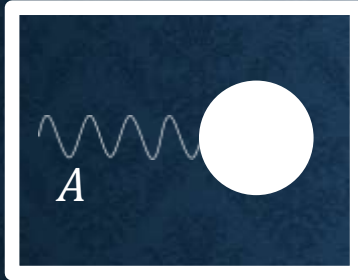
Instead of showing the rigorous algebraic calculations, we will look at schematic illustrations that represent the final results.

$$J \sim [Agg] + A_{dc}g\delta g$$



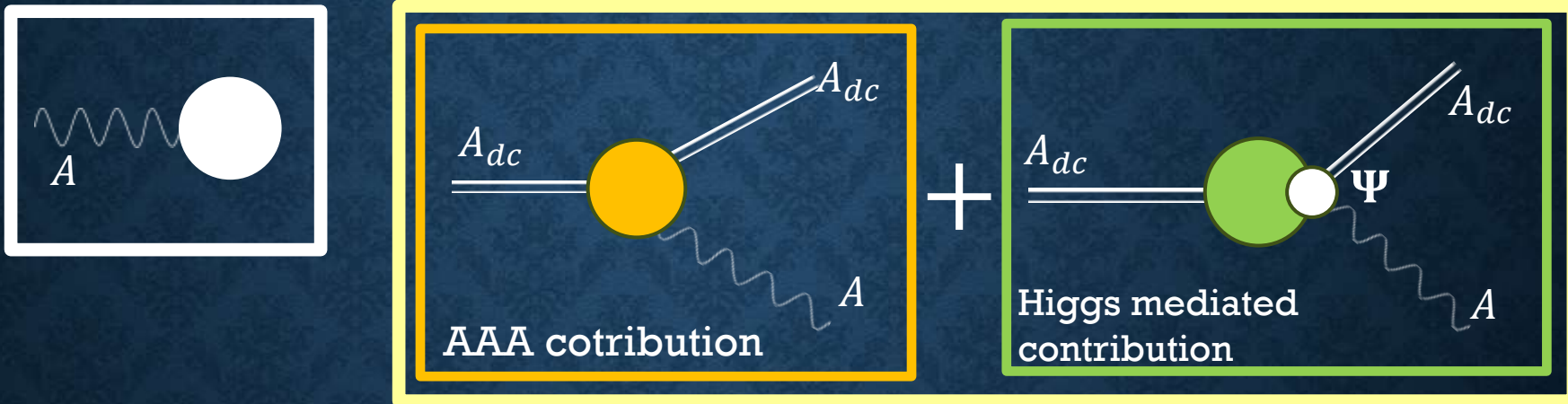
Instead of showing the rigorous algebraic calculations, we will look at schematic illustrations that represent the final results.

$$J \sim \boxed{Agg} + A_{dc}g\delta g \quad \delta g \sim \textcolor{blue}{A}_{dc} \cdot \textcolor{red}{A} + \textcolor{violet}{\delta\Delta} \quad \text{and} \quad \delta\Delta \sim \Psi \textcolor{brown}{A}_{dc} \cdot \textcolor{teal}{A}$$



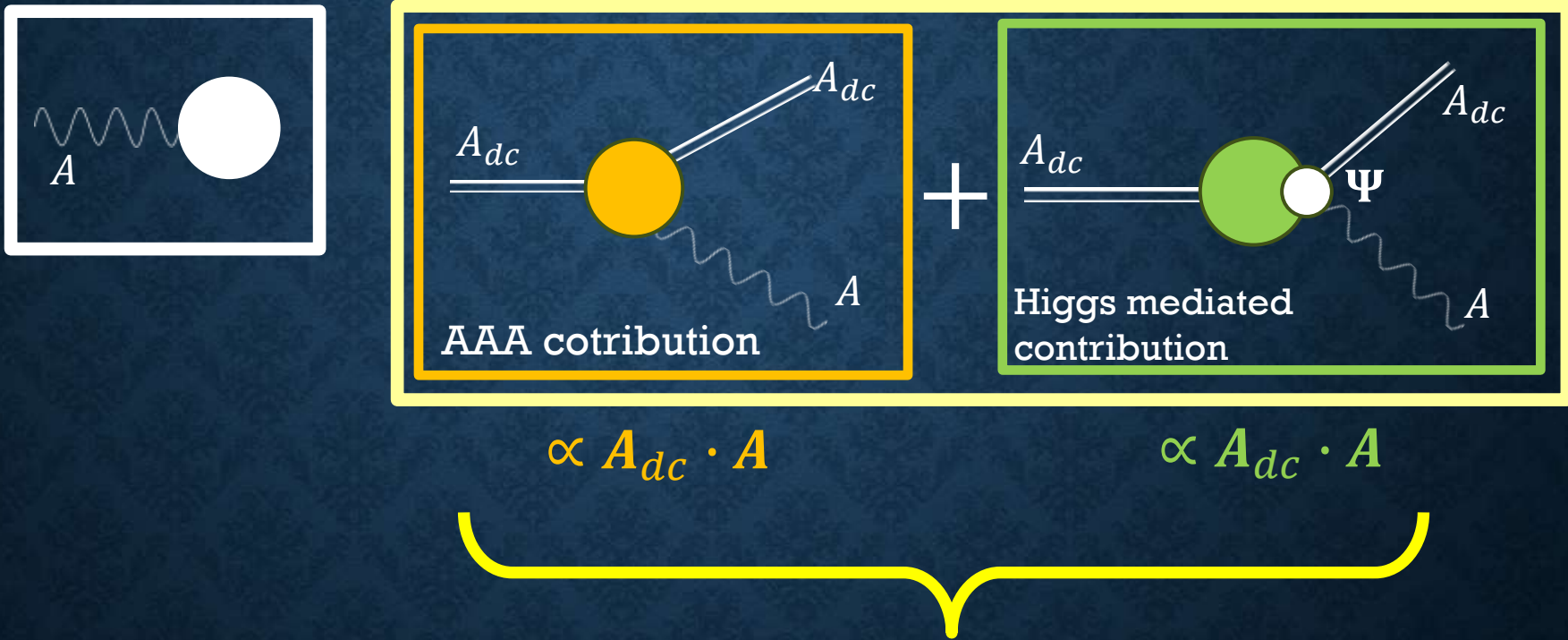
Instead of showing the rigorous algebraic calculations, we will look at schematic illustrations that represent the final results.

$$J \sim [Agg] + [A_{dc}g\delta g] \quad \delta g \sim A_{dc} \cdot A + \delta\Delta \quad \text{and} \quad \delta\Delta \sim \Psi A_{dc} \cdot A$$



Instead of showing the rigorous algebraic calculations, we will look at schematic illustrations that represent the final results.

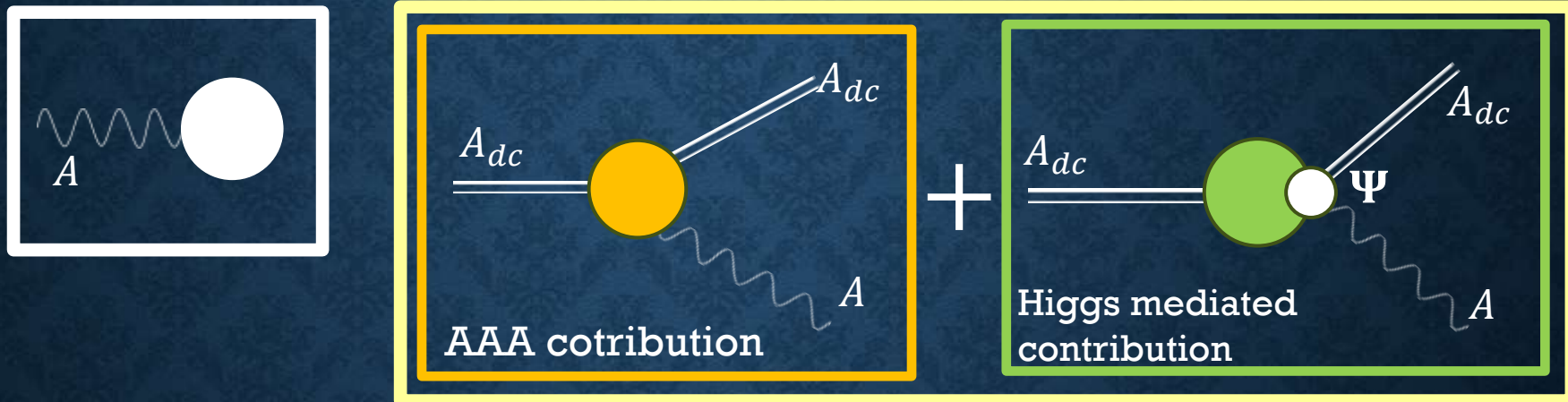
$$J \sim [Agg] + [A_{dc}g\delta g] \quad \delta g \sim A_{dc} \cdot A + \delta\Delta \quad \text{and} \quad \delta\Delta \sim \Psi A_{dc} \cdot A$$



Nonequilibrium corrections due to the
Doppler fluctuation of flow $\propto A_{dc} \cdot A$

Instead of showing the rigorous algebraic calculations, we will look at schematic illustrations that represent the final results.

$$J \sim [Agg] + [A_{dc}g\delta g] \quad \delta g \sim A_{dc} \cdot A + \delta\Delta \quad \text{and} \quad \delta\Delta \sim \Psi A_{dc} \cdot A$$



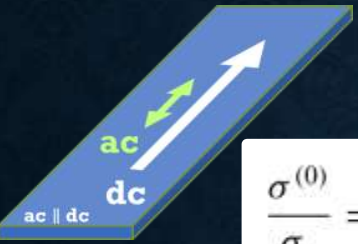
Then, the complex conductivity is given by

$$\sigma = \frac{J}{E} \sim \frac{[A] + [A_{dc} \cdot A] + [\Psi A_{dc} \cdot A]}{A}$$

Complex conductivity formula

T. Kubo, Phys. Rev. Applied **23**, 054091 (2025)

$ac \parallel dc$ case



$$\sigma = \sigma^{(0)} + \sigma^{(1)} + \sigma^{(2)}$$

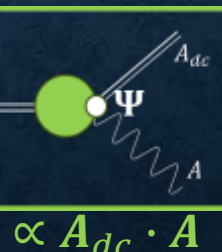
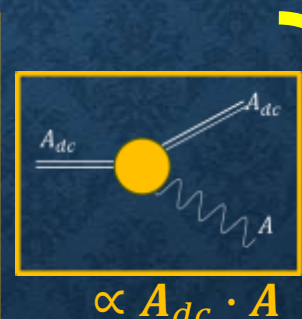
$$\frac{\sigma^{(0)}}{\sigma_n} = \int \frac{d\epsilon}{\hbar\omega} (\text{Re } G_b \text{ Re } G'_b + \text{Re } F_b \text{ Re } F'_b) (f_{\text{FD}} - f'_{\text{FD}}) + i \int \frac{d\epsilon}{\hbar\omega} (\text{Re } G_b \text{ Im } G'_b + \text{Re } F_b \text{ Im } F'_b) (2f_{\text{FD}} - 1), \quad (41)$$

$$\frac{\sigma^{(1)}}{\sigma_n} = \frac{8s}{\hbar\omega} \int \frac{d\epsilon}{\hbar\omega} \text{Re } F_b \text{ Im } F_b \text{ Re } G'_b (f_{\text{FD}} - f'_{\text{FD}}) + i \frac{2s}{\hbar\omega} \int \frac{d\epsilon}{\hbar\omega} [2 \text{Re } F_b \text{ Im } F_b \text{ Im } \{G_b + G'_b\} + \{(\text{Re } F'_b)^2 - (\text{Re } F_b)^2 + (\text{Im } F_b)^2 - (\text{Im } F'_b)^2\} \text{ Re } G_b] (2f_{\text{FD}} - 1), \quad (42)$$

AAA
contribution

$$\frac{\sigma^{(2)}}{\sigma_n} = \frac{2s\Psi}{\hbar\omega} \int \frac{d\epsilon}{\hbar\omega} (\text{Re } F_b \text{ Re } G'_b - \text{Re } G_b \text{ Re } F'_b) \times (f_{\text{FD}} - f'_{\text{FD}}) + i \frac{2s\Psi}{\hbar\omega} \int \frac{d\epsilon}{\hbar\omega} \{\text{Re } G_b \text{ Im}(F_b - F'_b) + \text{Re } F_b \text{ Im}(G_b + G'_b)\} (2f_{\text{FD}} - 1). \quad (43)$$

Higgs
mediated
contribution

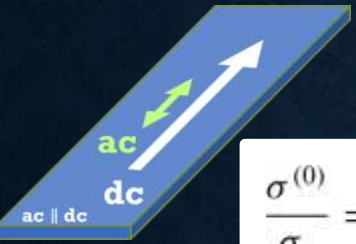


Nonequilibrium corrections due
to the Doppler fluctuation of flow
 $\propto A_{dc} \cdot A$

Complex conductivity formula

T. Kubo, Phys. Rev. Applied **23**, 054091 (2025)

$ac \parallel dc$ case



$$\sigma = \sigma^{(0)} + \sigma^{(1)} + \sigma^{(2)}$$

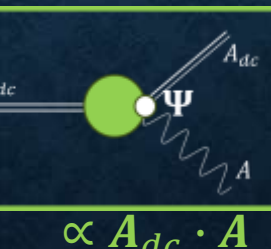
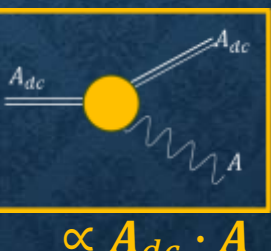
$$\begin{aligned} \frac{\sigma^{(0)}}{\sigma_n} &= \int \frac{d\epsilon}{\hbar\omega} (\text{Re } G_b \text{ Re } G'_b + \text{Re } F_b \text{ Re } F'_b) (f_{\text{FD}} - f'_{\text{FD}}) \\ &+ i \int \frac{d\epsilon}{\hbar\omega} (\text{Re } G_b \text{ Im } G'_b + \text{Re } F_b \text{ Im } F'_b) (2f_{\text{FD}} - 1), \end{aligned} \quad (41)$$

$$\begin{aligned} \frac{\sigma^{(1)}}{\sigma_n} &= \frac{8s}{\hbar\omega} \int \frac{d\epsilon}{\hbar\omega} \text{Re } F_b \text{ Im } F_b \text{ Re } G'_b (f_{\text{FD}} - f'_{\text{FD}}) \\ &+ i \frac{2s}{\hbar\omega} \int \frac{d\epsilon}{\hbar\omega} [2 \text{Re } F_b \text{ Im } F_b \text{ Im } \{G_b + G'_b\} + \{(\text{Re } F'_b)^2 \\ &- (\text{Re } F_b)^2 + (\text{Im } F_b)^2 - (\text{Im } F'_b)^2\} \text{ Re } G_b] (2f_{\text{FD}} - 1), \end{aligned} \quad (42)$$

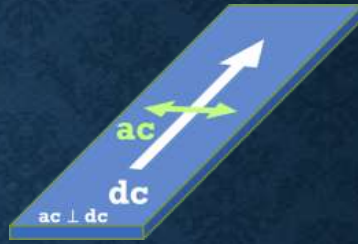
AAA contribution

$$\begin{aligned} \frac{\sigma^{(2)}}{\sigma_n} &= \frac{2s\Psi}{\hbar\omega} \int \frac{d\epsilon}{\hbar\omega} (\text{Re } F_b \text{ Re } G'_b - \text{Re } G_b \text{ Re } F'_b) \\ &\times (f_{\text{FD}} - f'_{\text{FD}}) + i \frac{2s\Psi}{\hbar\omega} \left\{ \text{Re } G_b \text{ Im } (F_b - F'_b) \right. \\ &\left. + \text{Re } F_b \text{ Im } (G_b + G'_b) \right\} (2f_{\text{FD}} - 1). \end{aligned} \quad (43)$$

Higgs mediated contribution



$ac \perp dc$ case



$$\sigma = \sigma^{(0)}$$

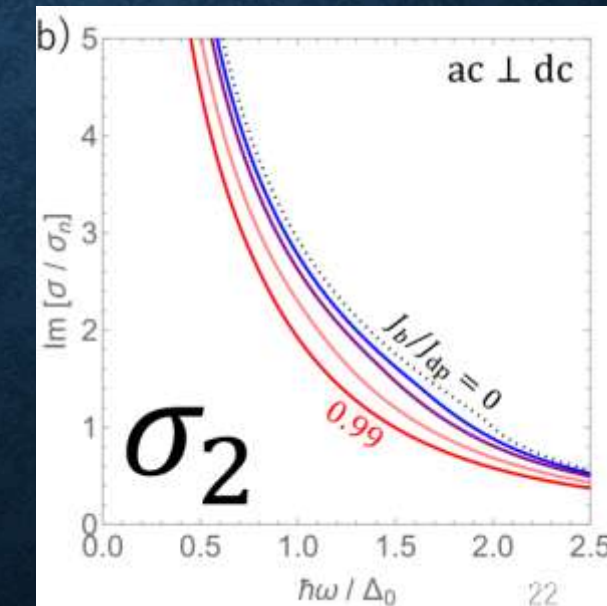
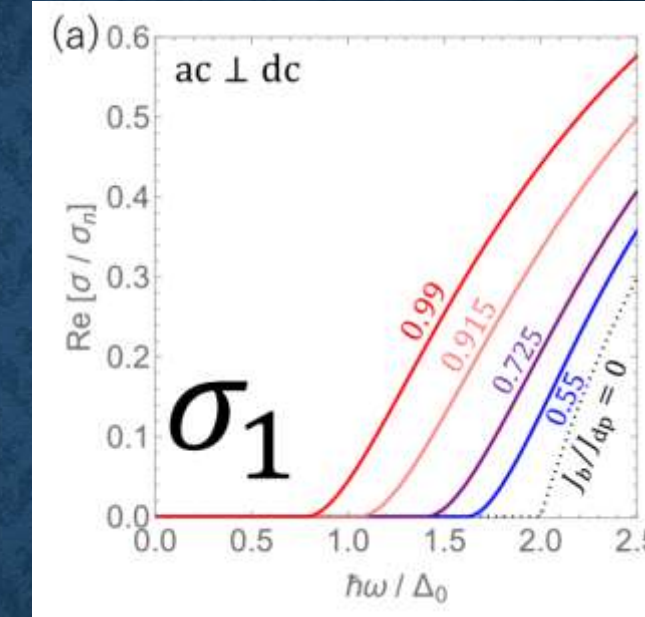


$$\begin{aligned} \frac{\sigma^{(0)}}{\sigma_n} &= \int \frac{d\epsilon}{\hbar\omega} (\text{Re } G_b \text{ Re } G'_b + \text{Re } F_b \text{ Re } F'_b) (f_{\text{FD}} - f'_{\text{FD}}) \\ &+ i \int \frac{d\epsilon}{\hbar\omega} (\text{Re } G_b \text{ Im } G'_b + \text{Re } F_b \text{ Im } F'_b) (2f_{\text{FD}} - 1), \end{aligned} \quad (41)$$

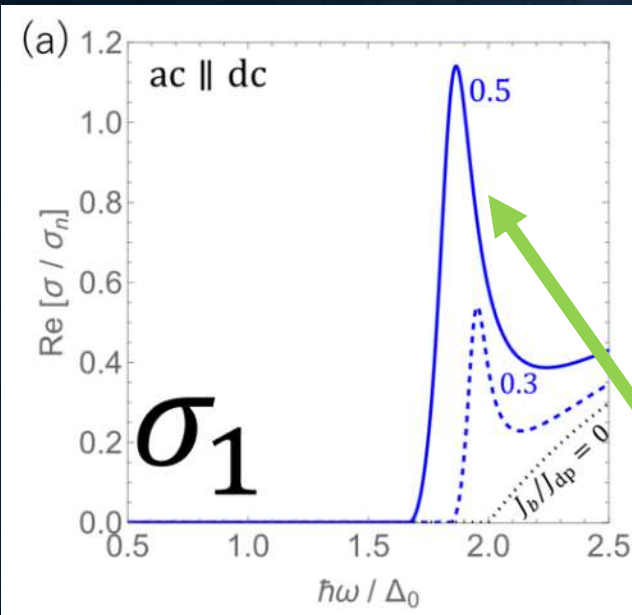
No Doppler fluctuation

Nonequilibrium corrections due to the Doppler fluctuation of flow $\propto A_{dc} \cdot A$

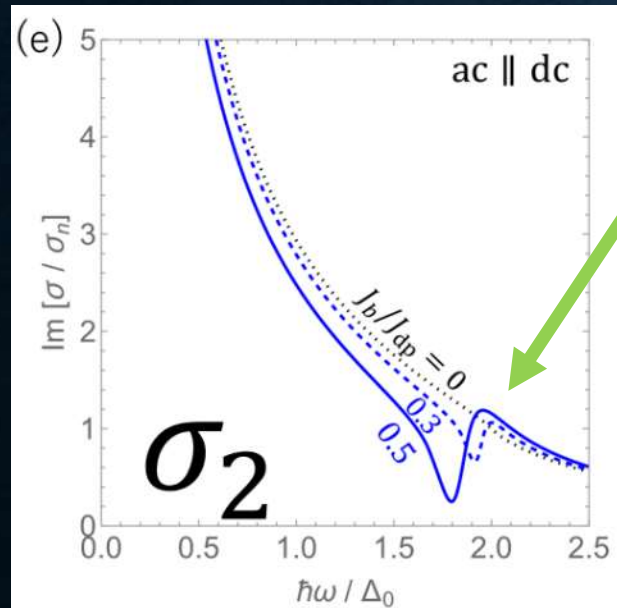
ac \perp dc



$ac \parallel dc$

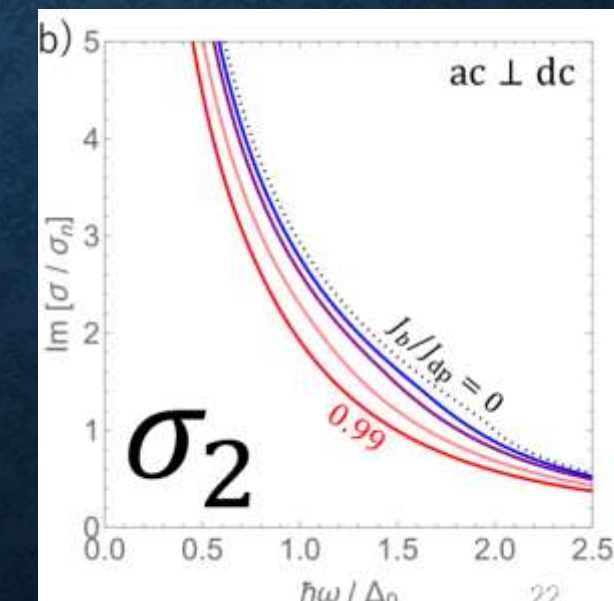
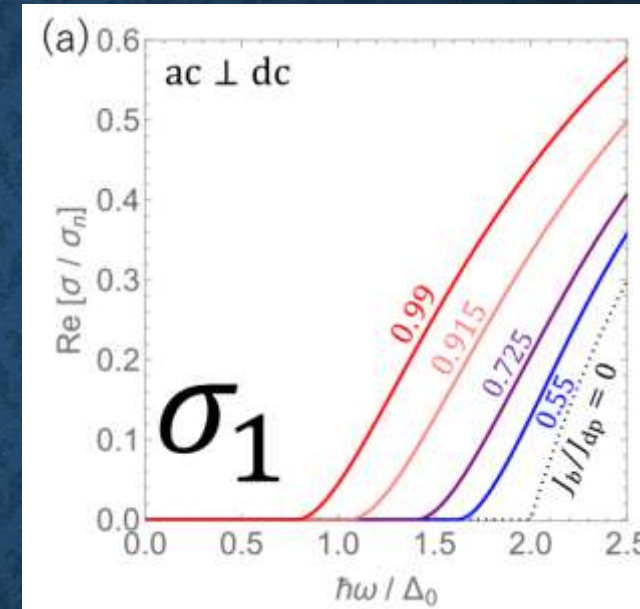


Resonance peak due
to the **Higgs** mode.



Already observed in
experiments!
S. Nakamura et al.,
PRL **122**, 257001 (2019)

$ac \perp dc$



To calculate the kinetic inductance, we just go back to its definition.

$$L_k = \frac{E}{\dot{J}_s} \xrightarrow{J_s \propto e^{-i\omega t}} L_k = \frac{1}{\omega \sigma_2} \xrightarrow{} L_k(J) = L_k(0) \left\{ 1 + \boxed{C} \left(\frac{J}{J_{dp}} \right)^2 + \dots \right\}$$

For $(T, \omega) \rightarrow (0, 0)$, we can analytically calculate the coefficient C

To calculate the kinetic inductance, we just go back to its definition.

$$L_k = \frac{E}{\dot{J}_s} \xrightarrow{J_s \propto e^{-i\omega t}} L_k = \frac{1}{\omega \sigma_2} \xrightarrow{} L_k(J) = L_k(0) \left\{ 1 + \boxed{C} \left(\frac{J}{J_{dp}} \right)^2 + \dots \right\}$$

For $(T, \omega) \rightarrow (0, 0)$, we can analytically calculate the coefficient C

$ac \perp dc$
case



$$C = C^{(0)} \simeq 0.136$$

To calculate the kinetic inductance, we just go back to its definition.

$$L_k = \frac{E}{\dot{J}_s} \xrightarrow{J_s \propto e^{-i\omega t}} L_k = \frac{1}{\omega \sigma_2} \xrightarrow{} L_k(J) = L_k(0) \left\{ 1 + \boxed{C} \left(\frac{J}{J_{dp}} \right)^2 + \dots \right\}$$

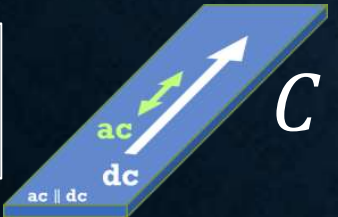
For $(T, \omega) \rightarrow (0, 0)$, we can analytically calculate the coefficient C

$ac \perp dc$
case



$$C = C^{(0)} \simeq 0.136$$

$ac \parallel dc$
case



$$C = C^{(0)} + C^{(1)} + C^{(2)} \simeq 0.409$$

$$\begin{aligned} & \approx 0.136 \\ & (23\%) \quad (23\%) \end{aligned}$$

Two yellow arrows pointing towards each other, labeled ≈ 0.136 and (23%) . Below them, two green arrows pointing towards each other, labeled (23%) .

$$\begin{aligned} & \approx 0.136 \\ & (23\%) \quad (23\%) \end{aligned}$$

Two yellow arrows pointing towards each other, labeled ≈ 0.136 and (23%) . Below them, two green arrows pointing towards each other, labeled (23%) .

To calculate the kinetic inductance, we just go back to its definition.

$$L_k = \frac{E}{\dot{J}_s} \xrightarrow{J_s \propto e^{-i\omega t}} L_k = \frac{1}{\omega \sigma_2} \xrightarrow{} L_k(J) = L_k(0) \left\{ 1 + \boxed{C} \left(\frac{J}{J_{dp}} \right)^2 + \dots \right\}$$

For $(T, \omega) \rightarrow (0, 0)$, we can analytically calculate the coefficient C

Microscopic theory of nonequilibrium superconductivity

T. Kubo, Phys. Rev. Applied **22**, 044042 (2024)

T. Kubo, Phys. Rev. Applied **23**, 054091 (2025)

$ac \perp dc$
case



$$C = C^{(0)} \simeq 0.136$$

$ac \parallel dc$
case



$$C = C^{(0)} + C^{(1)} + C^{(2)} \simeq 0.409$$

≈ 0.136
(23%)
(2.0956)
 ≈ 0.409
(43%)
(4.177)
AAA Higgs

To calculate the kinetic inductance, we just go back to its definition.

$$L_k = \frac{E}{\dot{J}_s} \xrightarrow{J_s \propto e^{-i\omega t}} L_k = \frac{1}{\omega \sigma_2} \xrightarrow{} L_k(J) = L_k(0) \left\{ 1 + \boxed{C} \left(\frac{J}{J_{dp}} \right)^2 + \dots \right\}$$

For $(T, \omega) \rightarrow (0, 0)$, we can analytically calculate the coefficient C

Microscopic theory of nonequilibrium superconductivity

T. Kubo, Phys. Rev. Applied **22**, 044042 (2024)

T. Kubo, Phys. Rev. Applied **23**, 054091 (2025)

Semi-phenomenological

J. R. Clem and V. G. Kogan, Phys. Rev. B **86**, 174521 (2012).

T. Kubo, Physical Review Research **2**, 033203 (2020).

$ac \perp dc$
case



$$C = C^{(0)} \simeq 0.136$$

$ac \parallel dc$
case



$$C = C^{(0)} + C^{(1)} + C^{(2)} \simeq 0.409$$

$\simeq 0.136$
 (23%)
 $(2.0\% \text{ KAA})$
 $(2.0\% \text{ Higgs})$
 (43%)
 (17%)

To calculate the kinetic inductance, we just go back to its definition.

$$L_k = \frac{E}{\dot{J}_s} \xrightarrow{J_s \propto e^{-i\omega t}} L_k = \frac{1}{\omega \sigma_2} \xrightarrow{} L_k(J) = L_k(0) \left\{ 1 + \boxed{C} \left(\frac{J}{J_{dp}} \right)^2 + \dots \right\}$$

For $(T, \omega) \rightarrow (0, 0)$, we can analytically calculate the coefficient C

Microscopic theory of nonequilibrium superconductivity

T. Kubo, Phys. Rev. Applied **22**, 044042 (2024)

T. Kubo, Phys. Rev. Applied **23**, 054091 (2025)

Semi-phenomenological

J. R. Clem and V. G. Kogan, Phys. Rev. B **86**, 174521 (2012).

T. Kubo, Physical Review Research **2**, 033203 (2020).

$ac \perp dc$
case



$$C = C^{(0)} \simeq 0.136$$

$ac \parallel dc$
case



$$C = C^{(0)} + C^{(1)} + C^{(2)} \simeq 0.409$$

$\simeq 0.136$
(23%)
(20.95%)
(43%)
(40.17%)
Higgs

Fast experiment (Frozen n_s)
 $C \simeq 0.136$

To calculate the kinetic inductance, we just go back to its definition.

$$L_k = \frac{E}{\dot{J}_s} \xrightarrow{J_s \propto e^{-i\omega t}} L_k = \frac{1}{\omega \sigma_2} \xrightarrow{} L_k(J) = L_k(0) \left\{ 1 + \boxed{C} \left(\frac{J}{J_{dp}} \right)^2 + \dots \right\}$$

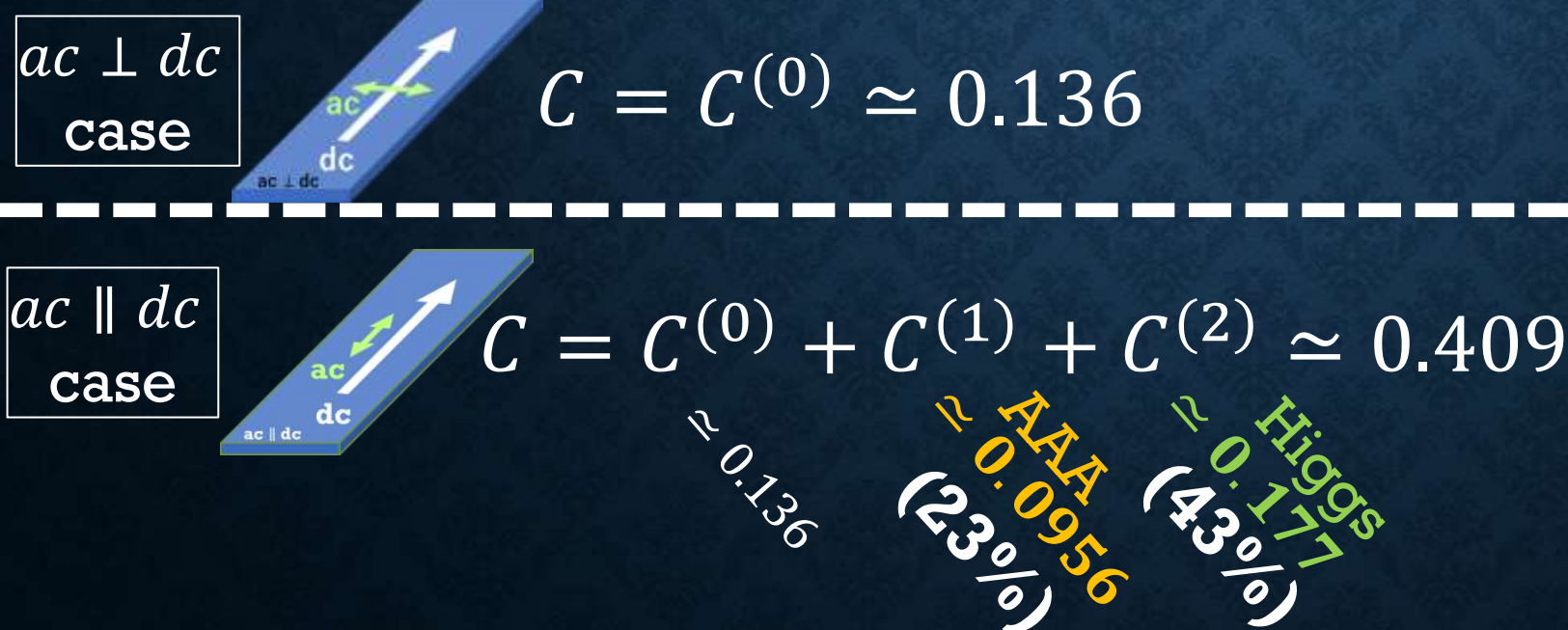
For $(T, \omega) \rightarrow (0, 0)$, we can analytically calculate the coefficient C

Microscopic theory of nonequilibrium superconductivity

T. Kubo, Phys. Rev. Applied **22**, 044042 (2024)
T. Kubo, Phys. Rev. Applied **23**, 054091 (2025)

Semi-phenomenological

J. R. Clem and V. G. Kogan, Phys. Rev. B **86**, 174521 (2012).
T. Kubo, Physical Review Research **2**, 033203 (2020).

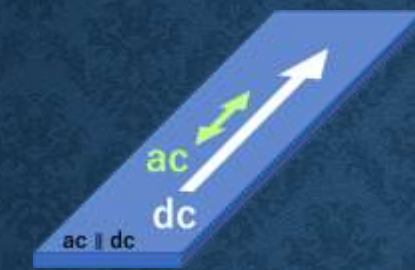


Fast experiment (Frozen n_s)
 $C \simeq 0.136$

Slow experiment (Oscillating n_s)
 $C \simeq 0.409$

“C” from the Keldysh-Eilenberger theory, which is a microscopic theory of **nonequilibrium** superconductivity and is applicable at any temperature ($0 \leq T \leq T_c$) and for arbitrary mean free path.

$$C \simeq 0.4$$

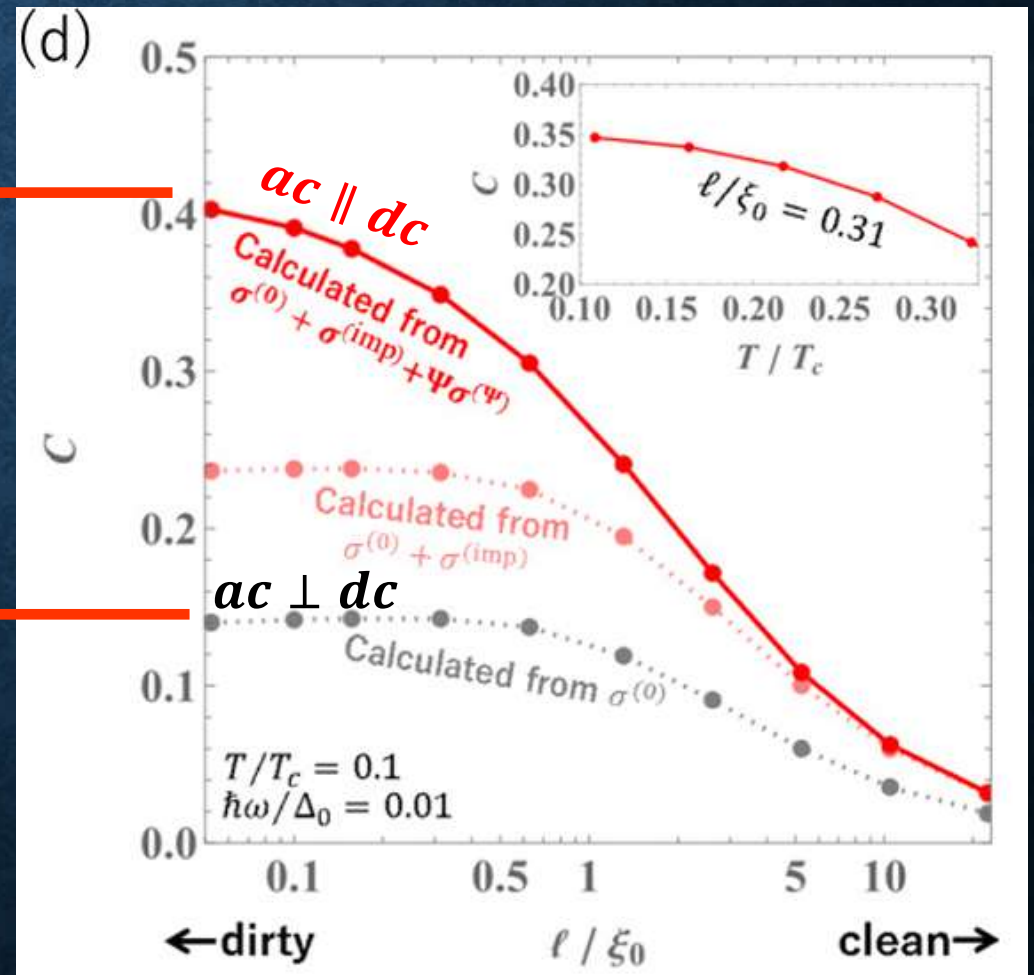


Consistent with the dirty limit result obtained from the Keldysh-Usadel

$$C \simeq 0.14$$



$$L_k(J_b) = L_k(0) \left\{ 1 + \textcolor{red}{C} \left(\frac{J_b}{J_{dp}} \right)^2 + \dots \right\}$$



We have finally come to understand the **true meaning** of the semi-phenomenological approach: frozen and oscillating n_s

[When Does it happen?]

What has long been believed

Frozen n_s

The ac frequency is so **fast** that
the superfluid density cannot follow it.
(Fast experiment)

We have finally come to understand the **true meaning** of the semi-phenomenological approach: frozen and oscillating n_s

[When Does it happen?]

What has long been believed

Frozen n_s

The ac frequency is so **fast** that
the superfluid density cannot follow it.
(Fast experiment)

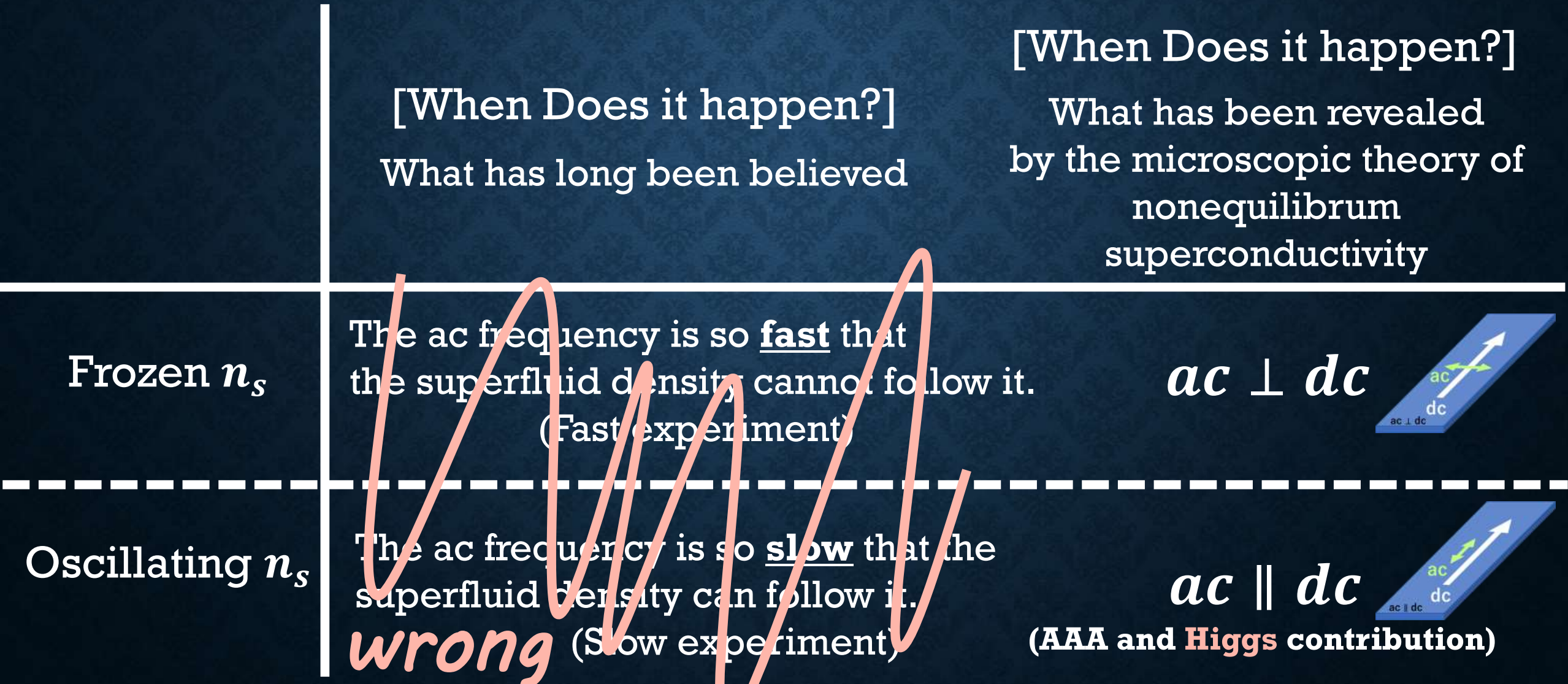
Oscillating n_s

The ac frequency is so **slow** that the
superfluid density can follow it.
(Slow experiment)

We have finally come to understand the **true meaning** of the semi-phenomenological approach: frozen and oscillating n_s

	[When Does it happen?]	[When Does it happen?]
	What has long been believed	What has been revealed by the microscopic theory of nonequilibrium superconductivity
Frozen n_s	The ac frequency is so fast that the superfluid density cannot follow it. (Fast experiment)	
Oscillating n_s	The ac frequency is so slow that the superfluid density can follow it. (Slow experiment)	163

We have finally come to understand the **true meaning** of the semi-phenomenological approach: frozen and oscillating n_s

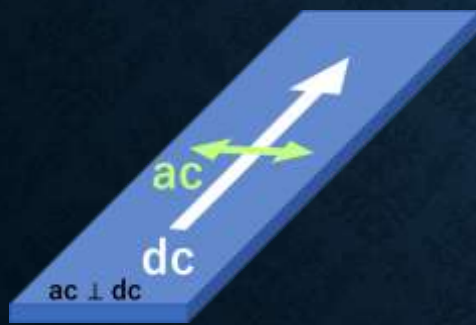


Summary of this part

The Higgs mode is ubiquitous in superconducting devices.

The current dependence of the kinetic inductance is a representative example.

$$L_k(J) = L_k(0) \left\{ 1 + C \left(\frac{J}{J_{dp}} \right)^2 + \dots \right\}$$



$ac \perp dc$
case

$$C = C^{(0)} \simeq 0.136$$



$ac \parallel dc$
case

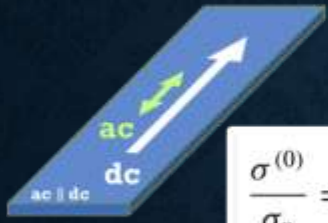
$$C = C^{(0)} + C^{(1)} + C^{(2)} \simeq 0.409$$

0.136
0.0956
(23%)
0.177
(43%)
Higgs

Complex conductivity formula

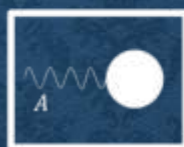
T. Kubo, Phys. Rev. Applied 23, 054091 (2025)

$ac \parallel dc$ case



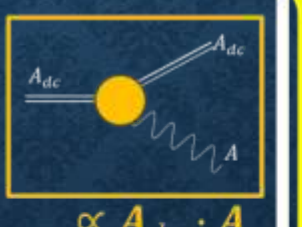
$$\sigma = \sigma^{(0)} + \sigma^{(1)} + \sigma^{(2)}$$

$$\begin{aligned} \frac{\sigma^{(0)}}{\sigma_n} &= \int \frac{d\epsilon}{\hbar\omega} (\text{Re } G_b \text{ Re } G'_b + \text{Re } F_b \text{ Re } F'_b) (f_{\text{FD}} - f'_{\text{FD}}) \\ &+ i \int \frac{d\epsilon}{\hbar\omega} (\text{Re } G_b \text{ Im } G'_b + \text{Re } F_b \text{ Im } F'_b) (2f_{\text{FD}} - 1), \end{aligned} \quad (41)$$



AAA contribution

$$\begin{aligned} \frac{\sigma^{(1)}}{\sigma_n} &= \frac{8s}{\hbar\omega} \int \frac{d\epsilon}{\hbar\omega} \text{Re } F_b \text{ Im } F_b \text{ Re } G'_b (f_{\text{FD}} - f'_{\text{FD}}) \\ &+ i \frac{2s}{\hbar\omega} \int \frac{d\epsilon}{\hbar\omega} [2 \text{Re } F_b \text{ Im } F_b \text{ Im } \{G_b + G'_b\} + \{(\text{Re } F'_b)^2 \\ &- (\text{Re } F_b)^2 + (\text{Im } F_b)^2 - (\text{Im } F'_b)^2\} \text{ Re } G_b] (2f_{\text{FD}} - 1), \end{aligned} \quad (42)$$



Higgs mediated contribution

$$\begin{aligned} \frac{\sigma^{(2)}}{\sigma_n} &= \frac{2s\Psi}{\hbar\omega} \int \frac{d\epsilon}{\hbar\omega} (\text{Re } F_b \text{ Re } G'_b - \text{Re } G_b \text{ Re } F'_b) \\ &\times (f_{\text{FD}} - f'_{\text{FD}}) + i \frac{2s\Psi}{\hbar\omega} \int \frac{d\epsilon}{\hbar\omega} \{ \text{Re } G_b \text{ Im } (F_b - F'_b) \\ &+ \text{Re } F_b \text{ Im } (G_b + G'_b) \} (2f_{\text{FD}} - 1). \end{aligned} \quad (43)$$



$ac \perp dc$ case



$$\sigma = \sigma^{(0)}$$

$$\begin{aligned} \frac{\sigma^{(0)}}{\sigma_n} &= \int \frac{d\epsilon}{\hbar\omega} (\text{Re } G_b \text{ Re } G'_b + \text{Re } F_b \text{ Re } F'_b) (f_{\text{FD}} - f'_{\text{FD}}) \\ &+ i \int \frac{d\epsilon}{\hbar\omega} (\text{Re } G_b \text{ Im } G'_b + \text{Re } F_b \text{ Im } F'_b) (2f_{\text{FD}} - 1), \end{aligned} \quad (41)$$

No Doppler fluctuation

Nonequilibrium corrections due to the Doppler fluctuation of flow $\propto A_{dc} \cdot A$

Summary of this lecture

Research and development of superconducting resonators, which lie at the intersection of various fields, represent one of the most important efforts to pioneer 21st-century physics.

